

Dissertation zur Erlangung des Doktorgrades
der Fakultät für Chemie und Pharmazie
der Ludwig-Maximilians-Universität München

Studies on Stable Formulations for a Hydrophobic Cytokine

Andrea Hawe
aus München

Juni 2006

Erklärung

Diese Dissertation wurde im Sinne von § 13 Abs. 3 bzw. 4 der Promotionsordnung vom 29. Januar 1998 von Herrn Prof. Dr. Wolfgang Frieß betreut.

Ehrenwörtliche Versicherung

Diese Dissertation wurde selbstständig, ohne unerlaubte Hilfe erarbeitet.

München, am 26. Juni 2006

A handwritten signature in cursive script, reading "Andrea Hawe", followed by a horizontal line.

(Andrea Hawe)

Dissertation eingereicht am 26. Juni 2006

1. Gutachter: Prof. Dr. Wolfgang Frieß

2. Gutachter: Prof. Dr. Gerhard Winter

Mündliche Prüfung am 21. Juli 2006

Acknowledgements

The presented thesis was written at the Department of Pharmacy, Pharmaceutical Technology and Biopharmaceutics at the Ludwig-Maximilians-University in Munich under supervision of Prof. Dr. Wolfgang Frieß.

First of all, I want to express my gratitude to my supervisor Prof. Dr. Wolfgang Frieß for the possibility to join his research group and especially for his professional and enthusiastic guidance of my work, as well as all the scientific input and advice he gave me. Furthermore, I very much appreciate that he offered me great opportunities to present the work at numerous congresses all over the world. Thank you for the pleasant working climate that made the development of this thesis not just possible, but a fulfilling and exciting time.

I want to thank Prof. Dr. Gerhard Winter for his dedicated leadership of the chair, his commitment to enable us these outstanding working conditions and numerous social activities, like skiing in winter, barbecue in summer and many more. Thank you a lot for the scientific and personal advice and taking over the co-referee.

Many thanks to all colleagues from research group Prof. Frieß and from research group Prof. Winter likewise who shared the time here in Munich with me, for support and numerous activities in daylight and night time. Special thanks to my direct lab-colleagues Matthias Ganz and Stefanie Schüle for the overall nice time we had together in our lab. Thanks also to my indirect lab neighbor Sandra Herrmann for the daily doorway chats. For all the support by taking over practical work, helping in the student lab and by literature supply, I want to thank our technical assistants Ingrid Hiltman, Imke Leitner and Patricia Settele.

I am indebted to Boehringer Ingelheim in Biberach for the general support of the work with material and the possibility to use their lab equipment. Special thanks to Dr. Karoline Bechtold-Peters who managed the delicate organization of the material and to Franz Nothelfer, who advised us in preparative chromatography.

I want to acknowledge the companies Schott AG for providing divers glass vials and Becton Dickinson GmbH for providing pre-filled syringes for my work.

Many thanks to Prof. Dr. Geoffrey Lee at the Department of Pharmaceutical Technology at the Friedrich-Alexander University of Erlangen-Nuernberg for the possibility to use the

modulating DSC, Prof. Dr. Udo Bakowsky from the Department of Pharmaceutical Technology and Biopharmaceutics at the Philipps University in Marburg for performing the AFM measurements and Dr. Stefan Wittmer from LOT Oriel in Darmstadt for performing the disc centrifugation experiments.

From the Department of Chemistry and Pharmacy of the LMU in Munich I want to thank Dr. Svetlana Mintova and Dr. Norbert Stock for taking the SEM pictures. Further, Wolfgang Wünschheim for his help with the powder diffractometer and Dr. Sascha Correll for analyzing my samples with the Low Temperature X-ray Diffractometer.

The student assistants Frank Schaubhut, Katja Schmid and Sarah Mikisch are acknowledged for the good job they have done. It was a pleasure to work with you.

Outside the university I want to thank my flat mates Andrea, Kerstin, Johanna and Seval for their ongoing friendship, Julia for the great time we had during studying and for all the advice. Katrin, some special thanks for your friendship over the last years.

My parents, my sister Martina, my brothers Simon and Benno and my grandmother, I want to thank for all the encouragement and support they gave me in all the years.

Finally, I want to thank Michael for being a great colleague here at the university and for all your help and for my work, especially the proof-reading of the thesis. Most important I want to thank you for your love.

For my parents

Table of Contents

Chapter 1

Introduction and Objectives of the Thesis

1.	INTRODUCTION	2
2.	FORMULATION OF HYDROPHOBIC PROTEINS	3
2.1	Hydrophobicity of Proteins	3
2.2	Hydrophobic Proteins used as Pharmaceuticals.....	4
2.3	Solubility of Hydrophobic Proteins	4
2.4	Protein Adsorption	6
3.	HUMAN SERUM ALBUMIN AS STABILIZER FOR PROTEINS	9
3.1	HSA as Excipient in Protein Formulation	11
3.2	Development of HSA-free formulations	13
3.2.1	Lyo- and Cryoprotection	14
3.2.2.	Protein Adsorption	14
3.2.3.	Protein Solubility.....	16
4.	CONCLUSIONS	17
5.	OBJECTIVES OF THE THESIS	18
6.	REFERENCES	18

Chapter 2

Characterization of Cytokine Solubility and Particle Formation in Presence of Human Serum Albumin

1.	INTRODUCTION	26
2.	MATERIALS AND METHODS	27
2.1	Materials	27
2.2	Methods	27
2.2.1	Turbidity Measurement	27
2.2.3	Light Obscuration.....	27
2.2.4	Dynamic Light Scattering (DLS)	28
2.2.5	Zetapotential.....	28
2.2.6	SDS-PAGE.....	28
2.2.7	Fluorescence Spectroscopy	28
2.2.8	Attenuated Total Reflection- FTIR Spectroscopy (ATR-FTIR).....	29
2.2.9	Atomic Force Microscopy (AFM).....	30
2.2.10	Disc centrifugation	30
3.	RESULTS AND DISCUSSION	31
3.1	Characterization of Cytokine-HSA Formulations at Different pH and Ionic Strength Conditions	31
3.1.1	Effect of pH and Salt on Turbidity	31
3.1.2	SDS-PAGE of the Precipitated Material	38
3.1.3	Fluorescence Spectroscopy of Cytokine-HSA Mixtures	39
3.1.4	Particle Size Analysis in Cytokine-HSA Formulations.....	42
3.2	Studies on HSA-placebo Formulations.....	49
3.2.1	Batch to Batch Variations of unstabilized-HSA.....	49
3.2.2	Impact of NaCl, Na-N-Acetyltryptophanate and Na-Octanoate on HSA.....	53
4.	CONCLUSIONS	56
5.	REFERENCES	57

Chapter 3

Physico-chemical Characterization of the Freezing Behavior of Mannitol-Human Serum Albumin Formulations

1.	INTRODUCTION	61
2.	MATERIAL AND METHODS	62
2.1	Materials	62
2.2	Methods	62
2.2.1	Differential Scanning Calorimetry (DSC)	62
2.2.2	Cryomicroscopy	63
2.2.3	Low Temperature X-ray Powder Diffraction (LTXRD)	63
3.	RESULTS AND DISCUSSION	64
3.1	DSC Studies of Stabilized-HSA and Mannitol	64
3.2	Impact of HSA-Quality on the Freezing-Behavior of Mannitol	65
3.3	Influence of the Applied Scanning Rate on Thermal Behavior of Mannitol-HSA Formulations	68
3.4	Influence of Na-Octanoate, Na-N-Acetyltryptophanate and NaCl on the Freezing Behavior of Mannitol	68
3.5	Influence of Na-Octanoate, Na-N-Acetyltryptophanate and NaCl on the Freezing Behavior of unstabilized-HSA and Mannitol	70
3.6	Influence of NaCl on Freezing Behavior of Mannitol with Stabilized-HSA	71
3.7	Determination of T _c with Cryomicroscopy	72
3.8	Analytics of the Mannitol Freezing Behavior with LTXRD	73
4.	CONCLUSIONS	74
5.	REFERENCES	75

Chapter 4

Physico-chemical Lyophilization Behavior of Mannitol-Human Serum Albumin Formulations

1.	INTRODUCTION	78
2.	MATERIALS AND METHODS	79
2.1	Materials	79
2.2	Methods	79
2.2.1	Lyophilization Process	79
2.2.2	X-ray Powder Diffraction (XRD).....	80
2.2.3	Differential Scanning Calorimetry (DSC)	80
2.2.4	Karl-Fischer Titration.....	80
2.2.5	Turbidimetry	80
2.2.6	High Pressure Size Exclusion Chromatography (HP-SEC)	81
3.	RESULTS AND DISCUSSION	82
3.1.	Lyophilization of the System Mannitol-HSA-NaCl	82
3.1.1	Drying Process	82
3.1.2	Residual Moisture Content.....	83
3.1.3	Morphology, Crystallinity and Thermal Properties of Lyophilized Products with Mannitol, Stabilized-HSA and NaCl	84
3.2.	Storage Stability of the Lyophilized Formulations.....	88
3.2.1	Changes in the Product Morphology Upon Storage	88
3.2.2	Stability of HSA during Storage.....	90
4.	CONCLUSIONS	94
5.	REFERENCES	95

Chapter 5

Impact of Freezing Procedure and Annealing on the Physico-chemical Properties and the Formation of Mannitol Hydrate in Mannitol-Sucrose-NaCl Formulations

1.	INTRODUCTION	98
2.	MATERIALS AND METHODS	99
2.1	Materials	99
2.2	Methods	99
2.2.1	Low Temperature X-ray Powder Diffraction (LTXRD)	99
2.2.2	Differential Scanning Calorimetry (DSC) of the Frozen Solutions.....	100
2.2.3	Lyophilization	100
2.2.4	Differential Scanning Calorimetry (DSC) of Lyophilized Products.....	101
2.2.5	Temperature-Modulated-DSC (TMDSC) of Lyophilized Samples.....	101
2.2.6	X-ray Powder Diffraction (XRD).....	101
2.2.7	Karl-Fischer Titration.....	101
3.	RESULTS AND DISCUSSION	102
3.1.	Impact of NaCl on the Physico-chemical Properties of Mannitol-Sucrose Formulations.....	102
3.1.1.	DSC of Mannitol-Sucrose-NaCl Formulations in the Frozen State.....	102
3.1.2.	DSC and XRD of Lyophilized Mannitol-Sucrose Formulations.....	105
3.1.3.	Impact of NaCl on Lyophilized Mannitol-Sucrose-Formulations	107
3.2.	Impact of Annealing on the Formation of Mannitol Hydrate	109
3.2.1.	LTXRD of Mannitol-Sucrose-Formulations at Different Annealing Conditions	109
3.2.2.	XRD of Lyophilized Samples Produced with Different Lyophilization Cycles.....	110
4.	CONCLUSIONS	113
5.	REFERENCES	114

Chapter 6

Development of Stable HSA-free Formulations for a Hydrophobic Cytokine

1.	INTRODUCTION	117
2.	MATERIALS AND METHODS	118
2.1	Materials	118
2.1.1	Proteins and Excipients	118
2.1.2	Containers.....	118
2.2	Methods	118
2.2.1	Turbidimetry	119
2.2.2	UV-Spectroscopy	120
2.2.3	High Pressure Size Exclusion Chromatography (HP-SEC)	120
2.2.4	Reversed Phase High Pressure Liquid Chromatography (RP-HPLC).....	121
2.2.5	Dynamic Light Scattering (DLS)	121
2.2.6	Attenuated Total Reflection-FTIR Spectroscopy (ATR-FTIR).....	122
2.2.7	Microcalorimetry.....	123
2.2.8	Lyophilization	123
2.2.9	Powder X-ray Diffraction (XRD).....	123
2.2.10	Karl-Fischer Titration.....	123
3.	RESULTS AND DISCUSSION	124
3.1	Impact of pH and Ionic Strength on Cytokine Aggregation	124
3.1.1	Turbidity and HP-SEC Studies.....	124
3.1.2	Dynamic Light Scattering (DLS)	127
3.2	Temperature Induced Changes of the Cytokine	130
3.2.1	FTIR-studies.....	131
3.2.2	Dynamic Light Scattering Studies.....	139
3.3	Cytokine Adsorption to Vials.....	141
3.3.1	Influence of pH, Glycine Concentration and Container Type on Cytokine Adsorption.....	142
3.3.2	Influence of Polysorbate 20 on Cytokine Adsorption	143
3.4	Short-time Cytokine Stability in Solution	145
3.4.1	Influence of pH on Cytokine Stability.....	145
3.4.2	Influence of Ionic Strength on Cytokine Stability	148
3.4.3	Influence of Excipients on Cytokine Stability	149

3.5	Freeze-Thaw Stability	151
3.6	Long-term Stability of Liquid and Lyophilized Formulations	153
3.6.1	Long-term Stability of Liquid Cytokine Formulations.....	155
3.6.2	Stability of Lyophilized Formulation	158
3.6.3	Comparison of Liquid and Lyophilized Formulation.....	164
4.	CONCLUSIONS	165
5.	REFERENCES	167

Chapter 7

Summary of the Thesis.....	171
----------------------------	-----

List of Abbreviations

ACN	Acetonitrile
AFM	Atomic Force Microscopy
ATR	Attenuated Total Reflection
BSA	Bovine Serum Albumin
DCM	Dichloromethane
DLS	Dynamic Light Scattering
DSC	Differential Scanning Calorimetry
FNU	Formazine Nephelometric Units
FTIR	Fourier Transformation Infrared Spectroscopy
HP-SEC	Size Exclusion High Pressure Liquid Chromatography
HSA	Human Serum Albumin
LTXRD	Low Temperature X-ray Powder Diffraction
Ph. Eur.	European Pharmacopoeia
pI	Isoelectric point
RP-HPLC	Reversed Phase High Pressure Liquid Chromatography
SDS	Sodium Dodecyl Sulfate
SEM	Scanning Electron Microscopy
T _c	Collapse Temperature
T _g	Glass Transition
T _g '	Glass Transition of the Maximally Freeze-Concentrated Solution
T _m	Denaturation Temperature or Melting Temperature
TMDSC	Temperature Modulated Differential Scanning Calorimetry
Trp	Tryptophane
XRD	X-ray Powder Diffraction

Chapter 1

Introduction and Objectives of the Thesis

Abstract

In the general introduction the formulation development for hydrophobic proteins is discussed. The low solubility of these proteins often combined with a strong tendency to adsorb on different materials during processing or storage are the major challenges during formulation development. Human Serum Albumin (HSA) is frequently used as excipient to overcome the mentioned problems. As HSA is gained from human plasma, its use is always related to the risk of blood born pathogens, as well as batch to batch variations. Furthermore, specific analytics for the active protein are difficult in presence of an excess of HSA. Therefore, ways need to be found to circumvent the use of HSA in protein formulations. Possible approaches for the development of HSA-free formulations for hydrophobic proteins are described in Chapter 1.

Keywords: hydrophobic proteins, solubility, adsorption, HSA

1. Introduction

With the first successful production of recombinant somatostatin, a peptide hormone consisting of 14 amino acids in 1977 [1] and shortly later the production of recombinant insulin [2] the starting point for the tremendous increase of biotechnological products on the pharmaceutical market was set. At about the same time it was accomplished to produce murine monoclonal [3] and later chimeric and humanized antibodies [4,5]. Approved by the FDA in 1982, human insulin was the first genetically engineered consumer health product on the market. Since then, numerous products including recombinantly produced antibodies, proteins and peptides have entered the market and currently about 225 are under development [6].

One critical step for the production of a protein as pharmaceutical product is the development of a stable formulation, as proteins are complex molecules which are susceptible for various degradation mechanisms and instability reactions [7,8]. It is a great challenge to maintain the native and functional structure of a protein during pharmaceutical processing, production, storage and the final application at the patient. The first step is getting insight into the characteristics of the particular protein and identifying possible instability reactions. To achieve this goal the development of analytical techniques which are capable to detect and quantify structural and activity relating changes in the protein is inevitable. In pre-formulation studies the basic knowledge on the protein is gained and the optimum conditions, concerning pH, buffer system, ionic strength and protein concentration have to be determined [9]. Based on this information the further development of a liquid or lyophilized formulation can proceed. Depending on the protein and the type of formulation the addition of excipients and stabilizers has to be evaluated. Thereby, it is a general concept to keep the formulation as simple as possible. The knowledge of the physico-chemical properties of the selected excipients during freezing and in the dried state if using a solid formulation is very important. To avoid failures in protein formulations, one has to be aware of the fact that the physico-chemical properties of excipients can affect protein stability and activity. Therefore, the focus must not be solely set on the protein alone, but on the formulation as a complex system. Protein formulation is an interesting and multifarious field that requires a structured but flexible procedure to achieve the desired goal of a stable formulation.

2. Formulation of Hydrophobic Proteins

2.1 Hydrophobicity of Proteins

Proteins are macromolecules consisting of forty to several hundreds L-amino acids connected via peptide bonds. Both, the size of the protein and the amino acid composition govern the characteristics of the particular protein e.g. folding, hydrophobicity and solubility. When a protein is folded in an aqueous environment about 80% of the hydrophobic amino acids are buried in the interior of the protein without having contact to the surrounding water molecules [10]. Various scales for the classification of amino acids according to their hydrophobicity are available. One example is the scale developed by Cowan and Whittaker (1990) using RP-HPLC which ranges from 0 to 1 (1=high hydrophobicity), with some examples shown in Table 1 [11].

Table 1: Amino acids and hydrophobicity value classified by Cowan and Whittaker (1990) [11].

amino acid	value
Alanine	0.660
Leucine	0.988
Isoleucine	1.000
Methionine	0.846
Tryptophane	0.914
Phenylalanine	0.983

Basically, the residues present on the surface of a protein affect the hydrophobicity of the protein. Each amino acid contributes to the measured surface hydrophobicity in relation to the protein structure as a whole and the composition of the residues on the protein surface [12]. Based on this assumption a more sophisticated classification of the hydrophobicity of amino acids was developed by Berggren et al. (2002), by studying the partitioning of proteins and peptides in an aqueous two-phase system. Generally, the classification of the hydrophobicity of amino acids strongly depends on the experimental setup and therefore the various scales often differ in the prediction of the hydrophobicity of the different amino acids [13]. A novel approach is the prediction of the average surface hydrophobicity of a protein by mathematical models which are based on the amino acid composition and the three-dimensional structure of the protein [14,15].

2.2 Hydrophobic Proteins used as Pharmaceuticals

Many proteins that are used as pharmaceuticals, e.g. interferons, interleukins or growth factors are considered as hydrophobic. The hydrophobicity of these proteins is further increased, when they are recombinantly produced in *Escherichia coli* (*E. coli*) as host cells, as glycosilation is not possible in *E. coli*. Human Interferon beta-1b (INF- β -1b) for example is glycosilated at a single site at Asn 80 at the end of helix C [16]. The lack of glycosilation in the recombinant human INF- β -1b (rHINF- β -1b), produced in *E. coli* increases the hydrophobicity of the protein, which is reflected in the retention time in RP-HPLC with a C18 column [17]. Two major issues that have to be overcome during formulation development for hydrophobic proteins are the low solubility and the adsorption of the active protein to surfaces, e.g. filters, tubes, pumps or primary packaging materials.

2.3 Solubility of Hydrophobic Proteins

The low solubility of hydrophobic proteins becomes an issue, when the target concentration for the formulation cannot be achieved. Already during preformulation studies the point of solubility needs to be addressed. For a protein it is not possible to determine one definite solubility value, as solubility is a function of pH, ionic strength and the presence of further excipients. Generally, solubility is lowest at the isoelectric point (pI) of a protein, due to the zero net charge of the molecules. Shaw et al. (2002) produced variants of ribonuclease Sa with isoelectric points from 4.6 to 10.2 (pI of the wild type: 3.5) by exchanging individual amino acids [18]. They showed that the minimum solubility of the variants lies within one pH unit around the pI and the solubility increases at higher and lower pH values [18]. Another example is insulin, with a maximum solubility below 0.1 mg/ml at its pI at pH 5.4, while the solubility is higher than 30 mg/ml at pH below 4.0 or above 7.0 [19]. Hydrophobic proteins often show a solubility below 1.0 mg/ml at physiological pH, e.g. 0.8 mg/ml for G-CSF [20] or 0.05 mg/ml for rhINF- β -1b [21].

The solubility of a protein needs to be tested as function of the pH, generally in the range of pH 3.0 to 10.0. However, at the acidic and alkaline end of the pH-range physical and chemical instability reactions are more likely to occur. Table 2 summarizes chemical instabilities that are characteristic for acidic and alkaline pH conditions.

Table 2: Chemical instability reactions of proteins at low and high pH [7,22].

acidic pH-range	alkaline pH-range
deamidation of asparagine and glutamine	deamidation of asparagine and glutamine via a cyclic imid or hydrolysis (pH 7-12)
oxidation of methionine (< pH 4)	oxidation of cysteine
proteolysis of aspartic acid (dilute acid)	β -elimination
cleavage of aspartic acid-X (very acidic)	shift of disulphide bonds

Chemical and physical instability reactions of proteins, as well as potential analytical techniques to determine these reactions are discussed extensively in literature for example in the reviews of Manning et al. (1989) [7], Wang (1999 and 2005) [22,23], Chi et al. (2003) [8] and Reubsaet et al. (1998) [24]. For the selection of the appropriate formulation pH a balance between sufficient solubility and stability has to be found.

Besides the selection of an optimum formulation pH, there are several approaches available to achieve the target concentration. The structural modification of a protein is one way to increase its solubility, with the conjugation with polyethylene glycol (PEG) being the most relevant method. Besides the low solubility, PEGylation can overcome several other problems related to the use of proteins as pharmaceuticals e.g. immunogenicity, susceptibility to enzymatic degradation, rapid kidney clearance and the related a short circulating half-live in vivo [25-27]. For the covalent conjugation PEG derivatives with activated functional groups are linked to reactive amino acids, e.g. lysine, cysteine, histidine, arginine, aspartic acid, glutamic acid, serine, treonine, tyrosine respectively the N-terminal amino group or the C-terminal carboxylic acid [28].

Another way to enhance protein solubility is the addition of excipients with surfactants, cyclodextrins, amino acids and salts being most effective. For parenteral protein formulations non-ionic surfactants, mostly polysorbate 20 and 80 are used. Besides the increase of solubility, surfactants can prevent adsorption of protein on surfaces and aggregation, which can be induced by the formation of interfaces e.g. during freeze-thawing or agitation [8]. Several mechanisms for the stabilizing effect of surfactants are postulated. One is that surfactants can directly bind to the protein surface, which was shown for example for human growth factor (hGH) [29,30]. The binding of surfactant to a protein can lead to a stabilization or destabilization depending on the protein. Additionally, the surface tension of a protein solution is lowered by surfactants and with it

the driving force for aggregation and adsorption is decreased [22]. Surfactants compete with proteins for the adsorption to surfaces, which leads to a stabilization of the protein, which was shown by Kreilgaard et al. (1998) for recombinant human factor XIII and polysorbate 20 [31]. Polysorbate 80 protected lactate dehydrogenase (LDH) from denaturation during freeze-thawing by hindering the interaction of LDH with ice and the amount of polysorbate 80 required for the protection correlated with the ice crystal surface area [32].

Cyclodextrins, which are cyclic oligosaccharides composed of six to eight dextrose units, can be used to enhance the solubility of proteins. For i.v. application chemically modified β -cyclodextrins, e.g. 2-hydroxypropyl- β -cyclodextrins (HPCD) were used to increase the solubility of Interleukin-2 (IL-2), ovine Growth Factor (O-GH) and Bovine Insulin [33]. Other examples are the use of cyclodextrins for a nasal formulation [34] or a parenteral formulation of Interferon- β [35]. Furthermore, cyclodextrins can reduce aggregation and precipitation of proteins, but on the other hand thermal degradation can be favored [36,37].

Protein solubility is further a function of the ionic strength and the used salt type. Salts, respectively anions and cations can be classified by their chaotrope effect (salting in), respectively cosmotrope (salting out) effect [38]. A stabilizing or salting out effect is achieved when macromolecules result in preferential hydration of the protein, whereas binding of salts to the protein surface often leads to a destabilizing, salting in effect [39,40]. In some cases, the solubility of a protein can be enhanced at its isoelectric points when low salt concentrations are added [41]. Especially in early developed formulations, HSA was frequently used to stabilize hydrophobic proteins used in low concentration, which is further discussed in section 3 of the introduction.

2.4 Protein Adsorption

Hydrophobic proteins, which are often used at low concentration, are susceptible to surface adsorption resulting in a reduced protein concentration in the final product. For recombinant human Interleukin-11 (rhIL-11), used at a concentration of 1 $\mu\text{g/ml}$ a reduction of activity by more than 40% after three hours at room temperature was caused by the adsorption of the protein on the glass container [42]. Adsorption can occur on all kinds of surfaces, e.g. filling equipment, tubes, filters or packaging materials. Especially during filtration processes, when the protein solution gets in contact with large filter surfaces the risk of protein adsorption is very high. Therefore, protein adsorption needs to be considered during production and formulation development. The selection of the container material can also impact the degree of protein adsorption. Schwarzenbach et al. (2002) demonstrated with atomic force microscopy (AFM) that the adhesion force

of Interferon- α -2a (INF α -2a) was reduced by 40% when using glass type I+, which has a specially treated surface instead of glass type I [43].

Norde (1995) reviewed the principles of protein adsorption on solid surfaces and described the different stages of the process [44]. The mechanism of adsorption is shown in Figure 1. Before a protein can adsorb to a surface, it needs to be transported to the surface (1). The basic mechanisms are diffusion and convective transport by laminar or turbulent flow. While the velocity of transport is increasing with protein concentration, the attachment of the protein to the surface is concentration independent. After binding to the surface (2) the protein can undergo structural reorientations (3). Adsorption is usually an irreversible process. However, desorption of protein (4) can be achieved by surface active ingredients [45]. Desorption of lysozyme from a polysulfone (PES) membrane with surfactants was shown by Kaplan et al. (2002) [46]. Finally the protein is transported away from the surface again by diffusion or convective transport (5).

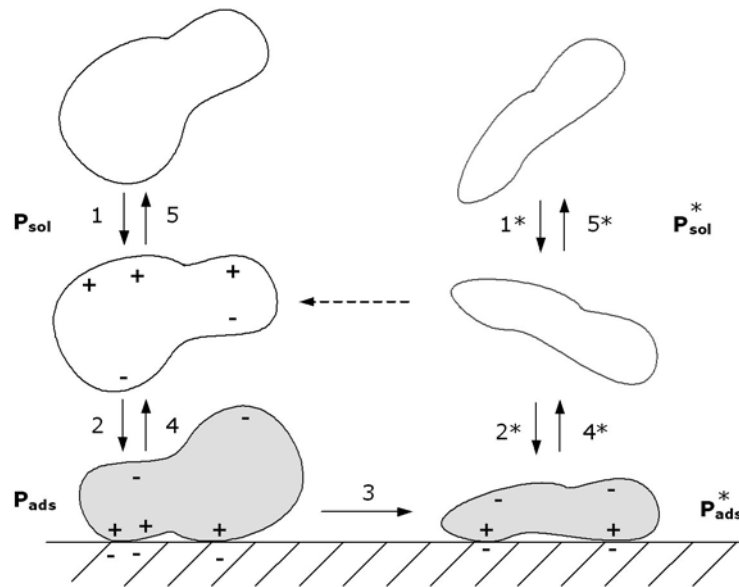


Figure 1: Protein adsorption mechanism of a protein on a surface. P_{sol} and P_{ads} are the native state of the protein in solution and after adsorption. P^* are structurally perturbed states of the protein [44].

Numerous factors can impact the kinetics and the degree of adsorption of the particular protein on surfaces, e.g. protein concentration, temperature, pH, ionic strength and the presence of further excipients [44,47,48]. The hydrophobic or hydrophilic properties of the surface further govern the adsorption process. Spontaneous adsorption can occur when the change in Gibbs Energy ($\Delta_{ads}g$) is negative, by a decrease in enthalpy ($\Delta_{ads}h$) or increase in entropy ($\Delta_{ads}s$) at a constant temperature as shown in equation (1) [46].

$$\Delta_{ads}g = \Delta_{ads}h - T\Delta_{ads}s \quad (1)$$

Generally, the adsorption process is driven by hydrophobic interactions and hydrogen bonding [49]. In addition, electrostatic interactions between charged surfaces and proteins, which are surrounded by counter ions to form electrical double layers, play an important role. The charged surface attraction occurs when protein and surface exhibit opposite charges. The electrical double layers can overlap and potential differences in net charge are balanced by the incorporation of counter ions between protein and surface [50]. The highest affinity of a protein to a surface is achieved, when the opposite charges of protein and surface result in a net charge of zero.

Adsorption is associated with a structural reorientation of the protein on the surface, which often leads to irreversible denaturation. Vermeer et al. (1998) identified an increase in α -helical structures from 0.0% to 17% and a decrease of β -sheet structure from 76% to 32% for a mouse monoclonal immunoglobulin (isotype 1) with circular dichroism (CD) after adsorption to Teflon particles [51]. In a formulation containing 0.05 to 0.2 mg/ml Interleukin-2 (IL-2) more than 97% of the initial activity was lost after 24 hours circulation in silicone rubber tubing, whereas only 20% to 30% of the activity loss can be attributed to adsorbed protein [52]. This indicates that activity loss is often more pronounced than the decline of the concentration after adsorption and associated with structural changes [52]. The tremendous activity loss is especially a problem when protein solutions are delivered via continuous infusions or when delivery devices e.g. micro pumps are applied. Tzannis et al. (1997) analyzed the time course of the adsorption process for IL-2 and found rapid adsorption after 10 minutes combined with a loss α -helical in favor of β -sheet structures. After five hours the residual concentration in solution decreased not significantly anymore. However, the adsorbed molecules undergo structural changes and the β -sheet structures disappear in favor of the original α -helix elements, as well as random structural elements [52]. Jørgensen et al. (1999) showed that already after 20 minutes the concentration of four peptide epidermal growth factor (EGF) receptor ligands was reduced to 33% to 73% on polyethylene, 15% to 46% on polystyrene and 12% to 29% on glass tubes due to adsorption [53].

Protein adsorption can be minimized by the addition of surfactants to the formulation. Zhang and Ferrari (1999) showed that Albumin adsorption onto silicon surfaces was reduced by polysorbate 20 [54]. Adsorption of three model proteins (hen egg white lysozyme, bovine serum albumin and ribonuclease A type IIA) onto different surfaces was reduced up to 30% by increasing the sugar concentrations, with trisaccharides being more effective than disaccharides and monosaccharides [48]. The addition of an excess of Human Serum Albumin to the active protein is another common approach to reduce the loss of the active protein due to adsorption.

3. Human Serum Albumin as Stabilizer for Proteins

Human Serum Albumin is the most abundant protein in human plasma, where it is the major transport protein for fatty acids, as well as for different metabolites, drugs and organic compounds. After synthesis in the liver the non-glycosylated HSA is exported into the blood, where it is present at a concentration of about 0.6 mM. HSA is composed of 585 amino acids and contains 17 disulphide bonds within each molecule. The dominating secondary structural elements are alpha-helices with about 67%. The heart-shaped structure consists of three repeating subdomains I-III, which contain two subdomains each [55]. Several binding sites in the different subdomains of HSA are characterized. The interaction of HSA with fatty acids and other components is extensively discussed in literature [56-58].

In the pharmaceutical field HSA is used as drug substance and as excipient for the stabilization of other proteins. Generally, HSA is extracted from human plasma and therefore implicates problems associated with human blood derived products like the risk of blood born pathogens and batch to batch variations. Figure 2 shows a scheme of the production process for commercial HSA.

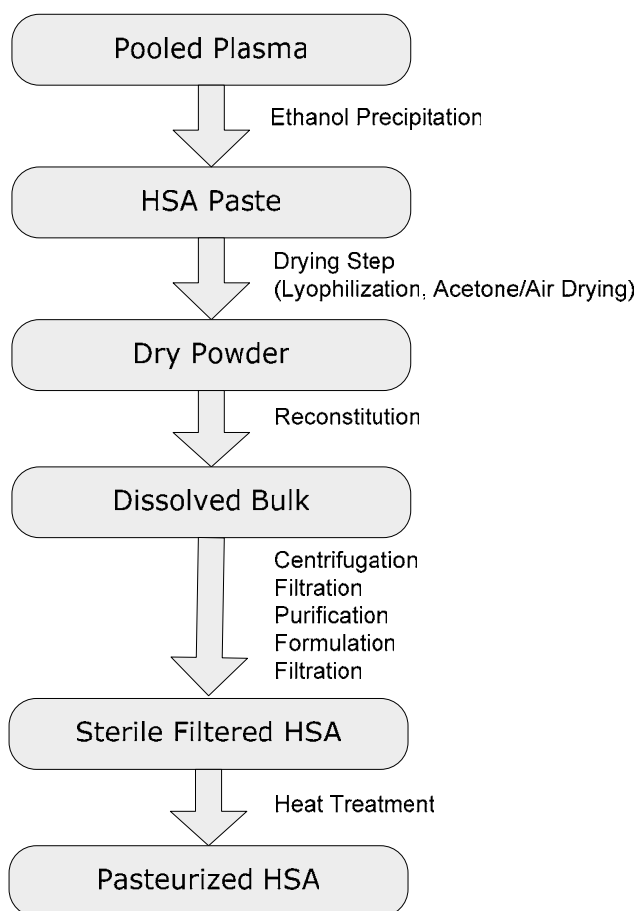


Figure 2: Scheme for commercial production of HSA out of human plasma [59].

HSA for the application as drug substance or stabilizers in protein formulations is gained from pooled human plasma using the Cohn fractionation process with HSA precipitating in the last fraction [60]. After precipitation a wet, crude HSA paste is obtained, which requires further drying and purification steps. A prerequisite for the use of HSA as drug substance or excipient is the terminal pasteurization process for 10 hours at 60°C to guarantee viral inactivation [61].

The pasteurization process imposes an extreme temperature stress for the protein, which leads to denaturation and aggregation if no further excipients are added. The melting temperature (T_m) can be used to estimate the thermal stability of a protein. Without stabilizers the melting temperature of HSA lies at 59.9°C at a formulation pH of 7.4 [62]. The sodium salt of caprylic acid and the sodium salt of the amino acid N-acetyltryptophanate are used to increase the thermal stability of HSA by increasing T_m [63,64]. Arakawa and Kita (2002) postulate that the increase in T_m by Na-caprylate cannot solely explain the stabilizing effect and they assume that Na-caprylate binds to the denatured form of HSA as well and thereby reduces the tendency of the molecules to aggregate [65]. Na-N-acetyltryptophanate on the other hand can diminish oxidation, by protecting the sulfhydryl groups of HSA [62]. The FDA specifies the addition of 0.08 mmol Na-caprylate or a combination of 0.08 mmol Na-caprylate and 0.08 mmol Na-N-acetyltryptophanate per gram HSA at a formulation pH of 6.9 together with 0.15 M NaCl [61].

In several approaches recombinant human albumin (rHA) was used to circumvent the mentioned problems of blood born pathogens and batch to batch variations. Tarelli et al. (1998) demonstrated that rHA had equal capacity to stabilize thyroid-stimulating hormone, Interleukin-15 and granulocyte colony-stimulating factor in lyophilized formulations as plasma derived HSA [66]. Matsushita et al. (2004) offered a functional analysis of rHA and of different sub domains for pharmaceutical applications [67]. Bosse et al. (2005) reported equivalent safety and pharmacodynamic behavior of rHA and plasma derived HSA in a double blind, randomized, phase I trial on 500 volunteers including three dose levels [68]. However, rHA is not routinely used in the field of protein formulation, due to the still high material costs.

3.1 HSA as Excipient in Protein Formulation

HSA is frequently used as stabilizer in liquid and lyophilized formulations, to prevent protein adsorption and to stabilize the active protein. Examples for commercial products that contain HSA as stabilizer are shown in Table 3.

Table 3: Examples for commercial protein formulations with HSA as excipient [69,70].

protein	products available
Antithrombin III	Atenativ® (lyophilized)
Botulinum neurotoxin complex	BOTOX® (lyophilized), BOTOX® COSMETIC (lyophilized)
Factor VIII	Fanhdi® (lyophilized), Haemate®HS (lyophilized), Monoclote-P® (lyophilized), Recombinate® (lyophilized), Kogenate® (lyophilized)
Immunoglobulins	Gammagard® S/D (lyophilized), Sandoglobulin® (lyophilized), BabyBIG® (lyophilized), CytoGam® (liquid), RespiGam (liquid), Zevalin™ (liquid)
Interferons alpha and beta	Avonex® (lyophilized), Alferon N Injection® (liquid), Betaseron® (lyophilized), Rebif® (liquid)
Modified human beta-glucocerebrosidase	Ceredase® (liquid)
Protein C	Ceprothin® (lyophilized)
Recombinant alpha-1-proteinase inhibitor	Aralast™ (lyophilized)
Streptokinase	Streptase® (lyophilized)
Urokinase	Abbokinase® (lyophilized)
Fibrinogen (human), thrombin	Crosseal™ (frozen solution)

For lyophilized formulations it is essential to add stabilizers that protect the active protein against freezing and drying associated stress. During freezing the low temperature, the formation of ice crystals, the increasing concentration of protein and excipients in the remaining amorphous phase, as well as possible phase separations and pH shifts are displaying stress for the protein. By the addition of cryoprotective excipients the active protein can be protected against freezing induced damages. Removal of the protein

hydration shell is the major issue during the drying process and lyoprotective excipients can be applied for stabilization.

An overview and explanation of the stabilization mechanisms of different excipients is given in the reviews of Wang (2000) [70] and Arakawa et al. (2001) [72]. The mechanism of preferential exclusion explains the stabilizing effect of many cryoprotectors [73]. After drying water substitute hypothesis [74] and glass dynamics hypothesis [75] are important stabilizing mechanisms not only for proteins. Sugars like trehalose or sucrose, which are amorphous after lyophilization and exhibit a high glass transition temperature, provide a good stabilization in the dried state. Recently, it was shown by Cicerone et al. (2003), that the addition of glycerol to trehalose increased protein stability although the glass transition temperature (T_g) was substantially lowered [76].

Human Serum Albumin can act as lyoprotector and cryoprotector during lyophilization and can further reduce the loss of active protein due to adsorption [71]. Anchordoquy and Carpenter (1996) showed that BSA is capable to stabilize Lactate Dehydrogenase (LDH) during lyophilization and prevent its activity by inhibiting the dissociation of the tetramer in the frozen state, as well as by preferential exclusion, whereby the stabilizing effect is increasing with BSA concentration [77].

Because of the unspecificity of protein adsorption on surfaces, the loss of the active protein can be minimized by the addition of an excess of a second protein e.g. HSA which saturates the binding sites of a surface. Dawson et al. (1992) describe that the use of 0.05% to 0.1% HSA inhibits protein adsorption and stabilizes different hydrophobic cytokines (Interleukins IL-1 α , IL-1 β , IL-3, macrophage colony-stimulating factor) during lyophilization [78]. The addition of 0.1% HSA to formulations of the peptides EGF and TGF- α can prevent absorption on polyethylene, polystyrene and glass tubes measured after 24 hours; while for HB-EGF and Betacellulin 0.1% HSA was not sufficient to prevent adsorption on glass [53].

Development of significant analytical tools to characterize the protein and its degradation products is a prerequisite for a successful formulation development. In formulation with HSA as stabilizer, the presence of a second protein often in a 10 to 50 fold surplus compared to the active protein makes specific analytics difficult. In spectroscopic and chromatographic methods the signal of the active protein is often superimposed and disturbed by HSA. To analyze the active protein next to HSA, specific methods like ELISA [79], selective precipitation [80], western-blot or BIACORE are applied.

Immunogenicity is often associated with the application of protein drugs. The most prominent example is the incidence of pure red cell aplasia (PRCA) caused by recombinant human erythropoietin formulations, which coincided with a formulation change in 1998. Here HSA was substituted by a combination of polysorbate 80 and glycine for the European market [81]. A controversial discussion on possible reasons for

PRCA aroused and two main theories emerged. With the change of the formulation the prefilled syringes were changed and uncoated rubber stoppers were used. Leachates from the stopper were made responsible for the immunogenicity reaction [82]. On the other Hermeling et al. (2003) showed that the presence of micelle-associated epoetin in the formulations can induce the formation of antibodies against epoetin [83]. The theory was rebutted by Villalobos et al. (2005) [84]. Structural changes, in particular aggregation is known to induce the risk of immunogenicity reactions in the patient [85]. HSA itself exhibits a low risk for immunogenicity, however in presence of a second protein the formation of mixed aggregates can lead to immunogenicity reactions. The formation of mixed aggregates was shown for rhINF α [86,87] and recombinant streptokinase [88].

3.2 Development of HSA-free Formulations

HSA is mostly used in low dose formulations of hydrophobic proteins, due to its solubilizing effect, its ability to reduce protein adsorption and its stabilizing properties. In the development of new protein formulations HSA is omitted as far as possible, because of the already discussed disadvantages related to its application. Furthermore, there is the trend to replace existing formulations which contain HSA as excipient by HSA-free formulations. For the replacement of HSA, alternative approaches need to be found which provide sufficient stabilization and solubilization of the protein. Furthermore, the loss of protein due to adsorption needs to be prevented. Several examples for the replacement of HSA are available on the market and in literature. In Eprex[®] (Epoetin- α) HSA was replaced by polysorbate 80 and glycine as excipients. For the HSA-free formulation of Avonex[®] (Interferon- β -1a) arginine and polysorbate 20 were employed. Ruiz et al. (2003) describe a preformulation study for the development of a HSA-free formulation for recombinant human Interferon- α -2b (rhINF- α -2b), where they achieved stable formulations by adding polysorbate 80, EDTA-Na₂ and PEG 400 [88]. In a lyophilized formulation of recombinant streptokinase, HSA was successfully replaced by glycine and sucrose in a formulation that further contained sodium glutamate and phosphate buffer at a pH of 7.4 [89]. For recombinant factor VIII SQ, the combination of NaCl as crystalline bulking agent with L-histidine and sucrose as amorphous stabilizers together with polysorbate 80 provided a stable lyophilized formulation without HSA [90]. From the described examples it is obvious that the use of non-ionic surfactants in combination with sugars and amino acids are common approaches for the development of HSA-free formulations.

3.2.1 Lyo- and Cryoprotection

In its function as lyo- and cryoprotector HSA can be replaced by sugars, e.g. sucrose, trehalose, sugar alcohols e.g. mannitol and amino acids e.g. glycine, histidine, arginine. Thereby, it is important to have sufficient amorphous excipient in the lyophilized product to stabilize the active protein, by formation of hydrogen bonds and/or providing a glassy matrix [91]. Mannitol as single component can be dried in rapid processes due to its high eutectic temperature and thereby forms elegant cakes. However, due to its tendency to crystallize it is often not able to provide sufficient stabilization for the active protein [92]. Here mixtures of mannitol with sucrose or trehalose, respectively glycine are possible alternatives [93,94]. For the lyophilization of these mixed systems it is important to select the optimum ratio of the excipients and to adjust the lyophilization process to obtain a high degree of crystallization of the bulking agent. A partially crystallized bulking agent can lead to stability problems, if crystallization occurs upon storage. During crystallization, hydrate water can be released leading to an increase in residual moisture of the lyophilized cake. Further the hydrogen bonds between excipient and protein, which are necessary to stabilize the protein, can no longer be preserved in the crystalline state [92].

3.2.2 Protein Adsorption

When formulating hydrophobic proteins without HSA protein adsorption needs to be prevented. A possible approach to overcome protein adsorption is the addition of sugars to the formulation. Uncharged sugars can be adsorbed to negatively charged surfaces and can so modify the surface forces. This was shown by Claesson et al. (1996) for the adsorption of sucrose to an aluminosilicate which reduced the double layer force [95]. However, surface changes by adsorbed sugar molecules were excluded as the prevalent mechanism, by which sugars can reduce protein adsorption since the described effect was observed for different proteins independent of the hydrophobic or hydrophilic properties of the particular surface [48]. Thus, it was concluded that preferential exclusion of the sugar from the protein surface can explain the effect of a reduced adsorption in the presence of sugar. Adsorbed, as well as denatured protein molecules exhibit a larger surface area as compared to the native state, which is thermodynamically unfavorable and leads to a shift of the equilibrium towards the native state.

An increase in ionic strength can also reduce protein adsorption. This was shown for human Apotransferrin, whose adsorption onto a silicon titanium dioxide surface at pH 8.0 could be significantly reduced by increasing the NaCl concentrations [96]. Ramsden and Prenosil (1994) ascribe the reduced adsorption to a lowering of the surface potential

which can lead to a higher repulsive energy barrier [96]. By increasing the ionic strength in the formulations the electrostatic interactions between the protein and the surface can be weakened. Greene et al. (2005) quantified the adsorption of IgG adsorption onto chemically modified PPE membranes of different charges. They determined a reduced adsorption of IgG upon the addition of NaCl independent of the charge of the surface and concluded that adsorption was driven by unspecific electrostatic interactions [97].

The degree of protein adsorption depends on formulation pH, as the pH strongly affects the charge of both the protein and in some cases also of the surface. Glass for example usually exhibits a negative charge in the pH-range feasible for protein formulations. Only in an extreme acidic environment far below pH 2.0 positively charged sites are present on the surface of glass [98]. Protein adsorption is typically most pronounced at the pI of the protein [96]. Maximum adsorption of Human Plasma Albumin was measured close to its pI at about pH 4.7 on polystyrene latex, silver iodide, polyoxymethylene, hematite and silica surfaces. As the highest adsorption was measured at the pI of Human Plasma Albumin independent of the materials, it was assumed the pH dependency of protein adsorption is rather due to the properties of the protein than to changed surface conditions at different pH values [99]. Especially for large proteins like ovalbumin and BSA the highest affinity to polystyrene was determined at their pI and Kondo and Higashitani (1992) concluded that hydrophobic interactions between the surface and the protein are most important [100]. On the other hand, high adsorption rates were also found when the protein and the surface exhibit opposite charges, which was shown for the IgG adsorption onto chemically modified PPE membranes of different charges [97].

A highly effective approach to prevent protein adsorption is the use of surfactants. Surfactants can reduce protein adsorption either by having an effect on the surface or by altering the solution properties. The hydrophobicity of a surfactant appeared to be most important for the reduction of Salmon Calcitonin (sCT) and BSA adsorption on glass, as polysorbate 20 was more effective than more hydrophilic poloxamer 188 or ionic surfactants [101]. Numerous other examples, describing the use of polysorbates to reduce adsorption are available in literature [54,101]. For example, the adsorption of HSA to polyethylene sheets was reduced by 35% to 40% when 0.05% polysorbate 20 was added to the formulations [54]. Surfactants can not only prevent protein adsorption. Already adsorbed protein can as well be desorbed from a surface upon the addition of surfactants. Feng et al. (1995) showed that polysorbate 20 removed about 40% of adsorbed HSA and 80% of adsorbed High Density Lipoproteins (HDL) from a polyethylene surface, while only a marginal desorbing effect was achieved for adsorbed IgG and fibrinogen under similar conditions [102].

Besides the addition of adsorption reducing excipients to the formulation, the issue of adsorption can be addressed by the selection of the materials which are employed during processing and storage. During processing especially filter materials, which provide large surfaces, are critical factors. For the final formulation, special containers with reduced susceptibility for adsorption like glass type I⁺ can be employed to minimize protein adsorption [43].

3.2.3 Protein Solubility

During the development of HSA-free formulations the low solubility of hydrophobic proteins can become a major problem. Especially at physiological pH, solubility often lies below 1.0 mg/ml, e.g. 0.8 mg/ml for G-CSF [20] or 0.05 mg/ml for rhINF- β -1b [21]. Protein solubility is a function of pH; however, the pH of optimum solubility not necessarily correlates with the pH of optimum stability. Rnase T1 shows the highest stability, determined by the free energy of unfolding ΔG (H₂O) at its isoelectric point at pH 4.0, at which the protein exhibits the lowest solubility [103]. Therefore, a compromise between adequate solubility and sufficient stability of the active protein needs to be found when selecting the formulation pH.

It was already described in 2.3 that protein solubility is a function of the ionic strength and the type of salt which is added to the formulation. As there is no general rule how solubility is influenced by the addition of salt, this point needs to be evaluated for the particular protein. Salts can stabilize proteins, which is for example described by Callahan et al. (2001) who showed that NaCl increased the thermal stability of brain derived neurotropic factor (BDNF) and thereby improved the shelf-life stability [104]. On the other hand, RNase A did not aggregate at pH 3.0 when exposed to 75°C for 24 hours, unless NaCl was added, which weakened the distinct charge-charge repulsions between the RNase A monomers that inhibited aggregation without NaCl [105]. Again, the addition of salt must not affect the stability of the active proteins.

Furthermore, the addition of surfactants can enhance protein solubility and stability. Surfactants can limit protein degradation during processes in which interfaces are created, e.g. liquid/air interfaces during filling, liquid/solid interfaces when ice crystals form during freezing or liquid/air interfaces during reconstitution of lyophilized cakes [106]. Surfactants accumulate at the particular interfaces, thus the protein concentration at the interface is reduced and the protein is protected from surface-induced denaturation [107]. For example polysorbate 80 successfully stabilized lactate dehydrogenase (LDH) during freeze-thawing [32]. For the development of HSA-free formulations a combination of various approaches can lead to a successful stabilization of the active protein.

4. Conclusions

Various approaches to overcome the issues of low solubility and the tendency to adsorb on surfaces arising during the formulation of hydrophobic proteins are available. HSA can be used to solve these problems as it is an excellent stabilizer and solubility enhancing excipient. However, its use is related with the concerns of blood born pathogens, batch to batch variations and immunogenicity when mixed aggregates are formed. Furthermore, the development of specific analytics for the active protein is often very demanding. By selecting optimum solution pH, ionic strength, excipients and container materials the solubility of a protein as well as its tendency to adsorb on surfaces can be influenced. In numerous cases the development of HSA-free formulations is feasible.

5. Objectives of the Thesis

The goal of the thesis was to analyze the impact of the formulation conditions on the stabilization of a hydrophobic cytokine. A standard way to formulate the cytokine at physiological pH is using HSA as excipient. Based on a lyophilized formulation with mannitol as bulking agent and HSA as stabilizer analogous to commercially available systems, our intention was to elucidate the impact of HSA-stabilizers, NaCl and pH on particle formation and stability of the cytokine in the liquid state (Chapter 2). In addition, we wanted to clarify the role of NaCl on the lyophilization behavior of the system HSA-mannitol. The goal was to understand how freezing, lyophilization and a subsequent storage of the formulations are influenced by NaCl and the HSA-stabilizers (Chapter 3 and 4). The use of HSA as excipient is related to the risk of blood born pathogens, enhanced immunogenicity, as well as to analytical difficulties. Therefore, the second major objective was to replace HSA in the cytokine formulation and to develop stable HSA-free formulations. For the lyophilized formulations HSA should be replaced by sucrose as amorphous stabilizer and the first studies focused on the physico-chemical properties of the system mannitol-sucrose during lyophilization (Chapter 5). To achieve a stable HSA-free formulation, cytokine adsorption and solubility needed to be addressed and optimal formulation conditions had to be found for a liquid as well as a lyophilized formulation (Chapter 6).

Thus, the main objectives of the thesis were:

1. Characterization of the HSA-containing formulation of the hydrophobic cytokine with focus on the impact of NaCl and pH on particle formation and protein stability (Chapter 2).
2. Characterization of the system HSA-mannitol during freezing and lyophilization with focus on the influence of NaCl and the HSA-stabilizers on the physico-chemical properties (Chapter 3 and 4).
3. Find the optimum formulation and lyophilization conditions for the system mannitol-sucrose to achieve a product of crystalline mannitol and amorphous sucrose, with a reduced content of mannitol hydrate (Chapter 5).
4. Develop a stable HSA-free formulation for the hydrophobic cytokine (Chapter 6).

6. References

1. K. Itakura, T. Hirose, R. Crea, A. D. Tiggs, D. Heyneker. Expression in *Escherichia coli* of a chemically synthesized gene for the hormone somatostatin. *Science* **198**:1056-1063 (1977).
2. D. V. Goeddel, D. G. Kleid, F. Bolivar, H. L. Heyneker, D. G. Yansura, R. Crea, T. Hirose, A. Kraszewski, K. Itakura, A. D. Riggs. Expression in *Escherichia coli* of chemically synthesized genes for human insulin. *Proc. Natl. Acad. of Sci.* **76**:106-110 (1979).
3. G. Kohler, C. Milstein. Continuous cultures of fused cells secreting antibody of predefined specificity. *Nature* **256**:495-497 (1975).
4. S. L. Morrison, M. J. Johnson, L. A. Herzenberg, V. T. Oi. Chimeric human antibody molecules: mouse antigen-binding domains with human constant region domains. *Proc. Natl. Acad. of Sci.* **81**:6851-6855 (1984).
5. P. T. Jones, P. H. Dear, J. Foote, M. S. Neuberger, G. Winter. Replacing the complementarity-determining regions in a human antibody with those from a mouse. *Nature* **321**:522-525 (1986).
6. "Medicines in Development: Biotechnology, survey 2006", available at <http://www.phrma.org/files/Biotech%202006.pdf> (2006).
7. M. C. Manning, K. Patel, R. T. Borchardt. Stability of Protein Pharmaceuticals. *Pharm. Res.* **6**:903-918 (1989).
8. E. Y. Chi, S. Krishnan, T. W. Randolph, J. F. Carpenter. Physical Stability of Proteins in Aqueous Solutions: Mechanisms and Driving Forces in Nonnative Protein Aggregation. *Pharm. Res.* **20**:1325-1336 (2003).
9. E. J. McNally, C. E. Lockwood. The Importance of a Thorough Preformulation Study. In "Protein formulation and Delivery" edited by E. J. McNally, Marcel Dekker Inc., p. 111-139 (2000).
10. J. A. Thomson, B. A. Shriley, G. R. Grimsley, C. N. Pace. Conformational Stability and Mechanism of folding of Ribonuclease T1. *J. Biol. Chem.* **264**:11614-11620 (1989).
11. R. Cowan, R. G. Whittaker. Hydrophobicity indexes for amino acid residues as determined by high-performance liquid chromatography. *Peptide Res.* **3**:75-80 (1990).
12. K. Berggren, A. Wolf, J. A. Asenjo, B. A. Andrews, F. Tjerneld. The surface exposed amino acid residues of monomeric proteins determine the partitioning in aqueous two-phase systems. *Biochim. Biophys. Acta* **1596**:253-268 (2002).
13. V. V. Nauchitel, R. L. Somorjai. Spatial and free energy distribution patterns of amino acid residues in water soluble proteins. *Biophys. Chem.* **51**:327-336 (1994).
14. S. Moelberg, E. Emberly, C. Tang. Correlation between sequence hydrophobicity and surface-exposure pattern of database proteins. *Protein Sci.* **13**:752-762 (2004).
15. J. C. Salgado, I. Rapaport, J. A. Asenjo. Is it possible to predict the average surface hydrophobicity of a protein using only its amino acid composition? *J. Chromat. A.* **1075**:133-143 (2005).
16. M. Karpusas, A. Whitty, L. Runkel, P. Hochman. The structure of human interferon- β : implications for activity. *Cell. Mol. Life Sci.* **54**:1203-1216 (1998).
17. J. Utsumi, S. Yamazaki, K. Hosoi, S. Kimura, K. Hanada, T. Shimazu, H. Shimizu. Characterization of *E. coli*-Derived Recombinant Human Interferon- β as Compared with Fibroblast Human Interferon- β . *J. Biochem.* **101**:1199-1208 (1987).
18. K. L. Shaw, G. B. Grimsley, G. I. Yakovlev, A. A. Makarov, C. N. Pace. The effect of net charge on the solubility, activity, and stability of ribonuclease Sa. *Protein Sci.* **10**:1206-1215 (2001).
19. M. J. Akers, M. R. DeFelippis. Peptides and Proteins as Parenteral Solutions. In: *Pharmaceutical Formulation Development of Peptides and Proteins* edited by S. Frokjaer and L. Hovgaard, The Taylor and Francis Series in Pharmaceutical Sciences (2000).

20. C. Gregg, O. Kinstler. Chemical modifications of granulocyte-colony stimulating factor (G-CSF) bioactivity. United States Patent, US 6,017,876 (2000).
21. L. S. Lin, M. G. Kunitani, M. S. Hora. Interferon- β -1b (Betaseron®); A Model for Hydrophobic Therapeutic Proteins. *Pharm. Biotechnol.* **9**:275-301 (1996).
22. W. Wang. Instability, stabilization and formulation of liquid protein pharmaceuticals. *Int. J. Pharm.* **185**:125-188 (1999).
23. W. Wang. Protein Aggregation and its inhibition in biopharmaceuticals. *Int. J. Pharm.* **289**:1-30 (2005).
24. J. L. E. Reubsaet, J. H. Beijnen, A. Bult, R. J. van Maanen, J. A. D. Marchal, W. J. M. Underberg. Analytical techniques used to study the degradation of proteins and peptides: chemical instability. *J. Pharm. Biom. Anal.* **17**:955-978 (1998).
25. Y. S. Wang, S. Youngster, M. Grace, J. Bausch, R. Bordens, D. F. Wyss. Structural and biological characterization of pegylated recombinant interferon alpha-2b and its therapeutic implications. *Adv. Drug Del. Rev.* **54**:547-570 (2002).
26. K. Rajender Reddy, M. W. Modi, S. Pedder. Use of peginterferon alfa-2 (40KD) (Pegasys®) for the treatment of hepatitis C. *Adv. Drug Delivery Rev.* **54**:571-586 (2002).
27. J. M. Harris, R. B. Chess. Effect of PEGylation on Pharmaceuticals. *Nature Rev.* **2**:214-221 (2002).
28. M. J. Roberts, M. D. Bentley, J. M. Harris. Chemistry for peptide and protein pegylation. *Adv. Drug Delivery Rev.* **54**:459-476 (2002).
29. M. Katakam, L. N. Bell, A. K. Banga. Effect of surfactant on the physical stability of recombinant human growth hormone. *J. Pharm. Sci.* **84**:713-716 (1995).
30. N. B. Bam, J. L. Cleland, J. Yang, M. C. Manning, J. F. Carpenter, R. F. Kelley, T. W. Randolph. Tween Protects Recombinant Human Growth Hormone against agitation-induced Damage via Hydrophobic Interactions. *J. Pharm. Sci.* **87**:1554-1559 (1998).
31. L. Kreilgaard, L. S. Jones, T. W. Randolph, S. Frokjaer, J. M. Flink, M. C. Manning, J. F. Carpenter. Effect of Tween 20 on Freeze-Thawing- and Agitation-Induced Aggregation of Recombinant Human Factor XIII. *J. Pharm. Sci.* **87**:1597-1559 (1998).
32. A. Hillgren, J. Lindgren, M. Aldén. Protection mechanism of Tween 80 during freeze-thawing of a model protein, LDH. *Int. J. Pharm.* **237**:57-69 (2002).
33. M. Brewster, M. Hora, J. Simpkins, N. Bodor. Use of 2-Hydroxypropyl- β -cyclodextrin as a Solubilizing and Stabilizing Excipient for Protein Drugs. *Pharm. Res.* **8**:792-795 (1991).
34. S. C. Quay, H. R. Costantino. Intranasal formulations of interferon beta free of stabilizers that are proteins or polypeptides. PCT Int. Appl. WO2005120551 (2005).
35. M. D. Del Curto. Stabilized interferon liquid formulations. PCT Int. Appl. WO20055058346 (2005).
36. A. Cooper. Effect of cyclodextrins on the thermal stability of globular proteins. *J. Am. Chem. Soc.* **114**:9208-9209 (1992).
37. S. Branchu, R. T. Forbes, P. York, H. Nyqvist. A central composite design to investigate the thermal stabilization of lysozyme. *Pharm. Res.* **16**:702-708 (1999).
38. Y. Koga, P. Westh, J. V. Davies, K. Miki, K. Nishikawa, H. Katayanagi. Toward Understanding the Hofmeister Series. 1. Effect of Sodium Salts of Some Anions on the Molecular Organization of H₂O. *J. Phys. Chem.* **108**:8533-8541 (2004).
39. T. Arakawa, S. N. Timasheff. Preferential Interactions of Proteins with Salts in Concentrated Solutions. *Biochem.* **21**:6545-6552 (1982).
40. T. Arakawa, S. N. Timasheff. Mechanism of Protein Salting In and Salting Out by Divalent Cation Salts: Balance between Hydration and Salt Binding. *Biochem.* **23**:5912-5923 (1984).
41. F. Rothstein. Differential precipitation of proteins: science and technology. *Bioprocess Technol.* **18**:115-208 (1994).

-
42. C. Page, P. Dawson, D. Woolacott, R. Thorpe, An. Mire-Sluis. Development of a Lyophilization Formulation that Preserves the Biological Activity of the Platelet-inducing Cytokine Interleukin-11 at Low Concentrations. *J. Pharm. Pharmacol.* **52**:19-26 (2000).
 43. M. S. Schwarzenbach, P. Reimann, V. Thommen, M. Hegner, M. Mumenthaler, J. Schwob, H. J. Güntherodt. Interferon α -2a interactions on Glass Vial Surfaces Measured by Atomic Force Microscopy. *PDA J. Pharm. Sci. Tech.*, **59**:78-89 (2002).
 44. W. Norde. Adsorption of Proteins at Solid-Liquid Interfaces. *Cells Mat.* **5**:97-112 (1995).
 45. W. Norde, F. MacRitchie, G. Nowicka, J. Lyklema. Protein adsorption at solid-liquid interfaces: reversibility and conformation aspects. *J. Coll. Interf. Sci.* **112**:447-456 (1986).
 46. M. C. Kaplan, A. Jégou, B. Chaufer, M. Rabiller-Baudry, M. C. Michalsky. Adsorption of lysozyme on membrane material and cleaning with non-ionic surfactant characterized through contact angle measurements. *Desalination* **146**:149-154 (2002).
 47. F. Y. Oliva, L. B. Avalle, O. R. Cámara, C. P. De Pauli. Adsorption of human serum albumin (HSA) onto colloidal TiO₂ particles, Part I. *J. Coll. Interf. Sci.* **261**:299-311 (2003).
 48. J. R. Wendorf, C. J. Radke, H. W. Blanch. Reduced Protein Adsorption at Solid Interfaces by Sugar Excipients. *Biotech. Bioeng.* **87**:565-573 (2004).
 49. L. Marchal-Heussler. Adsorption of Drugs. In: Encyclopedia of Surface and Colloidal Science, Marcel Dekker, New York; pp. 294-306 (2002).
 50. W. Norde, J. Lyklema. The adsorption of human plasma albumin and bovine pancreas ribonuclease at negatively charged polystyrene surfaces. IV: The charge distribution in the adsorbed state. *J. Coll. Interf. Sci.* **66**:285-294 (1978).
 51. A. W. P. Vermeer, M. G. E. G. Bremer, W. Norde. Structural Changes of IgG induced by heat treatment and by adsorption onto a hydrophobic Teflon surface studied by circular dichroism spectroscopy. *Biochim. Biophys. Acta.* **1425**:1-12 (1998).
 52. S. T. Tzannis, W. J. M. Hrushesky, P. A. Wood, T. M. Przybycien. Adsorption of a Formulated Protein on a Drug Delivery Device Surface. *J. Coll. Interf. Sci.* **189**:216-228 (1997).
 53. P. E. Jørgensen, L. Eskildsen, E. Nexø. Adsorption of EGF receptor ligands to test tubes – a factor with implications for studies on the potency of these peptides. *Scan. J. Clin. Lab. Invest.* **59**:191-198 (1999).
 54. M. Zhang, M. Ferrari. Reduction of Albumin Adsorption onto Silicon Surfaces by Tween 20. *Biotechnol. Bioeng.* **56**:618-625 (1999).
 55. X. M. He, D. C. Carter. Atomic structure and chemistry of human serum albumin. *Nature* **358**:209-215 (1992).
 56. J. A. Hamilton. Fatty acid interactions with proteins: what X-ray crystal and NMR solution structures tell us. *Prog. Lipid Res.* **43**:177-199 (2004).
 57. P. A. Zunszain, J. Ghuman, T. Komatsu, E. Tsuchida, S. Curry. Crystal structural analysis of human serum albumin complexed with hemin and fatty acid. *BMC Struct. Biol.* **3**:no pp given (2003).
 58. S. Curry, H. Mandelkow, P. Brick, N. Franks. Crystal structure of human serum albumin complexed with fatty acid reveals an asymmetric distribution of binding sites. *Nat. Struct. Biol.* **5**:827-835 (1998).
 59. J. J. Lin, J. D. Meyer, J. F. Carpenter, M. C. Manning. Stability of Human Serum Albumin During Bioprocessing: Denaturation and Aggregation During Processing of Albumin Paste. *Pharm. Res.* **17**:391-396 (2000).
 60. E. J. Cohn, L. E. Strong, W. L. Hughes Jr, D. J. Mulford, J. N. Ashworth, M. Melin, H. L. Taylor. Preparation and properties of serum and plasma proteins. IV. A system for the separation into fractions of the proteins and lipoprotein components of biological tissues and fluids. *J. Am. Chem. Soc.* **68**:459-475 (1946).
 61. U.S. Food and Drug Administration, Code of Federal Regulations, Title 21, Volume 7: §640.80 Albumin (Human), revised as on April 1 (2004).

62. M. Anraku, Y. Tsurusaki, H. Watanabe, T. Maruyama, U. Kragh-Hansen, M. Otagiri. Stabilizing mechanisms in commercial albumin preparations: octanoate and N-acetyl-L-tryptophanate protect human serum albumin against heat and oxidative stress. *Biochim. Biophys. Acta* **1702**:9-17 (2004).
63. G. Scatchard, L. E. Strong, W. L. Hughes Jr., J. N. Ashworth, A. H. Sparrow. Chemical, clinical, and immunological studies and the products of human plasma fractionation. XXVI. The properties of human serum albumin at low salt content. *J. Clin. Invest.* **24**:671-679 (1945).
64. G.A. Ballou, P.D. Boyer, J. M. Luck, G. F. Lum. The heat coagulation of human albumin. *J. Biol. Chem.* **153**:589-605 (1944).
65. T. Arakawa, Y. Kita. Stabilizing effect of caprylate and acetyltryptophanate on heat-induced aggregation of bovine serum albumin. *Biochim. Biophys. Acta*, **1479**:32-36 (2000).
66. E. Tarelli, A. Mire-Sluis, H. A. Tivnann, B. Bolgiano, D. T. Crane, C. Gee, X. Lemercinier, M. L. Althayde, N. Sutcliffe, P. H. Corran, B. Rafferty. Recombinant Human Albumin as a Stabilizer for Biological Materials and for the Preparation of International Reference Reagents. *Biologicals* **26**:331-346 (1998).
67. S. Matsushita, Y. Isima, V. T. G. Chuang, H. Watanabe, S. Tanase, T. Maruyama, M. Otagiri. Functional Analysis of Recombinant Human Serum Albumin Domains for Pharmaceutical Applications. *Pharm. Res.* **21**:1924-1932 (2004).
68. D. Bosse, M. Praus, P. Kiessling, L. Nyman, C. Andresen, J. Waters, F. Schindel. Phase I Comparability of Recombinant Human Albumin and Human Serum Albumin. *J. Clin. Pharmacol.* **45**:57-67 (2005).
69. Rote Liste 2005, Arzneimittelverzeichnis für Deutschland (einschließlich EU-Zulassungen und bestimmter Medizinprodukte). Bundesverband der Pharmazeutischen Industrie (BPI), Verband Forschender Arzneimittelhersteller (VFA).
70. B. S. Chang, S. Y. Patro. Freeze-drying Process Development for Protein Pharmaceuticals. In: Lyophilization of Biopharmaceuticals, editors H. R. Costantino, M. J. Pikal, AAPS Press Arlington (2004).
71. W. Wang. Lyophilization and Development of Solid Protein Pharmaceuticals. *Int. J. Pharm.* **203**:1-60 (2000).
72. T. Arakawa, S. J. Prestrelski, W. C. Kenney, J. F. Carpenter. Factors affecting short-term and long-term stability of proteins. *Adv. Drug Del. Rev.* **46**:307-326 (2001).
73. J. F. Carpenter, J. H. Crowe. The mechanism of cryoprotection of proteins by solutes. *Cryobiol.* **25**:244-255 (1988).
74. J. H. Crowe, J. F. Carpenter. An infrared spectroscopic study of the interactions of carbohydrates with dried protein. *Biochem.* **28**:3916-3922 (1989).
75. F. Franks, R. H. M. Hatley, S. F. Mathias. Materials science and the production of shelf-stable biologicals. *Bio. Pharm.* **4**:38, 40-2, 55 (1991).
76. M. T. Cicerone, A. Tellington, L. Trost, A. Sokolov. Substantially improved stability of biological agents in the dried form. *Bio. Proc. Int.* **1**:36-47 (2003).
77. T. J. Anchordoquy, J. F. Carpenter. Polymers Protect Lactate Dehydrogenase during Freeze-Drying by Inhibiting Dissociation in the Frozen State. *Arch. Biochem. Biophys.* **332**:231-238 (1996).
78. P. J. Dawson. Effect of formulation and freeze-drying on the long-term stability of rDNA-derived cytokines. *Dev. Biol. Stand.* **74**:273-82 (1992).
79. A. Braun, J. Alsenz. Development and Use of Enzyme-Linked Immunosorbent Assays (ELISA) for the Detection of Protein Aggregates in Interferon Alpha (INF α) Formulations. *Pharm. Res.* **14**:1394-1400 (1997).
80. J. D. Meyer, J. E. Matsuura, J. A. Ruth, E. Shefter, S. T. Patel, J. Bausch, E. Mc Gonigle, M. C. Manning. Selective Precipitation on Interleukin-4 Using Hydrophobic Ion Pairing: A Method For Improved Analysis of Proteins Formulated with Large Excesses of Human Serum Albumin. *Pharm. Res.* **11**:1492-1495 (1994).

81. A. Haselbeck. Epoetins: differences and their relevance to immunogenicity. *Cur. Med. Res. Opin.* **19**:430-432 (2003).
82. K. Boven, S. Stryker, J. Knight, A. Thomas, M. van Regenmortel, D. M. Kemeny, D. Power, J. Rossert, N. Casadevall. The increased incidence of pure red cell aplasia with an Eprex formulation in uncoated rubber stopper syringes. *Kidney Int.* **67**:2346-2353 (2005).
83. S. Hermeling, H. Schellekens, D. J. A. Crommelin, W. Jiskoot. Micelle-Associated Protein in Epoetin Formulations: A Risk Factor for Immunogenicity? *Pharm. Res.* **20**:1903-1907 (2003).
84. A. P. Villalobos, S. R. Gunturi, G. A. Heavner. Interaction of Polysorbate 80 with Erythropoietin: A Case Study in Protein-Surfactant Interactions. *Pharm. Res.* **22**:1186-1194 (2005).
85. S. Hermeling, D. J. A. Crommelin, H. Schellekens, W. Jiskoot. Structure-Immunogenicity Relationships of Therapeutic Proteins. *Pharm. Res.* **21**:897-903 (2004).
86. A. Braun, L. Kwee, M. A. Labow, J. Alsenz. Protein Aggregates Seem to Play a Key Role Among the Parameters Influencing the Antigenicity of Interferon Alpha (INF- α) in Normal and Transgenic Mice. *Pharm. Res.* **14**:1472-1478 (1997).
87. E. Hochuli. Interferon immunogenicity: technical evaluation of interferon- α 2a. *J. Interf. Cytokine Res.* **17**(Suppl. 1):15-21 (1997).
88. L. Ruiz, N. Reyes, L. Duany, A. Franco, K. Aroche, E. H. Rando. Long-term stabilization of recombinant human interferon α 2b in aqueous solution without serum albumin. *Int. J. Pharm.* **264**:57-72 (2003).
89. M. López, L. R. González, N. Reyes, J. Sotolongo, V. Pujol, K. Aroche Tech. Stabilization of a freeze-dried recombinant streptokinase formulation without serum albumin. *J. Clin. Pharm. Therap.* **29**:367-373 (2004).
90. T. Österberg, A. Fatouros, M. Mikaelsson. Development of a Freeze-Dried Albumin-Free Formulation of Recombinant Factor VIII SQ. *Pharm. Res.* **14**:892-898 (1997).
91. L. Chang, D. Shepard, J. Sun, D. Ouelette, K. L. Grant, X. Tang, M. J. Pikal. Mechanism of Protein Stabilization by Sugars During Freeze-Drying and Storage: Native Structure Preservation, Specific Interaction, and/or Immobilization in a Glassy Matrix. *J. Pharm. Sci.* **94**:1427-1444 (2005).
92. K. Izutsu, S. Kojima. Excipient crystallinity and its protein-structure stabilizing effect during freeze-drying. *J. Pharm. Pharmacol.* **54**:1033-1039 (2002).
93. R. Johnson, C. Kirchhoff, H. Gaud. Mannitol-Sucrose Mixtures-Versatile Formulations for Protein Lyophilization. *J. Pharm. Sci.* **91**:914-922 (2002).
94. W. Lei, D. Q. Wang, S. L. Nail. Freeze-Drying of Proteins from a Sucrose-Glycine Excipient System: Effect of Formulation Composition on the Initial Recovery of Protein Activity. *AAPS Pharm. Sci. Tech.* **6**:150-157 (2005).
95. P. M. Claesson, H. K. Christenson, J. M. Berg, R. D. Neuman. Interaction between Mica Surfaces in the Presence of Carbohydrates. *J. Coll. Interf. Sci.* **172**:415-424 (1995).
96. J. J. Ramsden, J. E. Prenosil. Effect of Ionic Strength on Protein Adsorption Kinetics. *J. Phys. Chem.* **98**:5376-5381 (1994).
97. G. Greene, H. Radhakrishna, R. Tannenbaum. Protein binding properties of surface-modified porous polyethylene membranes. *Biomat.* **26**:5972-5982 (2005).
98. S. Sjöberg. Silica in aqueous environment. *J. Non-Cryst. Sol.* **196**:51-57 (1996).
99. W. Norde, F. MacRitchie, G. Nowicka, J. Lyklema. Protein Adsorption at Solid-Liquid interfaces: Reversibility and Confirmation Aspects. *J. Coll. Interf. Sci.* **112**:447-456 (1985).
100. A. Kondo, K. Higashitani. Adsorption of model proteins with wide variation in molecular properties on colloidal particles. *J. Coll. Interf. Sci.* **150**:344-351 (1992).
101. M. R. Duncan, J. M. Lee, M. P. Warchol. Influence of surfactants upon protein/peptide adsorption to glass and polypropylene. *Int. J. Pharm.* **120**:179-88 (1995).

102. M. Feng, A. B. Morales, A. Poot, T. Beugeling, A. Bantjes. Effects of Tween 20 on the desorption of proteins from polymer surfaces. *J. Biom. Sci. Polymer Edition* **7**:415-425 (1995).
103. C. N. Pace, D. V. Laurents. RNase A and T1: pH dependence and folding. *Biochem.* **29**:2520-2525 (1990).
104. W. J. Callahan, L. O. Narhi, A. A. Kosky, M. J. Treuheit. Sodium Chloride Enhances the Storage and Conformational Stability of BDNF and PEG-BDNF. *Pharm. Res.* **18**:261-266 (2001).
105. A. M. Tsai, J. H. van Zanten, M. J. Betenbaugh. II. Electrostatic Effect in the Aggregation of Heat Denatured RNase A and Implications for Protein Additive Design. *Biotechnol. Bioeng.* **59**:281-285 (1998).
106. T. W. Randolph, L. S. Jones. Surfactant-protein interactions. *Pharm. Biotechnol.* **13**:159-175 (2002).
107. P. A. Gunning, A. R. Mackie, A. P. Gunning, N. C. Woodward, P. J. Wilde, V. J. Morris. Effect of Surfactant Type on Surfactant-Protein Interactions at the Air-Water Interface. *Biomacromol.* **5**:984-991 (2004).

Chapter 2

Characterization of Cytokine Solubility and Particle Formation in Presences of Human Serum Albumin

Abstract

The impact of pH and NaCl content on particle formation and solubility of the hydrophobic cytokine in a formulation with Human Serum Albumin (HSA) and mannitol as excipients was studied. A tremendous increase in turbidity at pH 5.0, close to the isoelectric point of HSA was observed. Dynamic light scattering (DLS), disc centrifugation, Atomic Force Microscopy (AFM) and light obscuration were used to characterize the turbidity causing particle formation process in the formulations. Here the high turbidity values mainly could be ascribed to particles of 500 to 1000 nm in size. SDS-PAGE showed that most of the cytokine precipitated at pH 5.0. As HSA used in the formulation further contained Na-octanoate and Na-N-acetyltryptophane, the impact of these stabilizers on unstabilized-HSA was evaluated. It could be shown that Na-octanoate and Na-N-acetyltryptophane were less effective in preventing the turbidity increase of unstabilized-HSA compared to NaCl. The HSA-cytokine precipitation at pH 5.0 was partially irreversible when the pH was re-adjusted to 7.0. Furthermore, the interactions between HSA and cytokine were weakened by NaCl, as determined by fluorescence spectroscopy. The positive effect of NaCl on the formulation could be attributed to a direct stabilization of HSA, which in consequence provided an overall stabilization of the cytokine.

Keywords: human serum albumin, cytokine, pH, NaCl, particle formation

1. Introduction

When formulating the hydrophobic cytokine especially the problems of aggregation and adsorption on containers due to its low solubility need to be overcome. At physiological pH the solubility of the cytokine is less than 0.05 mg/ml [1]. One possible approach for a formulation at physiological pH is the use of Human Serum Albumin (HSA) as stabilizing excipient. Chapter 1 provides a comprehensive discussion on the use of HSA as excipient for protein formulations. Generally, HSA is extracted from human plasma and therefore implicates problems associated with human blood derived products like the risk of blood born pathogens and batch to batch variations. According to the US Food and Drug Administration, HSA has to undergo pasteurization for ten hours at temperatures of 60°C at the end of various processing and purification steps [2]. As stabilizing excipients against heat induced stress Na-octanoate [3] and the amino acid derivative Na-N-acetyltryptophanate [4] are added. HSA is in addition stabilized by NaCl, which can inhibit the heat-induced aggregation of HSA [5]. NaCl and the other HSA-stabilizers brought into the formulations indirectly via HSA may induce problems, e.g. for proteins which are sensitive to ionic strength. Furthermore, they may impact the physico-chemical properties of other excipients, e.g. crystallization behavior or glass transitions which is critical in lyophilized formulations. The impact of the HSA-stabilizers on the physico-chemical properties of formulations with HSA and mannitol during freezing and lyophilization is outlined in Chapter 3 and 4. For formulations with HSA limited analytical methods are available, because HSA, which is often employed in a 10 to 50-fold excess, interferes with many analytical methods for the active protein.

In this study the hydrophobic model cytokine is used as a lyophilized formulation in combination with stabilized-HSA and mannitol as excipients in analogy to commercially available products. To estimate the role of different stabilizers on HSA, studies with different HSA-types were conducted, as well. The goal was to characterize the physical stability with special focus on aggregation in HSA-cytokine formulations under different pH and ionic strength conditions. To get comprehensive insight into the aggregation phenomena, various methods were used e.g. turbidimetry, DLS, disc centrifugation, AFM and light obscuration. We further wanted to analyze possible interactions between the hydrophobic cytokine and HSA by using fluorescence spectroscopy to understand the properties of the cytokine-HSA formulation under different pH and ionic strength conditions.

2. Materials and Methods

2.1 Materials

A lyophilized formulation with 0.25 mg/ml cytokine, 12.5 mg/ml mannitol and 12.5 mg/ml stabilized-HSA in analogy to commercially available formulations was used. This formulation further contained between 0.08% and 0.1% NaCl, deriving from HSA and from pH-adjustment. Unstabilized-HSA (Fraction V, 96% to 99% purity) from Sigma-Chemicals (Steinheim, Germany) was solid and contained no further excipients. Four different batches (072K7600, 072K7601, 033K7600, 033K7601) were used without further purification. Stabilized-HSA from Grifols (Langen, Germany) was used as 20% solution and contained 16 mmol Na-octanoate, 16 mmol Na-N-acetyltryptophanate, 130 to 160 mmol/l sodium and max 2 mmol/l potassium. As HSA-free cytokine material a bulk with 1.2 mg/ml cytokine in 20 mM glycine at pH 3.0 was employed. The production of this HSA-free cytokine bulk material is described in Chapter 6. NaCl, Na-octanoate and N-Acetyl-DL-tryptophanate were purchased from Sigma (Steinheim, Germany). KCl, LiCl, NaCH₃COO, NH₄Cl, KSCN and KI were purchased from Merck (Darmstadt, Germany). All salts were of reagent grade and used without further purification.

2.2 Methods

2.2.1 Turbidity Measurement

Turbidity measurement was performed with a NEPHLA turbidimeter (Dr. Lange, Düsseldorf, Germany). Light ($\lambda=860\text{nm}$) was sent through the samples and the scattered light was measured at 90° angle. The system was calibrated with formazine as standard and the results were given in formazine nephelometric units (FNU).

2.2.2 Light Obscuration

Particles $\geq 1\text{ }\mu\text{m}$ were determined by light obscuration measurement using PAMAS – SVSS-C Sensor HCB-LD-25/25 (Partikelmess- und Analysensysteme GmbH, Rutesheim, Germany). Five aliquots of 0.3 ml were analyzed of each sample.

2.2.3 Dynamic Light Scattering (DLS)

DLS, performed on a Zetasizer Nano (Malvern, Herrenberg, Germany) was used to characterize protein molecules and particles in the range from 1 to 1500 nm. The Zetasizer Nano is operating with a 4 mW He-Ne-Laser at 633 nm and non invasive back-scatter technique (NIBS). The size distribution by intensity and volume was calculated from the correlation function using the multiple narrow mode of the Dispersion Technology Software from Malvern (version 4.00).

2.2.4 Zetapotential

The zetapotential was determined with the Zetasizer Nano (Malvern, Herrenberg, Germany). The measurements were performed in the automatic measurement mode using disposable capillary cells (Malvern DTS 1060).

2.2.5 SDS-PAGE

Non-reducing denaturing SDS-PAGE was used to analyze formulations containing HSA and the cytokine. NuPAGE[®] 10% and 12% Bis-Tris gels 1 mm, 10 wells (Invitrogen, Karlsruhe, Germany) and NuPAGE[®] MOPS running buffer was used for the separation. The electrophoresis was performed at a constant current of 0.03 A per gel. NuPAGE[®] LDS sample buffer was added to the samples, which were denatured for 10 minutes at 95°C. 20 µl of the solution were loaded to each well. The amount of protein per well ranged between 0.1 to 0.3 µg cytokine, 5 to 15 µg HSA, or 1 to 5 µg HSA when analyzed as single component. The gels were stained with SilverXPress[®] Silver Staining Kit, respectively Colloidal Blue Staining Kit (Invitrogen, Karlsruhe, Germany).

2.2.6 Fluorescence Spectroscopy

Fluorescence spectroscopy was performed using a Varian Cary Eclipse (Darmstadt, Germany). The impact of pH on the fluorescence of cytokine, HSA and a combination was studied. HSA was used in a constant concentration of 0.5 mg/ml, while the cytokine concentration was varied. HSA-cytokine interactions were studied at pH 3.0 and pH 4.5 with 0.0% and 0.1% NaCl, all buffered with 2 mM glycine. For the first studies the solutions were measured in 3.0 ml cuvettes at a constant temperature of 20°C with an excitation wavelength of 280 nm at an excitation slit of 5 nm. The emission was recorded from 260 to 450 nm at an emission slit of 5 nm and a scanning rate of 120 nm/sec. The PMT voltage of the detector was set to 400 V. To study protein-protein interactions

300 µl of the samples were analyzed in 96-well plates at a constant temperature of 20°C. Excitation wavelength was 280 nm at an excitation slit of 5 nm and emission was recorded from 260 to 450 nm at an emission slit of 5 nm and a scanning rate of 30 nm/second. The PMT voltage of the detector was set to 600 V.

Fluorescence quenching was monitored to evaluate the degree of HSA-cytokine interaction. Therefore, the fluorescence of the individual components, as well as of the combination was analyzed for the respective conditions. The degree of interaction was determined using equation (1). A high value for F_0/F can be attributed to stronger interactions between the two proteins [6].

$$\text{Degree of interaction} = F_0/F \quad (1)$$

F_0 = calculated sum of the fluorescence intensity (290 to 450nm) of the individual proteins

F = measured fluorescence intensity (290 to 450 nm) of solution containing both proteins

2.2.7 Attenuated Total Reflection- FTIR Spectroscopy (ATR-FTIR)

FTIR spectroscopy was performed on a Tensor 27 (Bruker Optics, Ettlingen, Germany) using the Bio-ATR unit. The spectra were recorded from 4000 to 850 cm^{-1} wavenumbers in attenuated total reflectance (ATR) mode at 20°C. Each measurement was the average of 240 scans. After analysis, the particular buffer spectrum was subtracted from the protein spectrum. The spectra were further processed by an off-set correction, forming the second derivative and vector normalization. The structural similarity between the second derivatives of the spectra was calculated via a spectral correlation coefficient r according to equation (2) [7,8].

$$r = \frac{\sum (x_i - x^*) (y_i - y^*)}{\left[\sum (x_i - x^*)^2 \sum (y_i - y^*)^2 \right]^{1/2}} \quad (2)$$

x_i and y_i are the corresponding peak intensities of various wave numbers i (second derivative of amide band I from 1700 to 1600 cm^{-1}) in reference (x) and sample spectra (y). x^* and y^* are the average intensities of reference and sample spectra from 1700 to 1600 cm^{-1} .

2.2.8 Atomic Force Microscopy (AFM)

AFM was conducted by Prof. Dr. U. Bakowsky at the Department of Pharmaceutical Technology and Biopharmaceutics at the Philipps University, Marburg with a Nanoscope VI Dimension Bioscope (Veeco Instruments, Santa Barbara, US). As imaging technique the tapping mode in air was used. Interactions between the sample and the tip were below 300 pN. Type I cantilevers with a nominal spring constant of 36 nN/nm were applied. The scanning speed was adjusted to the respective scanned area and ranged between 0.25 and 2 Hz at a resolution of 512 * 512 pixels, independent of width of the scanned area. All experiments were performed under atmospheric pressure at 25°C / 60% RH.

2.2.9 Disc centrifugation

The CPS disc centrifugation system (LOT-Oriel GmbH, Darmstadt, Germany) was used to determine the size distribution of the particles in the range of 20 nm to 2 µm. The measurements were performed by Dr. Stefan Wittmer, LOT Oriel Darmstadt. 200 µl of the protein solution was applied on the disc, which was rotating with 22000 to 24000 rpm. A density gradient from 7% to 2% sucrose was built up within the disc. At the edge of the disc the particles were detected with a light source of 470 nm. The time required for the particles to reach the edge of the disc, as well as the absorption signal were transformed to a particle size distribution, using Stokes-Law and Mie-theory.

3. Results and Discussion

3.1 Characterization of Cytokine-HSA Formulations at Different pH and Ionic Strength Conditions

3.1.1 Effect of pH and Salt on Turbidity

An elevated turbidity can be a sign for the presence of larger aggregates and precipitated material within a formulation. Figure 1 shows the turbidity and the particles larger than 1 μm for a formulation with 0.25 mg/ml cytokine, 12.5 mg/ml stabilized-HSA and 12.5 mg/ml mannitol. At pH 7.4 a turbidity of 6 FNU was measured. When the pH of the formulations was lowered the turbidity increased sharply and reached a maximum of about 100 FNU at pH 5.0. Furthermore, light obscuration showed that the number of particles, in particular the particles of 1 to 2 μm in size (compare 3.1.4, Figure 16), increased significantly when the pH was lowered to 5.0. The correlation between the data from light obscuration with the turbidity data was in agreement with literature [9].

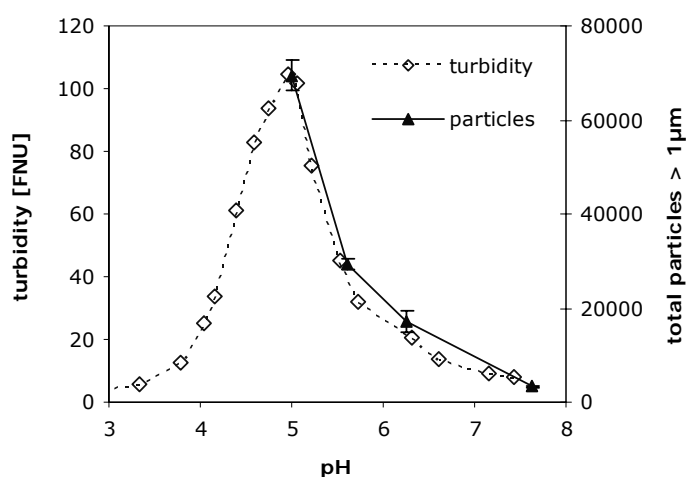


Figure 1: Turbidity and total number of particles larger 1 μm determined by light obscuration of 0.25 mg/ml cytokine, 12.5 mg/ml stabilized-HSA and 12.5 mg/ml mannitol between pH 3.0 and 7.4.

Since turbidity measurement offered the advantage of being less time- and material consuming the technique was used as a characterization tool in the subsequent study.

A possible explanation for the increased turbidity and protein precipitation at pH 5.0 could be found when the isoelectric points (pI) of the proteins were considered. For the cytokine the pI, at which it shows the lowest solubility, is located at pH 9.2 [10]. For HSA a pI between 4.8 and 4.9 is described [11]. The turbidity maximum at pH 5.0 was close to the isoelectric point of HSA. At its pI, protein-protein interactions are favored due to a reduced interaction energy barrier, which can lead to aggregation [12]. Consequently,

Saso et al. (1998) described, that HSA showed that highest level of heat-induced aggregates in the pH range of 4.5 to 5.0 [5]. For the cytokine-HSA formulation the turbidity increase at pH 5.0 pointed to either a precipitation of HSA itself or a combination of HSA-cytokine. Furthermore, it could be possible that HSA was no longer capable to provide sufficient stabilization of the formulation, leading to a precipitation of the cytokine.

NaCl is known to stabilize HSA against heat-induced aggregation [5] by increasing the melting temperature (T_m) [13]. As an increase in ionic strength can further impact the solubility of proteins, the turbidity of the formulation with 0.25 mg/ml cytokine, 12.5 mg/ml stabilized-HSA and 12.5 mg/ml mannitol was studied from pH 7.4 to 3.0 upon the addition of NaCl (Figure 2).

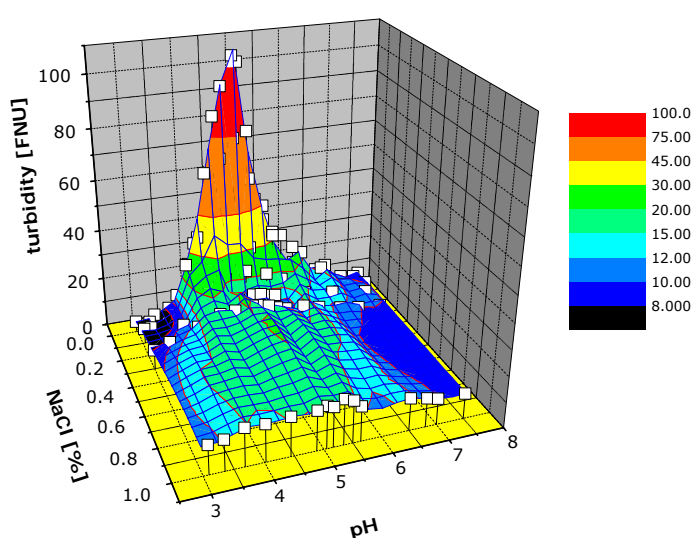


Figure 2: Turbidity of 0.25 mg/ml cytokine, 12.5 mg/ml stabilized-HSA and 12.5 mg/ml mannitol with 0.0% to 0.3% NaCl from pH 7.4 to 3.0.

It was obvious that the addition of NaCl could significantly reduce the turbidity increase at pH 5.0, indicating a stabilizing effect of NaCl on the formulations. For NaCl concentrations between 0.2% and 0.9% turbidity at pH 5.0 reached a plateau phase of about 20 FNU. This wide plateau phase pointed at a rather unspecific stabilizing effect of NaCl, probably induced by electrostatic effects. At pH 7.4, the turbidity was slightly lower without NaCl, which required further investigations.

To evaluate whether the turbidity preventing effect was specific for NaCl, the influence of various salts on the turbidity of the cytokine-HSA formulation was evaluated. It is generally difficult to predict the direct effect of salts on protein stability, as it is influenced by various factors, e.g. type of protein, pH, ionic strength, mechanism of

interaction [12]. Anions and cations can be classified by their chaotrope effect (salting in), respectively cosmotrope (salting out) effect as shown in Figure 3.

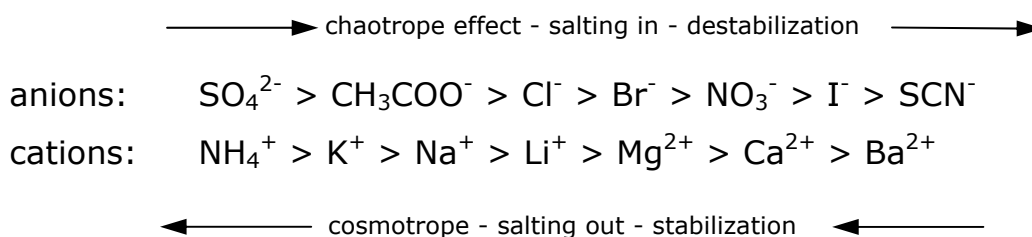


Figure 3: Classification of anions and cations according to their chaotrope, respectively cosmotrope properties [14].

A stabilizing or salting out effect is achieved when the addition of salt leads to a preferential hydration of the protein, whereas binding of salts to the protein often yields a destabilizing, salting in effect [15,16]. Low concentrations of salts usually increase the solubility of proteins by non-specific electrostatic interactions. Different salts (KCl, LiCl, NaCH_3COO , NH_4Cl , KI, and KSCN) were added to the formulation of 0.25 mg/ml cytokine, 12.5 mg/ml HSA and 12.5 mg/ml mannitol at a concentration to provide an ionic strength of $\mu=0.009$ or $\mu=0.034$. Table 1 summarizes the turbidity maxima measured for the different salts at ionic strength of $\mu=0.009$ and $\mu=0.034$. The resulting turbidity maxima were located at pH 5.0 for all studied conditions. The exception was KSCN at an ionic strength of $\mu=0.034$ where the maximum turbidity was shifted to pH 4.0. Without the addition of salt a maximum turbidity of about 100 FNU was measured at pH 5.0. All tested salts led to a decline of the maximum turbidity at pH 5.0. It was evident that the more chaotrope salts KSCN and KI were less effective in preventing the turbidity increase at pH 5.0. When used at the lower ionic strength NaCl and KCl were superior to the other salts in preventing the turbidity increase at pH 5.0. When increasing the ionic strength to 0.034 NaCl, KCl, LiCl, NaCH_3COO and NH_4Cl all reached comparable values of about 19 to 21 FNU at pH 5.0. The cation appeared to have a minor impact on the turbidity preventing effect. This pointed at an unspecific effect of electrostatic interactions which led to the lowered turbidity at pH 5.0. The stabilizing effect of NaCl is advantageous due to the physiological compatibility of NaCl and the fact that it is brought into the formulations as HSA stabilizer. For this reason exclusively NaCl was used to improve the solubility of the formulation in the further progress of the studies.

Table 1: Maximum turbidity in FNU at pH 5.0 for the cytokine-HSA formulation after the addition of different salts at ionic strength of $\mu=0.009$ and $\mu=0.034$.

	$\mu = 0.009$		$\mu = 0.0345$	
	c [%]	turbidity pH 5.0 [FNU]	c [%]	turbidity pH 5.0 [FNU]
NaCl	0.05	34.7	0.2	18.9
KCl	0.06	36.4	0.26	19.9
LiCl	0.04	49.3	0.15	19.1
NaCH ₃ COO	0.07	49.0	0.28	21.0
NH ₄ Cl	0.05	54.7	0.18	18.08
KI	0.14	65.4	0.57	37.4
KSCN	0.06	55.8	0.23	35.4*

*turbidity maximum at pH 4.0 with 86.2 FNU

One point to be clarified was the reversibility of the precipitation at pH 5.0. In order to elucidate this issue the formulation pH was lowered to 5.0 and re-adjusted back to 7.4 (Figure 4).

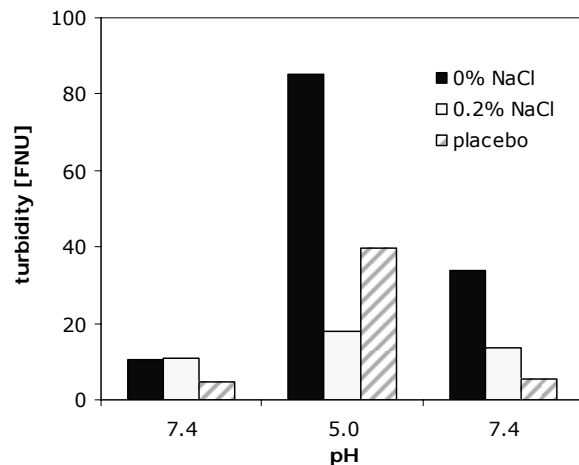


Figure 4: Turbidity at pH-shift from 7.4 to 5.0 of cytokine-HSA formulation (0.25 mg/ml cytokine, 12.5 mg/ml stabilized-HSA and 12.5 mg/ml mannitol) with 0.0% and 0.2% NaCl compared to a placebo formulation (12.5 mg/ml unstabilized-HSA and 12.5 mg/ml mannitol).

Formulations with 0.25 mg/ml cytokine, 12.5 mg/ml stabilized-HSA and 12.5 mg/ml mannitol, respectively a placebo-formulation with 12.5 mg/ml unstabilized-HSA were compared. Unstabilized-HSA was used to eliminate a potential effect of the HSA-stabilizers on turbidity and to show solely the properties of HSA. The turbidity of the cytokine-HSA formulation increased from about 10 FNU at pH 7.4 to 85 FNU at pH 5.0. Immediately after the pH-shift a residual turbidity of 38 FNU was measured at pH 7.4

and a constant level of 33 FNU was reached after approximately 90 minutes. This indicated that precipitation, triggered by the lowering of the pH, was at least partially irreversible. When 0.2% NaCl was added to the formulations the turbidity increased from 11 FNU at pH 7.4 to 18 FNU at pH 5.0 and remained with 13 FNU about 2 FNU higher than initially. For a placebo-formulation with 12.5 mg/ml unstabilized-HSA precipitation and elevated turbidity levels of about 40 FNU at pH 5.0 were observed as well. In contrast to the cytokine-HSA formulation the precipitation of unstabilized-HSA was completely reversible and the turbidity dropped to the initial value of about 4 FNU. This indicated that the cytokine or a combination of cytokine-HSA were responsible for the irreversibility of the precipitation.

To further clarify the stabilizing influence of NaCl on the turbidity profile of the cytokine-HSA formulation, the turbidity of unstabilized-HSA and cytokine as individual components was studied between pH 3.5 and 7.0 at increasing NaCl concentrations. In a formulation with 12.5 mg/ml unstabilized-HSA turbidity stepped up at decreasing pH and reached a maximum at pH 4.5 (Figure 5a). With 0.1% NaCl the turbidity increase was reduced and at 0.25% and 0.5% NaCl completely inhibited. Thus, it could be stated that NaCl offered a direct stabilization of HSA against precipitation at pH 5.0. A stabilizing effect of NaCl on HSA and BSA is also described in literature. Saso et al. (1998) showed a stabilizing effect of NaCl on heat induced aggregation of HSA [5]. Yamasaki and Yano (1990, 1991) reported that the denaturation temperature of BSA between pH 4.5 to 9.0 was increased with rising ionic strength after adding 0.001 to 1.0 M (0.0058% to 5.8%) NaCl. This stabilizing effect was ascribed to a screening effect of NaCl on the electrostatic forces and the inhibition of crevice formation within the molecule in the vicinity of ²¹²Trp [17,18]. This screening effect of NaCl on electrostatic forces was as well reflected in the lower zeta potential values of HSA in presence of NaCl (compare Figure 19, section 3.2.1).

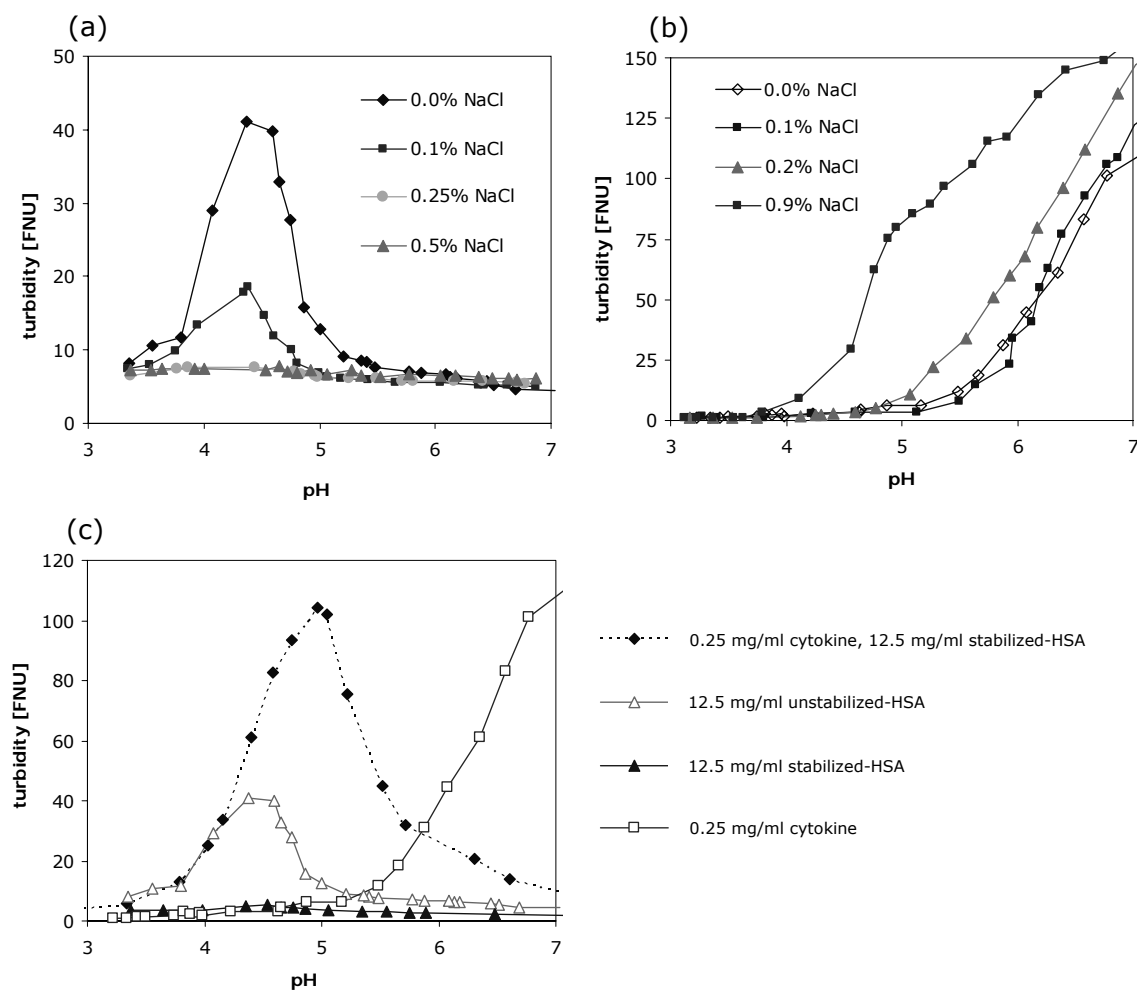


Figure 5: Turbidity of 12.5 mg/ml unstabilized-HSA with 0.0% to 0.5% NaCl (a) and 0.25 mg/ml cytokine with 0.0 to 0.9% NaCl (b) at pH 3.0 to 7.0. In (c) the turbidity of the Cytokine-HSA formulation is compared to the individual components.

Compared to the cytokine-HSA formulation with a turbidity maximum at pH 5.0, the turbidity maximum was located at pH 4.5 for HSA as single component. This shift could be explained by the zeta potential of the formulations (Figure 6). For the cytokine-HSA formulation a zeta potential of 0 mV, which marks the pI was found at pH 5.2. This was approximately 0.5 pH-units higher than for HSA as single component, where 0 mV was reached at pH 4.7. Thus, the zeta potential was shifted to higher pH values due to the addition of the cytokine. In the studied pH range the cytokine, with its pI of 9 was highly positively charged. Above pH 5.5 it was not feasible to determine the zeta potential of the cytokine due to the beginning precipitation and its low solubility. Generally, the pI of a protein mixture is found between the pI values of the individual proteins depending on the ratio. This was for example shown by Rezwan et al. (2005) for Bovine Serum Albumin and Lysozyme adsorbed on colloidal particles [19].

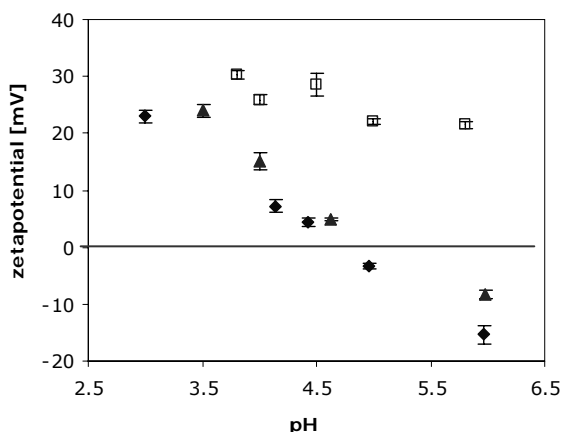


Figure 6: Zetapotential of 0.25 mg/ml cytokine (□), 12.5 mg/ml HSA (◆) and a combination of 0.25 mg/ml cytokine and 12.5 mg/ml HSA (▲) measured in a buffer with 5 mM glycine at pH 3.0 to 6.0.

The cytokine as individual component revealed a completely different turbidity profile between pH 3.0 and 7.0 as compared to HSA (Figure 5b). The turbidity increased when the pH was raised from 3.0 to 7.0 when the formulation pH approached the pI of the cytokine at 9.2. Upon the addition of NaCl, precipitation was fostered and the turbidity stepped up already at lower pH values. Huang et al. (2005) demonstrated for human recombinant Interferon- α -2a by isothermal titration calorimetry, that the attraction between the protein monomers were increased by the addition of NaCl with the consequence of aggregation induced by hydrophobic interactions and decreasing electro-repulsive forces between the protein molecules [20]. At pH 5.0, however, turbidity values below 10 FNU were found for the cytokine with 0.0% to 0.2% NaCl. This indicated a sufficient solubility under these conditions if the cytokine was present alone. A comprehensive discussion on the impact of NaCl on the cytokine aggregation and stability is found in Chapter 6.

Figure 5c compares the turbidity of the cytokine-HSA formulation with those of the individual components. Unstabilized-HSA reached the maximum turbidity of about 40 FNU at pH 4.5. Due to the stabilizers and NaCl this turbidity increase could be inhibited in formulations with stabilized-HSA, which was shown for NaCl and unstabilized-HSA in Figure 5a. Formulations with 0.25 mg/ml cytokine were clear at pH 5.0 and the turbidity increase started first when the pH exceeded 5.5. For the combination of cytokine and stabilized-HSA the turbidity resulted in a turbidity curve, which resembled those of HSA as single component, however, with a higher maximum value of 100 FNU. In the concentration applied for the formulation the stabilizers were not capable to prevent the turbidity increase. Still it was unclear if the precipitation was caused by the cytokine, HSA or a combination of the two proteins.

3.1.2 SDS-PAGE of the Precipitated Material

To analyze the composition of the precipitated material SDS-PAGE was performed at pH 7.0 and pH 5.0. At pH 5.0 the turbid solution (TS) was centrifuged and both the supernatant (SN) and the precipitated material (P) were investigated. The HSA-gel showed that only traces of HSA were found in the precipitated fraction (Figure 7a). In contrast, the cytokine was present to a similar degree in the supernatant and the precipitated fraction (Figure 7b). Comparing the cytokine bands it was obvious that the precipitated fraction contained a high portion of cytokine.

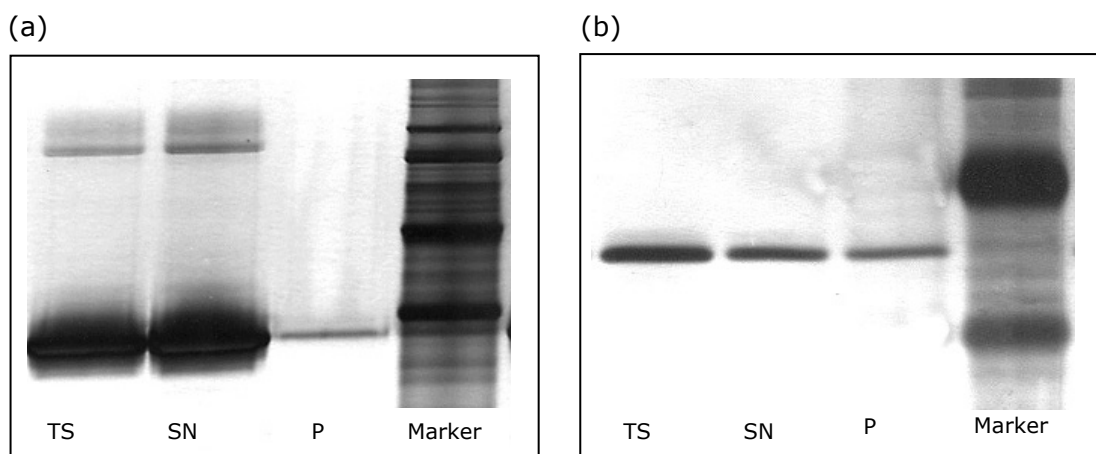


Figure 7: SDS-PAGE of the cytokine-HSA formulation at pH 5.0 showing the turbid solution (TS), the supernatant (SN) and the precipitated fraction (P) of HSA (a) and the cytokine (b).

The results from SDS-PAGE were in agreement with turbidity studies. For HSA as single component the HSA-stabilizers and especially NaCl provided sufficient stabilization to prevent a turbidity increase over the pH-range. In the presence of the cytokine, however, sufficient stabilization could no longer be provided.

3.1.3 Fluorescence Spectroscopy of Cytokine-HSA Mixtures

The high turbidity of 100 FNU for the cytokine-HSA formulation compared to 10 FNU for the cytokine and 40 FNU for unstabilized-HSA at pH 5.0 pointed at interactions between the two proteins. To gain insight into the interactions between HSA and the cytokine at different conditions, isothermal titration calorimetry [21], nuclear magnetic resonance spectroscopy [22], equilibrium dialysis [23], fluorescence spectroscopy or chromatography [23] would be possible techniques. In the context of this project, fluorescence spectroscopy was used to evaluate the interaction between HSA and cytokine. Both proteins contain Trp residues in their amino acid sequences, HSA one at position 214 and the cytokine molecule two Trp near the surface (position 22 and 143) and one in the hydrophobic core (position 79). Trp residues of a protein can be excited at 280 nm and show characteristic emission spectra with maxima between 310 to 350 nm, depending on the environment [24,25].

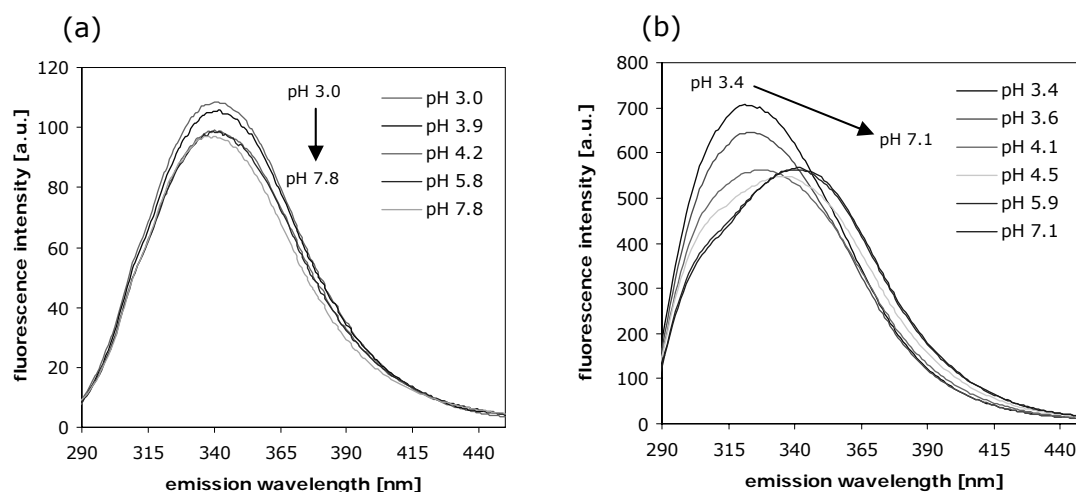


Figure 8: Emission spectra of 0.01 mg/ml cytokine (a) and 0.5 mg/ml HSA (b) in 2 mM glycine between pH 2.8 and 7.8 after excitation at 280 nm.

In the emission spectra of the cytokine as individual component the maximum was located at 340 nm independent of the formulation pH (Figure 8a). An emission maximum of 340 nm can be attributed to Trp residues on the protein surface, which have contact with bound water and other polar groups [24]. With increasing pH values the fluorescence intensity declined, but no shift of the maximum occurred. This revealed that the microenvironment of the Trp residues of the cytokine was not affected by the pH change and potential associated structural changes [26]. An increased intensity of fluorescence which is not combined with a red shift of the maximum was also described for Bovine Growth Hormone upon a pH shift from neutral to acid [27]. For HSA the lowering of the pH was accompanied with a shift of the emission maximum from 340 nm between pH 7.8 and pH 4.8, to 326 nm at pH 3.9 and 321 nm between pH 3.5 and

pH 2.8 (Figure 8b). The blue shift of the spectra at lower pH values indicated an exposure of the Trp residues to a less polar environment and a loss of contact to water. For the evaluation of protein-protein interactions increasing cytokine concentrations were added to a constant amount of 0.5 mg/ml HSA. The interaction was evaluated for pH 3.0 and pH 4.5 without and with 0.1% NaCl. Due to the beginning cytokine precipitation above pH 5.0 it was not feasible to include higher pH values in the study. In Figure 9 the spectra of HSA, cytokine and the combination of HSA with cytokine are shown exemplarily for pH 3.0

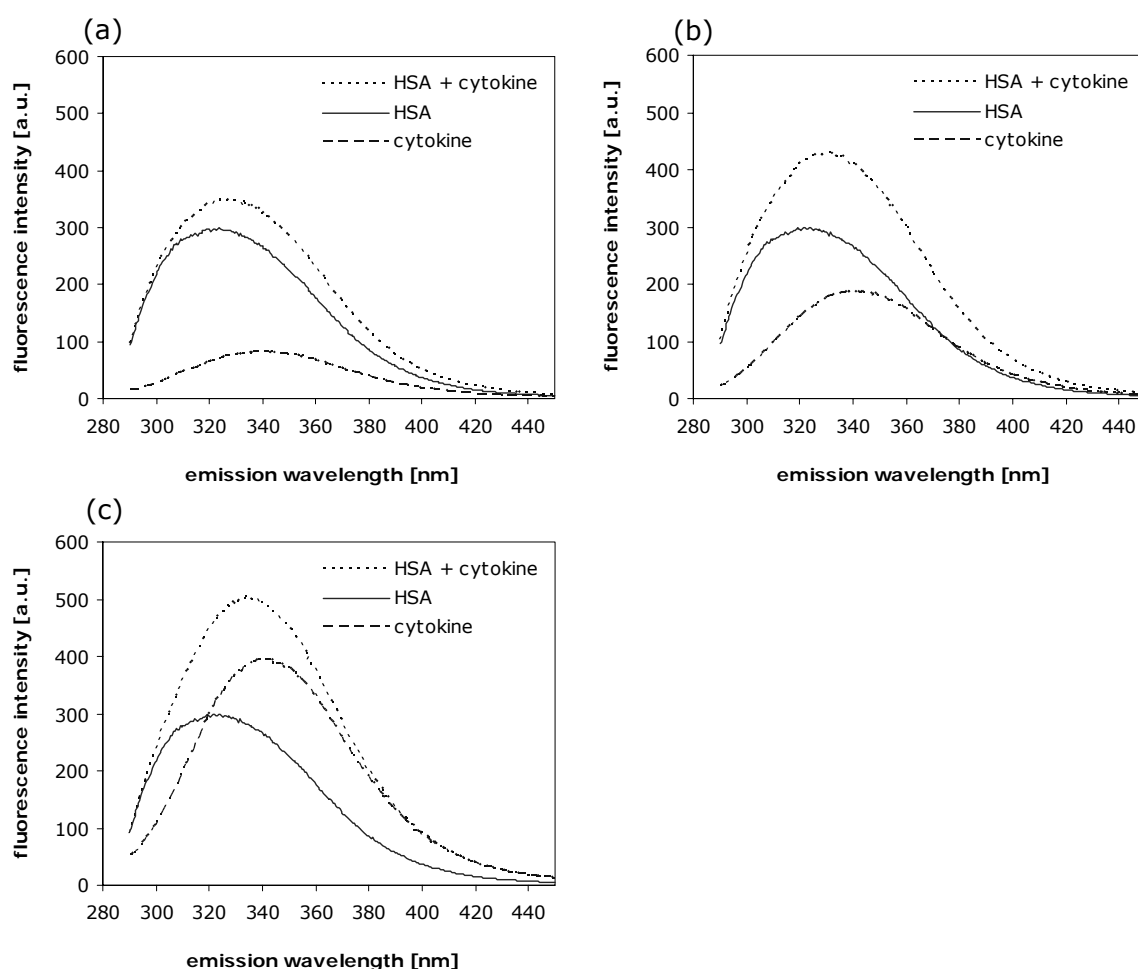


Figure 9: Emission spectra of 0.5 mg/ml HSA with 0.02 mg/ml cytokine (a), 0.04 mg/ml cytokine (b) and 0.1 mg/ml cytokine (c) in 2 mM glycine at pH 3.0 after excitation at 280 nm.

The degree of interactions was determined as F_0/F , with F_0 as the calculated sum of the fluorescence intensity (290 to 450nm) of the individual protein and F as the measured intensity of a solution with both proteins [6]. A higher value of F_0/F indicated stronger protein-protein interactions. For the combination of HSA and the cytokine the interaction parameter F_0/F was increasing at higher cytokine concentrations. At pH 3.0 the interaction parameter F_0/F raised from about 1.1 at 0.02 mg/ml to 1.3 at 0.1 mg/ml

cytokine (Figure 10a). This indicated that interactions occurred to a greater extent at higher cytokine concentrations when HSA was present in excess. The addition of 0.1% NaCl did not impact the strength of the interactions determined at pH 3.0. Significantly stronger interactions between HSA and the cytokine were measured without NaCl at pH 4.5 (Figure 10b). F_0/F increased from 1.15 to 1.53 when adding 0.02 and 0.1 mg/ml cytokine to 0.5 mg/ml HSA. The addition of 0.1% NaCl weakened the interactions between HSA and cytokine, obvious by lower values of F_0/F , which were comparable to pH 3.0.

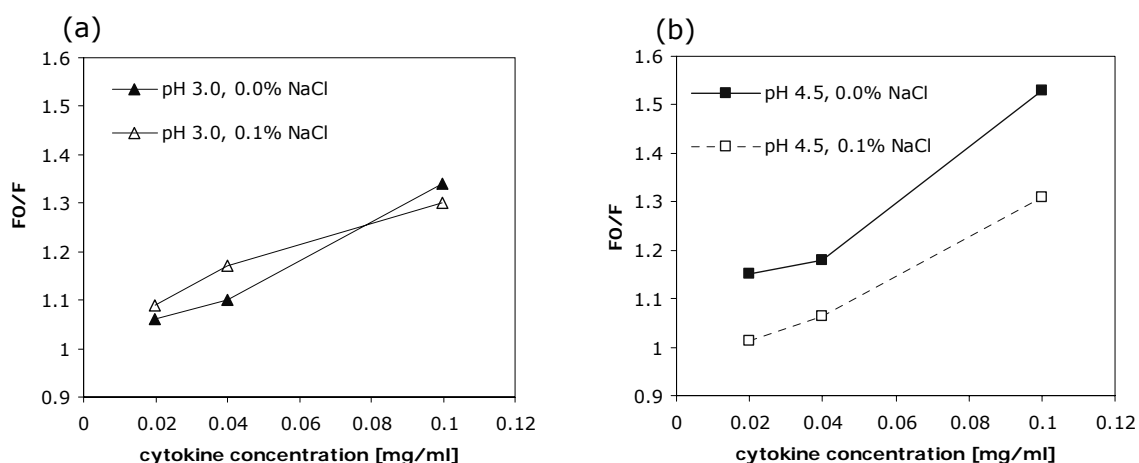


Figure 10: Interaction parameter F_0/F for the combination of 0.5 mg/ml HSA with cytokine at pH 3.0 (a) and pH 4.5 (b) with different NaCl concentrations.

Besides the direct stabilizing effect of NaCl on HSA, the reduced interaction between HSA and the cytokine by adding NaCl at pH 4.5 could offer a further explanation for the prevention of the turbidity increase in the cytokine-HSA formulation with the maximum at pH 5.0.

3.1.4 Particle Size Analysis in Cytokine-HSA Formulations

One goal of the study was to characterize the particle formation in cytokine-HSA formulations depending on pH and NaCl concentration. So far, only turbidimetry was used to characterize aggregation and particle formation. However, different particle fractions especially very small particles below 30 nm, as well as larger particles in the μm -range may not sufficiently be reflected by turbidimetry. Therefore, various methods complementing each other, namely DLS, disc centrifugation and light obscuration were used to monitor particle formation. For the DLS-measurements the short-term intensity fluctuations of scattered light, which are caused by random Brownian motion of the particles are used to calculate the particle size. The measuring range for DLS experiments is typically 1 nm to 5 μm , in exceptional cases up to 10 μm . The upper limit depends on particle density and the incipient sedimentation [28]. Particles of 1 μm and larger can be determined by light obscuration. Disc centrifugation is a method equivalent to analytical ultracentrifugation that can provide information on particles of 20 nm to 2 μm in size. Furthermore, AFM was utilized to visualize the particles formed with pH-changes.

The DLS size-distribution by volume showed a peak with a mean diameter of 5 to 9 nm in the cytokine-HSA formulation without and with 0.2% NaCl between pH 7.0 and 5.0 (Figure 11a,b). This first peak dominated the size distribution by volume with maximum intensities by volume of about 30% for all studied conditions. The cytokine-HSA formulation is dominated by the 50-fold excess of HSA compared to the cytokine. Therefore, the literature values described for HSA can be used as reference values. For native HSA at neutral pH, a mean diameter of 6 to 7 nm and for aggregated HSA a broad peak at 30 to 100 nm was described by Sotum and Christiansen (1997) [29]. Lowering the pH of the cytokine-HSA formulation resulted in a shift of the monomer peak from 4.8 nm at pH 7.0 to 7.5 nm at pH 5.0 without NaCl and from 5.6 nm to 6.5 nm with 0.2% NaCl. A second peak with a maximum between 30 and 60 nm, deriving from aggregated protein, with an intensity of approximately 0.1% was present in all samples. In samples without NaCl a third particle class with a maximum of about 500 nm at pH 5.5 and about 1500 nm at pH 5.0 appeared (Figure 11c,d). The tremendous turbidity increase below pH 5.5 in NaCl-free samples could essentially be attributed to this third population.

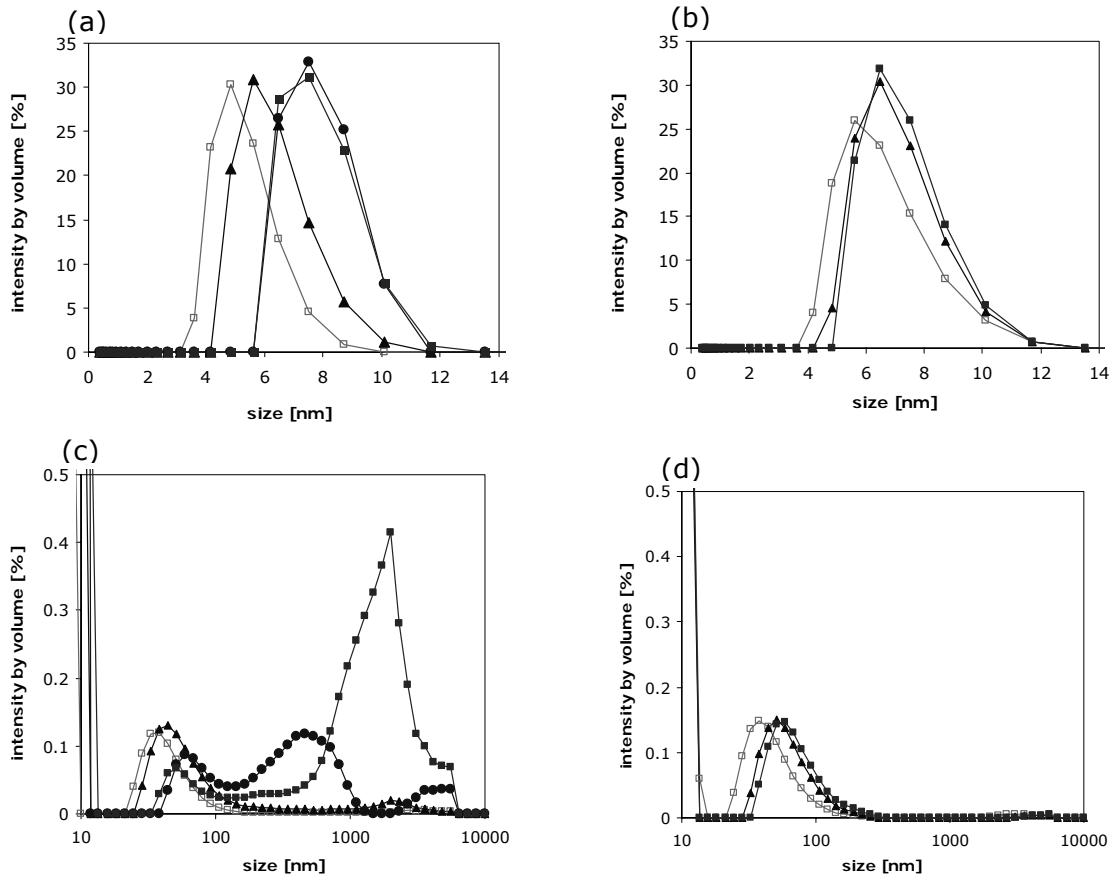


Figure 11: DLS size-distribution by volume of the cytokine-HSA formulation in water (a,c) and 0.2% NaCl (b,d) at pH 7.4 (—□—), 6.0 (—▲—), 5.5 (—●—) and 5.0 (—■—).

Regarding the integrated peak areas of the DLS size-distribution by volume a decline in the area of the first peak between 0 and 15 nm and the second species between 15 to 120 nm in favor of larger species was obvious when the pH was lowered without NaCl added (Figure 12a). The fact that the integrated area between 15 and 120 nm declined at pH 5.5 and 5.0 demonstrated that the turbidity increase could mainly be attributed to particles larger than 120 nm. The addition of 0.2% NaCl could inhibit the turbidity increase to a maximum of 20 FNU at pH 5.0 compared to 100 FNU without NaCl. In samples with 0.2% NaCl less than 1.5% of integrated area of the size distribution by volume could be attributed to the particles larger than 120 nm (Figure 12b). This further strengthened the assumption that particles larger than 120 nm were mainly responsible for the tremendous turbidity increase at pH 5.0. The result were in agreement with Mahler et al. (2005) who showed for IgG1 formulations that turbidity determined at 350 and 550 nm could be attributed to medium sized aggregates and furthermore was in correlation with particles of 1 to 2 μm determined by light blockage [9]. In the size distribution by number more than 99% of the intensity derived from particles smaller than 10 nm.

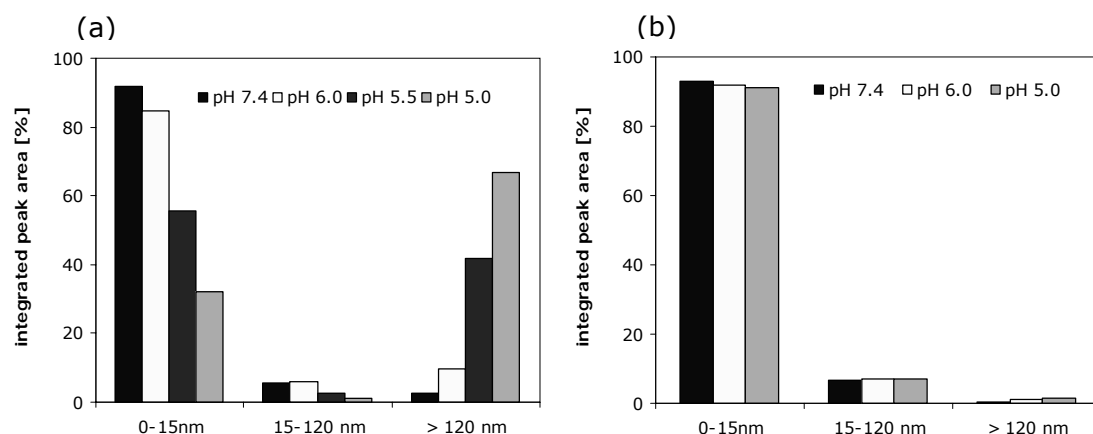


Figure 12: Integrated peak area of the DLS size-distribution by volume in % of the total AUC for cytokine-HSA formulations without NaCl (a) and 0.2% NaCl (b) at pH 7.4 to 5.0.

Due to the high scattering intensities of larger particles DLS experiments can reach a limit when samples contain multiple particle classes. These systems can be analyzed by disc centrifugation, which is an alternative to analytical ultracentrifugation. The size distribution obtained by disc centrifugation is based on the sedimentation velocity of particles within the density gradient of the disc. This sedimentation velocity is depending on particle size and density under the influence of centrifugal forces. Bondoc and Fritzpatrick (1998) used disc centrifugation to determine the hydrodynamic diameter of adenovirus monomers, dimers, trimers and aggregates [30]. Other examples found in literature are the application of disc centrifugation to classify the size of polymer latex [31,32], UV-absorbers [33], nanoparticles [34], immunoglobulins [35] and E. coli inclusion bodies [36].

With the density gradient from 7% to 2% sucrose built up within the disc the smallest particles to be detected were 20 nm. Particles with a size below 20 nm would require unfeasible runtimes of several hours. The main particle sizes determined by disc centrifugation ranged between 20 nm and 1 μ m in cytokine-HSA formulations at pH 7.0 and pH 5.0 without and with 0.2% NaCl (Figure 13). At pH 7.0 the size-distribution by weight indicated slightly larger particles for samples with 0.2% NaCl than for samples without NaCl. Without NaCl 50% of the intensity by weight derived from particles smaller than 32 nm compared to 40 nm when 0.2% NaCl was added. However, at pH 7.0 about 95% of the intensity could be ascribed to particles smaller than 100 nm without and with 0.2% NaCl. When lowering the pH of the NaCl-free formulation to 5.0 a significant shift of the size-distribution by weight to larger particles was observed. More the 50% of the intensity by weight could be attributed to particles larger than 100 nm. For the samples with 0.2% NaCl 95% of the intensity by weight derived from particles smaller than 100 nm.

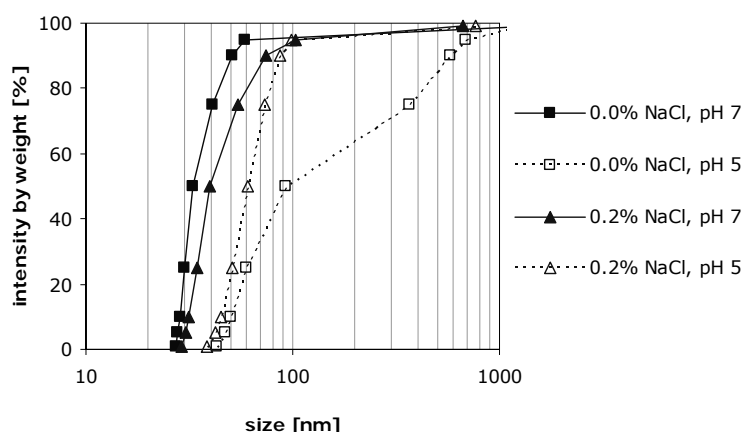


Figure 13: Cumulative particle size distribution by weight of cytokine-HSA with 0.0% NaCl and 0.2% NaCl at pH 7.0 and pH 5.0 determined with disc centrifugation.

AFM was used to size and visualize particles in the nm-range. Contrary to the other evaluated techniques, AFM studies at pH 5.0 were omitted because of the presence of particles in the μm -range, which can interfere with the analytics. From the data collected by AFM it is possible to visualize the particles, which is exemplarily shown in Figure 14 for the formulation at pH 7.0 focusing on the small objects smaller than 10 nm. These small objects between 6 and 10 nm were present at pH 7.0, 6.0 and 5.5.

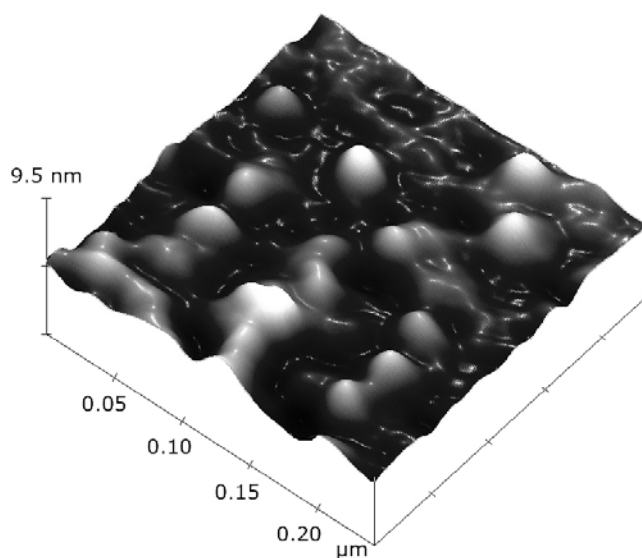


Figure 14: 3D visualization of 0.25 mg/ml cytokine, 12.5 mg/ml stabilized-HSA at pH 7.0.

To size the objects in the samples line-scans were used, which are exemplarily shown for a sizing of 30 nm objects at pH 7.0 and 600 nm objects at pH 5.5 (Figure 15). At pH 7.0, 6.0 and 5.5, small globular objects with a size between 6 and 10 nm, as well as particles in the size range from 22 to 35 nm were present. Thereby, the samples at pH 7.0

possessed the most homogenous distribution with small globular objects of 6 to 10 nm, and also larger objects with a medium size of 29.4 nm. At pH 6.0 objects with an average size of 31.2 nm and some particles with a diameter of about 80 nm were detected in the sample besides the aforementioned fraction at 6 to 10 nm. The incipient precipitation at pH 5.5 was reflected in particles with a diameter of 200 to 400 nm. Beside these particles, smaller particles of 6 to 10 nm and 32.4 nm were detected.

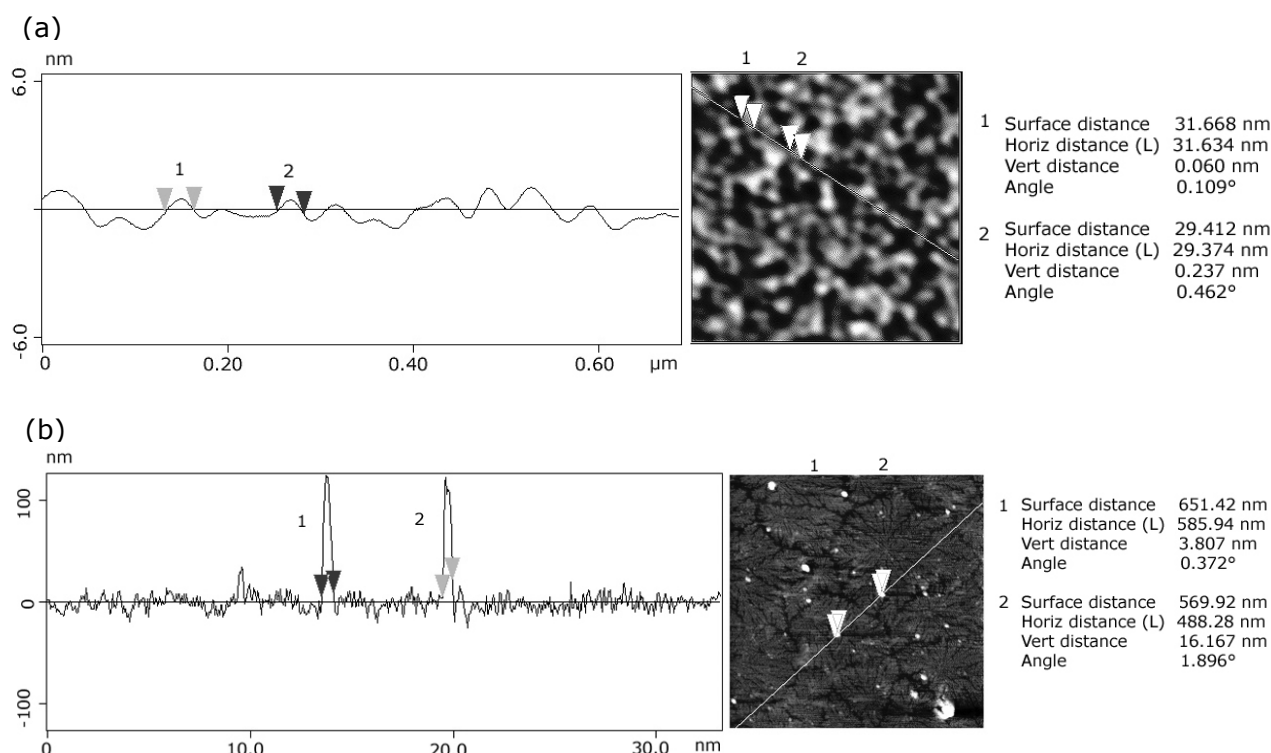


Figure 15: Line scans to size particles of 0.25 mg/ml cytokine, 12.5 mg/ml stabilized-HSA at pH 7.0 (a) and pH 5.5 (b).

The so far described methods focused on the characterization of the nm-range. Light obscuration was used to determine the number of particles $\geq 1 \mu\text{m}$. In the absence of NaCl, an immense increase in particles at pH 5.0, especially in the size range between 1 and 2 μm was observed, due to precipitation of the protein (Figure 16a,c). This increase in particles was reflected in the significant turbidity increase for the formulation at pH 5.0. The total number of particles $\geq 1 \mu\text{m}$ at pH 7.0 and 6.0 was slightly higher compared to the solutions without the addition of NaCl. In the presence of 0.2% NaCl similar amounts of particles $\geq 1 \mu\text{m}$ were measured at pH 7.0, 6.0 and 5.0 (Figure 16b,d). The addition of NaCl can be beneficial to inhibit the formation of particles $\geq 1 \mu\text{m}$, upon lowering the pH.

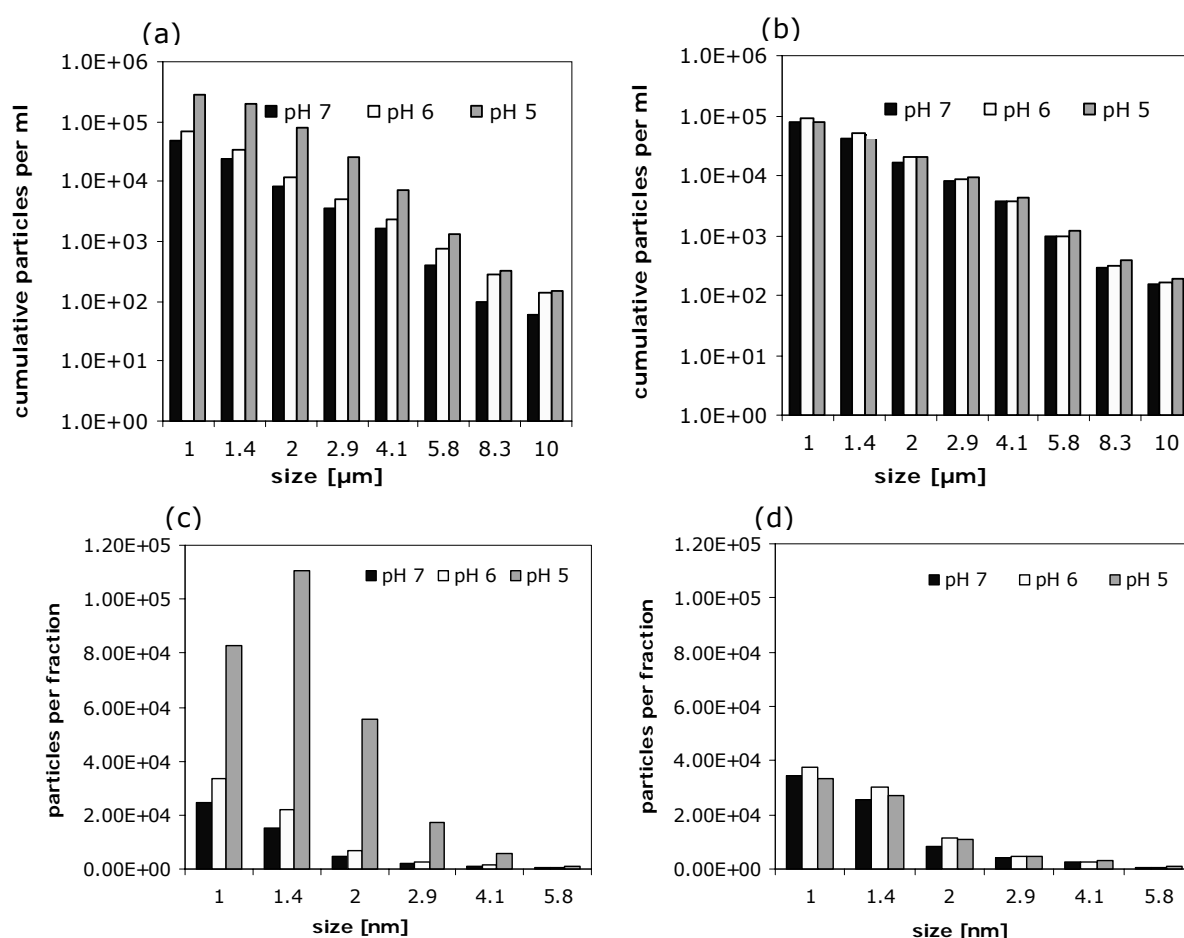


Figure 16: Cumulative particle size distribution of cytokine-HSA formulation with 0.0% NaCl (a) and 0.2% NaCl (b) and particles per ml with 0.0% NaCl (c) and 0.2% NaCl (d) at pH 7.0, 6.0 and 5.0.

A summary of the results obtained by DLS, disc centrifugation and AFM is displayed in Table 2. In contrast to disc centrifugation and light obscuration, DLS and AFM were capable to detect particles in the range of 5 to 10 nm, which represented most of the protein in the samples by number. Extreme long experimental times would be required to determine protein particles smaller than 20 nm by disc centrifugation. Despite of the diverse measuring principle, DLS and AFM provided comparable particle size results between 5 and 500 nm, whereby AFM offered no quantitative information. On the other hand samples containing a mixture of small and large particles e.g. the cytokine-HSA formulation at pH 5.0 were problematic for DLS. The intensity of the scattered light is proportional to the diameter to the power of 6 and therefore, the scattering signal of large particles could superimpose the signal of smaller particles. Particles of a medium size of 30 to 100 nm were detected by disc centrifugation, DLS and AFM for all pH-values. DSL showed that the area of the medium fraction decreased from 5.5% to 1.0% when the pH was lowered from 7.0 to 5.0 in favor of the larger, turbidity inducing

particles. Particles with a size of about 1000 to 1500 nm were detected by DLS and disc centrifugation. In the DLS size distribution the intensity by volume was below 0.1% in the size range above 120 nm. However, the integrated area under the peak compared to the total AUC increased from 2.7% at pH 7.0 to 66.9% at pH 5.0. With disc centrifugation at pH 7.0 about 1% of the intensity by weight derived from particles larger than 100 nm compared to 48% at pH 4.8. Light obscuration showed that the number of particles $\geq 1 \mu\text{m}$ increased when the pH was lowered from 7.0 to 5.0.

Table 2: Main particle sizes of the cytokine-HSA formulation without NaCl determined with DLS, AFM and disc centrifugation.

pH	DLS	AFM	Disc centrifugation
7.4	0-15 nm (max: 4.8 nm) / 91.8% ⁽¹⁾ 15-120 nm (max: 35 nm) / 5.5% ⁽¹⁾ > 120 nm (no max) / 2.7% ⁽¹⁾	6-10 nm 29.4 nm \pm 3.2 nm	20-50 nm / 90% ⁽²⁾ 50-100 nm / 96% ⁽²⁾ 100-1000 nm / 99% ⁽²⁾
6.0	0-15 nm (max: 5.6 nm) / 84.5% ⁽¹⁾ 15-120 nm (max: 44 nm) / 5.9% ⁽¹⁾ > 120 nm (no max) / 9.5% ⁽¹⁾	6-10 nm 31.2 nm \pm 3.8 nm 80 nm	-
5.5	0-15 nm (max: 7.5 nm) / 55.7% ⁽¹⁾ 15-120 nm (max: 58 nm) / 2.6% ⁽¹⁾ > 120 nm (max: 450 nm) / 41.7% ⁽¹⁾	6-10 nm 32.4 nm \pm 3.5 nm 200-400 nm	-
5.0	0-15 nm (max: 7.5 nm) / 84.5% ⁽¹⁾ 15-120 nm (max: 60 nm) / 1.0% ⁽¹⁾ > 120 nm (max: > 1000 nm) / 66.9% ⁽¹⁾	Not feasible due to large particles	20-50 nm / 10% 50-100 nm / 52% ⁽²⁾ 100-1000 nm / 97% ⁽²⁾

⁽¹⁾ integrated area of the size distribution by volume

⁽²⁾ cumulative intensity by weight

With all methods it could be shown that particle formation was increased when the formulation pH was lowered from 7.0 to 5.0. It was further obvious that NaCl provided a stabilizing effect and could significantly reduce the formation of particles in the formulations.

3.2 Studies on HSA-Placebo Formulations

Within the progress of the study it was observed that stabilized-HSA behaved significantly different as compared to unstabilized-HSA. In addition, various batches of Sigma-HSA showed significant differences in their turbidity profile over the pH-range. To elaborate these findings two selected batches of unstabilized-HSA were compared by turbidity measurement, SDS-PAGE, FTIR, zetapotential measurement and DLS. For the cytokine-HSA formulation stabilized-HSA, which contained the excipients NaCl, Na-octanoate and Na-N-acetyltryptophanate was used. To clarify the role of these stabilizers on the behavior of the formulation the impact of the stabilizers on HSA at different pH and ionic strength conditions was studied.

3.2.1 Batch to Batch Variations of Unstabilized-HSA

Turbidity scans of the analyzed Sigma-batches revealed significant differences in their profile and turbidity maximum (Figure 17). The turbidity maxima of the four different batches ranged between 9 and 42 FNU and were located between pH 4.5 and 4.8.

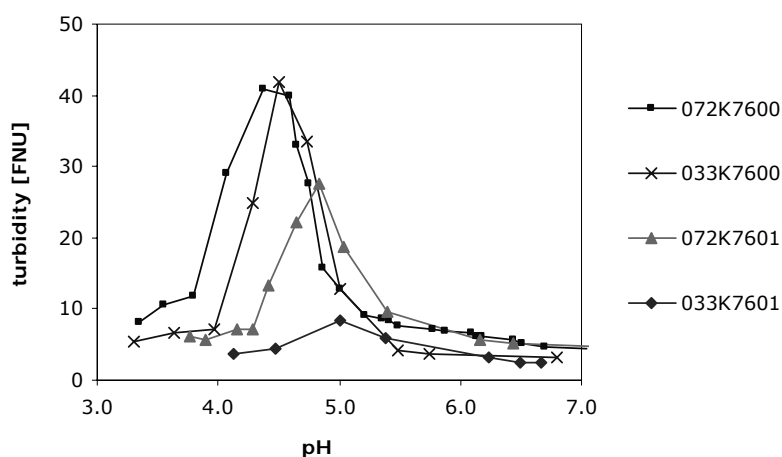


Figure 17: Turbidity of different batches of 12.5 mg/ml unstabilized-HSA between pH 7.0 and 3.0.

For a more detailed characterization, the batches 033K7600 and 033K7601 were selected, as they were comparable in shelf-life, time-point of opening and storage conditions. Although the batches provided a comparable history, the turbidity increase for batch 033K7600 with a maximum above 40 FNU was more pronounced than for batch 033K7601 (Figure 18a,b). The stabilizing effect of NaCl on the two batches was similar. The addition of 0.2% NaCl led to a constant low turbidity of about 3 to 4 FNU from pH 7.0 to 3.5 for both batches.

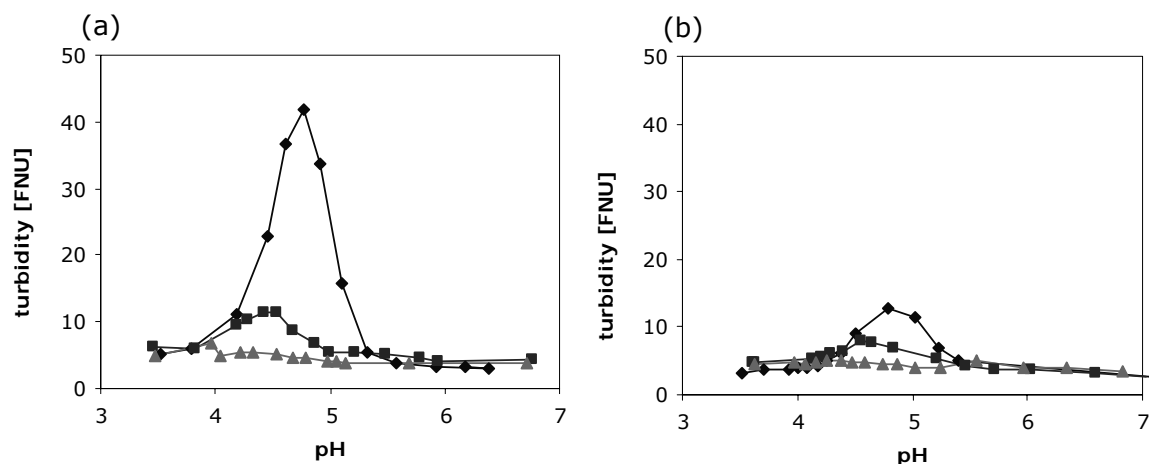


Figure 18: Turbidity of 12.5 mg/ml unstabilized-HSA batch 033K7600 (a) and 033K7601 (b) between pH 7.0 and 3.5 with 0.0% (—◆—), 0.1% (—■—) and 0.2% (—▲—) NaCl.

Analyzed by DLS the monomer peak of the more pH sensitive batch 033K7600 was shifted to a greater extent to larger sizes compared to batch 033K7601 when the pH was lowered from 7.0 to 6.0, respectively 4.8 (Figure 19a). In addition, batch 033K7600 showed higher intensities of about 0.4% in the size range larger than 30 nm at pH 4.8 which also could explain the higher turbidity of this batch (Figure 19b).

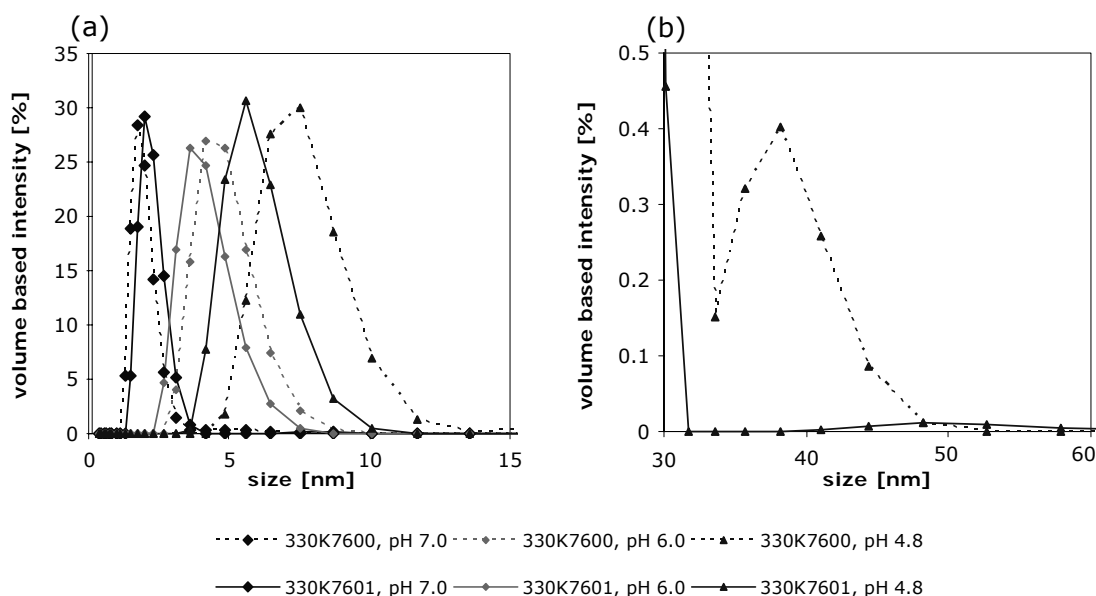


Figure 19: DLS size distribution by volume of 12.5 mg/ml unstabilized-HSA of the batches 033K7600 and 033K7601 at pH 7.0, 6.0 and 4.8 from 0 to 15 nm (a) and 30 to 60 nm (b).

The two compared batches of unstabilized-HSA showed similar zeta potential profiles over the pH-range, whereby a zeta potential of 0 mV was measured at pH 5.0 without and with

0.2% NaCl for both qualities (Figure 20). With 0.2% NaCl lower zeta potential values were measured due to the screening effect of NaCl on the charge of HSA.

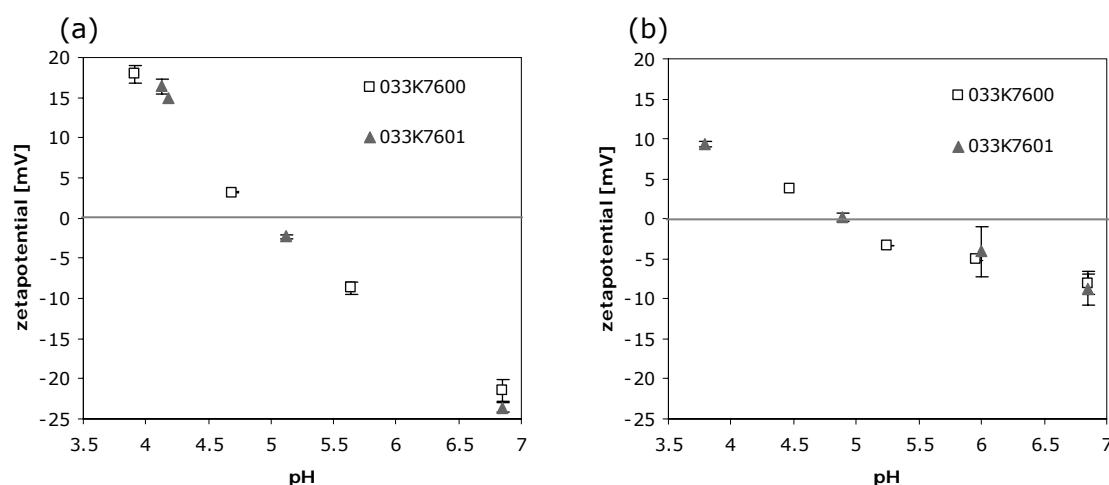


Figure 20: Zetapotential of the two batches of 12.5 mg/ml unstabilized-HSA measured in water (a) and 0.2% NaCl (b) from pH 3.5 to 7.0.

SDS-PAGE was used to characterize the composition of the two batches of unstabilized-HSA, compared to stabilized-HSA with respect to monomer, aggregation and impurities at pH 7.0 and 4.8 (Figure 21).

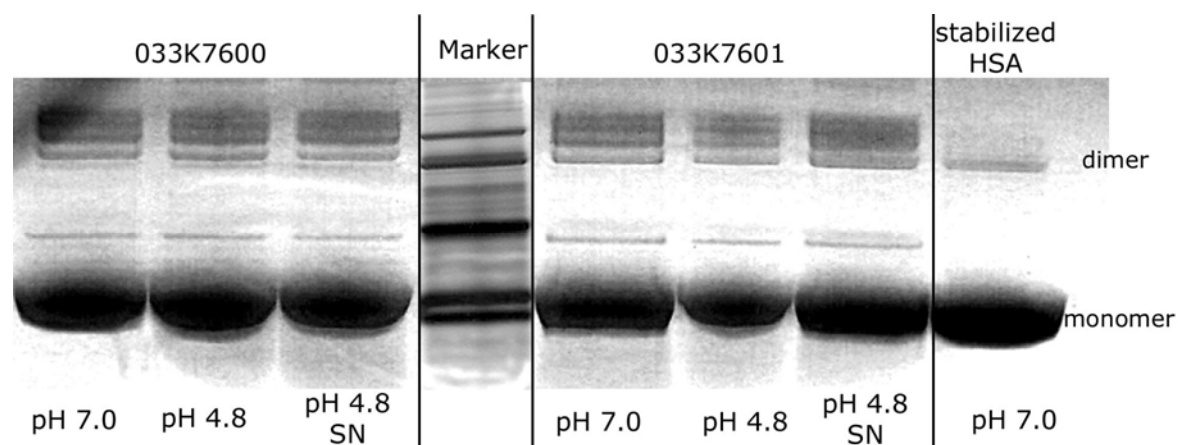


Figure 21: SDS-PAGE of Sigma-HSA batch 033K7600, batch 033K7601 and stabilized-HSA (6.25 µg protein per well) at pH 7.0 and pH 4.8, as well as the supernatant (SN) at pH 4.8 after centrifugation.

SDS-PAGE showed no significant differences between the two batches of unstabilized-HSA under the studied pH conditions. For both batches the HSA-monomer and dimer band and several bands deriving from potential impurities were found. Stabilized-HSA

was characterized by higher purity and far less bands. Only the monomer band and a small dimer band were present in the gel for stabilized-HSA.

The secondary structure of HSA at pH 7.0 and 4.8 without and with 0.2% NaCl was characterized by ATR-FTIR using the second derivative of the amide I band (Figure 22). In the second derivative the band at 1654 cm^{-1} could be assigned to α -helical structures, which are the dominating elements within the HSA molecules. An α -helix content of 67% was described by He and Carter (1992), who published the crystal structure of Human Serum Albumin at 2.8 \AA resolution [37]. A second band with a maximum at 1633 cm^{-1} at pH 7.0, which was shifted to 1628 cm^{-1} at pH 4.8 was present in the spectra. The band at 1630 cm^{-1} was attributed to intramolecular β -sheet within the HSA molecule as proposed by Wang et al. (2005) [8]. Since crystallographic studies of BSA/HSA revealed the absence of β -sheet structures, Murayama and Tomida (2004) offered an extensive explanation for the band at 1630 cm^{-1} for BSA. They assigned it to short segment chains that are connecting α -helical segments [38]. When lowering the pH in the studied HSA-formulations from 7.0 to 4.8 a slight shift of the band from 1633 cm^{-1} at pH 7.0 to 1628 cm^{-1} at pH 4.8 could be observed. The presence of a band around 1620 cm^{-1} , which is generally indicative for the formation of intermolecular β -sheets [39], was not observed after the pH-shift to 4.8. Intermolecular β -sheets are one sign for aggregation that occurs, e.g. during thermal denaturation [40].

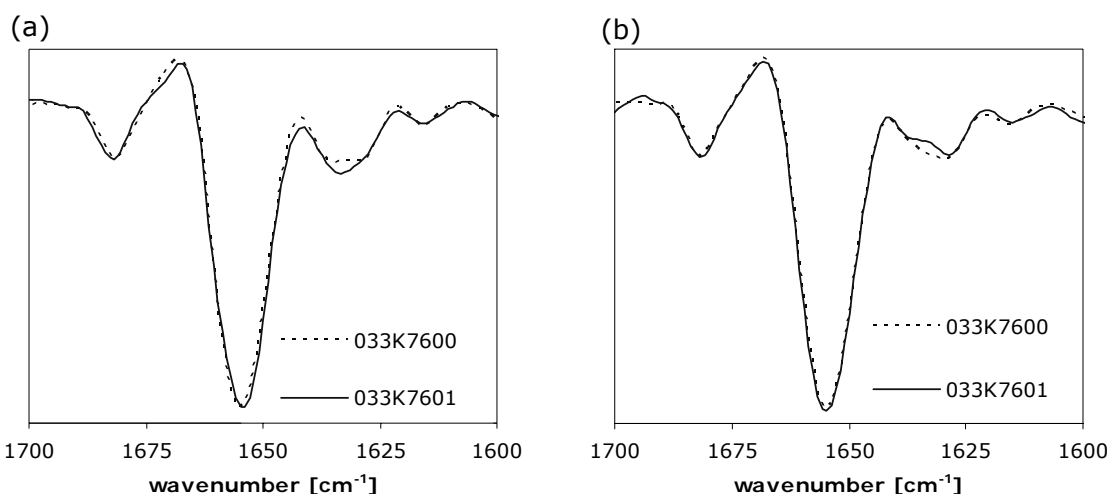


Figure 22: ATR-FTIR second-derivative of 12.5 mg/ml Sigma-HSA batches 033K7600 and 033K7601 without NaCl at pH 7.0 (a) and pH 4.8 (b).

Although a significant turbidity increase at pH 4.8 was measured at least for batch 033K7600, this was not reflected in the secondary structure measured by FTIR. The spectra of the two batches revealed a high degree of similarity at the studied pH conditions, which was also reflected in the spectral correlation coefficient (Table 3).

Table 3: Spectral correlation coefficient of amide I band (1700 to 1600 cm⁻¹) setting 033K7600 as sample and 033K7601 as reference.

	0.0% NaCl	0.2% NaCl
pH 7.0	99.77%	99.73%
pH 4.8	99.88%	99.86%

Thus, the studies pointed at a difference between the HSA-batches regarding the precipitation behavior at pH 4.8, close to the pI of the protein, which was monitored by turbidity measurement and DLS. Despite this behavior, SDS-PAGE and FTIR revealed no significant differences in aggregation and secondary structure. A possible explanation for the variations between the batches could be the degree of purity. Batch 033K7600, which tended to higher turbidity values at pH 4.8 had a purity of 98% according to the certificate of analysis compared to a purity of 99% for batch 033K7601. Even though no definite explanation for the different behavior of batches was found, the occurrence of batch to batch variations needed to be taken into consideration when using the unstabilized-HSA as raw material.

3.2.2 Impact of NaCl, Na-N-Acetyltryptophanate and Na-Octanoate on HSA

When used as excipient in the cytokine-HSA formulation, HSA stabilized with Na-octanoate, Na-N-acetyltryptophanate and NaCl was exclusively used due to regulatory requirements. The FDA requires the addition of 0.08 mM Na-octanoate and 0.08 mM Na-N-acetyltryptophanate, respectively 0.16 mM Na-octanoate per gram HSA to stabilize the protein against heat-induced stress during the pasteurization process [2]. For a solution with 12.5 mg/ml HSA the addition of 2 mM stabilizers is hence required. Stabilized-HSA exhibited a constant turbidity below 5 FNU over the pH-range, compared to a significant increase above 50 FNU at pH 4.8 for some batches of unstabilized-HSA. To elucidate the differences between stabilized and unstabilized-HSA, the impact of the different stabilizers on the turbidity of unstabilized-HSA over the pH-range was to be analyzed. Batch 033K7600 was used, as this batch showed the most pronounced turbidity increase at pH 4.8 without further stabilization.

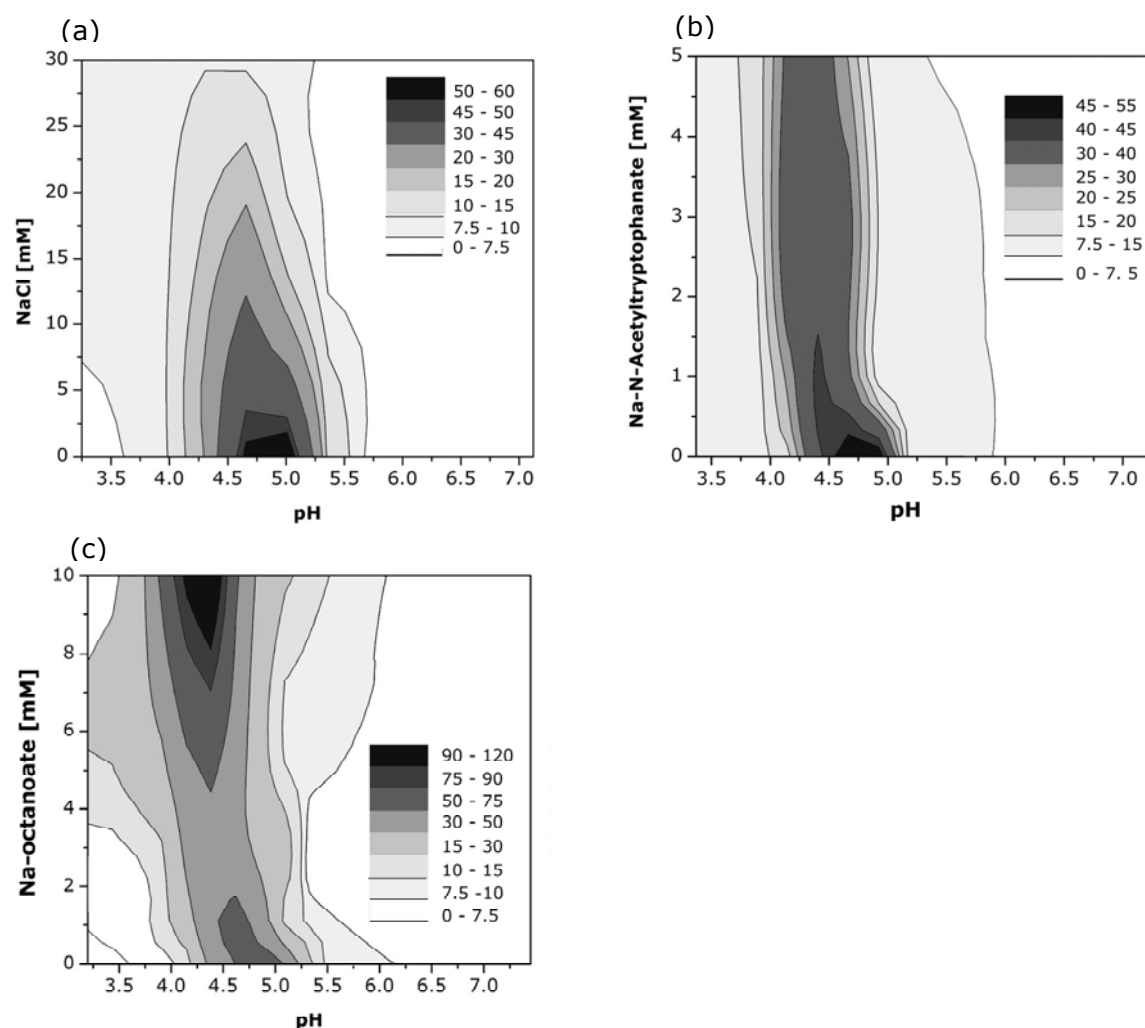


Figure 23: Turbidity in FNU of 12.5 mg/ml unstabilized-HSA (batch: 033K7600) with 0 to 30 mM NaCl (a), 0 to 5 mM Na-N-acetyltryptophanate (b) and 0 to 10 mM Na-octanoate (c) at pH 3.0 to 7.0.

The initial turbidity of 12.5 mg/ml unstabilized-HSA (batch 033K7600) in water was 7 FNU at pH 7.0. By adding increasing NaCl concentrations the tremendous turbidity increase at pH 4.8 could be significantly reduced (Figure 23a). At concentrations of 30 mM NaCl (0.17%) the turbidity ranged between 7 and 10 FNU from pH 7.0 to 3.0. A further increase in NaCl concentration up to 175 mM (1.01%) did not lead to further reduction of the maximally measured turbidity (data not shown). Na-N-acetyltryptophanate was added to HSA up to a concentration of 5 mM (0.25%). Higher concentrations were omitted, due to the poor solubility of the substance. The addition of Na-N-acetyltryptophanate led to a shift of the turbidity maximum to pH 4.5, while the maximum turbidity could only be decreased to values between 30 and 40 FNU (Figure 23b). This emphasized, that Na-N-acetyltryptophanate played a minor role in the suppression of the precipitation at the pI of HSA. The addition of 1 to 4 mM Na-octanoate resulted in a less distinct decrease of turbidity compared to Na-N-acetyltryptophanate. The

turbidity maximum was shifted to pH 4.5, comparable to Na-N-acetyltryptophante (Figure 23c). A further increase in Na-octanoate to a concentration between 5 and 10 mM initiated higher turbidities with maximum values above 110 FNU. Na-octanoate and Na-N-acetyltryptophante are known to bind to the same high affinity site II located in the subdomain IIIA of HSA [41,42]. The comparable effect on turbidity could therefore be assigned to the fact that both substances use the same stabilizing binding mechanism. In Figure 24 the impact of the Na-octanoate and Na-N-acetyltryptophante, respectively in combination with NaCl on unstabilized is shown.

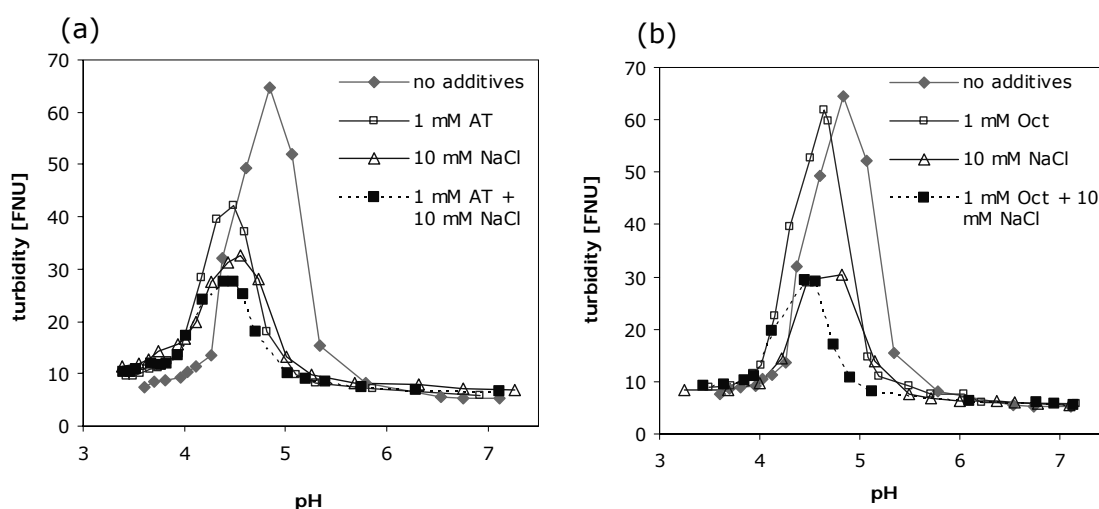


Figure 24: Impact of Na-N-acetyltryptophanate (AT), Na-octanoate (Oct), NaCl and a combination of the stabilizers on the turbidity of 12.5 mg/ml unstabilized-HSA from pH 3.5 to 7.2.

Apparently, NaCl played the major role in the prevention of the turbidity increase at pH 4.8, while the other stabilizers led to a shift of the turbidity maximum to lower pH values. The slightly better stabilization of Na-N-acetyltryptophanate compared to Na-octanoate could be assigned to an increased ionic strength in the formulations with Na-N-acetyltryptophanate. The ionic strength was increased for formulations with Na-N-acetyltryptophanate, because the poorly soluble compound was dissolved above pH 11 and the pH was adjusted to 7.0 by using HCl/NaOH.

4. Conclusions

For the studied formulation with 0.25 mg/ml cytokine, 12.5 mg/ml stabilized-HSA and 12.5 mg/ml mannitol a significant increase in turbidity was observed, when the pH was lowered, reaching a maximum above 100 FNU at pH 5.0. SDS-PAGE revealed that at pH 5.0 most of the cytokine was found in the precipitate. The particle formation process was characterized by DLS, disc centrifugation, AFM and light obscuration. The formulations contained mostly monomers of 5 to 10 nm and a second particle population at 20 to 50 nm. In highly turbid formulations e.g. when the pH of the cytokine-HSA formulation was lowered to 5.0 a third population at 500 to 1000 nm emerged. Studies with HSA placebo formulation made clear that Na-octanoate and Na-N-acetyltryptophanate used in the concentrations to stabilize HSA only played a minor role in preventing the turbidity increase at pH 5.0. However, the addition of NaCl provided a stabilizing effect on the formulation, as the turbidity increase at pH 5.0 could be significantly reduced. Fluorescence spectroscopy further revealed that the interactions between HSA and the cytokine were weaker in the presence of NaCl at pH 4.5. The HSA-cytokine precipitation at pH 5.0 was partly irreversible, when the pH was adjusted back to 7.4. This irreversibility could become an issue e.g. during pH-adjustment with acid when the pH drops below 7.4 into the turbidity region at least temporarily in some areas of a batch. Besides of a reduction of the cytokine-HSA interactions by NaCl, it is essential to provide sufficient stabilization of HSA by NaCl to achieve an overall stable cytokine-HSA formulation.

5. References

1. L. S. Lin, M. G. Kunitani, M. S. Hora. Interferon- β -1b (Betaseron®); A Model for Hydrophobic Therapeutic Proteins. *Pharm. Biotechnol.* **9**:275-301 (1996).
2. U.S. Food and Drug Administration, Code of Federal Regulations, Title 21, Volume 7: §640.80 Albumin (Human), revised as on April 1, 2004.
3. G. Scatchard, L. E. Strong, W. L. Hughes Jr., J. N. Ashworth, A. H. Sparrow. Chemical, clinical, and immunological studies and the products of human plasma fractionation. XXVI. The properties of human serum albumin at low salt content. *J. Clin. Invest.* **24**:671-679 (1945).
4. G. A. Ballou, P. D. Boyer, J. M. Luck, G. F. Lum. The heat coagulation of human albumin. *J. Biol. Chem.* **153**: 589-605 (1944).
5. L. Saso, G. Valentini, E. Grippa, M. G. Leone, B. Silvestrini. Effect of selected substances on heat-induced aggregation of Albumin, IgG and Lysozyme. *Res. Com. Mol. Pathol. Pharmacol.* **102**:15-28 (1998).
6. M. A. H. Capelle, R. Gurny, T. Avinte. High Throughput Screening of Protein-Protein Interactions. Proc. 5th World Meeting on Pharm. Biopharm. Pharm. Tech. Geneva (2006).
7. S. L. Wang, S. Y. Lin, M. J. Li, Y. S. Wei, T. F. Hsieh. Temperature effect on the structural stability, similarity and reversibility of human serum albumin in different states. *Biophy. Chem.* **114**:205-212 (2005).
8. S. L. Wang, Y. S. Wei, S. Y. Lin. Subtractive similarity method used to study the infrared spectra of proteins in aqueous solution. *Vibrat. Spectroscopy* **31**:313-319 (2003).
9. H. C. Mahler, R. Müller, W. Frieß, A. Delille, S. Matheus. Induction and analysis of aggregates in a liquid IgG1-antibody formulation. *E. J. Pharm. Biopharm.* **59**:407-417 (2005).
10. S. Hershenson, J. Thomson. Isoelectric focusing of recombinant interferon- β . *Appl. Theor. Electrophr.* **1**:123-124 (1989).
11. M. Houska, E. Brynda. Interactions of proteins with polyelectrolytes at solid/liquid interfaces: sequential adsorption of albumin and heparin. *J. Colloid. Interf. Sci.* **188**:243-250 (1997).
12. E. Y. Chi, S. Krishnan, T. W. Randolph, J. F. Carpenter. Physical Stability of Proteins in Aqueous Solution: Mechanism and Driving Forces in Nonnative Protein Aggregation. *Pharm. Res.* **20**:1325-1336 (2003).
13. M. Yamasaki, H. Yano, K. Aoki. Differential scanning calorimetric studies on bovine serum albumin: I Effects of pH and ionic strength. *Int. J. Biol. Macromol.* **12**:263-268 (1990).
14. Y. Koga, P. Westh, J. V. Davies, K. Miki, K. Nishikawa, H. Katayanagi. Toward Understanding the Hofmeister Series. 1. Effect of Sodium Salts of Some Anions on the Molecular Organization of H₂O. *J. Phys. Chem.* **108**:8533-8541 (2004).
15. T. Arakawa, S. N. Timasheff. Preferential Interactions of Proteins with Salts in Concentrated Solutions. *Biochem.* **21**:6545-6552 (1982).
16. T. Arakawa, S. N. Timasheff. Mechanism of Protein Salting In and Salting Out by Divalent Cation Salts: Balance between Hydration and Salt Binding. *Biochem.* **23**:5912-5923 (1984).
17. M. Yamasaki, H. Yano. Differential scanning calorimetric studies on bovine serum albumin: I. Effects of pH and ionic strength. *Int. J. Bio. Macromol.* **12**:263-268 (1990).
18. M. Yamasaki, H. Yano. Differential scanning calorimetric studies on bovine serum albumin: II. Effects of neutral salts and urea. *Int. J. Bio. Macromol.* **13**:322-328 (1991).
19. K. Rezwani, L. P. Meier, L. J. Gauckler. A Prediction Method for the Isoelectric Point of Binary Protein Mixtures of Bovine Serum Albumin and Lysozyme Adsorbed on Colloidal Titania and Alumina Particles. *Langmuir* **21**:3493-3497 (2005).
20. S. L. Huang, F. Y. Lin, C. P. Yang. Microcalorimetric studies of the effects on the interactions of human recombinant interferon- α 2a. *Eur. J. Pharm. Sci.* **24**:545-552 (2005).

21. A. Velazquez-Campoy, S. A. Leavitt, E. Freire. Characterization of protein-protein interactions by isothermal titration calorimetry. *Methods in Molec. Biol.* **261**:35-54 (2004).
22. L. Quin, O. Vinogradova, A. M. Gronenborn. Protein-protein interactions probed by nuclear magnetic resonance spectroscopy. *Meth. in Enzymolog.* **339**:377-389 (2001).
23. S. Beeckmans. Chromatographic Methods to Study Protein-Protein Interactions. *Methods* **19**:278-305 (1999).
24. A. S. Ladokhin. Fluorescence Spectroscopy in Peptide and Protein Analysis. in Encyclopedia of Analytical Chemistry. R. A. Meyers (Ed.), 5762-5779 (2000).
25. W. Jiskoot, A. J. W. G. Visser, J. N. Herron, M. Sutter. Fluorescence Spectroscopy. In Methods for Structural Analysis of Protein Pharmaceuticals. Eds. W. Jiskoot, D. J. A. Crommelin. AAPS Press (2005).
26. V. K. Sharma, D. S. Kalonia. Temperature- and pH-Induced Multiple Partially Unfolded States of Recombinant Human Interferon- α 2a: Possible Implications in Protein Stability. *Pharm. Res.* **20**:1721-1729 (2003).
27. T. H. Holzman, J. J. Dougherty Jr., D. N. Brems, N. E. MacKenzie. pH-Induced Conformational States of Bovine Growth Hormone. *Biochem.* **29**:1255-1261 (1990).
28. V. M. Gun'ko, A. V. Klyueva, Y. N. Levchuk, R. Lebeda. Photon Correlation Spectroscopy investigations of proteins. *Adv. Coll. Interf. Sci.* **105**:201-238 (2003).
29. P. C. Sontum, C. Christiansen. Photon Correlation Spectroscopy applied to characterisation of denaturation and thermal stability of human albumin. *J. Pharm. Biomed. Anal.* **16**:295-302 (1997).
30. L. L. Bondoc Jr, S. Fritzpatrick. Size distribution analysis of recombinant adenovirus using disc centrifugation. *J. Indust. Microbiol. Biotechnol.* **20**:317-322 (1998).
31. E. M. Verdurmen, J. G. Albers, A. L. Geramn. Polybutadiene latex particle size distribution analysis utilizing a disk centrifuge. *Colloid. Polym. Sci.* **272**:57-63 (1994).
32. P. Navabpour, C. Rega, C. J. Lloyd, D. Attwood, P. A. Lovell, P. Geraghty, D. Clarke. Influence of concentration on the particle size analysis of polymer latexes using diffusing-wave spectroscopy. *Colloid. Polym. Sci.* **283**:1025-1032 (2005).
33. B. Herzog, A. Katzenstein, K. Quass, A. Stehlin, H. Luther. Physical properties of organic particulate UV-absorbers used in sunscreens I. Determination of particle size with fiber-optic quasi-elastic light scattering (FOQELS), disc centrifugation, and laser diffractometry. *J. Coll. Interf. Sci.* **271**:136-144 (2004).
34. A. Azioune, A. B. Slimane, L. Ait Hamou, A. Pleuvy, M. M. Chehimi, C. Perruchot, S. P. Armes. Synthesis and Characterization of Active Ester-Functionalized Polypyrrole-Silica Nanoparticles: Application to the Covalent Attachment of Proteins. *Langmuir* **20**:3350-3356 (2004).
35. G. Neal, E. Keshavarz-Moore, S. P. Ayazi. Ultra scale-down approach for the prediction of full-scale recovery of ovine polyclonal immunoglobulins used in the manufacture of snake venom specific fab fragment. *Biotechnol. Bioeng.* **81**:149-157 (2003).
36. H. H. Wong, B. K. O'Neill, A. P. J. Middelberg. Cumulative Sedimentation Analysis of Escherichia coli debris size. *Biotechnol. Bioeng.* **55**:556-564 (1997).
37. X. M. He, D. C. Carter. Atomic structure and chemistry of human serum albumin. *Nature* **358**:209-215 (1992).
38. K. Murayama, M. Tomida. Heat-Induced Secondary Structure and Conformation Change of Bovine Serum Albumin Investigated by Fourier Transform Infrared Spectroscopy. *Biochem.* **43**:11526-11532 (2004).
39. A. C. Dong, S. J. Prestrelski, S. D. Allison, J. F. Carpenter. Infrared Spectroscopic studies of lyophilization induced protein aggregation. *J. Pharm. Sci.* **84**:415-424 (1995).
40. E. Pauthe, J. Pelta, S. Patel, D. Lairez, F. Goubard. Temperature induced β -aggregation of fibronectin in aqueous solutions. *Biochim. Biophys. Acta* **1597**:12-21 (2002).

41. M. Anraku, Y. Tsurusaki, H. Watanabe, T. Maruyama, U. Kragh-Hansen, M. Otagiri. Stabilizing mechanisms in commercial albumin preparations: octanoate and N-acetyl-L-tryptophanate protect human serum albumin against heat and oxidative stress. *Biochim. et Biophys. Acta* **1702**:9-17 (2004).
42. U. Kragh-Hansen, V. T. G. Chuang, M. Otagiri. Practical aspects of the ligand-binding and enzymatic properties of human serum albumin. *Biol. Pharm. Bull.* **25**:695-704 (2002).

Chapter 3

Physico-chemical Characterization of the Freezing Behavior of Mannitol-Human Serum Albumin Formulations

Abstract

The goal of the study was to analyze the impact of the Human Serum Albumin (HSA) quality (stabilized or non-stabilized HSA), the addition of NaCl and the HSA-stabilizers Na-octanoate and Na-N-acetyltryptophanate on the freezing behavior of mannitol-HSA formulations. The focus was set on crystallization, T_g' (glass transition temperature of the maximally freeze-concentrated phase) and T_c (collapse temperature). Differential Scanning Calorimetry (DSC), cryomicroscopy and low temperature X-ray powder diffraction (LTXRD) were used to study the frozen state. In mannitol-HSA formulations, mannitol crystallization was inhibited and T_g' lowered to a greater extent by stabilized-HSA (containing Na-octanoate, Na-N-acetyltryptophanate and NaCl) than by unstabilized-HSA. Detailed DSC and LTXRD studies showed that in the concentrations used for the stabilization of HSA, NaCl led to changes in the freezing-behavior an effect which was less pronounced for the other stabilizers. NaCl further lowered the T_c which was determined by cryomicroscopy. As the freezing behavior governs the further lyophilization process, the changes have to be taken into consideration for the development of a lyophilization cycle to avoid collapse and instabilities.

Keywords: mannitol, HSA, NaCl, DSC, LTXRD, freezing

1. Introduction

Lyophilization is still the most frequently used technique to produce dry and stable protein formulations. Within the lyophilization process, the applied freezing protocol and a potential annealing step have a major effect on the subsequent drying procedure regarding drying-rate and drying-time [1-3]. The freezing process also governs the structure and morphology of the lyophilized products [4]. Thereby, the physico-chemical properties of the selected excipients are influenced by the presence of salts, which are often added as buffer components or stabilizers [5,6]. Salts can further be introduced into the formulation within the bulk purification process or by pH-adjustment. A slight increase in salt concentration can lead to significant changes of the physico-chemical properties of the excipients during freezing and drying [7-10]. Therefore, it is important to investigate and understand how the freezing step, the low temperature behavior and the subsequent drying process of a formulation are influenced by the salt concentration.

As model system a formulation with mannitol as crystallizing bulking agent and HSA as amorphous stabilizer is used. This combination is used to stabilize the cytokine in the HSA-containing, lyophilized formulation (compare Chapter 2). A combination of the HSA and mannitol as excipients for the stabilization of proteins is commonly described in literature and patents, especially for hydrophobic proteins like interleukins and interferons [11-13]. Mannitol is a standard excipient for lyophilization due to its excellent cake forming qualities. The nonreducing sugar alcohol can be dried under relatively harsh conditions, because of its high eutectic temperature of -1.5°C . The crystallization of mannitol during freezing and drying depends on various factors. Besides the employed mannitol concentration [4], the lyophilization process, especially the freezing rate [14,15] has a significant impact on mannitol crystallization and morphology. The presence of other excipients like lyoprotectants, buffer salts or proteins can promote and inhibit mannitol crystallization [16-19]. Thus, the crystallization behavior of mannitol in the frozen state needs to be studied to control the morphology of mannitol upon lyophilization. HSA is still a widely used excipient in both liquid and lyophilized protein formulations. Its application as stabilizing excipient in liquid and lyophilized formulations was already discussed in Chapter 1. According to the US Food and Drug Administration HSA used in protein formulations or as drug has to be pasteurized for 10 hours at temperatures up to 60°C [20]. Consequently, stabilization against the heat induced stress is required. The salt of the fatty acid Na-octanoate [21] and the amino acid derivative Na-N-acetyltryptophanate [22] protect HSA during the pasteurization process [23]. HSA is further stabilized by the addition of NaCl [20,21,24]. Thus the ionic strength in protein formulations stabilized with HSA increases inevitably and the physico-chemical properties can be affected due to the presence of the different stabilizers. The goal of this

study was to investigate the impact of NaCl and the other HSA-stabilizers on the physico-chemical properties of formulations containing mannitol and HSA during freezing and at low temperatures.

2. Material and Methods

2.1 Materials

Different types of HSA were used for the experiments, namely non-stabilized HSA from Sigma-Chemicals (Steinheim, Germany) and stabilized-HSA from Grifols (Langen, Germany). Stabilized-HSA from Grifols was used as 20% solution and contained 16 mmol Na-octanoate, 16 mmol Na-N-acetyltryptophanat and NaCl. For the experiments the solution was diluted to the desired concentration. Sigma-HSA was provided as a solid powder which contained 97% HSA according to the specifications and was used without further purification. Mannitol in the quality of Ph. Eur. was purchased from Caelo (Hilden, Germany) NaCl, Na-octanoate and N-acetyl-DL-tryptophante from Sigma (Steinheim, Germany). The pH of the solutions was adjusted to 7.0 ± 0.1 using HCl and NaOH. The declaration of the used concentrations was given in % [w/v] if not stated otherwise.

2.2 Methods

2.2.1 Differential Scanning Calorimetry (DSC)

DSC was used to study T_g' and crystallization behavior at low temperatures. Approximately 20 mg of the solution were analyzed in a crimped Al-crucible. The samples were frozen from 20°C to -70°C and reheated to 20°C with a standard scanning-rate of 10°C/min in a Netzsch DSC 204 Phoenix® (Selb, Germany), calibrated with Indium. T_g' (onset, point of inflection) and crystallization (onset, peak, enthalpy) of the excipients were determined during the heating scan.

2.2.2 Cryomicroscopy

The collapse temperature T_c , which is closely related to T_g' was determined by cryomicroscopy. To determine the collapse temperature 5 µl of the solutions were frozen on a microscopic slide with an average cooling rate of 5°C/min to -50°C on the cooling stage (Linkman THM 600 S, Surrey, UK) under a microscope (Olympus BX 50, Hamburg, Germany). After applying vacuum to the system a moving drying front could be observed, due to the sublimation of ice. Subsequently, the temperature was step-wise

increased until collapse occurred. When the region of collapse was identified the sample was re-cooled and smaller steps of 0.5°C with a lower heating rate were applied to bracket the collapse temperature. T_c was defined as the temperature at which the coherent and compact structure of drying front became fragile with pores.

2.2.3 Low Temperature X-ray Powder Diffraction (LTXRD)

Crystallization was studied with LTXRD using Cu- $K\alpha_1$ -radiation ($\lambda=154.06$ pm) on the powder diffractometer Stadi P from STOE (Darmstadt, Germany) with parafocused transmission geometry. Germanium was used as primary monochromator and the scattered X-rays were detected with a linear PSD area detector. The solutions were frozen in the rotating capillary (diameter 0.5 mm) in the cooling stage (Oxford Cryosystem) of the X-ray diffractometer. The diffraction patterns were analyzed with the program WinXPOW from STOE (Darmstadt, Germany). For the LTXRD experiment a temperature profile similar to the conditions during lyophilization was chosen. The samples were frozen to -40°C with a cooling rate of 0.5°C/min. At -40°C the first measurement under isothermal conditions was performed. The temperature was subsequently increased to -20°C at 1°C/min and several measurements were performed at designated time intervals. The temperature of -20°C was chosen as it represents the annealing temperature applied during lyophilization (compare Chapter 4). For mannitol it is possible to crystallize in the α -, β - and δ -modification. Furthermore crystallization of mannitol as hydrate during freezing and after lyophilization was reported [29]. Table 1 summarizes the characteristic mannitol peaks.

Table 1: Assignment of X-ray diffraction peaks to the different mannitol-modifications.

mannitol modification	main peaks [° 2- θ]	intensity [%]	peaks used for identification [° 2- θ]	references
α -mannitol	13.6	20	13.6	JCPDS-database Walter-Levy (1968)
	17.2	45	17.2	
	18.7	100		
β -mannitol	14.6	65	14.6	JCPDS-database
	16.8	85	16.8	Walter-Levy (1931)
	18.8	100	23.4	
	23.4	90		
δ -mannitol	9.7	100	9.7° 2- θ	JCPDS-database
	20.4	50	no peak at 17.9° 2- θ	Walter-Levy (1968)
mannitol	9.6	80	9.6° 2- θ	Yu et al. (1999) [29]
hydrate	17.9	100	17.9° 2- θ	

3. Results and Discussion

3.1 DSC Studies of Stabilized-HSA and Mannitol

DSC is an important tool to study the frozen state of formulations. Thereby, the glass transition of the maximally freeze-concentrated solution (T_g'), crystallization and melting processes can be measured. This information can be important for the frozen storage of protein formulations and at most for the development of appropriate lyophilization cycles.

For the first set of experiments the total solid content of the solutions was kept constant at 2.5% [w/v] and the ratio of mannitol to stabilized-HSA was varied. DSC analysis of the freezing process for a 2.5% mannitol solution indicated partial crystallization of mannitol during cooling. At low temperatures the nucleation of mannitol crystals prevailed [26]. Because of the remaining amorphous mannitol fraction, two glass transition points $Tg'_1 = -29.9^\circ\text{C}$ and $Tg'_2 = -26.1^\circ\text{C}$ (point of inflection) followed by a crystallization with an onset of -25°C where the nuclei grow to mature crystals [26] were detected during the rewarming of the solution (Figure 1).

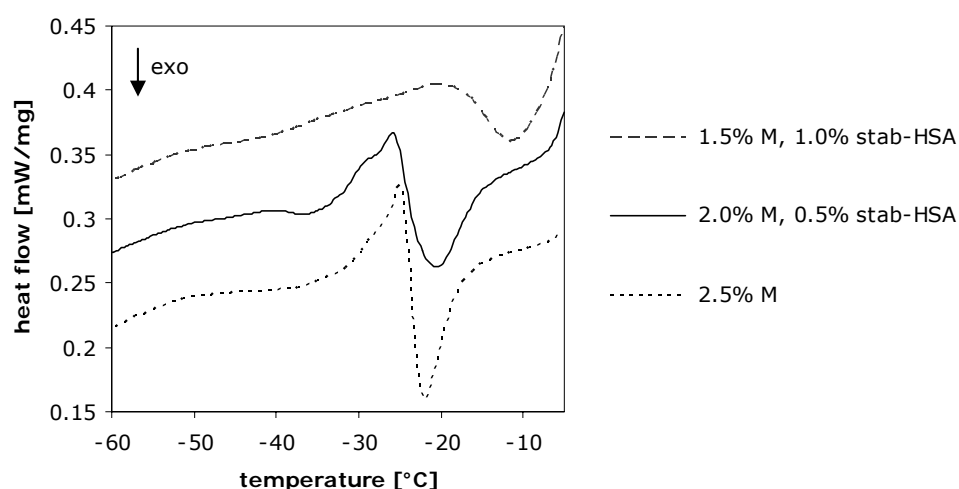


Figure 1: DSC heating scans of solutions with variable ratios of mannitol (M) to stabilized-HSA (HSA) at a total solid content of 2.5%.

This was in agreement with literature, which described the glass transition points at -32°C (Tg'_1) and -25°C (Tg'_2) for 10% mannitol [27,28]. Furthermore, it was described that at a higher cooling rate of $20^\circ\text{C}/\text{min}$ mannitol crystallization in solutions with 5% to 15% [w/v] cannot be observed during freezing, whereas reduced cooling rates of 5 to $10^\circ\text{C}/\text{min}$ led to partial crystallization. Even at slow cooling rates e.g. $1^\circ\text{C}/\text{min}$, that are typically used during lyophilization, mannitol only crystallizes partially during cooling, leading to additional crystallization during warming [14,27]. The addition of stabilized-

HSA as non-crystallizing solute had the effect that mannitol crystallization was delayed and inhibited (Figure 1). Onset and peak maximum of the crystallization were shifted to higher temperatures. A similar effect has been described for mannitol-BSA formulations in phosphate buffer [29]. The T_g' of the formulations was shifted to lower temperatures with increasing amounts of stabilized-HSA added (Table 2). The formulations with 2.5% mannitol respectively 2.0% mannitol and 0.5% stabilized-HSA showed nearly identical transition temperatures and crystallization behavior. At equal amounts of mannitol and stabilized-HSA in the solution the crystallization of mannitol was completely suppressed.

Table 2: T_g' , onset and peak maximum of mannitol crystallization in presence of stabilized-HSA in formulations with 2.5% total solid content.

mannitol [%]	stabilized-HSA [%]	$T_g'_1$ $T_g'_2$ [°C]	crystallization onset [°C]	peak maximum [°C]
2.5	0	-26.1 -29.9	-25.3	-22.1
2.0	0.5	-26.4 -30.5	-25.3	-21.1
1.5	1.0	-34.9	-17.3	-11.6
1.25	1.25	-35.2		

Stabilized-HSA itself contains NaCl, Na-octanoate and Na-N-acetyltryptophanate. It is well known that NaCl suppresses the crystallization of mannitol during freezing [5] and potentially lowers the T_g' of amorphous excipients [9].

3.2 Impact of HSA-Quality on the Freezing-Behavior of Mannitol

In order to study the impact of the HSA-quality on the low temperature behavior of mannitol in the formulation, increasing amounts of unstabilized-HSA, respectively stabilized-HSA were added to a constant mannitol concentration of 6.25%. With the constant amount of mannitol the crystallization enthalpies (area of the crystallization peak) of the different samples could be compared. The higher mannitol concentration was used because it was required for the LTXRD measurements due to the detection limit of the method.

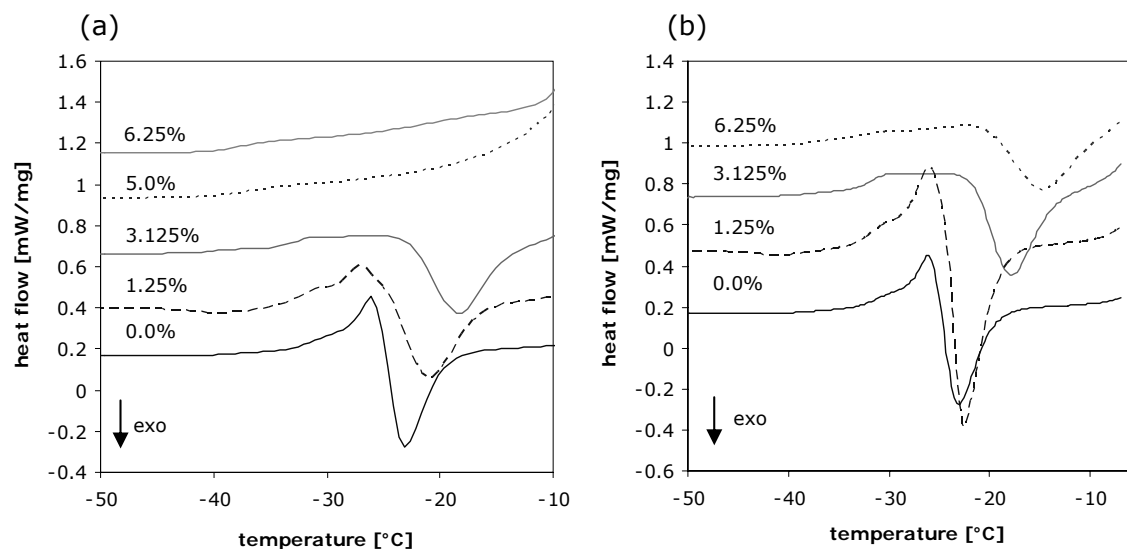


Figure 2: DSC heating scan of 6.25% mannitol with 0.0% to 6.25% stabilized-HSA (a) and 0.0% to 6.25% unstabilized-HSA (b) at 10°C/min.

In the DSC, mannitol crystallization was delayed and finally completely suppressed with increasing amounts of stabilized-HSA at a scanning rate of 10°C/min (Figure 2a and Table 3). In addition, stabilized-HSA influenced the T_g' of the formulations during freezing. Two T_g' values were detected up to a concentration of 3.125% stabilized-HSA, whereas only one T_g' was left at higher concentrations. The position of the T_g' was shifted to lower temperatures. Both results were in agreement with the studies conducted with 2.5% total solid content (compare 3.1). The same set of experiments was performed with unstabilized-HSA. By the addition of 3.125% to 6.25% unstabilized-HSA the crystallization of mannitol was delayed to higher temperatures and the crystallization enthalpy was decreasing (Figure 2b). This showed that HSA itself inhibited and delayed the crystallization of mannitol. However, T_g' was unaffected when adding unstabilized-HSA to the formulations. In the range of 1.25% to 6.25% unstabilized-HSA $T_g'_1$ was found at -31.5°C and $T_g'_2$ around -26°C. Both HSA-qualities had a significant impact on the crystallization behavior of mannitol during the heating scan of the DSC. At a concentration of 1.25% HSA, the onset of mannitol crystallization (-24.5°C) was unaffected by the addition of both, unstabilized and stabilized HSA (Figure 2). The peak maximum of the crystallization was located at -23.4°C for pure mannitol and was shifted to -22.5°C with the addition of 1.25% unstabilized-HSA, respectively to -20.9°C for stabilized-HSA. However, a higher crystallization enthalpy in the heating-scan was measured for 1.25% unstabilized-HSA containing mannitol solutions (-26.8 J/g) compared to 6.25% pure mannitol (17.1 J/g) or 6.25% mannitol with 1.25% stabilized-HSA (-17.0 J/g). The inhibitory effect of unstabilized-HSA on mannitol crystallization was less pronounced than that of stabilized-HSA, resulting in the increased crystallization

enthalpy during the rewarming for unstabilized-HSA. The lower crystallization enthalpy for mannitol as single component could be explained by the fact that mannitol had the chance to crystallize during the cooling scan, seen by an exothermal peak at -40°C (data not shown). A complete inhibition of mannitol crystallization was achieved by adding 6.25% stabilized-HSA, but not with 6.25% unstabilized-HSA. The DSC-data suggested that the studied HSA-qualities both had the ability to inhibit mannitol crystallization, with a stronger inhibitory effect seen for stabilized-HSA. Stabilized-HSA contained further additives, presumably NaCl which is known to inhibit mannitol crystallization.

Table 3: Tg'1, Tg'2 and crystallization (onset, peak maximum and enthalpy) of 6.25% mannitol with unstabilized-HSA and stabilized-HSA measured with DSC at 1°C/min, 5°C/min and 10°C/min.

HSA [%]	UNSTABILIZED-HSA		STABILIZED-HSA					
	10°C/min		10°C/min		5°C/min		1°C/min	
	Tg'1 Tg'2	crystalli- zation	Tg'1 Tg'2	crystalli- zation	Tg'1 Tg'2	crystalli- zation	Tg'1 Tg'2	crystalli- zation
0 (5:0)*	-31.2°C -27.1°C	-25.4°C ⁽¹⁾ -23.1°C ⁽²⁾ -17.1 J/g ⁽³⁾	-31.2°C -27.1°C	-25.4°C ⁽¹⁾ -23.1°C ⁽²⁾ -17.0 J/g ⁽³⁾	-34.0°C -29.4°C	-27.2°C ⁽¹⁾ -25.3°C ⁽²⁾ -10.4 J/g ⁽³⁾	-34.2°C -31.6°C	-28.9°C ⁽¹⁾ -27.9°C ⁽²⁾ -5.0 J/g ⁽³⁾
1.25 (5:1)*	-32.0°C -27.2°C	-24.6°C ⁽¹⁾ -22.6°C ⁽²⁾ -26.8 J/g ⁽³⁾	-32.9°C -28.1°C	-25.1°C ⁽¹⁾ -21.0°C ⁽²⁾ -17.0 J/g ⁽³⁾	-34.1°C -29.4°C	-27.9°C ⁽¹⁾ -26.5°C ⁽²⁾ -12.9 J/g ⁽³⁾	-35.1°C -31.8°C	-30.0°C ⁽¹⁾ -28.7°C ⁽²⁾ -5.3 J/g ⁽³⁾
3.125 (5:3)*	-31.4°C -25.0°C	-20.2°C ⁽¹⁾ -14.6°C ⁽²⁾ -12.5 J/g ⁽³⁾	-39.5°C -32.7°C	-22.5°C ⁽¹⁾ -18.4°C ⁽²⁾ -11.4 J/g ⁽³⁾	-34.6°C	-26.9°C ⁽¹⁾ -24.0°C ⁽²⁾ -8.8 J/g ⁽³⁾	-36.1°C	-31.4°C ⁽¹⁾ -29.6°C ⁽²⁾ -6.3 J/g ⁽³⁾
6.25 (5:5)*	-31.4°C -25.0°C	-20.2°C ⁽¹⁾ -14.6°C ⁽²⁾ -12.5 J/g ⁽³⁾	-37.7°C	no cryst.	-39.0°C	-14.6°C ⁽¹⁾ -11.3°C ⁽²⁾ -1.1 J/g ⁽³⁾	-40.4°C	-29.0°C ⁽¹⁾ -25.0°C ⁽²⁾ -6.6 J/g ⁽³⁾

* ratio of mannitol : HSA ⁽¹⁾ onset ⁽²⁾ peak maximum ⁽³⁾ enthalpy of crystallization

3.3 Influence of the Applied Scanning Rate on Thermal Behavior of Mannitol-HSA Formulations

In order to reflect the conditions predominating during lyophilization and to investigate how the scanning rate influences T_g' and the crystallization behavior of mannitol, the DSC was operated at 1°C/min, 5°C/min and 10°C/min for the heating and cooling-scans. At the scanning rates 1°C/min and 5°C/min 6.25% mannitol in a solution with 6.25% stabilized-HSA had the chance to crystallize during the cooling scan. As a consequence less material crystallized during heating resulting in a lowered crystallization enthalpy of -5.0 J/g at 1°C/min and -10.4 J/g at 5°C/min compared to -17.1 J/g at 10°C/min (Figure 4). It was already shown that mannitol crystallization was completely suppressed by the addition of more than 3.125% stabilized-HSA to 6.25% mannitol at a scanning rate of 10°C/min. At a scanning rate of 1°C/min and 5°C/min mannitol crystallization was detected up to a concentration 6.25% stabilized-HSA.

Comparing the results obtained with the different scanning rates it became obvious that the thermal events occurred at lower temperatures, when 1°C/min, respectively 5°C/min were used (Table 3). T_g' is a kinetic parameter and therefore depends on the applied scanning rate [26] with a shift to lower temperatures at reduced scanning rates [30]. This has to be considered for the development of a lyophilization cycle due to the lower cooling rates that are frequently used.

3.4 Influence of Na-Octanoate, Na-N-Acetyltryptophanate and NaCl on the Freezing Behavior of Mannitol

A more pronounced inhibitory effect on crystallization and the lowering of T_g' was noticeable for stabilized-HSA compared to unstabilized-HAS (compare 3.2). The solution of 6.25% stabilized-HSA used for the DSC experiments contained 5 mM (0.08%) Na-octanoate and 5 mM (0.13%) Na-N-acetyltryptophanate and at least 31.5 mM (0.19%) NaCl. In the concentrations actually used for stabilizing HSA, Na-N-actyltryptophanate and Na-octanoate showed no significant inhibition of mannitol crystallization (Figure 3). Whereas 5 mM Na-octanoate showed no impact on T_g' , $T_g'_1$ was lowered by 1.0°C and $T_g'_2$ by 1.5°C in the presence of 5 mM Na-N-actyltryptophanate. In contrast NaCl had a major influence on the low temperature behavior of mannitol. At a concentration of 0.19% NaCl the suppression of mannitol crystallization and the decrease of $T_g'_1$ by 3.9°C and $T_g'_2$ by 2.8°C. The HSA-stabilizers, principally NaCl were responsible for the differences in the low-temperature behavior in formulations with stabilized and unstabilized-HSA

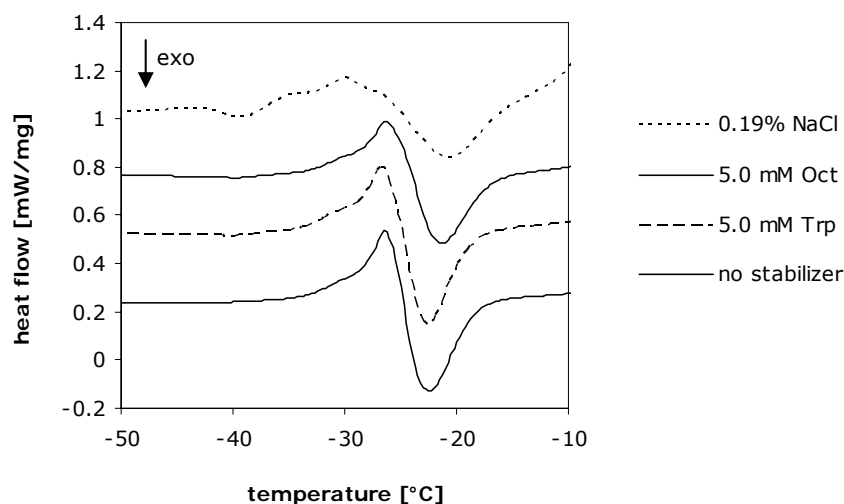


Figure 3: DSC heating scan of 6.25% mannitol with 5 mM Na-N-acetyltryptophanate (Trp), 5 mM Na-octanoate (Oct) and 0.19% NaCl at 10°C/min.

The impact of 0.05% to 1.0% NaCl on the low temperature behavior of 6.25% mannitol solution is shown in Figure 4a. The addition of NaCl inhibited mannitol crystallization and delayed it to higher temperatures. At the same time T_g' was significantly lowered in a linear way (Figure 4b).

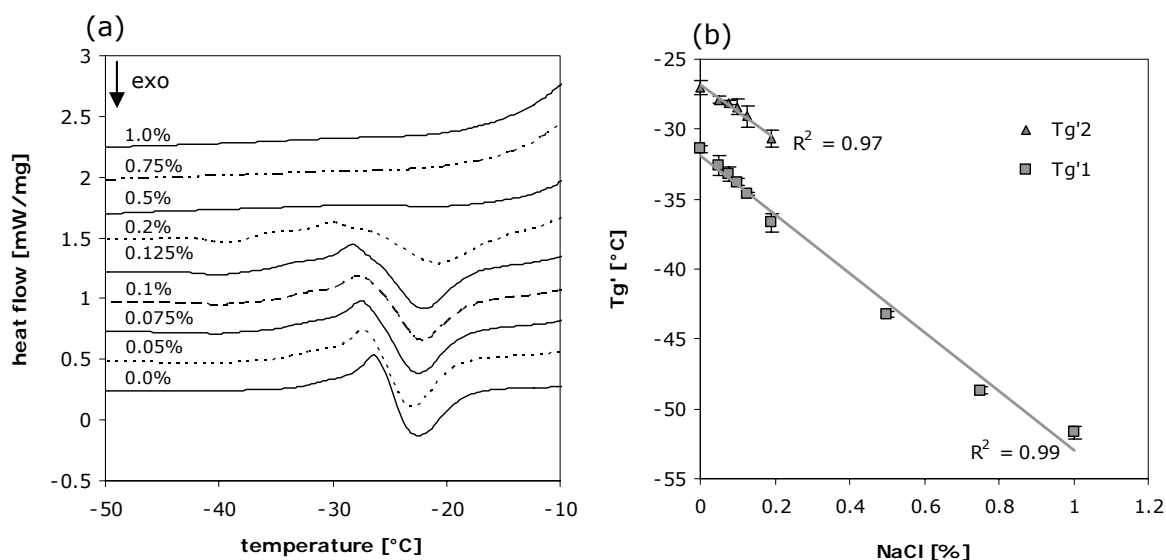


Figure 4: DSC heating scan at 10°C/min of 6.25% mannitol with 0.0% to 1.0% NaCl (a) and $T_g'1$ and $T_g'2$ plotted for 0.0% to 1.0% NaCl.

The shift of T_g' in formulations with NaCl could be due to the very low T_g' of NaCl itself, which lies below -60°C [31]. NaCl can act as plasticizer by increasing the amount of unfrozen water in the amorphous phase, leading to a lowering of the T_g' of amorphous excipients. As lyophilization has to be conducted at product temperatures below T_g'

[32,36], the samples with the lowered T_g' have to be dried at reduced product temperatures resulting in longer, less efficient drying processes.

3.5 Influence of Na-Octanoate, Na-N-Acetyltryptophanate and NaCl on the Freezing Behavior of Unstabilized-HSA and Mannitol

The impact of the stabilizers was further investigated using the DSC heating scan at 10°C/min for the more complex formulations composed of 6.25% mannitol and 6.25% unstabilized-HSA. Mannitol crystallization was less affected by 5 mM Na-octanoate or 5 mM Na-N-acetyltryptophanate than by the addition of 0.19% NaCl (Figure 5). By adding a combination of the stabilizers (5 mM Na-N-acetyltryptophanate, 5 mM Na-octanoate, 0.19% NaCl) to a solution with 6.25% mannitol and 6.25% unstabilized-HSA, the low temperature behavior of the formulation resembled that of a formulation with stabilized-HSA.

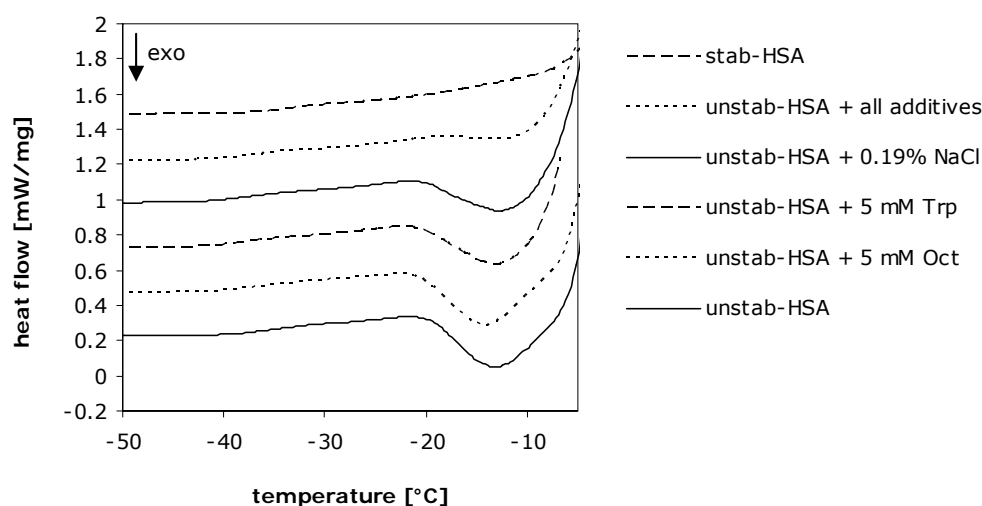


Figure 5: DSC heating scan at 10°C/min of 6.25% unstabilized-HSA and 6.25% mannitol, without additives, 5 mM Na-octanoate (Oct), 5 mM Na-N-acetyltryptophanate (Trp), 0.19% NaCl and a combination of all stabilizers compared to 6.25% stabilized-HSA and 6.25% mannitol.

The crystallization of mannitol was inhibited and T_g' was shifted to lower temperatures. These data demonstrated that the HSA-stabilizers, especially NaCl, were responsible for the changed freezing behavior of mannitol-HSA.

3.6 Influence of NaCl on Freezing Behavior of Mannitol with Stabilized-HSA

As it is crucial to consider the lowered T_g' for the development of a lyophilization cycle to avoid collapse, the impact of NaCl was further investigated. The focus was set on NaCl, as it had the most pronounced effect of the HSA-stabilizers during freezing. Therefore, the addition of NaCl to mixtures of mannitol and stabilized-HSA at a ratio of 1:1 was analyzed with DSC and LTXRD. This ratio was chosen for the more detailed studies as it is often found in protein formulation and commercial lyophilized products [12]. Due to the detection limit of the LTXRD, the solutions with a higher total solid content of 6.25% HSA, respectively mannitol were used. DSC revealed a significant shift of T_g' to lower temperatures upon the addition of NaCl (Figure 6).

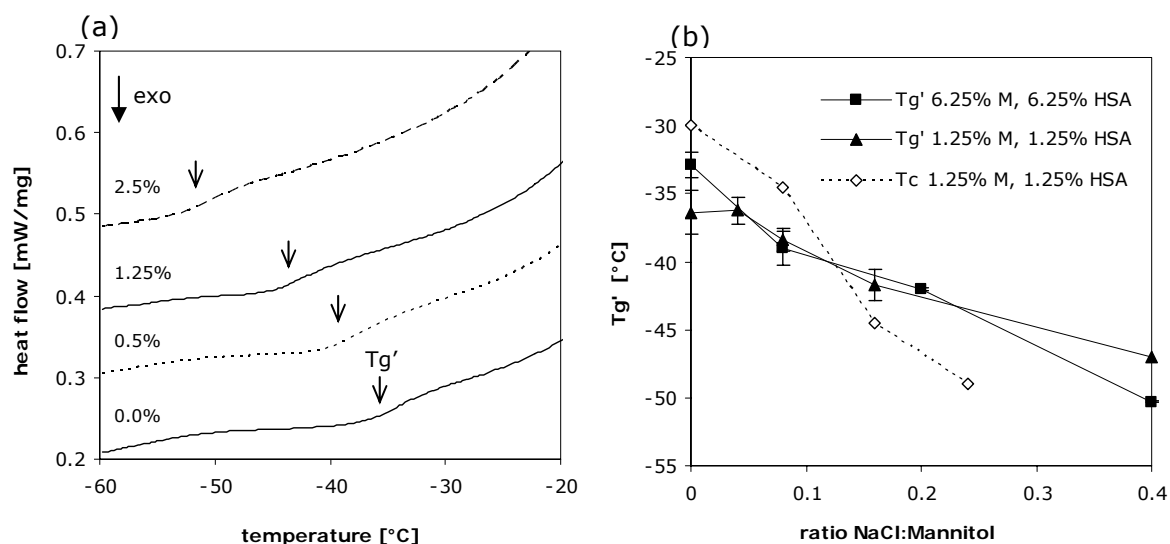


Figure 6: DSC heating scan of 6.25% mannitol and 6.25% stabilized-HSA, 0.05 to 2.5% NaCl (a) and T_g' and T_c of 6.25% mannitol and 6.25% stabilized-HSA compared to 1.25% mannitol and 1.25% stabilized-HSA plotted against the ratio of NaCl to mannitol (b).

The addition of 0.5% NaCl lowered the T_g' of 1.25% mannitol and 1.25% stabilized-HSA in a linear way from -37°C to -47°C . The results could be confirmed by solutions containing the 5-fold total solid. With the addition of 0.5% to 2.5% NaCl to a solution of 6.25% stabilized-HSA and 6.25% mannitol a comparable depression of T_g' was detected (Figure 6a). At a T_g' near -50°C measured for the high NaCl concentrations, the development of a feasible and economical lyophilization process is hardly possible. The results showed that it is not the total amount of NaCl present in the sample but the ratio of NaCl to other excipients in a formulation that determined the degree of the lowering of the T_g' (Figure 6b). This can be ascribed to the fact that the T_g' is concentration independent for diluted systems [34].

3.7 Determination of T_c with Cryomicroscopy

Cryomicroscopy was used to determine the collapse temperature T_c of the solutions. T_c is the temperature at which the interstitial water in the frozen matrix becomes significantly mobile [35]. To avoid collapse during lyophilization the product temperature has to be kept below T_c . The collapse temperature approximately coincides with the T_g' measured by DSC [32,33] and usually lies about 2°C higher than T_g' [36]. In Figure 7 the behavior of 1.25% mannitol and 1.25% stabilized-HSA with 0.2% NaCl as an example is visualized.

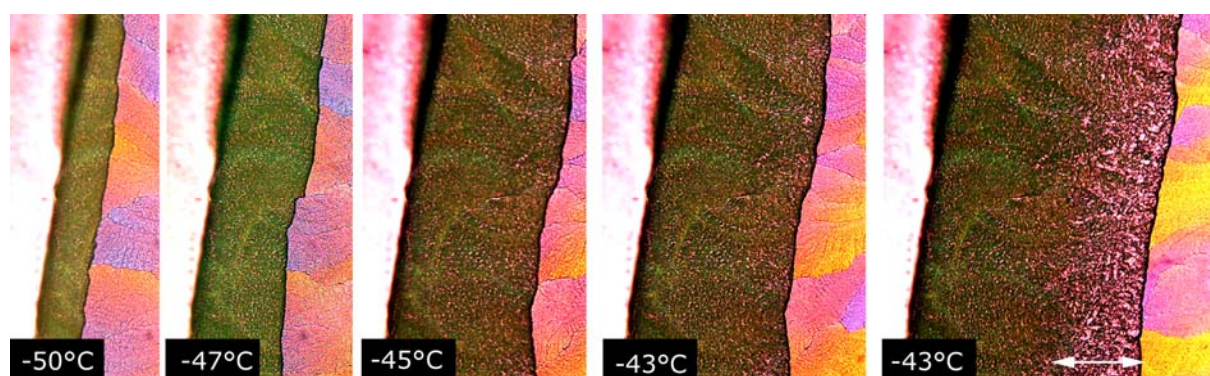


Figure 7: Cryomicroscopy of 1.25% mannitol and 1.25% stabilized-HSA, 0.2% NaCl from -50°C to -45°C. The arrow marks the collapsed area.

The dark section represents the moving drying front. The bright section derives from the frozen solution, with colors created by the utilization of polarization filters to achieve a better contrast between the drying front and the frozen solution. At temperatures between -50°C and -45°C the drying front was compact and did not show structural changes. At -43°C the drying front lost its compact structure. Holes and cracks appeared, through which the colored background became visible. The collapse temperature was approximated to range between -45°C and -43°C. In the progress of the experiment smaller temperature steps were used and T_c was finally determined to be -44.5°C.

T_c and T_g' both were lowered by the addition of NaCl (Figure 6b). The results from the cryomicroscopic experiment suggested substantial differences between T_c and T_g' with higher values for 0.0% and 0.1% NaCl and lower values for 0.2% to 0.3% NaCl. This could be explained by the different experimental set ups and time-temperature profiles used in DSC and cryomicroscopy. While DSC is working with a constant dynamic heating scan of 10°C/min, cryomicroscopy is working with isothermal and dynamic segments and lower scanning rates. The lower scanning rates could explain the steeper decline of T_c and the shift to lower temperatures compared to the DSC experiments. In the DSC thermal events were shifted to lower temperatures when the scanning rate was reduced. Knopp et al. (1998) determined lower values for the T_c of sucrose solutions using

cryomicroscopy compared to T_g' with a T_c of -37.7°C measured for 5% and 10% sucrose, while the T_g' lies at -32.0°C [37]. However, sucrose solutions at higher concentrations (above 40%) can exhibit two transitions. The transition at -40°C is usually assigned to the real glass transition, while the transition at -32°C is due to the onset of melting of ice crystals [38]. The T_c below -45°C for mannitol stabilized-HSA formulations with 0.2% and 0.3% NaCl could become critical during lyophilization.

3.8 Analytics of the Mannitol Freezing Behavior with LTXRD

DSC offers information on crystalline and amorphous phases in the frozen state. However, it is not possible to identify and characterize the crystalline phases according to their composition and modifications [39]. With LTXRD it is possible to identify and characterize multiple crystalline phases [40,41]. Because of the detection limit of LTXRD the higher mannitol concentration of 6.25% had to be used.

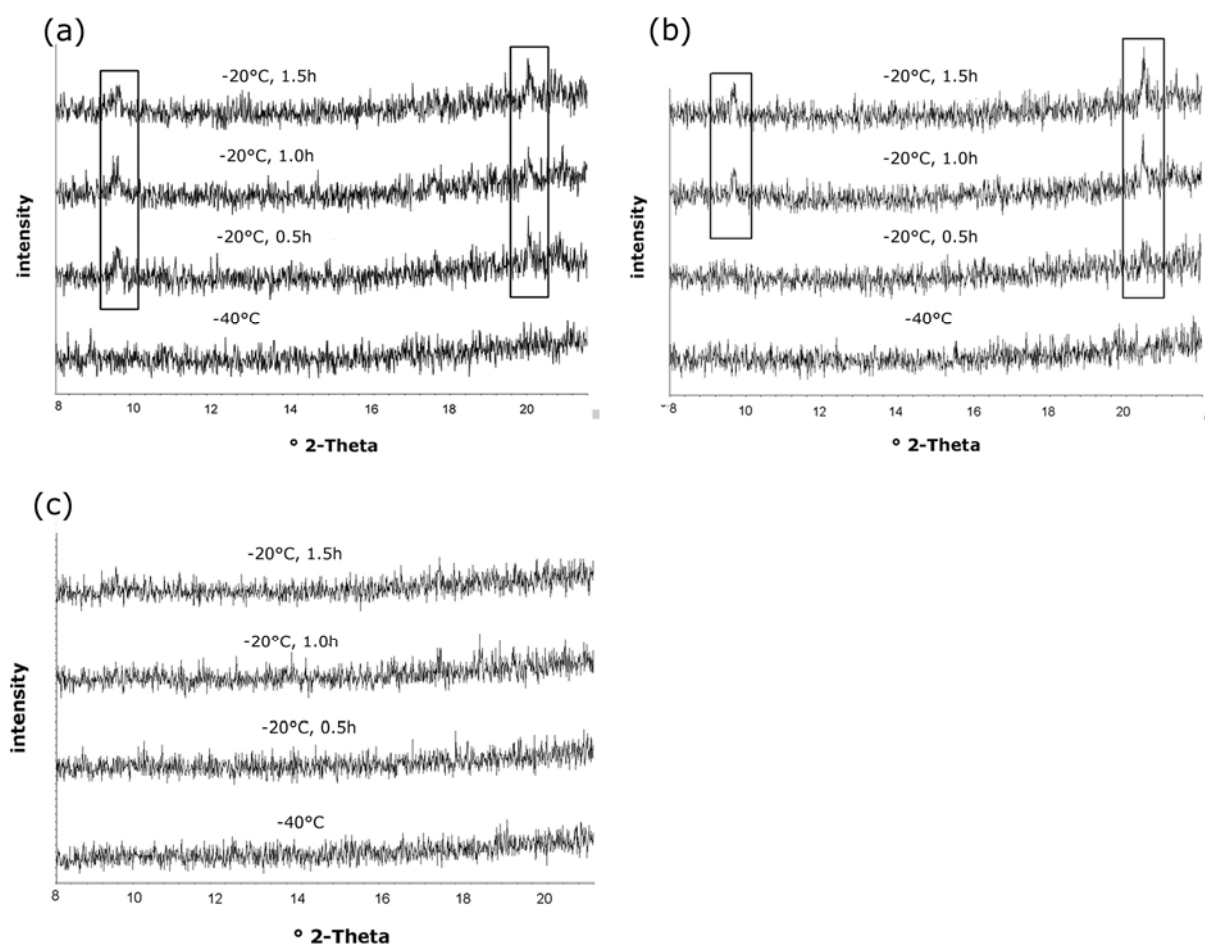


Figure 8: LTXRD of 6.25% mannitol and 6.25% stabilized-HSA with 0.0% NaCl (a), 1.25% NaCl (b) and 2.5% NaCl (c) after cooling to -40°C and during the 3 scans of the annealing phase at -20°C .

After freezing a solution with 6.25% mannitol and 6.25% stabilized-HSA to -40°C in the LTXRD no peaks of crystalline material could be detected besides the peaks of ice. After the temperature was increased to -20°C mannitol crystallized in the δ -modification, as could be seen by the peak at $9.7^{\circ} 2\text{-}\theta$ and $20.4^{\circ} 2\text{-}\theta$ and the absence of a signal at $17.9^{\circ} 2\text{-}\theta$ (Figure 8a). The addition of 1.25% NaCl delayed the crystallization of mannitol. Here at the end of the first scan at -20°C after approximately 20 minutes a peak at $20.4^{\circ} 2\text{-}\theta$ appeared. In the further course of the annealing phase the peaks gained in intensity (Figure 8b). Increasing the NaCl concentration to 2.5% led to a complete inhibition of crystallization and no crystalline material was detected with the LTXRD (Figure 8c). Unlike in LTXRD, no crystallization was measured in the heating scan of the DSC for solutions with 6.25% mannitol and 6.25% stabilized-HSA. Generally, the kinetic mechanism of crystallization is influenced by temperature [42]. During the dynamic heating scan of the DSC at $10^{\circ}\text{C}/\text{min}$ mannitol did not have the chance to crystallize, while the isothermal steps in the LTXRD provided enough time for crystallization.

4. Conclusions

DSC showed that unstabilized-HSA, stabilized-HSA and NaCl can delay and inhibit the crystallization of mannitol, which was confirmed by LTXRD. Thereby, stabilized-HSA showed a different behavior than unstabilized-HSA because of the presence of NaCl, Na-octanoate and Na-N-acetyltryptophanate. In the particular concentration used for the stabilization of HSA, NaCl had the most distinct impact on the low temperature behavior of mannitol. Already the addition of small quantities of NaCl shifted T_g' and T_c of mannitol formulations to lower temperatures, which could become critical for a freeze-drying process with respect to collapse. The study showed that the freezing step had a significant effect on the physico-chemical properties of mannitol-HSA formulations, which can affect the subsequent drying process and the physico-chemical properties of the lyophilized products. The study demonstrated that already the freezing step has a significant effect on the behavior of the formulations with mannitol and HSA. It can be assumed that this affect the subsequent drying process and the physico-chemical properties of the lyophilized products. The lyophilization behavior of the formulations with stabilized-HSA and mannitol are described in Chapter 4 of the thesis.

5. References

1. L. Jingsong, T. Viverette, M. Virgin, M. Anderson, P. Dalal. A study of the impact of freezing on the lyophilization of a concentrated formulation with a high fill depth. *Pharm. Dev. Technol.* **10**:261-272 (2005).
2. J. A. Searles, J. F. Carpenter, T. W. Randolph. Annealing to Optimize the Primary Drying Rate, Reduce Freezing-Induced Drying Rate Heterogeneity, and Determine T_g' in Pharmaceutical Lyophilization. *J. Pharm. Sci.* **90**:872-887 (2001).
3. X. Lu, M. Pikal. Freeze-Drying of Mannitol-Trehalose-Sodium Chloride-Based Formulations: The impact of Annealing on Dry Layer Resistance to Mass Transfer and Cake Structure. *Pharm Dev. Technol.* **9**:85-95 (2004).
4. A. Cannon, E. Trappler. The influence of Lyophilization on the Polymorphic Behavior of Mannitol. *PDA J. Pharm. Sci. Technol.* **54**:13-22 (2000).
5. C. Telang, L. Yu, R. Suryanarayanan. Effective Inhibition of Mannitol Crystallization in Frozen Solutions by Sodium Chloride. *Pharm. Res.* **20**:660-667 (2003).
6. M. F. Mazzobre, M. P. Longinotti, H. R. Corti, M. P. Buera. Effect of Salts on the Properties of Aqueous Sugar Systems, in Relation to Biomaterial Stabilization. 1. Water Sorption Behavior and Ice Crystallization/Melting. *Cryobiol.* **43**:199-210 (2001).
7. L. M. Her, M. Deras, S. L. Nail. Electrolyte-Induced Changes in Glass Transition Temperatures of Freeze-Concentrated Solutes. *Pharm. Res.* **12**:768-772 (1995).
8. M. J. Akers, N. Milton, S. R. Byrn, S. L. Nail. Glycine Crystallization During Freezing: The Effect of Salt Form, pH, and Ionic Strength. *Pharm. Res.* **12**:1455-1461 (1995).
9. E. Y. Shalaev, F. Franks. Crystalline and Amorphous Phases in the Ternary System Water-Sucrose-Sodium Chloride. *J. Phys. Chem.* **100**:1144-1152 (1996).
10. H. Nicolajsen, A. Hvidt. Phase Behavior of the System Trehalose-NaCl-Water. *Cryobiol.* **31**:199-205 (1994).
11. W. H. Hanish, P. M. Fernandes, T. Taforo. Stable formulations for lipophilic IL-2 proteins. United States Patent 4,992,271 (1991).
12. N. Zander. Ready-to-use prothrombin time reagent containing recombinant tissue factor, antioxidant and human serum albumin. Eur. Pat. Appl. EP 942,284 A (1992).
13. R. M. Platz, N. Kimura, O. Satoh, L. C. Foster. Dry powder formulations of interferons. PCT Int. Appl, WO 953,1479 A1 (1995).
14. A. Pyne, R. Surana, R. Suryanarayanan. Crystallization of Mannitol below T_g' during Freeze-Drying in Binary and Ternary Aqueous Systems. *Pharm. Res.* **19**:901-908 (2002).
15. B. Lyuet, D. Rasmussen. Study by differential thermal analysis of the temperature of instability of rapidly cooled solutions of glycerol, ethylene glycol, sucrose and glucose. *Biodyn.* **10**:1167-1191 (1968).
16. M. J. Pikal, K. M. Dellermann, M. L. Roy, R. M. Rigglin. The Effects of Formulation Variables on the Stability of Freeze-Dried Human Growth Hormone. *Pharm. Res.* **8**:427-436 (1991).
17. A. Kim, M. Akers, S. Nail. The Physical State of Mannitol after Freeze-Drying: Effect of Mannitol Concentration, Freezing Rate and a Noncrystallizing Cosolute. *J. Pharm. Sci.* **87**:931-935 (1998).
18. B. Lueckel, D. Bodmer, B. Helk, H. Leuenberger. Formulations of Sugars with Amino Acids or Mannitol- Influence of Concentration Ratio on Properties of the Freeze-Concentrate and the Lyophilisate. *Pharm. Dev. Technol.* **3**:325-336 (1998).
19. X. Liao, R. Krishnamurthy, R. Suryanarayanan. Influence of the Active Pharmaceutical Ingredient Concentration on the Physical State of Mannitol- Implications in Freeze-Drying. *Pharm. Res.* **22**:1978-1985 (2005).

20. U.S. Food and Drug Administration, Code of Federal Regulations, Title 21, Volume 7: §640.80 Albumin (Human), revised as on April 1 (2004).
21. G. Scatchard, L. E. Strong, W. L. Hughes Jr., J. N. Ashworth, A. H. Sparrow. Chemical, clinical, and Immunological studies and the products of human plasma fractionation. XXVI. The properties of human serum albumin at low salt content. *J. Clin. Invest.* **24**:671-679 (1945).
22. G. A. Ballou, P. D. Boyer, J. M. Luck, G. F. Lum. The heat coagulation of human albumin. *J. Biol. Chem.* **153**: 589-605 (1944).
23. T. Arakawa, Y. Kita. Stabilizing effect of caprylate and acetyltryptophanate on heat-induced aggregation of bovine serum albumin. *Bioch. et Bioph. Acta.* **1479**:32-36 (2000).
24. L. Saso, G. Valentini, E. Grippa, M. G. Leone, B. Silvestrini. Effect of selected substances on heat-induced aggregation of Albumin, IgG and Lysozyme. *Res. Com. Mol. Pathol. Pharmacol.* **102**:15-28 (1998).
25. L. Yu, N. Milton, E. Groleau, D. Mishra, R. Vansickle. Existence of a Mannitol Hydrate during Freeze-Drying and Practical Implications. *J. Pharm. Sci.* **88**:196-198 (1999).
26. L. Yu. Amorphous pharmaceutical solids: preparation, characterization and stabilization. *Adv. Drug Del. Rev.* **48**:27-42 (2001).
27. R. Cavatur, N. Vemuri, A. Pyne, Z. Chrzan, D. Toledo-Velasquez, R. Suryanarayanan. Crystallization Behavior of Mannitol in Frozen Aqueous Solutions. *Pharm. Res.* **19**:894-900 (2002).
28. P. Meredith, A. Donald, R. Pyne. Freeze-Drying: In Situ Observations Using Cryoenvironmental Scanning Electron Microscopy and Differential Scanning Calorimetry. *J. Pharm. Sci.* **85**:631-637 (1996).
29. K. Izutsu, S. Kojima. Excipient crystallinity and its protein-structure-stabilizing effect during freeze-drying. *J. Pharm. Pharmacol.* **54**:1033-1039 (2002).
30. D. Q. M. Craig, P. G. Royall, V. L. Kett, M. L. Hopton. The relevance of the amorphous state to pharmaceutical dosage forms: glassy drugs and freeze-dried systems. *Int. J. Pharm.* **179**:179-207 (1999).
31. F. Franks. Solid Aqueous solution. *Pure Appl. Chem.* **65**:2527-2537 (1993)
32. M. J. Pikal. Freeze-drying of proteins: Part I: Process design. *Biopharm.* **3**:18-26 (1990).
33. M. J. Pikal. Freeze-drying of proteins: Part II: formulation selection. *Biopharm.* **3**:26-30 (1990).
34. T. Chen, D. M. Oakley. Thermal analysis of proteins of pharmaceutical interest. *Thermochim. Acta* **248**:229-244 (1995).
35. T. A. Jennings. Lyophilization: Introduction and Basic Principles. Interpharm Press, Colorado, USA (1999).
36. M. J. Pikal, S. Shah. The collapse temperature in freeze drying: dependence on measurement methodology and rate of water removal from the glassy phase. *Int. J. Pharm.* **62**:165-186 (1990).
37. S. A. Knopp, S. Chongprasert, S. L. Nail. The relationship between the TMDSC Curve of Frozen Sucrose Solutions and Collapse during Freeze-Drying. *J. Therm. Anal.* **54**:659-672 (1998).
38. E. Y. Shalaev, F. Franks. Structural Glass Transition and Thermophysical Processes in Amorphous Carbohydrates and their Supersaturated Solutions. *J. Chem. Soc. Faraday Trans.* **91**:1511-1517 (1995).
39. A. Pyne, R. Suryanarayanan. Phase Transitions of Glycine in Frozen Aqueous Solutions and during Freeze-Drying. *Pharm. Res.* **18**:1448-1454 (2001).
40. R. Cavatur, R. Suryanarayanan. Characterization of phase transition during freeze-drying by in situ X-ray powder diffractometry. *Pharm. Dev. Tech.* **3**:579-586 (1998).
41. R. Cavatur, R. Suryanarayanan. Characterization of frozen aqueous solutions by low temperature X-ray powder diffractometry. *Pharm. Res.* **15**:193-198 (1998).
42. N. Rodríguez-Hornedo, D. Murphy. Significance of Controlling Crystallization Mechanisms and Kinetics in Pharmaceutical Systems. *J. Pharm. Sci.* **88**:651-660 (1999).

Chapter 4

Physico-chemical Lyophilization Behavior of Mannitol-Human Serum Albumin Formulations

Abstract

The lyophilization behavior is influenced by the presence of salts. The impact of NaCl on drying-time and the morphology after lyophilization was studied for formulations with mannitol and HSA, using different freezing-protocols. The drying-process was monitored by thermocouples and microbalance technique. Karl-Fischer titration, DSC, XRD and SEM were used to study the products after lyophilization and 6 months storage at 2-8°C, 25°C / 60% RH and 40°C / 75% RH.

NaCl decreased the drying-time of mannitol-HSA formulations, indicating morphological changes, which was confirmed by XRD and SEM. Without NaCl exclusively δ -mannitol was formed, which remained physico-chemically stable upon storage for 6 months. With increasing NaCl concentrations more β -mannitol and finally amorphous products were formed, whereby the freezing-protocol determined how much NaCl was needed to achieve an amorphous product. Upon storage, the amorphous state could not be preserved and mannitol and NaCl crystallized, which could damage proteins in the formulations. However, regarding the stability of HSA in the lyophilized products, monitored by turbidimetry and HP-SEC, the addition of NaCl could prevent increases in turbidity and the loss of HSA-monomers upon storage. Here the benefit of NaCl on HSA stability outbalanced the potential drawbacks that morphological changes, like crystallization impose on protein stability in the lyophilized products.

Keywords: lyophilization, mannitol, HSA, morphology, storage stability

1. Introduction

For the development of lyophilized formulations it is essential to add excipients that stabilize proteins against stress and damage during freezing, drying and upon storage. One common way to achieve elegant and stable lyophilized products is combining a crystalline bulking agent, e.g. mannitol or glycine with a second excipient that remains amorphous and acts as lyoprotector e.g. sucrose, trehalose or human serum albumin (HSA) [1-4]. Morphology and physico-chemical properties of the selected excipients used to stabilize the active protein can be influenced by the presence of salts [5,6]. Therefore, it is important to investigate and understand how the lyophilization process and the lyophilized products are influenced by the salt concentration. As model system a formulation with mannitol as cake forming agent and HSA as amorphous stabilizer is used, based on the formulation of the hydrophobic cytokine. For mannitol it is described in literature, that both the applied lyophilization process [7,8] and the presence of other excipients like lyoprotectants, buffer salts or proteins have an impact on the morphology of mannitol and can both promote and inhibit mannitol crystallization [1,9,10]. HSA is used as cyro- and lyoprotector for lyophilization, especially in older formulations. HSA is stabilized against the heat induced stress during the required pasteurization process by Na-octanoate [11] and Na-N-acetyltryptophanate [12]. Further, HSA is stabilized by NaCl [12-15] with the consequence that the ionic strength in protein formulations stabilized with HSA is inevitably increased and the physico-chemical properties can be affected due to the presence of NaCl brought into the formulation.

Detailed studies of the low temperature behavior of formulations with mannitol and HSA are described in Chapter 3. It could be shown that mannitol crystallization was inhibited by the addition of HSA and NaCl. Comparing the different HSA-stabilizers, NaCl had the most pronounced effect on the low temperature behavior of the formulations. NaCl further led to a significant depression of the collapse temperature (T_c) and the glass transition of the maximally freeze-concentrated solutions (T_g') of the formulations. The outcome of the freezing-studies has to be taken into consideration for the development of the lyophilization process, as freezing governs the physico-chemical properties of the excipients during and after lyophilization. To avoid collapse for example the product temperature during the process has to be kept below the collapse temperature [16,17]. The focus of Chapter 4 was set on the impact of NaCl on the lyophilization process of mannitol-HSA-based formulations and the physico-chemical properties of the lyophilized products. Stabilized-HSA, which enhances the complexity of the formulations, was selected as excipient as it was the exclusively used HSA-quality in the lyophilized cytokine formulation.

2. Materials and Methods

2.1 Materials

Stabilized-HSA from Grifols (Langen, Germany) was used as 20% solution and further contained 16 mmol Na-octanoate, 16 mmol Na-N-acetyltryptophanate and 3.0% NaCl as stabilizers. For the experiments the solution was diluted to the desired concentration. Mannitol was purchased from Caelo (Hilden, Germany) and NaCl from Sigma (Steinheim, Germany). The basic formulation contained 1.25% mannitol and 1.25% stabilized-HSA. Based on this formulation the fraction of the excipients, the total solid concentration and the NaCl concentration was varied. The pH of the solution was adjusted to 7.0 ± 0.1 using NaOH or HCl.

2.2 Methods

2.2.1 Lyophilization Process

1.2 ml of the solution were dried in 2 R vials from Schott (Mainz, Germany) in the Epsilon 2-12 D freeze-drier from Christ (Osterrode, Germany). Four different freezing-protocols I to IV were used for the production of the samples (Table 1). Primary drying was conducted at a shelf-temperature of -5°C and a pressure of 0.1 mbar. For secondary drying the shelf-temperature was increased to 30°C , while the pressure was kept constant at 0.1 mbar.

Table 1: Lyophilization programs I-IV used for the studies.

program	freezing-protocol	freezing-rate
I	within 2 h to -50°C	$0.46^{\circ}\text{C}/\text{min}$
II	within 2 h to -50°C Annealing at -20°C for 2 h	$0.46^{\circ}\text{C}/\text{min}$
III	within 1 h to -50°C	$0.92^{\circ}\text{C}/\text{min}$
IV	freezing on pre-cooled shelves (-50°C)	$2.3^{\circ}\text{C}/\text{min}$

The lyophilization process was monitored by measuring the product temperature of selected vials with thermocouples [18]. The end point of primary-drying was reached when the temperature in the vial was exceeding the shelf-temperature. As second tool to monitor the drying process, a microbalance type CWS-40 (Christ, Osterrode, Germany) was used. With the microbalance it is possible to determine the actual drying-rate during the process. The end of the primary drying is reached when the drying rate falls below

3 mg/h [19]. The thermocouples were placed into vials on a completely filled shelf as well as in vials, which were located on an extra shelf in a distance of 5 cm to each other. The vials were placed separately to assure the comparability of the results with the data from the microbalance. The microbalance was also placed separately on an extra shelf in the freeze-drier.

2.2.2 X-ray Powder Diffraction (XRD)

The morphology of the lyophilized products was analyzed with X-ray powder diffraction (XRD) from $5-40^\circ 2-\Theta$, with steps of $0.05^\circ 2-\Theta$ and a duration of 2 seconds per step on the X-ray diffractometer XRD 3000 TT (Seifert, Ahrenburg, Germany), equipped with a copper anode (40 kV, 30 mA, wavelength 154.17 pm).

2.2.3 Differential Scanning Calorimetry (DSC)

The samples were analyzed with the Netzsch DSC 204 Phoenix® (Selb, Germany), calibrated with indium from 0°C to 150°C with a rate of $10^\circ\text{C}/\text{min}$. Approximately 10 mg of the lyophilized samples were analyzed in sealed Al-crucibles. The thermal events were analyzed in the heating scan of the DSC.

2.2.4 Karl-Fischer Titration

The residual moisture of the samples was analyzed by coulometric Karl-Fischer titration using the Aqua 40.00 titrator with a headspace module (Analytik Jena AG, Halle, Germany). For the measurement at least 10 mg of the lyophilized sample was heated to 80°C . The evaporated water was transferred into the titration solution and the amount of H_2O was determined.

2.2.5 Turbidimetry

The turbidity of the samples in formazine nephelometric units (FNU) was measured by 90° light scattering at $\lambda=860\text{ nm}$ with the NEPHLA turbidimeter (Dr. Lange, Düsseldorf, Germany) calibrated with formazine as standard. To evaluate the degree of turbidity the reference solutions I-IV of the European Pharmacopoeia method 2.2.1 (clarity and degree of opalescence of liquids) were used [20]. A stock solution was prepared by mixing hydrazine-sulfate (10 mg/ml) and hexamethylenetetramine (100 mg/ml) at a ratio of 1:1. After 24 hours the stock solution was further diluted with water to concentrations of 0.075 mg/ml hydrazine sulfate and 0.75 mg/ml

hexamethylenetetramine. The reference solutions were prepared by diluting the stock solution according to the Ph. Eur. and the corresponding turbidity in FNU was measured (Table 2).

Table 2: Composition of the reference solutions according to Ph. Eur., corresponding turbidity and degree of opalescence.

reference solution	diluted stock solution [ml]	water [ml]	turbidity [FNU]	degree of opalescence
I	5	95	3.2	clear (\leq Ref I)
II	10	90	6.1	slightly opalescent (\leq Ref II)
III	30	70	17.8	opalescent (\leq Ref III)
IV	50	50	29.4	very opalescent (\leq Ref IV)

2.2.6 High Pressure Size Exclusion Chromatography (HP-SEC)

HSA-aggregation was determined by HP-SEC on a HP1100 (Agilent Technologies, Waldbronn, Germany) using a TSKgel G3000SWxl column (Tosoh Biosep, Stuttgart, Germany) with a guard column. The running buffer was composed of 20 mM NaH_2PO_4 and 100 mM NaCl (pH 6.8). The analytics were performed at a flow rate of 0.5 ml/min with UV-detection at 280 nm.

3. Results and Discussion

3.1. Lyophilization of the System Mannitol-HSA-NaCl

3.1.1 Drying Process

The drying process, basically the length of primary drying is depending on the structure of the frozen matrix and with it the dry layer resistance. Thereby, the composition of the formulation and the applied freezing procedure, which determines the size of the ice crystals can influence the duration of primary drying [21,22]. The impact of the freezing protocol and the addition of NaCl to formulations with 1.25% mannitol and 1.25% stabilized-HSA on primary drying time were investigated using thermocouples and the microbalance technique. Samples dried after a regular freezing with 0.45°C/min (program I) exhibited the shortest primary drying time ($7.6 \text{ h} \pm 0.3 \text{ h}$, $n=3$) after vacuum was applied. Longer primary drying times were observed when the vials were frozen with a higher freezing-rate by placing them on pre-cooled shelves ($8.9 \text{ h} \pm 0.7 \text{ h}$, $n=3$) and after freezing with an annealing step ($9.9 \text{ h} \pm 0.1 \text{ h}$, $n=3$). Annealing can both increase and decrease the drying-rate. Searles et al. (2001) showed that annealing at a temperature above T_g' leads to a 3.5 fold increase in the primary-drying rate of sucrose-hydroxyethyl starch formulations, due to increased ice-crystal size and simplified amorphous structures [23]. On the other hand, Pikal et al. (2004) determined prolonged primary drying times for mannitol-trehalose-NaCl based formulations after annealing, as partial collapse was inhibited by the highly crystallized mannitol, leading to a more compact structure that offers a higher dry-layer resistance [24].

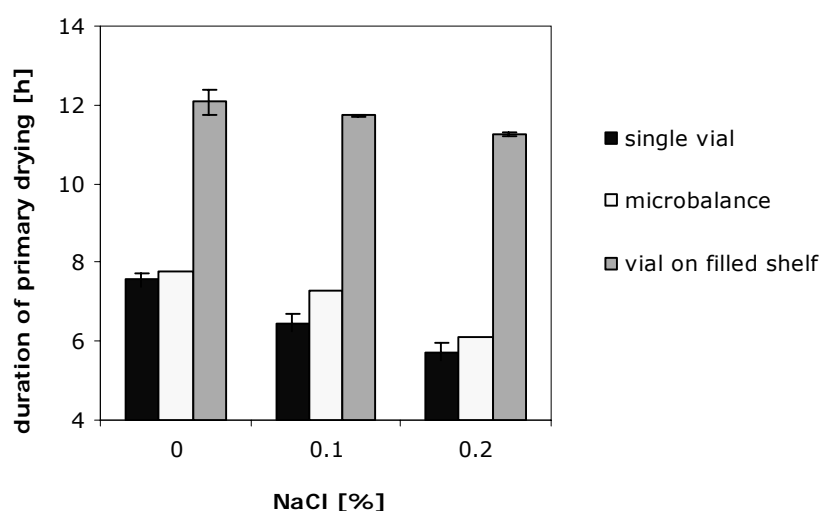


Figure 1: Primary drying time of 1.25% mannitol and 1.25% stabilized-HSA dried with program I.

The changes in primary drying time after the addition of NaCl to 1.25% mannitol and 1.25% stabilized-HSA dried with program I are shown in Figure 1. Thermocouples in separately placed vials and vials placed on a filled shelf, as well as the microbalance demonstrated shorter drying times with the addition of salt, indicating morphological and physico-chemical differences resulting from the presence of NaCl. Overall, the vials on the filled shelf required a longer drying time than individually vials placed on a separate shelf, due to the reduced energy transfer on a filled shelf [25].

3.1.2 Residual Moisture Content

The residual moisture of the samples with 1.25% mannitol and 1.25% stabilized-HSA was affected by NaCl (Figure 2). Up to 0.1% NaCl the water content ranged below 0.5%. For samples with 0.2% NaCl the residual moisture was drastically increased to approximately 2%, offering another indication for morphological or physico-chemical changes with an increase in NaCl concentration. It was shown in the freezing studies, that mannitol crystallization in mannitol-HSA formulations could be inhibited by the addition of NaCl, leading to a higher amorphous degree. The increase of the amorphous fraction can offer a possible explanation for the increase in residual moisture.

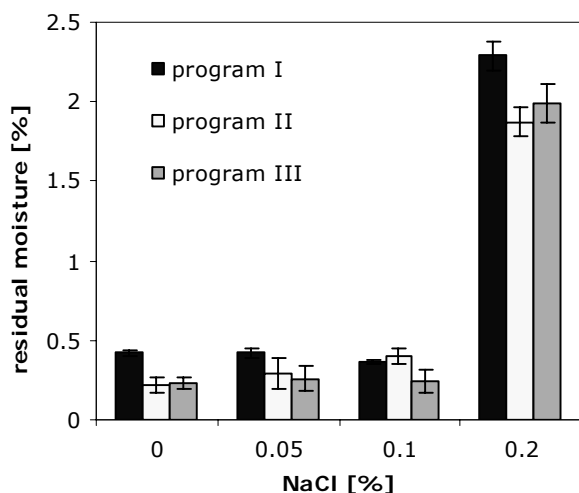


Figure 2: Residual moisture content of 1.25% mannitol and 1.25% stabilized-HSA with 0.0% to 0.2% NaCl after lyophilization with program I, II and III.

The higher residual moisture can affect protein stability during storage, as it can promote physical and chemical instabilities [26]. Water can act as reactant or product in chemical reactions [27]. The residual moisture in the amorphous lyophilized product further can promote crystallization and lead to a depression of the glass transition T_g , as water is acting as plasticizer [28,29].

3.1.3 Morphology, Crystallinity and Thermal Properties of Lyophilized Products with Mannitol, Stabilized-HSA and NaCl

Previous freezing studies had shown that mannitol crystallization could be inhibited by the addition of NaCl or HSA. This can affect the drying process and the physico-chemical properties of the lyophilized products. To explain the shorter primary drying time and higher residual moisture content for increasing NaCl concentrations, the morphology of lyophilized products with mannitol, HSA and NaCl was analyzed with XRD, DSC and SEM. After freeze-drying a 2.5% mannitol solution, peaks of all modifications (α -, β - and δ -mannitol) were found in the XRD pattern (Figure 3).

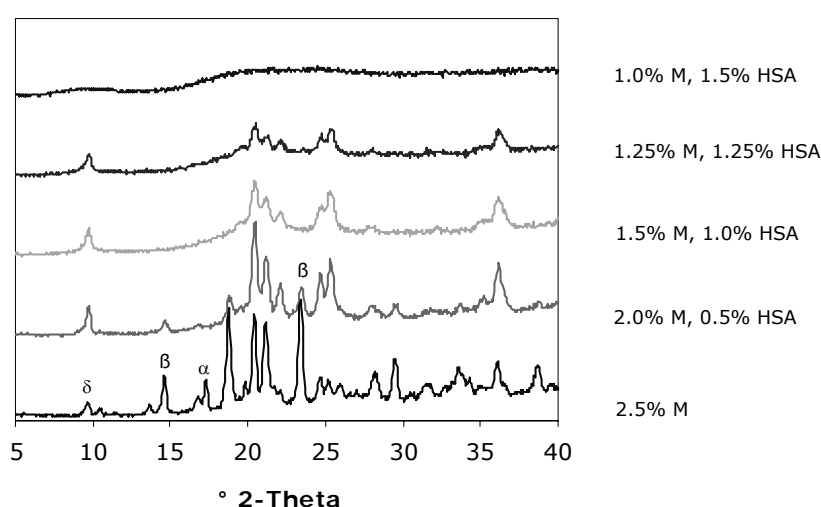


Figure 3: XRD diffraction pattern of variable ratios of mannitol (M) to stabilized HSA (HSA) lyophilized with program I from solutions with a total solid content of 2.5%.

With increasing amounts of stabilized-HSA, the α -modification disappeared first when 0.5% stabilized-HSA was added to the formulations. This was followed by a disappearance of the β -modification at 1.0% stabilized-HSA, leaving solely δ -mannitol. The critical ratio of mannitol to stabilized-HSA was 1:1, as the products were partially crystalline comprising δ -mannitol independent of the lyophilization program. The products were amorphous according to XRD when more than 50% of the lyophilized product was composed of HSA. For formulation with 1.25% mannitol and 1.25% stabilized-HSA the impact of NaCl and the applied freezing process on the morphology of the lyophilized products were studied with XRD. After lyophilization with program I, mannitol was present in the δ -modification for 0.0% to 0.1% NaCl (Figure 4a). By increasing the NaCl concentration to 0.15% the β -modification augmented. 0.2% NaCl led to pure β -mannitol and amorphous mannitol was found for 0.3% NaCl. Peaks of

crystalline NaCl (31.7° 2- Θ) could be detected when NaCl was used in concentrations higher than 0.1%.

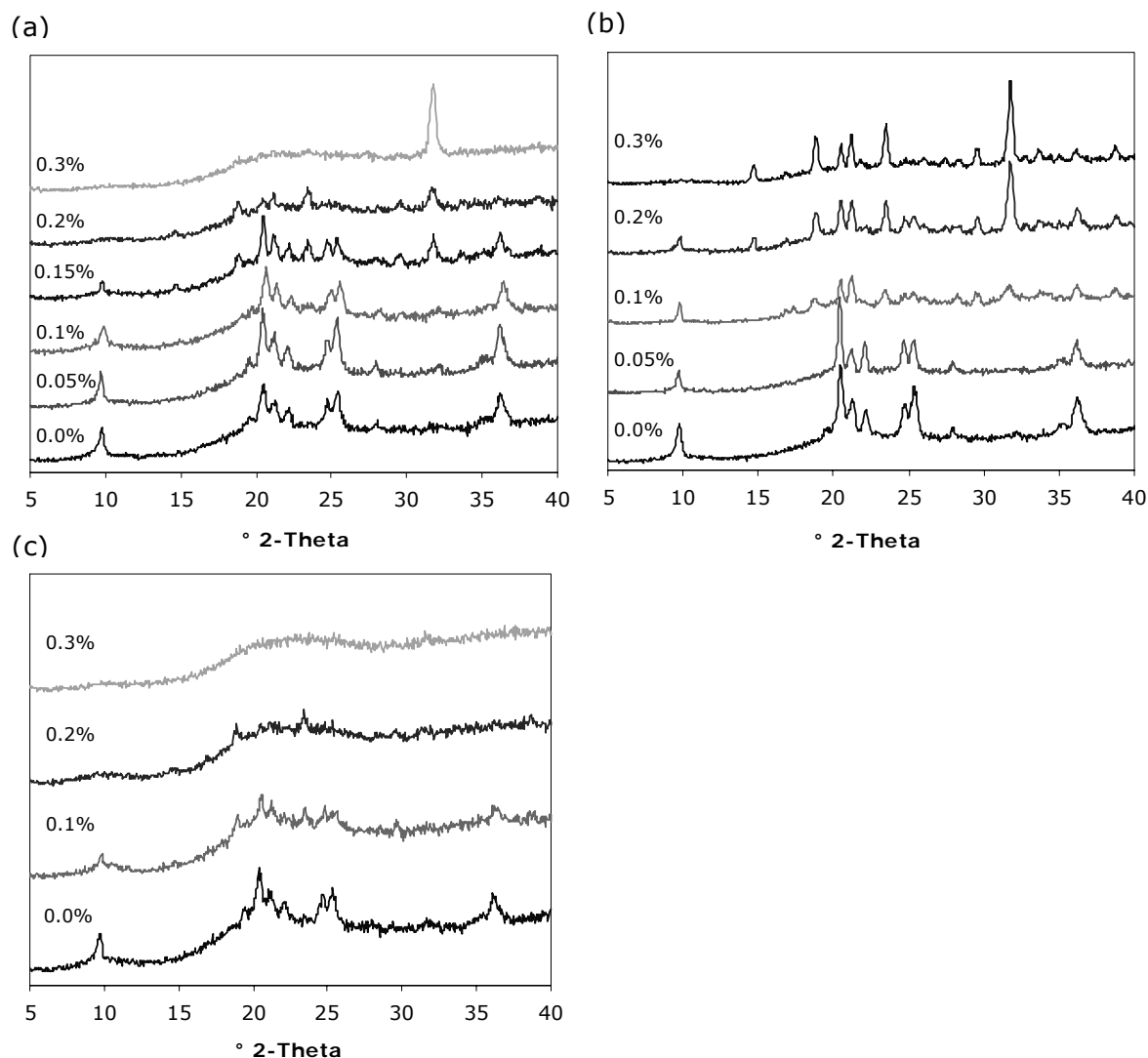


Figure 4: XRD diffraction pattern of 1.25% mannitol and 1.25% stabilized-HSA, 0.0% to 0.3% NaCl dried with program I (a), program II (b) and program III (c).

The change from crystalline to amorphous mannitol could also be visualized with SEM. Products without NaCl exhibited a relatively compact structure with ordered shaped edges and layers of crystalline appearance, which was in agreement with XRD data (Figure 5a). Increasing the NaCl content to 0.3% resulted in products, with a smooth network, an amorphous structure and first signs of collapse (Figure 5b). This could be used as an explanation for the decreased drying time of the samples with increasing NaCl content. The looser structure offered less product resistance during drying and therefore the sublimation rate was higher compared to products without NaCl.

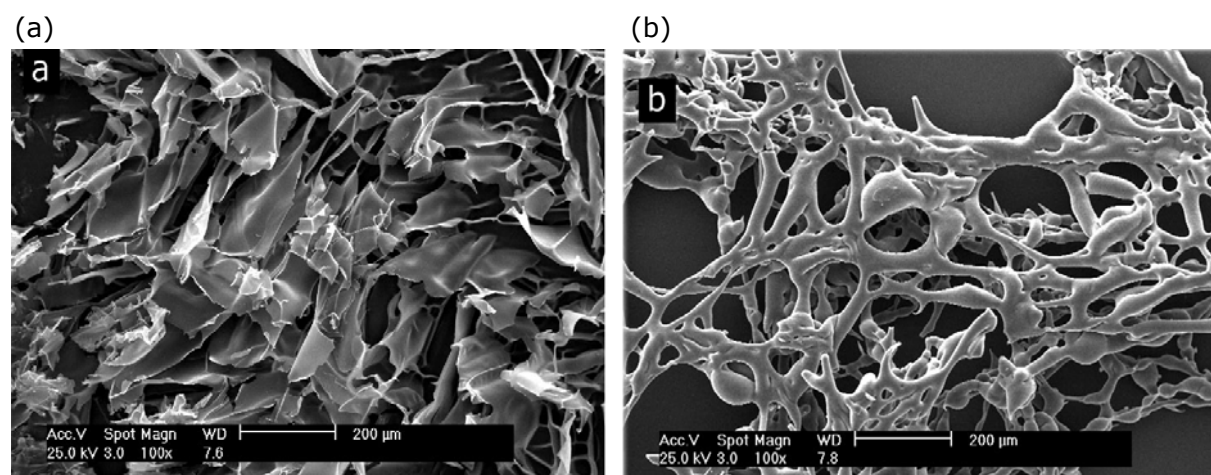


Figure 5: SEM of 1.25% mannitol and 1.25% stabilized-HSA without NaCl (a) and 0.3% NaCl (b).

For samples lyophilized with program I a broad peak with a maximum at 95°C to 100°C in the DSC heating scan could be detected in products containing 0.0% to 0.2% NaCl (Figure 6). The broad peak derived from HSA, as stabilized-HSA lyophilized without further excipients showed this characteristic peak as well. For formulations with mannitol and stabilized-HSA DSC did not detect a glass transition (T_g) which was indicative for the presence of amorphous material. This was in agreement with XRD for the samples without NaCl which demonstrated that these samples mainly consisted of crystalline mannitol. With increasing amounts of NaCl, mannitol remained partly amorphous according to XRD. However, no T_g was detected with DSC, which could be due to the broad peak, deriving from HSA that superimposed the signal of a possible T_g . At 0.3% NaCl, amorphous mannitol crystallized with an onset of 64°C and a maximum at 75°C. Between 120°C and 180°C the melting peaks of the different mannitol-modifications were detected. It is described in literature that δ -mannitol is transformed to β -mannitol at 130°C, with a subsequent melting at 150°C to 158°C [30]. The melting of the β - and the α -modification was found at 166°C to 168°C. As the lyophilized products were mixtures of HSA, NaCl and mannitol the melting points could differ from that of pure mannitol. NaCl shifts the melting points of the mannitol modifications to lower temperatures [31]. Overall, no T_g and no changes in the DSC chromatogram in the temperature range of 0°C to 40°C, which is relevant for storage, could be detected for the formulations consisting of 1.25% mannitol and 1.25% stabilized HSA with 0.0% to 0.3% NaCl (Figure 6).

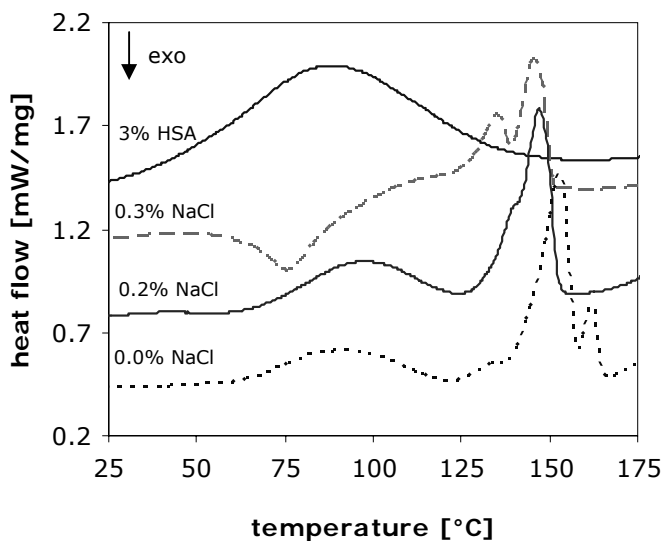


Figure 6: DSC heating-scan of 3% HSA and 1.25% mannitol and 1.25% stabilized-HSA with 0.0%, 0.2% and 0.3% NaCl dried with program I.

Drying the formulation with an additional annealing step (program II) led to samples with a higher crystallinity (Figure 4a). In this case peaks of crystalline β -mannitol were found for 0.3% NaCl, while these products were amorphous after the lyophilization with program I. The annealing was conducted at -20°C , which was above the onset of mannitol crystallization in DSC at -25°C , allowing mannitol to crystallize. The contrary effect of more amorphous samples could be achieved by applying a faster freezing rate of $0.9^{\circ}\text{C}/\text{min}$ (program III) or placing the vials on pre-cooled shelves (program IV), where an average freezing-rate of $2.3^{\circ}\text{C}/\text{min}$ was measured. The XRD patterns were equal for program III and IV, whereby NaCl stayed amorphous (Figure 4c).

For all studied lyophilization programs δ -mannitol was formed in the absence of NaCl, while the addition of NaCl led to a mixture of δ - and β -mannitol followed by β -mannitol and finally amorphous products. The lyophilization process affected at which NaCl concentration the transitions occurred.

3.2 Storage Stability of the Lyophilized Formulations

Excipients in the amorphous state are more suitable to stabilize proteins. Therefore, a potential crystallization of amorphous material during storage needs to be prevented. The addition of NaCl to formulations with 1.25% mannitol and 1.25% stabilized-HSA led to more amorphous products. It was evaluated whether the samples consisting of 1.25% mannitol and 1.25% stabilized-HSA with 0.0% to 0.2% NaCl were physico-chemically stable upon storage for 6 months at 2-8°C, 25°C / 60% RH and 40°C / 75% RH. Besides the physico-chemical stability, the impact of storage on HSA-stability at the different storage conditions was evaluated using turbidimetry and HP-SEC.

3.2.1 Changes in the Product Morphology upon Storage

After lyophilization formulations with 1.25% mannitol and 1.25% stabilized-HSA contained only δ -mannitol independent of the applied freezing protocol. Upon storage for 6 months no significant changes in the morphology could be observed at any temperature, indicating a morphologically stable system. It was described in literature that the δ -modification was less stable than the α - and β -modification [32]. Especially at elevated moisture levels e.g. during wet granulation δ -mannitol converts to β -mannitol [33]. The increase in residual moisture in the lyophilized products from 0.5% before storage to 1.5% to 3.0% (depending on the storage temperature) did not lead to a change in modifications. NaCl inhibited mannitol crystallization during lyophilization. The applied freezing-protocol determined the NaCl concentration at which complete inhibition of mannitol crystallization could be achieved (compare 3.1.3). After adding 0.2% NaCl to the formulation lyophilized with program I, peaks of β -mannitol at a very low intensity and NaCl ($31.7^\circ 2-\theta$) with an overall high content of amorphous material were detected (Figure 7a). When performing lyophilization with an annealing step (program II), a partly crystalline mixture of β - and δ -mannitol was achieved for formulations with 0.1% NaCl (Figure 7b). The low intensity of the NaCl peak at $31.7^\circ 2-\theta$ indicated an incomplete NaCl crystallization during the freeze-drying process. Lyophilization at a faster freezing rate (program III) resulted in amorphous products, when 0.1% NaCl was added (Figure 7c). During storage at 2-8°C, 25°C / 60% RH and 40°C / 75% RH mannitol and NaCl crystallized, indicated by an intensity increase of the peaks, with mannitol crystallizing prior to NaCl. This was in agreement with literature data for the crystallization order in the liquid state during freezing and rewarming, where NaCl crystallization takes place after the crystallization of mannitol, which is necessary for NaCl to inhibit the crystallization of mannitol [31]. During 6 months storage a formation of new mannitol modifications did not occur. Similar results were obtained by Cannon and Trappler (2000)

for lyophilized products with mannitol as single component stored for one year at room temperature [34].

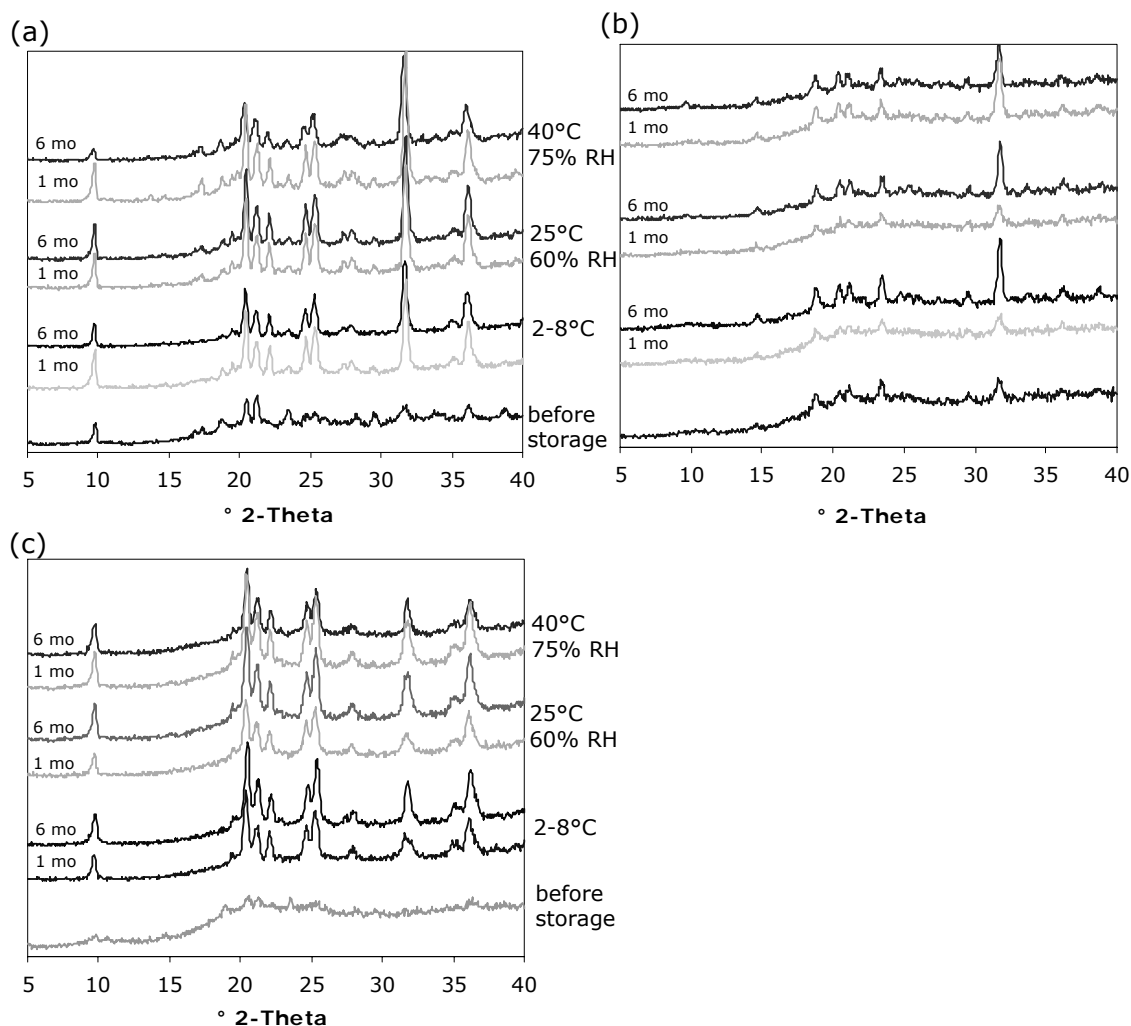


Figure 7: XRD of 1.25% mannitol and 1.25% stabilized-HSA, 0.1% (b,c) and 0.2% NaCl (a) dried with program I (a), program II (b) and program III (c) after 1 and 6 months at 2-8°C, 25°C / 60% RH and 40°C / 75% RH.

However, the amorphous or partially amorphous state created by adding NaCl to formulations with 1.25% mannitol and 1.25% stabilized-HSA could not be preserved over storage time. A stable amorphous state was for example achieved by increasing the fraction of stabilized-HSA to 1.5%, where mannitol remained amorphous after lyophilization and 24 months at 25°C / 60% RH (Figure 8).

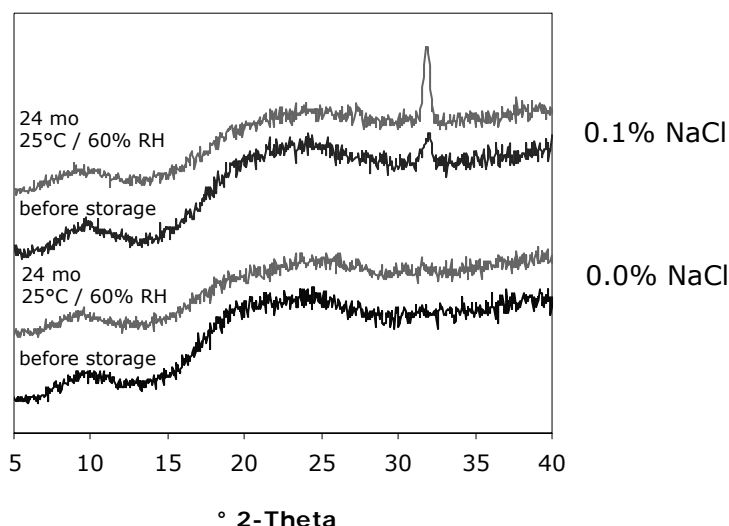


Figure 8: XRD of 1.5% stabilized-HSA and 1.0% mannitol without and with 0.1% NaCl, lyophilized with program I after lyophilization and 24 months at 25°C / 60% RH.

When adding 0.1% NaCl, the peak at 31.7° 2- θ was present and increased in intensity over time, while mannitol remained amorphous. It could be shown that the amorphous state created by NaCl was not stable upon storage. If NaCl is required e.g. as stabilizer for the active ingredient the fact that it crystallizes upon storage needs to be considered.

3.2.2 Stability of HSA during Storage

More important than the physico-chemical stability of the lyophilized product is the stability of a protein upon storage. To evaluate the stability of HSA over time, turbidity in FNU was monitored over the pH range from 7.5 to 3.0 and compared to the reference solutions I-IV of the European Pharmacopoeia method 2.2.1 [20]. By the pH scan the differences between the formulations became more obvious, as the increase in turbidity at pH 4.5 to 5.0 was more pronounced for stressed products. Additionally, aggregation was monitored with HP-SEC. Here the samples lyophilized with program I after 24 months at 25°C / 60% RH are shown exemplarily. Independent of the applied lyophilization process, clear solutions (turbidity < Ref I of Ph. Eur.) were obtained after reconstitution with water. The pH turbidity profile did not change after 6 months at 2-8°C (Figure 9a). After storage at 25°C / 60% RH and 40°C / 75% RH the turbidity increase at pH 5.0 was more obvious (Figure 9b-e). After 6 months at 25°C / 60% RH, respectively 40°C / 75% RH turbidities of 25-30 FNU, respectively 45-55 FNU were measured at pH 5.0, indicating damage of the protein at elevated temperatures. Furthermore, the turbidity of samples lyophilized with program II was about 4 FNU (25°C / 60% RH) and 10 FNU (40°C / 75% RH) higher compared to preparations dried with the other

programs. The more pronounced crystallinity and possible phase separation after annealing offered possible explanations.

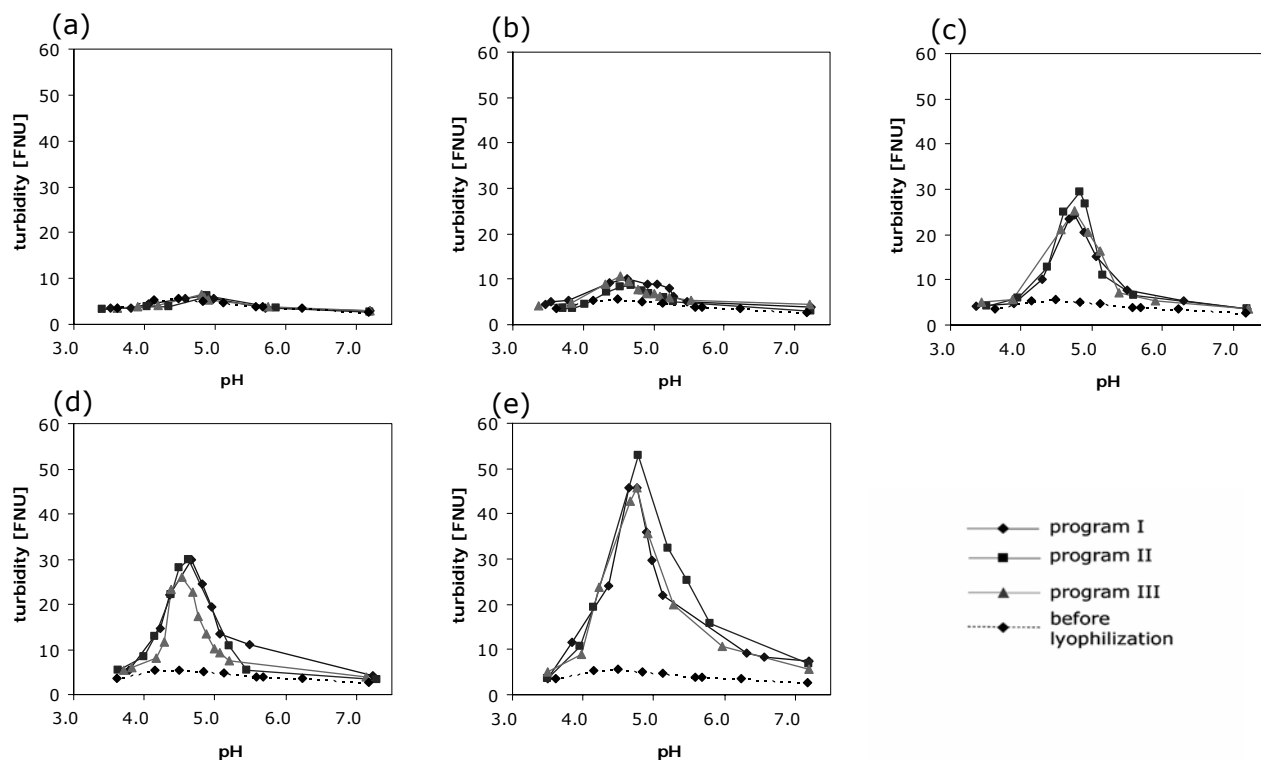


Figure 9: Turbidity of 1.25% mannitol and 1.25% stabilized-HSA upon storage at 2-8°C for 6 months (a), storage at 25°C / 60% RH for 1 month (b) and 6 months (c) and storage at 40°C / 75% RH for 1 month (d) and 6 months (e).

The addition of NaCl improved the stability over storage time for all applied freezing protocols. After 6 months storage at 2-8°C and 25°C / 60% RH there was no significant increase in turbidity at pH 4.5 to 5.0 for 0.1% and 0.2% NaCl (Figure 10). Consistent turbidities of 3.5 to 4.6 FNU over the studied pH-range, comparable to the solutions before lyophilization were measured. The turbidity increase at pH 4.5 to 5.0 could not completely be inhibited by NaCl after storage at 40°C / 75% RH. However, the turbidity maximum stayed below 10 FNU and the degree of opalescence was lower than Ref III of the European Pharmacopoeia with 7.6 FNU for 0.1% NaCl, respectively 6.4 FNU for 0.2% NaCl.

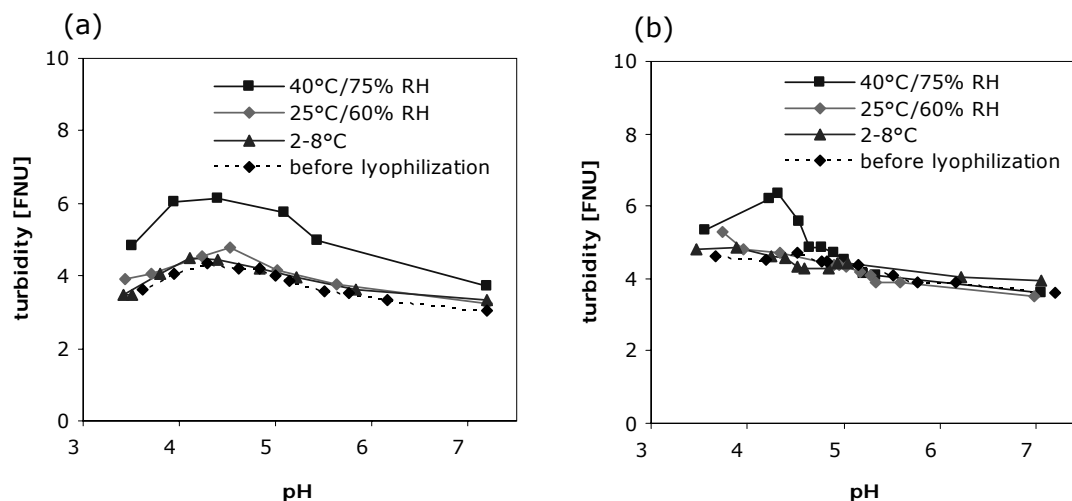


Figure 10: Turbidity of 1.25% mannitol and 1.25% stabilized-HSA with 0.1% NaCl (a) and 0.2% NaCl (b) dried with program I after 6 months storage at 2-8°C, 25°C / 60% RH and 40°C / 75% RH.

The stabilizing effect of NaCl on HSA seen in the turbidity data was further confirmed with HP-SEC. It was shown by HP-SEC for samples lyophilized with program I after 24 months storage at 25°C / 60% RH that higher monomer contents were found with increasing NaCl concentrations (Figure 11). The monomer content after lyophilization was $93\% \pm 0.5\%$ independent of the NaCl concentration.

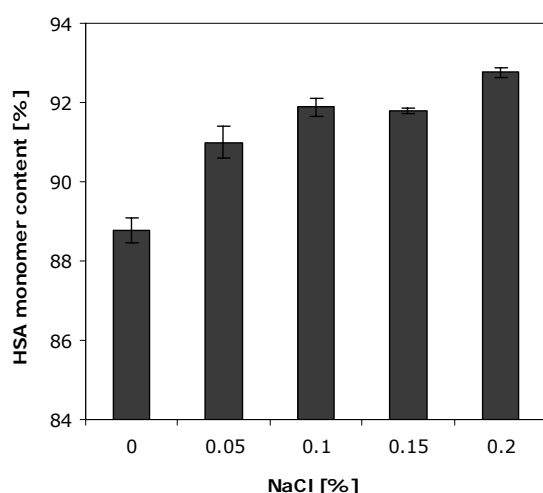


Figure 11: HSA-monomer content after reconstitution of 1.25% mannitol and 1.25% stabilized-HSA formulation with 0.0% to 0.2% NaCl, lyophilized with program I and 24 months storage at 25°C / 60% RH.

A stabilizing effect of NaCl on HSA, respectively BSA is also described in literature. In the solid state HSA generally exhibits a good thermo-reversible structural stability, which was

determined by FTIR from Wang et al. (2005) [35]. Higher melting temperatures (T_m) are detected by DSC with increasing NaCl concentrations in HSA solutions in the pH range from 5.6 to 7.0 [36]. Costantino et al. (1995a) showed for lyophilized recombinant human albumin (rHA) that aggregation upon high humidity incubation was reduced by NaCl due to the uptake of water in the vicinity of rHA by NaCl [37]. The secondary structure of rHA, was not significantly affected by the addition of NaCl [38]. Structural changes, in particular aggregation is known to induce the risk of immunogenicity reactions in the patient [39]. HSA itself exhibits a low risk for immunogenicity, however in presence of a second protein the formation of mixed aggregates can lead to immunogenicity reactions, which was e.g. shown for rhINF α [40,41].

Overall, the turbidity data showed a good stability of stabilized-HSA upon storage at 2-8°C for all studied lyophilization programs. At higher storage temperatures the samples produced with annealing (program II) exhibited higher turbidity values at pH 5.0, indicating destabilization. By NaCl addition, mannitol remained amorphous after lyophilization, but crystallized upon storage. Crystallization is known for its potential negative impact on protein integrity [3]. However, the addition of NaCl enhanced the stability of HSA independent of the applied freeze-drying program and the crystallization of mannitol upon storage. This indicated that the stabilizing effect of NaCl on HSA prevailed over a possible detrimental effect of mannitol crystallization upon storage.

4. Conclusions

The lyophilization behavior and the physico-chemical properties of the dried products are influenced by the presence of salts in the formulations. Therefore, the impact of NaCl on drying-time, crystallization and morphology was studied for formulations with mannitol and stabilized-HSA, using different freezing-protocols. A shorter drying-time for formulations with 1.25% mannitol and 1.25% stabilized-HSA was observed for three different lyophilization programs with increasing amounts of NaCl, due to morphological changes and a less compact cake structure. It could be shown by DSC, XRD and SEM that both NaCl-concentration and applied freezing-protocol had a significant impact on the physico-chemical properties of the formulations after lyophilization with differences in crystallinity and existing modifications. Without NaCl the lyophilized samples contained exclusively δ -mannitol for all studied freezing-protocols and remained physico-chemically stable upon storage for 6 months at 2-8°C, 25°C / 60% RH and 40°C / 75% RH. With increasing NaCl concentrations a larger fraction of β -mannitol was detected and finally amorphous products were formed. The applied freezing-protocol determined how much NaCl was needed to achieve an amorphous product. However, upon storage the amorphous state could not be preserved with the consequence that mannitol and NaCl crystallized. The data indicated that products without NaCl were more stable in their modifications. However, regarding the stability of HSA in the lyophilized products, monitored by a turbidity scan from pH 3.0 to 7.0 and HP-SEC, the addition of NaCl improved the stability of HSA upon storage. This could be referred to a direct stabilizing effect of NaCl on HSA upon storage, which is described in literature. For the studied systems the benefit of NaCl on protein stability outbalanced the potential drawbacks that morphological changes, like crystallization imposed on lyophilized products. Concluding, it can be stated that it is important to understand how NaCl is affecting the morphology and the protein in the formulation during lyophilization.

5. References

1. M. J. Pikal, K. M. Dellermann, M. L. Roy, R. M. Riggin. The Effects of Formulation Variables on the Stability of Freeze-Dried Human Growth Hormone. *Pharm. Res.* **8**:427-436 (1991).
2. R. Johnson, C. Kirchhoff, H. Gaud. Mannitol-Sucrose Mixtures-Versatile Formulations for Protein Lyophilization. *J. Pharm. Sci.* **91**:914-922 (2002).
3. K. Izutsu, S. Kojima. Excipient crystallinity and its protein-structure-stabilizing effect during freeze-drying. *J. Pharm. Pharmacol.* **54**:1033-1039 (2002).
4. K. Kasraian, T. M. Spitznagel, J. A. Juneau, K. Yim. Characterization of the Sucrose/Glycine/Water System by Differential Scanning Calorimetry and Freeze-Drying Microscopy. *Pharm. Dev. Technology.* **3**:233-239 (1998).
5. C. Telang, L. Yu, R. Suryanarayanan. Effective Inhibition of Mannitol Crystallization in Frozen Solutions by Sodium Chloride. *Pharm. Res.* **20**:660-667 (2003).
6. M. F. Mazzobre, M. P. Longinotti, H. R. Corti, M. P. Buera. Effect of Salts on the Properties of Aqueous Sugar Systems, in Relation to Biomaterial Stabilization. 1. Water Sorption Behavior and Ice Crystallization/Melting. *Cryobiol.* **43**:199-210 (2001).
7. A. Pyne, R. Surana, R. Suryanarayanan. Crystallization of Mannitol below T_g' during Freeze-Drying in Binary and Ternary Aqueous Systems. *Pharm. Res.* **19**:901-908 (2002).
8. B. Lyuet, D. Rasmussen. Study by differential thermal analysis of the temperature of instability of rapidly cooled solutions of glycerol, ethylene glycol, sucrose and glucose. *Biodyn.* **10**:1167-1191 (1968).
9. A. Kim, M. Akers, S. Nail. The Physical State of Mannitol after Freeze-Drying. Effect of Mannitol Concentration, Freezing Rate and a Noncrystallizing Cosolute. *J. Pharm. Sci.* **87**:931-935 (1998).
10. B. Lueckel, D. Bodmer, B. Helk, H. Leuenberger. Formulations of Sugars with Amino Acids or Mannitol-Influence of Concentration Ratio on Properties of the Freeze-Concentrate and the Lyophilizate. *Pharm. Dev. Technol.* **3**:325-336 (1998).
11. G. Scatchard, L. E. Strong, W. L. Hughes Jr., J. N. Ashworth, A. H. Sparrow. Chemical, clinical, and immunological studies and the products of human plasma fractionation. XXVI. The properties of human serum albumin at low salt content. *J. Clinical Invest.* **24**:671-679 (1945).
12. G. A. Ballou, P. D. Boyer, J. M. Luck, G. F. Lum. The heat coagulation of human albumin. *J. Biol. Chem.* **153**:589-605 (1944).
13. U.S. Food and Drug Administration, Code of Federal Regulations, Title 21, Volume 7: §640.80 Albumin (Human), revised as on April 1, 2004.
14. T. Arakawa, Y. Kita. Stabilizing effect of octanoate and adetyltrypthophanate on heat-induced aggregation of bovine serum albumin. *Biochim. Biophys. Acta* **1479**:32-36 (2000).
15. L. Saso, G. Valentini, E. Grippa, M. G. Leone, B. Silvestrini. Effect of selected substances on heat-induced aggregation of Albumin, IgG and Lysozyme. *Res. Com. in Mol. Pathology Pharmacol.* **102**:15-28 (1998).
16. M. J. Pikal. Freeze-drying of proteins: Part I: Process design. *Biopharm.* **3**: 17-26 (1990).
17. M. J. Pikal, S. Shah. The collapse temperature in freeze drying: dependence on measurement methodology and rate of water removal from the glassy phase. *Int. J. Pharm.* **62**:165-186 (1990).
18. S. Nail, L. Gatlin. Freeze-drying: Principles and practice. In K. E. Avis, H. A. Lieberman, L. Lachman (editors). *Pharmaceutical Dosage Forms: Parenteral Medications*, Vol. 2. New York: Marcel Dekker; pp 163-333 (1986).
19. C. Roth, G. Winter, G. Lee. Continuous Measurement of Drying Rate of Crystalline and Amorphous Systems during Freeze-Drying Using an In Situ Microbalance Technique. *J. Pharm. Sci.* **90**:1345-1355 (2001).
20. Clarity and degree of opalescence of liquids. *European Pharmacopoeia* p. 27-29 (2005).
21. D. E. Overcashier, T. W. Patapoff, C. C. Hsu. Lyophilization of Protein Formulations in Vials: Investigation on the Relationship between Resistance to Vapor Flow during Primary Drying and Small Scale Collapse. *J. Pharm. Sci.* **88**:688-695 (1999).
22. J. A. Searles, J. F. Carpenter, T. W. Randolph. The Ice Nucleation Temperature Determines the Primary Drying Rate of Lyophilization for Samples Frozen on a Temperature-Controlled Shelf. *J. Pharm. Sci.* **90**:860-871 (2001).

23. J. A. Searles, J. F. Carpenter, T. W. Randolph. Annealing to Optimize the Primary Drying Rate Heterogeneity, and Determine Tg' in Pharmaceutical Compositions. *J. Pharm. Sci.* **90**:872-887 (2001).
24. X. Lu, M. Pikal. Freeze-Drying of Mannitol-Trehalose-Sodium Chloride-Based Formulations: The Impact of Annealing on Dry Layer Resistance to Mass Transfer and Cake Structure. *Pharm. Tech. Dev.* **9**:85-95 (2004).
25. I. Presser. Innovative Online Messverfahren zur Optimierung von Gefriertrocknungsprozessen. Dissertation (2003).
26. E. D. Breen, J. G. Curley, D. E. Overcashier, C. C. Hsu, S. J. Shire. Effect of moisture on the stability of a lyophilized humanized monoclonal antibody formulation. *Pharm. Res.* **18**:1345-53 (2001).
27. E. Y. Shalae, G. Zografi. How Does Residual Water Affect the Solid-State Degradation of Drugs in the Amorphous State? *J. Pharm. Sci.* **85**:1137-1141 (1996).
28. D. J. Burnett, F. Thielmann, J. Booth. Determining the critical relative humidity for moisture-induced phase transitions. *Int. J. Pharm.* **287**:123-133 (2004).
29. Y. K. Roos, M. Cook. Plasticizing effect of water on thermal behavior and crystallization of amorphous food models. *J. Food Sci.* **56**:38-43 (1991).
30. A. Burger, J. Henck, S. Hetz, J. Rollinger, A. Weissnicht, H. Stottner. Energy/Temperature Diagram and Compression Behavior of the Polymorphs of D-Mannitol. *J. Pharm. Sci.* **89**:4 (2000).
31. C. Telang, R. Suryanarayanan, L. Yiu. Crystallization of D-Mannitol in Binary Mixtures with NaCl: Phase Diagram and Polymorphism. *Pharm. Res.* **20**:1939-1945 (2003).
32. L. Yu. Nucleation of One Polymorph by Another. *J. Am. Chem. Soc.* **125**:6380-6381 (2003).
33. T. Yoshinari, R. T. Forbes, P. York, Y. Kawashima. Moisture induced polymorphic transition of Mannitol and its morphological transformation. *Int. J. Pharm.* **247**:69-77 (2002).
34. A. Cannon, E. Trappler. The influence of Lyophilization on the Polymorphic Behavior of Mannitol. *PDA J. Pharm. Sci. Technol.* **54**:13-22 (2000).
35. S. L. Wang, S.Y. Lin, M. J. Li, Y. S. Wie, T. F. Hsieh. Temperature effect on the structural stability, similarity, and reversibility of human serum albumin in different states. *Bioph. Chem.* **114**:205-212 (2005).
36. M. Yamasaki, H. Yano, K. Aoki. Differential scanning calorimetric studies on bovine serum albumin: I. Effects of pH and ionic strength. *Int. J. Biol. Macromol.* **12**:263-268 (1990).
37. H. R. Costantino, K. Griebenow, P. Mishra, R. Langer, A. M. Klibanov. Fourier-transform infrared spectroscopic investigation of protein stability in the lyophilized form. *Biochim. Biophys. Acta* **1253**:69-74 (1995).
38. H. R. Costantino, R. Langer, A. M. Klibanov. Aggregation of a lyophilized pharmaceutical protein, recombinant human albumin: effect of moisture and stabilization by excipients. *Bio/Technol.* **13**:493-496 (1995).
39. S. Hermeling, D. J. A. Crommelin, H. Schellekens, W. Jiskoot. Structure-Immunogenicity Relationships of Therapeutic Proteins. *Pharm. Res.* **21**:897-903 (2004).
40. A. Braun, L. Kwee, M. A. Labow, J. Alsenz. Protein Aggregates Seem to Play a Key Role Among the Parameters Influencing the Antigenicity of Interferon Alpha (INF- α) in Normal and Transgenic Mice. *Pharm. Res.* **14**:1472-1478 (1997).
41. E. Hochuli. Interferon immunogenicity: technical evaluation of interferon- α 2a. *J. Interferon Cytokine Res.* **17** (Suppl. 1):15-21 (1997).

Chapter 5

Impact of Freezing Procedure and Annealing on the Physico-chemical Properties and the Formation of Mannitol Hydrate in Mannitol-Sucrose-NaCl Formulations

Abstract

The goal was to investigate the excipient system mannitol-sucrose as alternative HSA-free lyophilized formulations for the cytokine. Thereby, the impact of NaCl on the physico-chemical properties of mannitol-sucrose formulations during freezing and drying, with special focus on mannitol hydrate formation was investigated. Differential Scanning Calorimetry (DSC) and Low-temperature X-ray Powder Diffraction (LTXRD) were used to study the frozen solutions. After lyophilization the products were analyzed with DSC, Temperature-modulated DSC (TMDSC), X-ray Powder Diffraction (XRD) and Karl-Fischer titration. DSC showed an inhibition of mannitol crystallization by sucrose and NaCl during freezing. T_g' was lowered by both mannitol and NaCl. By the application of an annealing step during lyophilization mannitol crystallinity could be increased. However, lyophilization with an annealing step promoted the formation of mannitol hydrate. Mannitol hydrate is known to undergo conversion into the anhydrous polymorphs of mannitol upon storage with the consequence that the hydrate water is released. LTXRD revealed that mannitol hydrate was formed at temperatures below -30°C , but not at -27°C . The tendency that mannitol hydrate is predominantly formed at lower temperature was confirmed by XRD of lyophilized products, produced at different annealing temperatures.

Keywords: freezing, lyophilization, annealing, NaCl, mannitol hydrate

1. Introduction

In the HSA-containing cytokine formulation, mannitol was used as crystalline bulking agent and HSA as lyo- and cryoprotector. This combination of a crystalline bulking agent, e.g. mannitol or glycine with a second excipient that remains amorphous e.g. sucrose, trehalose or human serum albumin is a common way to achieve elegant lyophilized products [1-3]. Combinations of glycine with sucrose, respectively mannitol with sucrose are often employed. Johnson et al. (2002), as well as Passot et al. (2005) used a combination of 4% mannitol and 1% sucrose to successfully stabilize different proteins [4,5]. Liao et al. (2005) have studied the impact of an incooperated protein on the physical state of mannitol in formulations with mannitol and sucrose [6]. During lyophilization mannitol can crystallize in the α - β - or δ -modification or as mannitol hydrate depending on the applied freezing protocol, a potential annealing step and the process conditions during primary and secondary drying [7-9]. The presence of other excipients like buffer components, lyoprotectants or proteins can both inhibit and promote mannitol crystallization [10-12]. Especially salts, that are added as buffer components, isotonicity agents or stabilizers can have a major impact on the physico-chemical properties of mannitol and other excipients [13,14]. A slight increase in salt concentration can lead to significant changes of the physico-chemical properties of the excipients during freezing and drying [15-18]. The impact of NaCl on the system mannitol-HSA during freezing and lyophilization is subject of Chapter 3 and 4. Besides the anhydrous modifications, mannitol can exist as a metastable crystalline hydrate after lyophilization [19]. The presence of mannitol hydrate can lead to stability problems during storage due to the release of hydrate water upon its conversion into the anhydrous crystal forms. Therefore, it is important to develop lyophilization cycles that result in products free of mannitol hydrate. Johnson et al. (2002) showed that mannitol hydrate content can be reduced when performing the secondary drying at temperatures above 40°C [4]. Little is known about how an annealing procedure influences the formation of mannitol hydrate during lyophilization. Annealing is often applied for formulations with mannitol as bulking agent to maximize mannitol crystallization during the freezing-step. On the other hand, several approaches are described to produce amorphous mannitol as lyoprotector, e.g. by adding NaCl, boric acid or sodium tetraborate [13,20,21]. Only in the amorphous state mannitol is able to adequately stabilize the active protein via molecular interactions [22,23]. However, amorphous mannitol tends to crystallize upon storage and thereby loses its ability to stabilize the protein [2]. Therefore, the employment of mannitol as crystalline bulking agent in combination with an amorphous lyoprotector is the more promising approach. Thereby, it is essential to ensure mannitol crystallization during lyophilization. The crystallization of

an excipient upon storage can reduce storage stability. This was described by Kreilgaard et al. (1999) for *Humicola lanuginosa* Lipase formulated with sucrose, who attributed the reduced stability after crystallization to an increase in moisture content and a reduced glass transition (T_g) value of the remaining amorphous phase [24].

With respect to the planned development of HSA-free formulations for the cytokine, HSA was replaced by sucrose in its function as lyo- and cryoprotector. Different combinations of mannitol, sucrose and NaCl were used as model formulations for the studies. The impact of NaCl on the physico-chemical properties of the formulation during freezing, annealing and drying was investigated. For the frozen state the glass transition of the maximally freeze-concentrated solution (T_g') of the formulations and the crystallization of mannitol were monitored. The lyophilized products were analyzed regarding mannitol modifications, T_g and residual moisture. Special focus was set on the presence of mannitol hydrate in relation to the applied annealing steps, to find the optimum lyophilization conditions for the formulations.

2. Materials and Methods

2.1 Materials

Mannitol was obtained from Caelo (Hilden, Germany), sucrose from Suedzucker (Mannheim, Germany) and NaCl from Sigma (Steinheim, Germany).

2.2 Methods

2.2.1 Low Temperature X-ray Powder Diffraction (LTXRD)

Crystallization was studied with LTXRD using Cu-K α 1-radiation ($\lambda=154.06$ pm) on the powder diffractometer Stadi P from STOE (Darmstadt, Germany) with parafoocused transmission geometry. Germanium was used as primary monochromator and the scattered X-rays were detected with a linear PSD area detector. The sterile filtrated solutions were frozen in the rotating capillary (diameter 0.5 mm) in the cooling stage (Oxford Cryosystem) of the X-ray diffractometer. For the LTXRD experiment a temperature profile similar to the conditions during lyophilization was chosen. The samples were frozen to -50°C with a cooling rate of $0.5^\circ\text{C}/\text{min}$. At -50°C the first measurement under isothermal conditions was performed. The temperature was subsequently increased to the different annealing temperatures at $1^\circ\text{C}/\text{min}$ and several measurements were performed at designated time intervals. The diffraction patterns

were analyzed with the program WinXPOW from STOE (Darmstadt, Germany). The assignment of the XRD diffraction peaks of mannitol was performed according to Chapter 3.

2.2.2 Differential Scanning Calorimetry (DSC) of the Frozen Solutions

DSC was used to study the glass transition of the maximally freeze-concentrated solution (T_g') and the crystallization behavior of formulations with a total solid content of 5% [w/v] at low temperatures. Thereby, the ratio of mannitol to sucrose was varied and 0.05% to 0.2% NaCl were added to the formulations. Approximately 20 mg of the sterile filtrated solutions were analyzed in crimped Al-crucibles. The samples were frozen from 20°C to -70°C and reheated to 20°C with a standard scanning-rate of 10°C/min in a Netzsch DSC 204 Phoenix® (Selb, Germany), calibrated with Indium. T_g' (onset and point of inflection) and crystallization (onset, peak, enthalpy) of the excipients were determined during the heating scan.

2.2.3 Lyophilization

1000 µl of the formulations were dried in 2 R vials from Schott (Mainz, Germany) in the Epsilon 2-12 D freeze-drier from Christ (Osterrode, Germany). The samples were frozen to -50°C with a standard cooling rate of 0.45°C/min. Different annealing steps were used for the production of the samples (Table 1). Primary drying was conducted at a shelf-temperature of -15°C and a pressure of 0.045 mbar. For secondary drying the shelf-temperature was increased to 20°C, respectively 40°C at a pressure of 0.01 mbar.

Table 1: Lyophilization cycles used for the production of the samples.

process	annealing	secondary drying
I	without	20°C for 10 h
II	-20°C for 2 h	40°C for 8 h
III	-25°C for 2 h	40°C for 8 h
IIIa	-25°C for 2 h	20°C for 10 h
IV	-30°C for 2 h	40°C for 8 h

2.2.4 Differential Scanning Calorimetry (DSC) of Lyophilized Products

The lyophilized samples were analyzed with the Netzsch DSC 204 Phoenix® (Selb, Germany) from 0 to 150°C using scanning rates of 10°C/min. Approximately 10 mg of the lyophilized samples were analyzed in sealed Al-crucibles. The thermal events were analyzed in the heating scan of the DSC.

2.2.5 Temperature-Modulated-DSC (TMDSC) of Lyophilized Samples

The lyophilized samples were further analyzed with the Mettler Toledo DSC 822e (Giessen, Germany) in the modulating mode using 40 µl Al crucibles with Pin (ME 27331). The samples were scanned from 0 to 80°C at an average heating rate of 1.0°C/min at an amplitude of 0.5°C and a period of 0.8 minutes. The glass transitions were detected in the reversing heat curve.

2.2.6 X-ray Powder Diffraction (XRD)

The morphology of the lyophilized products was analyzed by X-ray powder diffraction (XRD) from 5-40° 2- θ , with steps of 0.05° 2- θ and a duration of 2 seconds per step on the X-ray diffractometer XRD 3000 TT (Seifert, Ahrenburg, Germany), equipped with a copper anode (40 kV, 30 mA, wavelength 154.17 pm).

2.2.7 Karl-Fischer Titration

The residual moisture of the samples was determined by coulometric Karl-Fischer titration using the Aqua 40.00 titrator with a headspace module (Analytik Jena AG, Halle, Germany). For the measurement at least 10 mg of the lyophilized sample was heated to 80°C for 10 minutes. The evaporated water was transferred into the titration solution and the amount of H₂O was determined. As reference material Apura Water Standard Oven 1% (Merck, Darmstadt Germany) was used and the recovery was considered for the calculation of the residual moisture of the samples.

To determine the amount of mannitol hydrate in the lyophilized sample Karl-Fischer was performed in the dynamic mode. The sample was heated with a heating rate of 5°C/min from 30 to 90°C and the water was simultaneously titrated.

3. Results and Discussion

3.1 Impact of NaCl on the Physico-chemical Properties of Mannitol-Sucrose Formulations

For the HSA-free formulations of the cytokine a total solid content of 5.0% [w/v] was planned, with mannitol as crystalline bulking agent and sucrose as amorphous stabilizer. The optimum ratio of mannitol to sucrose to produce formulations with crystalline mannitol and amorphous sucrose had to be found. The ratio of mannitol to sucrose was varied and 0.0% to 0.2% NaCl were added to the formulations. Before performing lyophilization, the physico-chemical properties of the formulations regarding T_g and crystallization were studied in the frozen state.

3.1.1 DSC of Mannitol-Sucrose-NaCl Formulations in the Frozen State

DSC indicated partial crystallization of mannitol during cooling for a 5.0% mannitol solution at scanning rates of 10°C/min. During the cooling scan the nucleation of mannitol crystals prevailed [25]. Because of the remaining amorphous mannitol fraction, two glass transitions Tg'_1 at -29.8°C and Tg'_2 at -25.5°C were measured, which were in agreement with literature [26,27]. The glass transition events were followed by mannitol crystallization with a peak maximum at -19.3°C during the rewarming of the sample. Here the nuclei, formed at low temperatures grow to mature crystals [25]. The addition of sucrose inhibited mannitol crystallization in the heating scan, indicated by a decreased enthalpy of crystallization and a shift of the peak maximum to higher temperatures (Figure 1a, b). When the sucrose fraction in the formulation exceeded 50%, mannitol crystallization was completely suppressed in the heating scan. In formulations with 4.0% mannitol and 1.0% sucrose three glass transition events Tg'_1 at -41.5°C, Tg'_2 at -32.2°C and Tg'_3 at -27.8°C could be detected. For a similar formulation with 4.0% mannitol, 1.0% sucrose in 10 mM Tris buffer Passot et al. (2005) described two glass transitions Tg'_1 at -41°C and Tg'_2 at -31°C, while Tg'_3 was not measured [5]. However, it is often difficult to detect the Tg' which is close to the onset of mannitol crystallization, even in solutions with mannitol as single component, as it can overlap with the subsequent mannitol crystallization [26]. The origin of multiple glass transition processes was discussed by Liao et al. (2005) who focused on the lowest Tg' for their studies [6]. With increasing amounts of sucrose, the two glass transitions at higher temperatures were no longer present, with only the glass transition at lower temperature remaining. The glass transition at lower temperatures was raised from -41.8°C for 4.0% mannitol and 1.0% sucrose to -33°C for 5.0% sucrose (Figure 1c).

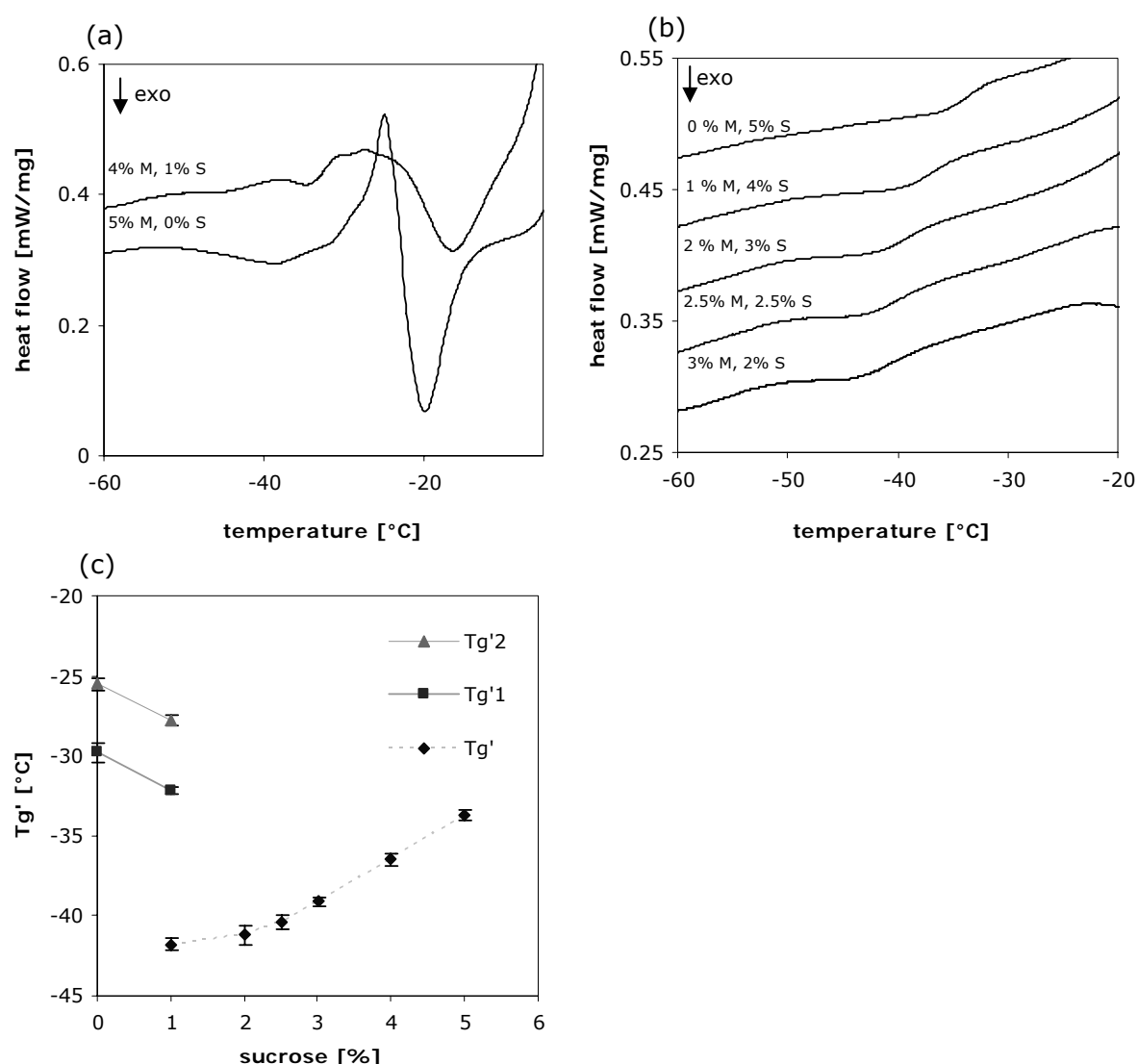


Figure 1: DSC heating curve (10°C/min) of mannitol (M) - sucrose (S) formulations with total solid content of 5.0% and different ratios of mannitol to sucrose (a and b). T_g' determined with DSC (n=3) with increasing sucrose concentrations (total solid content 5.0%) is shown in (c).

Liao et al. (2005) showed a constant T_g' of -43°C for mannitol to sucrose ratios between 1.5 and 3 and increasing T_g' values for mannitol to sucrose ratios below 1.5 for formulations with a total solid content of 7.0% using cooling rates of 20°C/min and heating rates of 5°C/min for the DSC measurements [6]. Upon the addition of NaCl to mannitol-sucrose formulations the T_g' of the formulations was lowered for all studied mannitol-sucrose combinations (Table 2).

Table 2: Tg' for mannitol-sucrose formulations with increasing amounts of NaCl.

	Tg' [°C] 0.0% NaCl	Tg' [°C] 0.05% NaCl	Tg' [°C] 0.1% NaCl	Tg' [°C] 0.2% NaCl
4.0% M - 1.0% S	-41.8	-42.1	-42.3	-43.3
3.0% M - 2.0% S	-41.2	-41.1	-41.7	-42.7
2.5% M - 2.5% S	-39.7	-40.4	-40.9	-41.9
2.0% M - 3.0% S	-39.1	-39.4	-40.9	-41.1
1.0% M - 4.0% S	-36.5	-37.5	-38.2	-38.8
0.0 %M - 5.0% S	-33.7	-34.0	-35.9	-37.3

The shift of Tg' in formulations with NaCl could be due to the very low Tg' of NaCl which lies below -60°C [28]. NaCl could act as plasticizer by increasing the amount of unfrozen water in the amorphous phase, leading to a depression of Tg'. The lowered Tg' in the formulations could further be indicative for the amorphous state of NaCl in the frozen state in the presence of mannitol and sucrose. When mannitol was present in the formulations the depression of Tg' by NaCl was less pronounced. While Tg' was lowered by 1.5 to 2.5°C in mannitol containing formulations, a decrease of 3.5°C is measured for 5.0% sucrose in the presence of 0.2% NaCl. In the amorphous state, mannitol itself can act as plasticizer and increase the amount of unfrozen water in the amorphous phase [12]. Even at the highest concentration of 4.0% mannitol and 1.0% sucrose, amorphous mannitol was existent, evident by the crystallization in the DSC heating-scan with an onset of -25°C (Figure 1a). At higher sucrose concentrations mannitol crystallization was further inhibited and the Tg' of the amorphous phase was lower compared to the Tg' of mannitol and sucrose as single components. This was ascribed to a higher amount of unfrozen water within the freeze-concentrate with increasing mannitol to sucrose ratio by Lueckel et al. (1998) [12]. A lowering of Tg' has to be considered for the development of the lyophilization cycles to avoid the higher mobility of the amorphous phase above Tg' and potential collapse during lyophilization. To avoid collapse the product temperature has to be kept below Tc, which ranges about 1 to 3°C higher than Tg' [29]. Besides the depression of Tg' NaCl inhibited mannitol crystallization in the DSC heating scan, exemplarily shown for 4.0% mannitol and 1.0% sucrose in Figure 2.

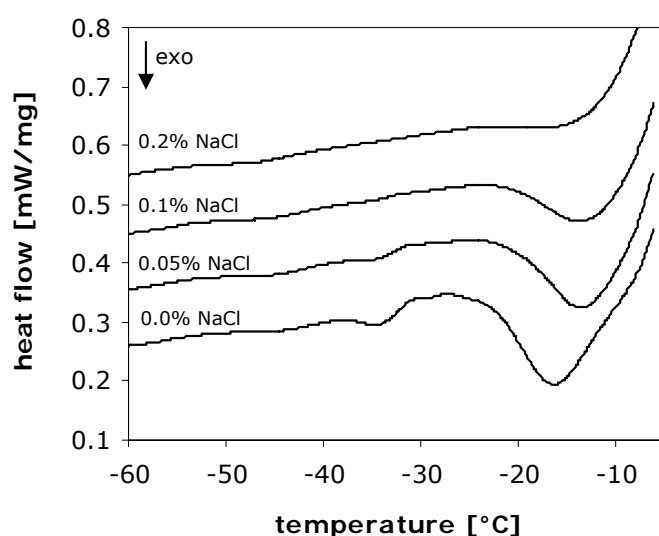


Figure 2: DSC heating scan of 4.0% mannitol and 1.0% sucrose with 0.0% to 0.2% NaCl.

3.1.2. DSC and XRD of Lyophilized Mannitol-Sucrose Formulations

For the stabilization of proteins the presence of an amorphous fraction in the lyophilized product is beneficial. Many attempts have been made to achieve amorphous mannitol to stabilize proteins, e.g. by using fast freezing rates or adding excipients that inhibit crystallization [13,20,21]. However, mannitol frequently crystallizes upon storage which can lead to stability problems for the protein. Crystalline mannitol loses its molecular interaction with proteins and with it the ability to stabilize the protein [2]. This indicates that the approach to produce amorphous mannitol as protein stabilizing component in a lyophilized formulation often fails. Therefore, a high degree of mannitol crystallization and the addition of a second amorphous stabilizer e.g. sucrose or trehalose is the favored route. To ensure sufficient mannitol crystallization during the lyophilization process the formulation compositions, as well as the lyophilization processes have to be optimized. The addition of amorphous excipients can inhibit mannitol crystallization, leading to partially crystalline system. This was shown for formulations with a total solid content of 5.0% and varying ratios of sucrose to mannitol. After lyophilization without annealing the products were largely amorphous when more than 2.5% sucrose was present (Figure 3a). In the DSC no crystallization was detected for 2.5% sucrose and 2.5% mannitol during freezing and rewarming. However, the lyophilized products were partially crystalline, indicating that crystallization occurred to a great extent during the drying process. This observation is in agreement with Pyne et al. (2001) [30]. The LTXRD experiments further supported this finding, as no peaks for crystalline mannitol appeared after freezing the samples to -50°C (Figure 8). In formulations with a 1:1 mannitol to

sucrose ratio, peaks of δ -mannitol (9.7° 2- θ) and β -mannitol (23.4° 2- θ) were detected. Furthermore, mannitol hydrate indicated by the peak at 17.9° 2- θ was present.

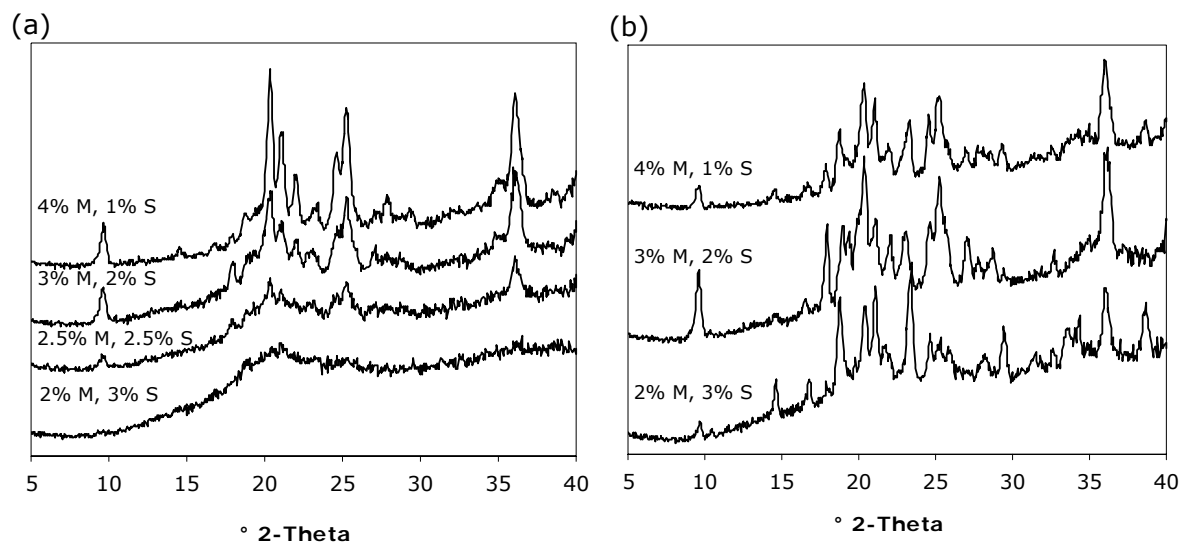


Figure 3: XRD of mannitol (M) - sucrose (S) formulations after lyophilization with process I (a) and with process IIIa which included an annealing step at -25°C for 2 hours (b).

In the first DSC heating scan of 2.5% mannitol and 2.5% sucrose, lyophilized with program I two glass transitions (T_g) at 12°C and 36°C followed by mannitol crystallization with an onset of 43.3°C and a peak maximum of 55.5°C were detected (Figure 4).

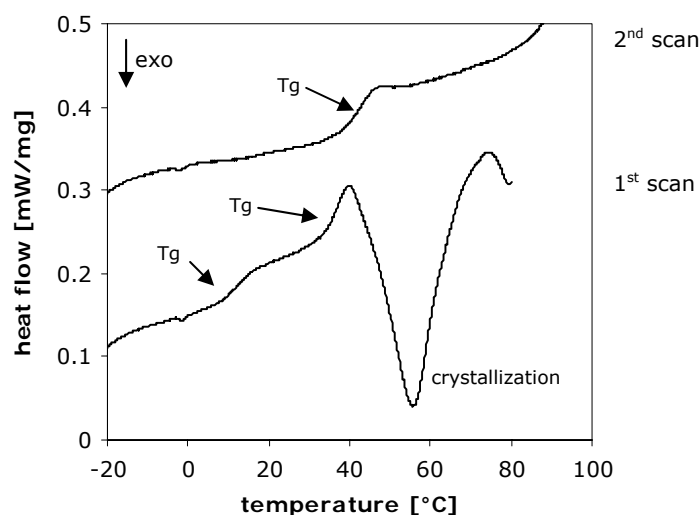


Figure 4: DSC heating scans of 2.5% mannitol and 2.5% sucrose lyophilized with program I.

The first glass transition at 12°C could be attributed to the amorphous mannitol fraction. For amorphous mannitol a T_g of 13°C was described by Kim et al. (1998) [11]. After the crystallization in the first DSC scan mannitol was present in the crystalline form, as confirmed by XRD (data not shown). Therefore, only the higher T_g at 42°C, which corresponds to sucrose remained in the second DSC-scan. Increasing the mannitol content to 3.0% and 4.0% led to a higher intensity of the mannitol peaks in the XRD. However, formulations with 3.0% mannitol and 2.0% sucrose, dried with program I also showed a crystallization event in the first scan pointing at the presence of amorphous mannitol. For 4.0% mannitol and 1.0% sucrose no crystallization was detected in the DSC heating scan. This could be ascribed to a high degree in mannitol crystallinity after lyophilization, which could be confirmed by the high sucrose T_g of 58°C. For lyophilized sucrose formulations with a residual moisture of 0.7% to 2.0% a T_g between 59°C and 63°C is described by te Booy et al. (1992) [31].

After lyophilization with annealing (program IIIa) a higher degree of crystallinity was achieved (Figure 3b). Thereby, mannitol crystallized mainly in the β-modification in formulations consisting of 2.0% mannitol and 3.0% sucrose, which were amorphous after lyophilization without annealing. Formulations with more than 2.0% mannitol were composed of β- and δ-mannitol, comparable to lyophilization without annealing. However, a larger fraction of mannitol hydrate (peak at 17.9° 2-θ) was present after drying the samples with annealing. This could be due to the fact that mannitol hydrate is a modification which emerges mainly at low temperatures during lyophilization. In the further progress of the study, the impact of annealing on the formation of mannitol hydrate was studied. Thereby, the focus was set on formulations consisting of 4.0% mannitol and 1.0% sucrose, as a high degree of mannitol crystallization can be achieved.

3.1.2 Impact of NaCl on Lyophilized Mannitol-Sucrose-Formulations

NaCl inhibited the crystallization of mannitol during freezing, which was shown by DSC for formulations with 4.0% mannitol and 1.0% sucrose (Figure 2). After lyophilization of 4.0% mannitol and 1.0% sucrose mannitol crystallization was observed for all studied NaCl concentrations and lyophilization cycles. Figure 5 shows the XRD diffraction patterns after lyophilization with program III.

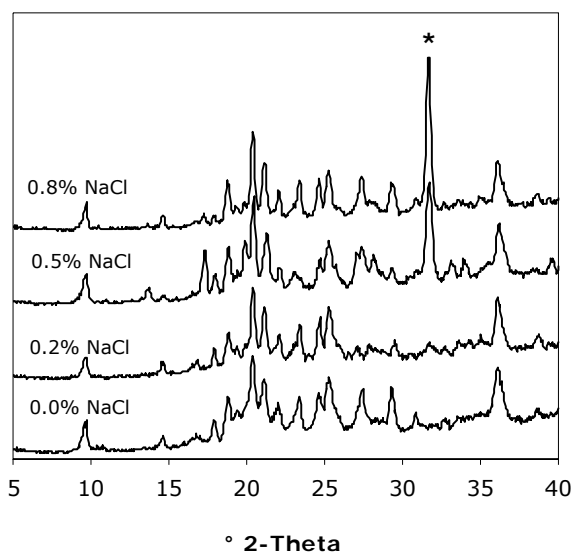


Figure 5: XRD of 4.0% mannitol and 1.0% sucrose with 0.0% to 0.8% NaCl (*marks characteristic peak of NaCl) lyophilized with program III.

For 0.0% to 0.8% NaCl mannitol crystallized as a mixture of the β - and δ -modification and mannitol hydrate (17.9° 2- θ), with a slight decline of the mannitol hydrate fraction at 0.8% NaCl. No crystallization events were measured in the DSC of the lyophilized products as well, indicating that mannitol and NaCl have crystallized during lyophilization. However, the T_g of the formulations was affected by the addition of NaCl. Both DSC and TMDSC showed that the T_g of the formulations was decreased by approximately 25°C when 0.4% NaCl was added to the formulations (Figure 6).

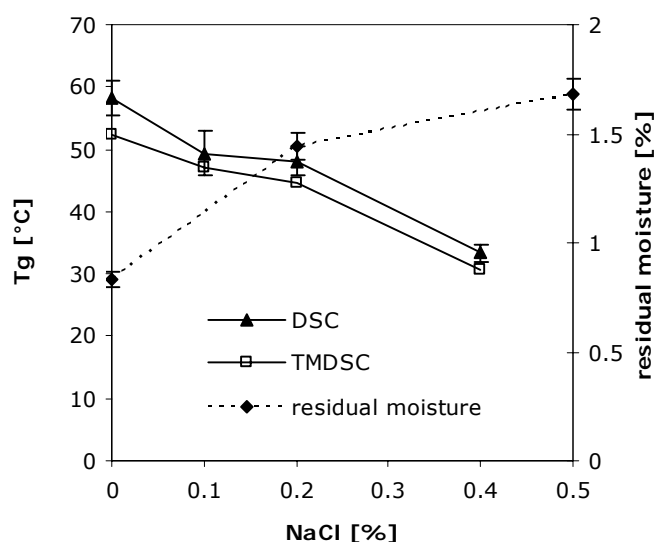


Figure 6: T_g determined with TMDSC and DSC (second scan) and residual moisture of 4.0% mannitol and 1.0% sucrose with 0.0% to 0.5% NaCl after lyophilization with program III.

The residual moisture increased from 0.8% without NaCl to 1.7% with 0.5% NaCl. This could explain the lowered glass transitions as water acts as plasticizer for the amorphous phase. Although mannitol crystallization was not affected by increasing NaCl concentrations, the lowered glass transition temperatures of the lyophilized products needs to be considered for the storage stability of a protein. A higher T_g is often beneficial for protein stability upon storage which was for example shown by Prestrelski et al. (1995) for Interleukin-2 [32]. However, Chang et al. (1996) demonstrated that storage of lyophilized recombinant human interleukin-1 receptor antagonist formulations below T_g was necessary, but not always sufficient to ensure long-term stability e.g. when the protein was already damaged during lyophilization process [33]. On the other hand, Davidson and Sun (2001) demonstrated for sucrose–raffinose formulations that an increase in T_g of the lyophilized samples was not related to a higher recovery of Glucose-6-phosphate Dehydrogenase activity after reconstitution when stored above T_g [34].

3.2 Impact of Annealing on the Formation of Mannitol Hydrate

To study the impact of annealing on the formation of mannitol hydrate, formulations with 4.0% mannitol and 1.0% sucrose were lyophilized with different lyophilization cycles. Furthermore, LTXRD was used to monitor crystallization of mannitol during an annealing step at low temperatures. For the LTXRD experiments solutions with higher concentrations (8.0% mannitol and 2.0% sucrose) were used, due to the detection limit of the method.

3.2.1 LTXRD of Mannitol-Sucrose-Formulations at Different Annealing Conditions

DSC offers information on crystalline and amorphous phases in the frozen state. However, with DSC it is not possible to identify and characterize the composition and modifications of the crystalline phase [35], which is on the other hand possible with LTXRD [36,37]. After freezing a formulation of 8.0% mannitol and 2.0% sucrose to -50°C with a cooling rate of 0.5°C/min no peaks of crystalline mannitol were detected (Figure 7). The cooling rate of 0.5°C/min was chosen as it is comparable to the cooling rate used during lyophilization. After an isothermal phase of one hour at -50°C the temperature was increased with 1.0°C/min to the annealing temperatures of -23°C, -27°C and -32°C, where three measurements were performed under isothermal conditions. After heating the samples to the annealing temperatures peaks of crystalline mannitol were detected. At -23°C and -27°C mannitol crystallized in the δ -modification,

seen by peaks at 9.7° 2- θ and 20.4° 2- θ (Figure 7a). Annealing at -32°C on the other hands led to a crystallization of mannitol hydrate which was evident by the peak at 17.9° 2- θ (Figure 7b). In the DSC heating scan mannitol crystallized with an onset of -25°C . At -32°C the crystallization process was decelerated as indicated by the lower intensity of the peaks in the first scan at -32°C .

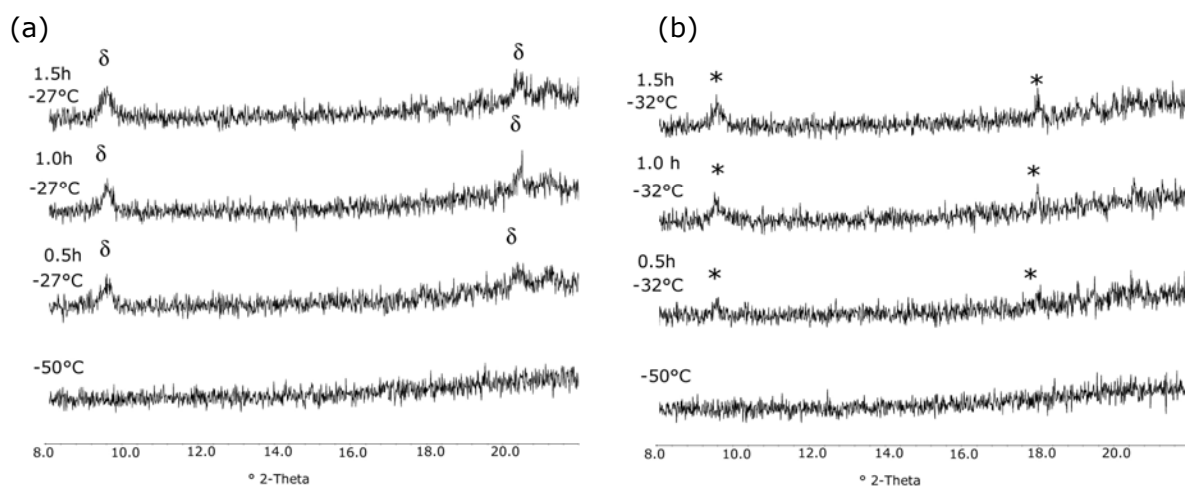


Figure 7: LTXRD of 8.0% mannitol and 2.0% sucrose after freezing to -50°C and during an isothermal annealing step at -27°C , with crystallization of δ -mannitol (a) and -32°C with crystallization of mannitol hydrate (marked with *) (b).

Thus, according to LTXRD annealing at a temperature of -32°C is not suitable due to formation of mannitol hydrate. To investigate whether the findings of the LTXRD could be transferred to formation of mannitol hydrate in lyophilized products, lyophilization was conducted at different annealing temperatures and the dried samples were analyzed by XRD.

3.2.2 XRD of Lyophilized Samples Produced with Different Lyophilization Cycles

The impact of annealing and secondary drying on the formation of mannitol hydrate during lyophilization was investigated for formulations of 4.0% mannitol and 1.0% sucrose without and with 0.2% NaCl. Annealing during lyophilization was conducted for 2 hours at shelf-temperatures of -20°C , -25°C or -30°C (Table 1). All processes resulted in a crystalline formulation, which was confirmed by DSC (data not shown). XRD revealed the presence of β - and δ -mannitol, as well as different amounts of mannitol hydrate (Figure 8a). The characteristic peak of mannitol hydrate at 17.9° 2- θ is enlarged in Figure 8b.

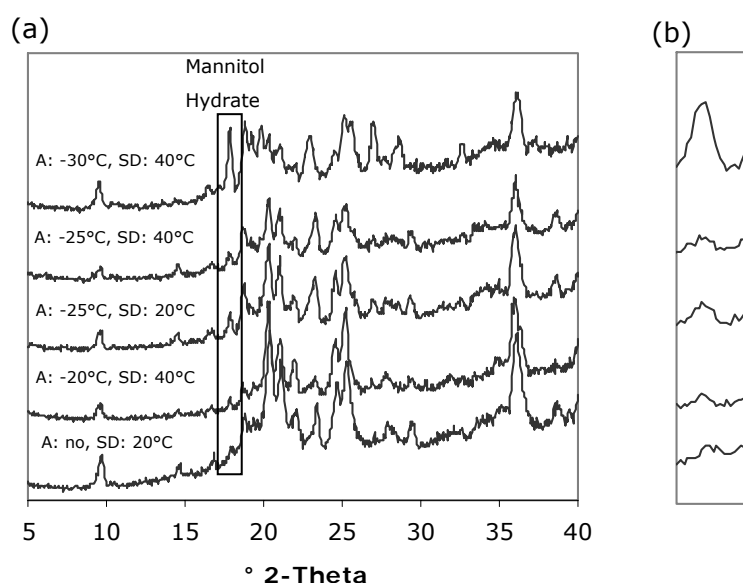


Figure 8: XRD of lyophilized 4.0% mannitol and 1.0% sucrose after different annealing (A) and secondary drying (SD) parameters (a) and mannitol hydrate peak at 17.9° 2- Θ (b).

To compare the amount of mannitol hydrate formed after the different processes, the peak area and the relative intensity of the mannitol hydrate peak at 17.9° 2- Θ were considered (Figure 9). The peak area was calculated by integrating the area under the peak from 17.4° 2- Θ to 18.4° Θ in the diffraction pattern. For the relative intensity the height of the mannitol hydrate peak was compared to the highest peak of the diffraction pattern, which was set as 100%. In formulations dried without annealing the lowest fraction of mannitol hydrate was formed, although secondary drying was performed at 20°C. Comparing the different annealing conditions the formation of mannitol hydrate was more distinct at lower annealing temperatures. This was in agreement with LTXRD, where mannitol hydrate was also formed at a lower temperature. The addition of 0.2% NaCl to the formulations slightly inhibited the formation of mannitol hydrate during lyophilization with annealing. However, NaCl tended to promote the formation of mannitol hydrate when annealing was waived. Comparing the different secondary drying temperatures less mannitol hydrate was formed when secondary drying was conducted at 40°C, which was in agreement with Johnson et al. (2002) [4]. However, the effect was less pronounced than the impact of the selected annealing temperature.

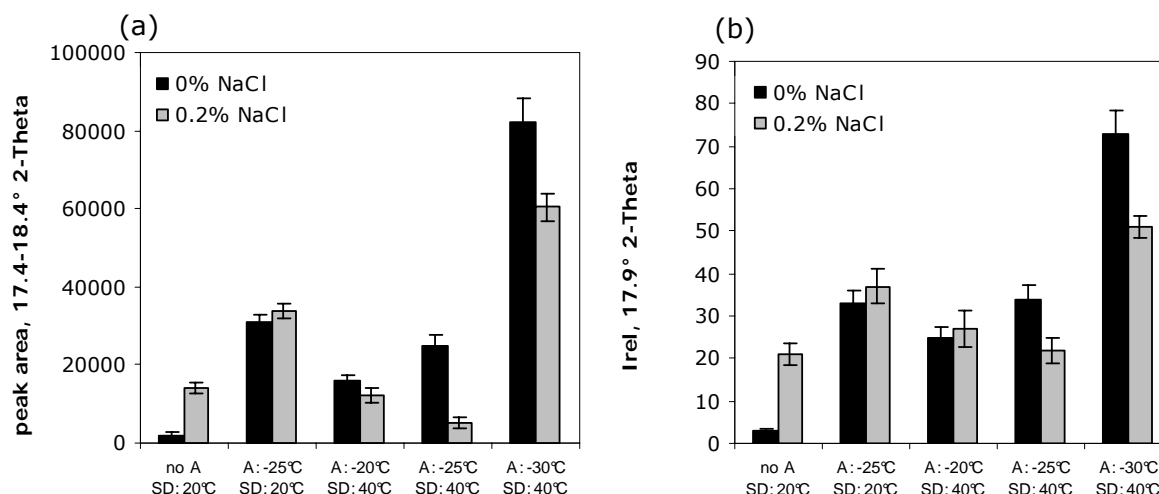


Figure 9: Peak area (a) and relative intensity (b) of mannitol hydrate peak after lyophilization of 4.0% mannitol and 1.0% sucrose without and with 0.2% NaCl using different annealing (A) and secondary drying (SD) conditions (n=3).

To estimate the amount of mannitol hydrate in the lyophilized formulation with 4.0% mannitol and 1.0% sucrose dried with program IV dynamic Karl-Fischer titration was performed (Figure 10). Water was released in two steps from the lyophilized product upon heating. The first step between 30 and 45°C could be attributed to the release of sorbed water and the second step from about 55 to 70°C mainly to the release of hydrate water from mannitol. In the second step about 0.6% water was released and in total the residual moisture content 1.1%. The data showed that about 15% to 20% of mannitol was present as hydrate, when calculated as hemihydrate in the worst case of annealing at -30°C.

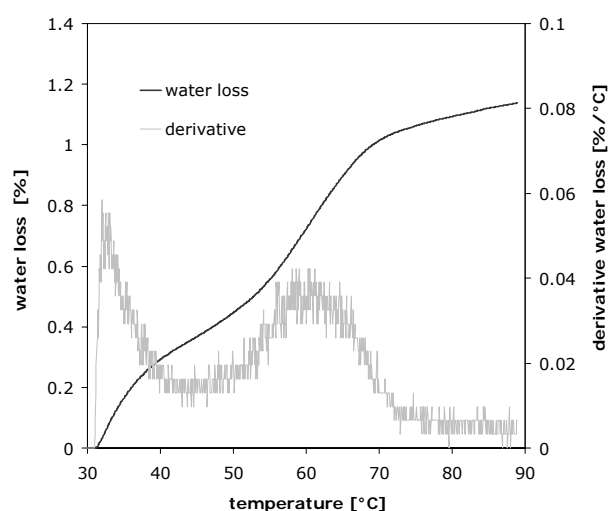


Figure 10: Water loss from 30 to 90°C determined with dynamic Karl-Fischer titration for 4.0% mannitol and 1.0% sucrose dried with program IV.

LTXRD and XRD both showed that annealing can promote the formation of mannitol hydrate. Although there were differences in volumes and containers used during lyophilization and for the LTXRD experiment it was evident that mannitol hydrate was formed especially at lower temperatures. Therefore, it is beneficial to conduct lyophilization without annealing if possible. For the formulations with 4.0% mannitol and 1.0% sucrose lyophilization without annealing was feasible, because mannitol crystallinity comparable to the processes with an extra annealing step was achieved. If annealing is required it is important to select a shelf temperature during annealing above -30°C to keep the level of mannitol hydrate as low as possible.

4. Conclusions

DSC results of the system mannitol-sucrose at low temperatures indicated a lowering of T_g' with increasing amounts of mannitol due to the plasticizing effect of mannitol on the amorphous phase. The addition of NaCl further reduced the T_g' of the formulations, which was more pronounced for formulations with lower mannitol contents. Mannitol crystallization during freezing was inhibited by sucrose and NaCl, resulting in partially crystalline systems. Lyophilization of 4.0% mannitol and 1.0% sucrose resulted in an extensive crystallization of mannitol, even without annealing. However, the T_g of these formulations was depressed by NaCl. Annealing increased mannitol crystallinity, but a higher mannitol hydrate content was often found after lyophilization of 4.0% mannitol and 1.0% sucrose with annealing. LTXRD of formulations with 8.0% mannitol and 2.0% sucrose showed that mannitol hydrate was preferably formed at lower annealing temperatures, while annealing at higher temperatures led to the formation of δ -mannitol. The results of LTXRD were confirmed by XRD after lyophilization, which showed that the highest amount of mannitol hydrate was formed after annealing at -30°C . NaCl enhanced the formation of mannitol hydrate when lyophilization was conducted without annealing. Compared to the impact of annealing the secondary drying temperature only played a minor role on the formation of mannitol hydrate. If annealing during lyophilization is necessary, a sufficient high temperature needs to be selected to avoid the formation of mannitol hydrate.

5. References

1. M. J. Pikal, K. M. Dellermann, M. L. Roy and R. M. Rigglin. The Effects of Formulation Variables on the Stability of Freeze-Dried Human Growth Hormone. *Pharm. Res.* **8**:427-436 (1991).
2. K. Izutsu, S. Kojima. Excipient crystallinity and its protein-structure-stabilizing effect during freeze-drying. *J. Pharm. Pharmacol.* **54**:1033-1039 (2002).
3. K. Kasraian, T. M. Spitznagel, J. A. Juneau, K. Yim. Characterization of the Sucrose/Glycine/Water System by Differential Scanning Calorimetry and Freeze-Drying Microscopy. *Pharm. Dev. Technol.* **3**:233-239 (1998).
4. R. Johnson, C. Kirchhoff, H. Gaud. Mannitol-Sucrose Mixtures-Versatile Formulations for Protein Lyophilization. *J. Pharm. Sci.* **91**:914-922 (2002).
5. S. Passot, F. Fonseca, M. Alarcon-Lorca, D. Rolland, M. Marin. Physical characterization of formulations for the development of two stable freeze-dried proteins during both dried and liquid storage. *Eur. J. Pharm. Biopharm.* **60**:335-348 (2005).
6. X. Liao, R. Krishnamurthy, R. Suryanarayanan. Influence of the Active Pharmaceutical Ingredient Concentration on the Physical State of Mannitol-Implications in Freeze-Drying. *Pharm. Res.* **22**:1978-1985 (2005).
7. A. Cannon, E. Trappier. The influence of Lyophilization on the Polymorphic Behavior of Mannitol. *PDA J. Pharm. Sci. Technol.* **54**:13-22 (2000).
8. A. Pyne, R. Surana, R. Suryanarayanan. Crystallization of Mannitol below T_g' during Freeze-Drying in Binary and Ternary Aqueous Systems. *Pharm. Res.* **19**:901-908 (2002).
9. X. Lu, M. Pikal. Freeze-Drying of Mannitol-Trehalose-Sodium Chloride-Based Formulations: The impact of Annealing on Dry Layer Resistance to Mass Transfer and Cake Structure. *Pharm Dev. Technol.* **9**:85-95 (2004).
10. M. J. Pikal, K. M. Dellermann, M. L. Roy, R. M. Rigglin. The Effects of Formulation Variables on the Stability of Freeze-Dried Human Growth Hormone. *Pharm. Res.* **8**:427-436 (1991).
11. A. Kim, M. Akers, S. Nail. The Physical State of Mannitol after Freeze-Drying: Effect of Mannitol Concentration, Freezing Rate and a Noncrystallizing Cosolute. *J. Pharm. Sci.* **87**:931-935 (1998).
12. B. Lueckel, D. Bodmer, B. Helk, H. Leuenberger. Formulations of Sugars with Amino Acids or Mannitol-Influence of Concentration Ratio on Properties of the Freeze-Concentrate and the Lyophilisate. *Pharm. Dev. Technol.* **3**:325-336 (1998).
13. C. Telang, L. Yu, R. Suryanarayanan. Effective Inhibition of Mannitol Crystallization in Frozen Solutions by Sodium Chloride. *Pharm. Res.* **20**:660-667 (2003).
14. M. F. Mazzobre, M. P. Longinotti, H. R. Corti, M. P. Buera. Effect of Salts on the Properties of Aqueous Sugar Systems, in Relation to Biomaterial Stabilization. 1. Water Sorption Behavior and Ice Crystallization/Melting. *Cryobiol.* **43**:199-210 (2001).
15. A. Hawe, W. Frieß, Physico-chemical Lyophilization Behavior of Mannitol, Human Serum Albumin Formulations. *Eur. J. Pharm. Sci.* **28**:224-232 (2006).
16. M. J. Akers, N. Milton, S. R. Byrn, S. L. Nail. Glycine Crystallization During Freezing: The Effect of Salt Form, pH, and Ionic Strength. *Pharm. Res.* **12**:1455-1461 (1995).
17. E. Y. ShalaeV, F. Franks. Crystalline and Amorphous Phases in the Ternary System Water-Sucrose-Sodium Chloride. *J. Phys. Chem.* **100**:1144-1152 (1996).
18. H. Nicolajsen, A. Hvidt. Phase Behavior of the System Trehalose-NaCl-Water. *Cryobiol.* **31**:199-205 (1994).
19. L. Yu, N. Milton, E. Groleau, D. Mishra, R. Vansickle. Existence of a Mannitol Hydrate during Freeze-Drying and Practical Implications. *J. Pharm. Sci.* **88**:196-198 (1999).

20. K. Izutsu, S. O. Ocheda, N. Aoyagi, S. Kojima. Effect of sodium tetraborate and boric acid on nonisothermal mannitol crystallization in frozen solutions and freeze-dried solids. *Int. J. Pharm.* **273**:85-93 (2004).
21. T. Yoshinari, R. T. Forbes, P. York, Y. Kawashima. Crystallisation of amorphous mannitol is retarded using boric acid. *Int. J. Pharm.* **258**:109-120 (2003).
22. K. K. Izutsu, S. Yoshioka, T. Terao. Effect of Mannitol Crystallinity on the Stabilization of Enzymes during Freeze-Drying. *Chem. Pharm. Bull.* **42**:5-8 (1994).
23. H. R. Costantino, J. D. Andya, P. A. Nguyen, N. Dasovich, T. D. Sweeney, S. J. Shire, C. C. Hsu, Y. F. Maa. Effect of Mannitol Crystallization on the Stability and Aerosol Performance of a Spray-Dried Pharmaceutical Protein, Recombinant Humanized Anti-IgE Monoclonal Antibody. *J. Pharm. Sci.* **87**:1406-1411 (1998).
24. L. Kreilgaard, S. Frokjaer, J. M. Flink, T. W. Randolph, J. F. Carpenter. Effects of Additives on the Stability of Humicola lanuginosa Lipase during Freeze-Drying and in the Dried Solid. *J. Pharm. Sci.* **88**:281-290 (1999).
25. L. Yu. Amorphous pharmaceutical solids: preparation, characterization and stabilization. *Adv. Drug Deliv. Rev.* **48**:27-42 (2001).
26. R. Cavatur, N. Vemuri, A. Pyne, Z. Chrzan, D. Toledo-Velasquez, R. Suryanarayanan. Crystallization Behavior of Mannitol in Frozen Aqueous Solutions. *Pharm. Res.* **19**:894-900 (2002).
27. P. Meredith, A. Donald, R. Payne. Freeze-Drying: In Situ Observations Using Cryoenvironmental Scanning Electron Microscopy and Differential Scanning Calorimetry. *J. Pharm. Sci.* **85**:631-637 (1996).
28. F. Franks. Solid Aqueous solution. *Pure Appl. Chem.* **65**:2527-2537 (1993).
29. M. J. Pikal, S. Shah. The collapse temperature in freeze drying: dependence on measurement methodology and rate of water removal from the glassy phase. *Int. J. Pharm.* **62**:165-186 (1990).
30. A. Pyne, K. Chatterjee, T. Suryanarayanan. Solute Crystallization in Mannitol-Glycine Systems – Implications on Protein Stabilization in Freeze-Dried Formulations. *J. Pharm. Sci.* **92**:2272-2282 (2003).
31. M. P. W. M. te Booy, R. A. de Ruiter, A. L. J. de Meere. Evaluation of the Physical Stability of Freeze-Dried Sucrose-Containing Formulations by Differential Scanning Calorimetry. *Pharm. Res.* **9**:109-114 (1992).
32. S. J. Prestrelski, K. A. Pikal, T. Arakawa. Optimization of lyophilization conditions for recombinant human interleukin-2 by dried-state conformational analysis using Fourier-transform infrared spectroscopy. *Pharm. Res.* **12**:1250-1259 (1995).
33. B. S. Chang, R. M. Beauvais, A. Dong, J. F. Carpenter. Physical Factors Affecting the Storage Stability of Freeze-Dried Interleukin-1 Receptor Antagonist: Glass Transition and Protein Confirmation. *Arch. Biochem. Bioph.* **331**:249-258 (1996).
34. P. Davidson, W. Q. Sun. Effect of Sucrose/Raffinose Mass Ratios on the Stability of Co-Lyophilized Protein During Storage above Tg. *Pharm. Res.* **19**:474-479 (2001).
35. A. Pyne, R. Suryanarayanan. Phase Transitions of Glycine in Frozen Aqueous Solutions and during Freeze-Drying. *Pharm. Res.* **18**:1448-1454 (2001).
36. R. Cavatur, R. Suryanarayanan. Characterization of phase transition during freeze-drying by in situ X-ray powder diffractometry. *Pharm. Dev. Tech.* **3**:579-586 (1998).
37. R. Cavatur, R. Suryanarayanan. Characterization of frozen aqueous solutions by low temperature X-ray powder diffractometry. *Pharm. Res.* **15**:193-198 (1998).

Chapter 6

Development of Stable, HSA-free Formulations for a Hydrophobic Cytokine

Abstract

Chapter 6 describes the characterization of the hydrophobic cytokine with respect to the influence of pH and ionic strength on aggregate formation and the thermal stability of the cytokine, as well as the development of HSA-free formulations. When the formulation pH exceeded 5.5 a precipitation of the cytokine led to a significant turbidity increase. Thereby, the increase in aggregates and turbidity determined by HP-SEC and DLS were more pronounced at a higher ionic strength. Especially at higher pH values protein adsorption was more distinct compared to pH 3.0. Protein adsorption could be minimized by the addition of polysorbate 20 or the use of glass type I⁺. FTIR showed that the denaturation temperature was decreased when the formulation pH was raised, indicating enhanced stability at lower pH values, which was confirmed by DLS.

Five liquid formulations in the pH range 3.5 to 4.5 and five lyophilized formulations in the pH range 4.0 to 5.0 were stored for 6 months at 2-8°C, 25°C / 60% RH and 40°C / 75% RH. The stability of these formulations was evaluated regarding aggregation and chemical modification. The stability was in each case better at lower pH values, which was in agreement with the higher denaturation temperatures measured by FTIR for the cytokine formulated at lower pH. For the lyophilized formulation at pH 4.0 stored at 40°C / 75% RH a discoloration of the reconstituted solutions was observable, which could be ascribed to an inversion of sucrose. Both liquid formulations at pH 3.5 and 4.0 and lyophilized formulations at pH 4.0 to 5.0 showed good stability when stored at 2-8°C. Thus, freeze-drying allowed formulating the cytokine at significantly higher pH. To avoid protein adsorption the addition of polysorbate 20 and the use of glass type I⁺ were feasible.

Keywords: hydrophobic cytokine, HSA-free formulation, protein adsorption, stability

1. Introduction

The model protein for the studies was a recombinant human cytokine with a molecular weight of about 20 kDa, which can be specified as very hydrophobic. The cytokine is produced in *E. coli* and therefore non-glycosylated [1]. During formulation development the hydrophobicity and the corresponding low solubility and adsorption phenomena were the major concerns that had to be overcome. One possible way is a formulation of the cytokine with HSA, which is an excellent stabilizer in liquid and lyophilized formulations. The properties of a HSA-containing formulation of the cytokine were characterized and discussed in Chapter 2. HSA can act as lyoprotector and cryoprotector during lyophilization [2]. Moreover, it reduces the loss of active protein due to adsorption, which poses a problem especially for low dose formulations of hydrophobic proteins [3,4]. However, HSA as excipient is generally extracted from human plasma and implicates the problems associated with human blood derived products. Besides the risk of blood born pathogens, batch to batch variations can occur. HSA itself exhibits a low risk of immunogenicity, whereas in presence of a second protein the formation of mixed aggregates can lead to immunogenicity reactions, which was e.g. shown for rhINF α [5,6]. Other issues emerging for HSA-containing formulations are the difficulties that occur during the development of analytical methods for the active protein in the formulations. With HSA, a second protein often present in a 10 to 50 fold excess compared to the active protein is brought into the formulation. This makes selective analytics of the active protein, as well as its aggregates and degradation products difficult and often impossible. Specific methods like ELISA [7], selective precipitation [8], western-blot or BIACORE are required to solve this analytical problem. For these reasons, HSA is avoided in the development of new formulations as far as possible. In its function as lyo- and cryoprotector, HSA can be replaced by other excipients e.g. sugars, sugar alcohols or amino acids. The concern of protein adsorption can be overcome by the addition of sugars [9] and most important by surfactants [10,11], e.g. poloxamer 188 or polysorbate 20 and 80. Another approach to minimize protein adsorption is the use of special containers with reduced susceptibility for adsorption, like glass type I⁺ [12].

The first studies focused on the optimization of formulation buffer and pH. Changes of the cytokine in relation to pH, ionic strength and temperature were evaluated using different analytical techniques to get an understanding of its structural characteristics. For selected pH and buffer conditions short-term stability studies over two weeks were conducted. In this context, the impact of NaCl and glycine concentration and the addition of further excipients (mannitol, trehalose, polysorbate 20) on the formation of aggregates were evaluated. Furthermore, the problem of protein adsorption needed to be considered, when selecting the containers and the constituents of the formulation. The

impact of pH, ionic strength and the presence of surfactants on the degree of protein adsorption were rated for different container materials. Besides these studies the freeze-thaw stability of the cytokine was tested, which was important for the subsequent development of lyophilized formulations. For the lyophilized cytokine formulations a combination of mannitol with sucrose was selected based on the results of the studies described in Chapter 5. Depending on the results of the preliminary studies five liquid formulations and five lyophilized formulations were to be selected. The stability of the formulations was evaluated over 6 months at 2-8°C, 25°C / 60% RH and 40°C / 75% RH.

2. Materials and Methods

2.1 Materials

2.1.1 Proteins and Excipients

The starting material contained 1.0 mg/ml cytokine formulated with 0.1% sodium dodecyl sulfate (SDS) at pH 5.5. Preparative size-exclusion chromatography was used to remove SDS using Sephadex G-25 columns (Amersham Biosciences, Uppsala, Sweden) equilibrated with 10mM NaOH (pH 12) as eluting buffer. The protein content of the fractions was determined with UV-spectroscopy at 280 nm. The fractions were further analyzed for the presence of SDS according to the European Pharmacopoeia. Therefore, 0.1 ml of the fraction was mixed with 0.1 ml 0.1% methylene blue solution and 2.0 ml diluted H₂SO₄ (5.5 ml concentrated H₂SO₄ in 100 ml H₂O). The aqueous solution was shaken out with 2.0 ml dichloromethane (DCM), whereby the ionic pair of methylene blue (Sigma, Steinheim, Germany) and SDS colored the DCM-phase blue. The samples were evaluated visually by means of reference solutions with known SDS contents. SDS from Merck (Hohenbrunn, Germany) was used for the reference solutions. After the buffer exchange with Sephadex-G25 column, the cytokine was intermediately formulated in 10 mM NaOH at pH 12. A concentrated stock solution of the particular buffer (200 mM) was added to the formulations and the pH was instantly adjusted with HCl.

As excipients for formulation development sucrose from Suedzucker (Mannheim, Germany), mannitol from Caelo (Hilden, Germany), polysorbate 20 from Serva (Heidelberg, Germany) and glycine and NaCl from Sigma (Steinheim, Germany) were employed without further purification.

2.1.2 Containers

2 R glass vials were a donation of Schott AG (Mainz, Germany). Two qualities of glass were employed, standard borosilicate glass type I and SCHOTT type I plus[®], which are based on standard type I glass. An additional layer of 0.1 to 0.2 μm of SiO_2 is coated onto the inner surface using the Plasma Impulse Chemical Vapor Deposition (PICVD) process. The vials were closed with unsiliconized butyl-lyophilization stoppers (Firma West, Eschweiler, Germany). BD Hypak SCF[™] glass prefilled 1 ml syringes were a donation of Becton Dickinson GmbH (Heidelberg, Germany). The prefilled syringes were used for the stability study of the liquid cytokine formulation. For the stability study 1.0 ml of the particular formulation was filled into the syringe barrel and subsequently the plunger, consisting of a stopper and a rod, was attached to the barrel from the back.

2.2 Methods

2.2.1 Turbidimetry

The NEPHLA turbidimeter (Dr. Lange, Düsseldorf, Germany) was used for turbidity measurements. The principle of turbidity measurement is 90° scattered light photometry. Light ($\lambda=860$ nm) is sent through the samples and the scattered light is measured at 90° angle. The system is calibrated with formazine as standard and the results are given in formazine nephelometric units (FNU). To evaluate the degree of turbidity the reference solutions I-IV of the European Pharmacopoeia method 2.2.1 (clarity and degree of opalescence of liquids) were used [13]. A stock solution was prepared by mixing hydrazine sulfate (10 mg/ml) and hexamethylenetetramine (100 mg/ml) at a ratio of 1:1. After 24 hours the stock solution was diluted with water to concentrations of 0.075 mg/ml hydrazine sulfate and 0.75 mg/ml hexamethylenetetramine (both from Sigma-Aldrich, Steinheim, Germany). The reference solutions were prepared with the diluted solution according to Table 1 and the turbidity in FNU was measured.

Table 1: Composition of the opalescence reference solutions and turbidity.

reference solution	diluted stock solution [ml]	water <i>R</i> [ml]	turbidity [FNU]	degree of opalescence
I	5	95	3.2	clear (\leq Ref I)
II	10	90	6.1	slightly opalescent (\leq Ref II)
III	30	70	17.8	opalescent (\leq Ref III)
IV	50	50	29.4	very opalescent (\leq Ref IV)

The method is not specific for proteins and therefore sample preparation is very important. To avoid disturbance by dust, all used buffer solutions were filtered (0.45 μm PES membrane). Further, the samples were degassed for about 20 seconds in an ultrasonic bath prior to the measurement.

2.2.2 UV-Spectroscopy

To determine the degree of protein adsorption, the protein content in the samples was determined with UV-spectroscopy using the Thermo Spectronic UV 1 from Thermo Electron Cooperation (Dreieich, Germany). The UV-absorption was measured at $\lambda=280\text{ nm}$. The protein content calculated using a molar extinction coefficient of 1.7.

2.2.3 High Pressure Size Exclusion Chromatography (HP-SEC)

Protein aggregation was determined by HP-SEC on a HP 1100 (Agilent Technologies, Waldbronn, Germany). A TSKgel G3000SWxl column (Tosoh Biosep, Stuttgart, Germany) with an adequate guard column was used. The running buffer was composed of 175 mM NaH_2PO_4 and 0.1% SDS with a pH adjusted to 6.8. The analytics were performed at a flow rate of 0.5 ml/min with UV-detection at 210 nm. The chromatograms were integrated manually with ChemStation (Agilent Technologies, Waldbronn, Germany) exemplarily shown in Figure 1

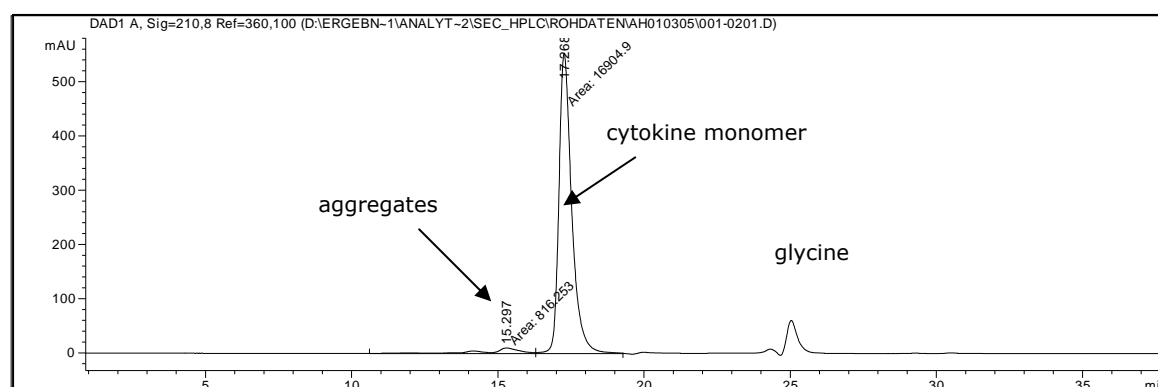


Figure 1: Example for integration of a HP-SEC chromatogram of 0.25 mg/ml cytokine.

Aggregation in % was determined by comparing the area under the curve (AUC) of dimers and lower aggregates with the AUC of the monomer peak. Further changes in the AUC over the storage time were considered.

2.2.4 Reversed Phase High Pressure Liquid Chromatography (RP-HPLC)

With RP-HPLC oxidation of methionine can be detected. RP-HPLC was performed according to Geigert et al. (1988) [14], using a Jupiter C4 column with 300 Å 5 µm 250*4.6 mm i.d. and a security guard C4, 4*3 mm (Phenomenex, Aschaffenburg, Germany), which was kept at 30°C for the analytics. A flow-rate of 1.0 ml/min was used and UV-detection at 214 nm. An elution gradient (Figure 2) was applied, using 10% acetonitrile (ACN) with 0.1% trifluoroacetic acid (TFA) and 100% acetonitrile with 0.1% trifluoroacetic acid (TFA) as eluents. The chromatograms were manually integrated with ChemStation (Agilent Technologies, Waldbronn, Germany).

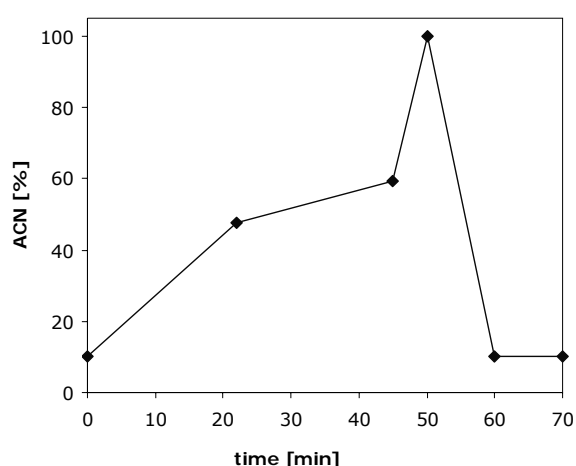


Figure 2: Elution gradient used for the RP-HPLC analytics.

2.2.5 Dynamic Light Scattering (DLS)

DLS performed on a Zetasizer Nano (Malvern, Herrenberg, Germany) was used to characterize the protein molecules and particles in the range from 1 nm to 1 µm. The Zetasizer Nano is operating with a 4 mW He-Ne-Laser at 633 nm and non invasive back-scatter technique (NIBS) at a constant temperature of 25°C. The measurements were conducted in the manual mode using 20 sub runs of 10 seconds. The size distribution by intensity and volume was calculated from the correlation function using the multiple narrow mode of the Dispersion Technology Software version 4.00 (Malvern, Herrenberg, Germany). Thereby, the resulting size distributions show the hydrodynamic diameter. The multiple narrow mode is an algorithm based on the non-negative least square method that deconvolutes the particle size distribution from the measured correlogram. To avoid a misinterpretation of signals deriving from noise a regulating parameter, the alpha-parameter defining the degree of smoothness in the distribution results is included in the NNLS algorithm. The alpha-parameter that represents the degree of noise in the

measured correlogram was set to 0.001 for the multiple narrow mode. To study the impact of temperature on changes of the protein, DLS was performed at a temperature profile from 20 to 75°C using steps of 2°C. At each temperature the samples were allowed to equilibrate for 2 minutes before the measurement consisting of 20 sub runs of 10 seconds.

2.2.6 Attenuated Total Reflection-FTIR Spectroscopy (ATR-FTIR)

FTIR-spectra were measured with the Tensor 27 (Bruker Optics, Ettlingen, Germany) using the Bio-ATR unit and the transmission cell. The spectra were recorded from wavenumbers of 4000 to 850 cm⁻¹ in the attenuated total reflectance (ATR) mode, respectively transmission mode at controlled temperatures. Each measurement was the average of 240 scans. After the analysis, the particular buffer spectrum was manually subtracted from the protein spectrum. The absorption spectra were further processed by an off-set correction and the second derivatives additionally by vector normalization. In the spectra the amide I band, deriving from C=O stretching vibrations is located at wavenumbers from 1700 to 1600 cm⁻¹. Hydrogen bonding influences the amide I and therefore changes in the secondary structure of the protein are reflected in the amide I band [15]. At wavenumbers from 1600 to 1500 cm⁻¹ the amide II band, deriving from N-H and C-N bending vibrations is found. In the second derivatives of the absorption spectra, the band components under the amide I and II band can be resolved. The structural similarity between the second derivatives of the spectra was calculated using the spectral correlation coefficient r [16,17]. The spectral correlation coefficient was calculated according to equation (1).

$$r = \frac{\sum (x_i - x^*) (y_i - y^*)}{\left[\sum (x_i - x^*)^2 \sum (y_i - y^*)^2 \right]^{1/2}} \quad (1)$$

In the equation, x_i and y_i are the corresponding peak intensities of various wave numbers i (second derivative of amide band I from 1700 to 1600 cm⁻¹) in reference (x) and sample spectra (y). x^* and y^* are the average intensities of reference and sample spectra from 1700 to 1600 cm⁻¹. To evaluate changes in the secondary structure with increasing temperatures, ramps from 20 to 90°C using 5°C steps were applied. At each temperature the sample was allowed to equilibrate for 120 seconds before the measurement.

2.2.7 Microcalorimetry

Microcalorimetry was performed with a VP-DSC (MicroCal[®], Milton Keynes, United Kingdom). All solutions with a protein concentration of 1 mg/ml were degassed for 5 minutes prior to the measurement. The scans were recorded from 20 to 90°C at a scanning rate of 1.0°C/min. Each measurement consisted of three scans: water against water, buffer against buffer and protein against buffer scan. The buffer scan was subtracted from the protein scan by the Origin[®] software.

2.2.8 Lyophilization

1000 µl of the formulations were dried in 2 R vials in the Epsilon 2-12 D freeze-drier from Christ (Osterrode, Germany). The samples were frozen to -50°C with a standard cooling rate of 0.45°C/min and kept at -50°C for 2 hours. Primary drying was conducted at a shelf-temperature of -15°C with a pressure of 0.045 mbar for 20 hours. For secondary drying the shelf-temperature was increased to 40°C for 10 hours. The vials were closed under N₂ atmosphere at a pressure of 800 mbar.

2.2.9 Powder X-ray Diffraction (XRD)

The morphology of the lyophilized products was analyzed with X-ray powder diffraction (XRD) from 5-40° 2- θ , with steps of 0.05° 2- θ and a duration of 2 seconds per step on the X-ray diffractometer XRD 3000 TT (Seifert, Ahrenburg, Germany), equipped with a copper anode (40 kV, 30 mA, wavelength 154.17 pm).

2.2.10 Karl-Fischer Titration

The residual moisture of the samples was analyzed by coulometric Karl-Fischer titration using the Aqua 40.00 titrator with a headspace module (Analytik Jena AG, Halle, Germany). The headspace method was validated against conventional Karl-Fischer titration, where anhydrous methanol was used to extract water from the lyophilized products. For the measurement at least 10 mg of the lyophilized sample was heated to 80°C for 10 minutes. The evaporated water was transferred into the titration solution and the amount of H₂O was determined. As reference material apura Water Standard Oven 1% (Merck, Darmstadt Germany) was used.

3. Results and Discussion

3.1 Impact of pH and Ionic Strength on Cytokine Aggregation

3.1.1 Turbidity and HP-SEC Studies

The selection of the optimum buffer composition and formulation pH is a prerequisite for the subsequent formulation development. According to literature a low pH combined with a low ionic strength is beneficial for the stability and the solubility of the used cytokine [18]. Thereby, glycine is suggested as appropriate buffering substance [18]. Based on this information the cytokine was formulated in 20 mM glycine at pH 3.0 as starting material for further studies. To investigate the impact of ionic strength and buffer concentration, glycine and NaCl concentrations were varied at a constant cytokine concentration of 0.25 mg/ml. The formulation pH was step-wise increased by adding NaOH and the corresponding turbidity was monitored from pH 3.0 to pH 9.0 (Figure 3).

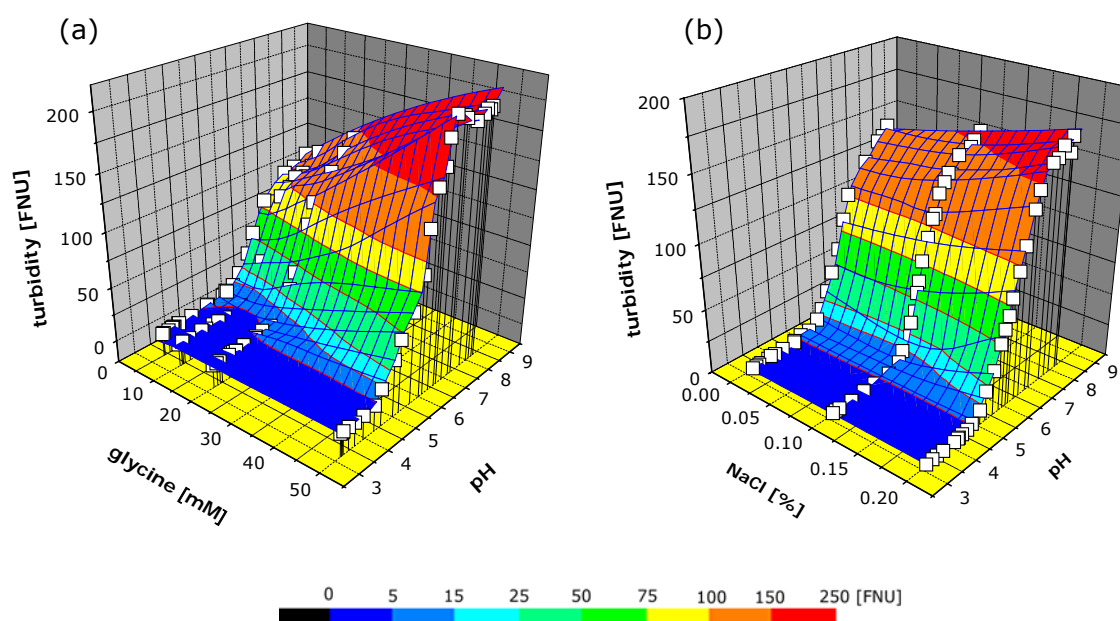


Figure 3: Turbidity of 0.25 mg/ml cytokine with 5 to 50 mM glycine (a) and with 20 mM glycine and 0.0% to 0.2% NaCl (b) from pH 3.0 to 9.0.

From 5 to 20 mM glycine turbidity ranged from 1 to 3 FNU at a pH between 3.0 and 5.0. The solutions were less turbid than reference solution I (3.2 FNU) of the European Pharmacopoeia and the degree of opalescence could be evaluated as clear. At these conditions the cytokine exhibited an adequate good solubility. A precipitation of the cytokine, noticeable by a steep increase in turbidity was measured when the pH was raised above 5.5 for all studied formulations. The turbidity increase could be ascribed to the declining solubility of the cytokine, as the pH approached the protein pI. A pI of 9.2

was determined with isoelectric focusing for the cytokine by Hershen et al. (1989) [19]. At its isoelectric point a protein exhibits a net charge of zero and with it its lowest solubility in aqueous media [20]. With increasing glycine concentrations the onset of the turbidity increase was shifted to lower pH values and maximum values above 150 FNU were measured. While samples with 5 to 20 mM glycine reached maximum turbidity values between 100 and 150 FNU at pH 9.0, maximum values of 200 FNU were measured at 50 mM glycine (Figure 3a). A similar effect was achieved when adding 0.1% (17 mM) and 0.2% (34 mM) NaCl to formulations containing 20 mM glycine. Here maximum turbidities of about 180 FNU were reached when 0.2% NaCl was added to the formulation (Figure 3b). With increasing NaCl concentrations in the formulations the onset for the turbidity increase was also shifted to lower pH-values. Turbidity was exceeding 3.2 FNU at approximately pH 4.5 for 0.0% to 0.2% NaCl, whereas it exceeded 3.2 FNU already at pH 3.6 for 0.9% NaCl (data not shown). However, the addition of NaCl had less impact on the turbidity increase compared to the addition of glycine. The effect of glycine can be partially attributed to its buffering effect. To increase the pH in presence of glycine, which has a pK_a of 2.4 [21], more NaOH was required to increase the pH. For formulation development it is important to note that the low pH range from 3.0 to 4.5 was appropriate due to low turbidity values.

Turbidity measurement detects larger protein aggregates, and all kind of particles in the formulations. To specify the formation of aggregates HP-SEC was employed to determine dimers and lower aggregates in formulations with 20 mM glycine from pH 3.0 to pH 6.0 (Figure 4).

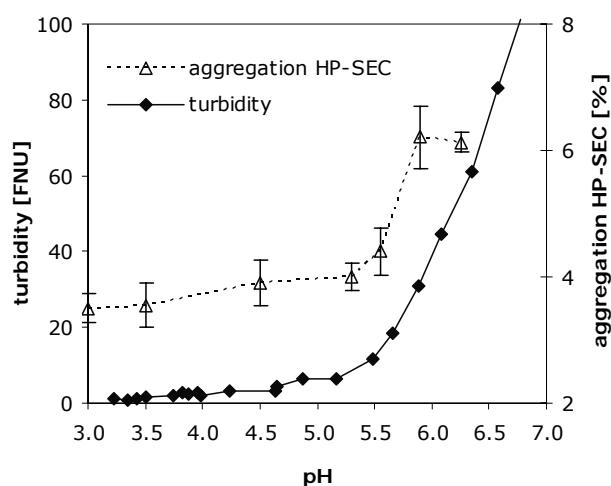


Figure 4: Turbidity and aggregation determined by HP-SEC and of 0.25 mg/ml cytokine formulated in 20 mM glycine between pH 3.0 and 6.3.

The starting material at pH 3.0 already contained about 3.5% aggregates, which probably can be assigned to the complex preparation method of the SDS-free bulk material which was described in point 2.1 of this chapter. However, no reference values concerning dimers and small aggregates in the HSA-containing formulation were available. Due to the 50-fold excess of HSA in the formulation it was not possible to separate the cytokine and its aggregated species from HSA by HP-SEC. In the HSA-free formulation, aggregation ranged from 3.6% to 4.4% between pH 3.0 and 5.5. Above pH 5.5 the area of the peaks of aggregated protein relative to area of the monomer peak significantly stepped up to 6.0%. The presence of larger aggregates, indicated by the high turbidity values above pH 5.5 was reflected in a substantial decrease of the total AUC of monomer and aggregates in the HP-SEC chromatograms. Larger aggregates, as well as precipitated protein were retained by the guard column and therefore not detected, but reflected in the decline of the AUC. Thus, HP-SEC revealed that the turbidity increase was associated with an aggregation of the cytokine at increasing pH values. For the formulations at pH 3.0 and pH 4.5 the aggregate content in presence of 0.2%, 0.5% and 0.9% NaCl was determined by HP-SEC. HP-SEC indicated an average increase in aggregates by 0.4% in samples with 0.0% to 0.9% NaCl when the pH was changed from pH 3.0 to 4.5 (Figure 5).

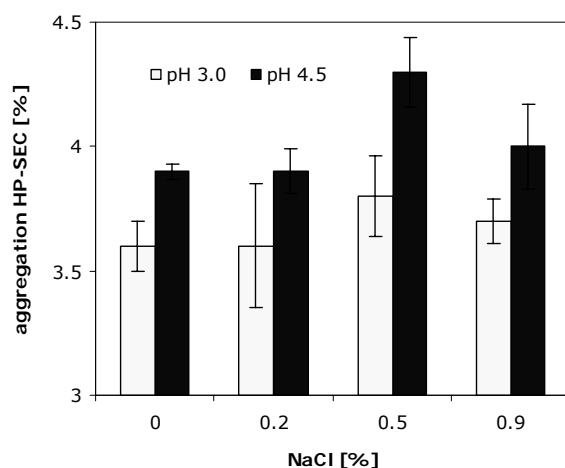


Figure 5: Aggregation determined by HP-SEC of 0.25 mg/ml cytokine in 20 mM glycine with 0.0% to 0.9% NaCl at pH 3.0 and 4.5.

For the samples with 0.9% NaCl, particularly at pH 4.5 the AUC of the chromatograms was slightly decreased. Here again precipitation of the cytokine occurred and was confirmed by the increased turbidity of about 20 FNU. To further clarify the impact of NaCl on cytokine formulations short-time stability studies are necessary, because a possible detrimental effect of an increased ionic strength can be amplified during storage.

The studies revealed a correlation between turbidity and formulation pH, respectively ionic strength. Thus, for formulation development the pH range from 3.0 to 4.5 appeared to be suitable, with lower glycine and NaCl concentrations being beneficial. Within the pH range from 3.0 to 4.5 no significant increase in aggregation was monitored at 5 to 20 mM glycine. However, the impact of pH and ionic strength on the cytokine needs to be studied in more detail with respect to structural changes during storage.

3.1.2 Dynamic Light Scattering (DLS)

Various methods are available to monitor protein aggregation e.g. HP-SEC, SDS-PAGE, turbidimetry, DLS or light obscuration. Thereby, each method is appropriate to detect certain species of aggregates. While dimers, trimers and oligomeric aggregates can be analyzed by HP-SEC, DLS covers the size range from 1 nm to 1 μ m and light obscuration detects particles larger than 1 μ m. To gain comprehensive insight into aggregation within a particular formulation the use of more than one technique is obligatory. Mahler et al. (2005) showed that DLS, turbidimetry and light obscuration were capable to detect different types of aggregates in monoclonal IgG1 antibody formulations upon mechanical stress in relation to surfactant concentration [22].

Aggregation of the cytokine was monitored with DLS as additional technique besides the already described HP-SEC and turbidity measurement. Thereby, changes in the size distribution by volume from pH 3.0 to 4.5 were studied for formulations with 0.25 mg/ml cytokine in 20 mM (Figure 6a). The cytokine monomers were reflected in the size distribution by volume in the main peak at a diameter of 5.1 nm. In comparison, for β -Lactoglobulin, a protein of 18.5 kDa the monomer peak was located at a diameter of 5.4 nm [23]. The second peak with a maximum at 13.5 nm could be assigned to aggregated protein [24]. A well-defined separation of monomers and dimers is generally not possible with DLS as the size resolution of the method is too low. The radii of particles have to differ by a factor higher than 2, the mass respectively by a factor of 8 in order to be resolved as two peaks [25]. However, the change of the size distribution can be used to evaluate the state of the cytokine at different conditions like pH or ionic strength. When the pH was raised from 3.0 to 4.5, the intensity of the peak at 13.5 nm increased linearly from 1.0% at pH 3.0 to 4.0% at pH 4.5 (Figure 6b). Similarly, HP-SEC pointed at a linearly increasing aggregation in the cytokine formulations from pH 3.0 to 4.5. Turbidity measurement showed that the formulations from pH 3.0 to pH 4.5 were all clear with turbidities below 3.2 FNU (data not shown).

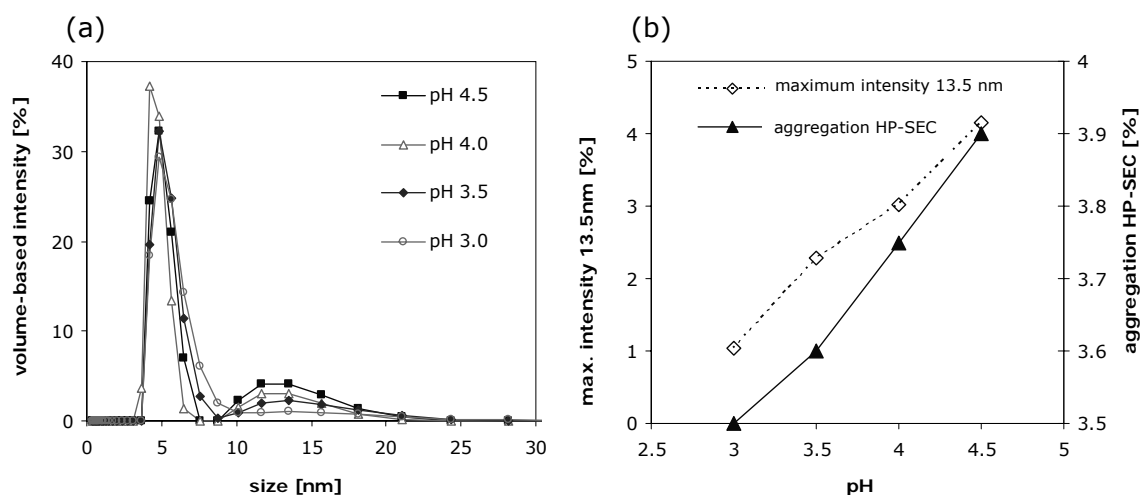


Figure 6: DLS size distribution by volume of 0.25 mg/ml cytokine in 20 mM glycine (a) and maximum intensity at 13.5 nm and aggregation determined by HP-SEC (b) for pH 3.0 to 4.5.

To evaluate how aggregation determined with HP-SEC was reflected in the size distribution by volume, cytokine samples with 0.9% to 13% aggregates were analyzed with DLS. Therefore, stressed (13% aggregates) and unstressed (0.9% aggregates) SDS-containing bulk material was mixed, DLS performed and aggregation determined with HP-SEC. Turbiditometry revealed that all used solutions were clear with a turbidity less than reference solution I. Before using the SDS-containing material, the size distribution by volume was compared with that of the cytokine formulated in glycine (Figure 7).

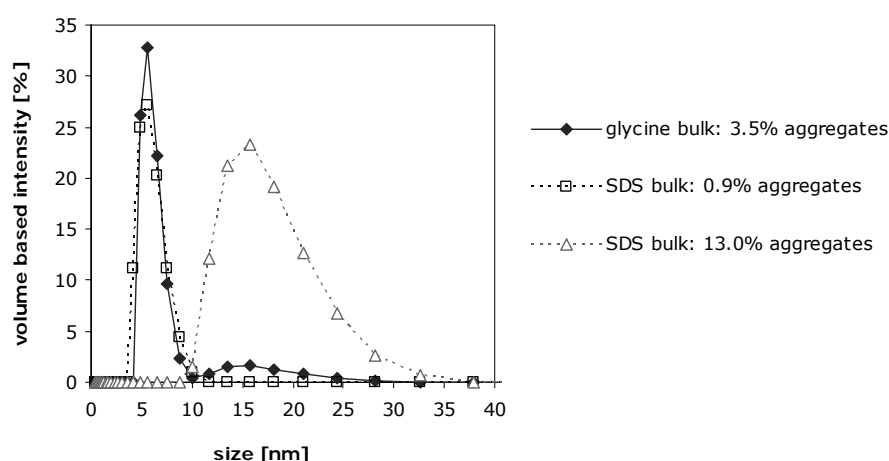


Figure 7: Size distribution by volume of SDS-bulk (1.7 mg/ml cytokine) with 0.9% and 13% aggregates and glycine bulk (0.25 mg/ml cytokine) with 3.5% aggregates.

The unstressed SDS-containing bulk material with 0.9% aggregates and the glycine bulk with 3.5% aggregates resulted in equal size-distributions in the DLS-measurements, only

differing in the intensity at 15 nm. In the size-distribution of the stressed SDS-containing bulk material (13% aggregates) the first peak was no longer present and the intensity at 15 nm increased significantly from 0.0% to 23.2%.

For the studied formulations DLS determined higher intensities between 10 and 30 nm when more aggregates were determined by HP-SEC. Figure 8 shows that the maximum intensity between 10 and 30 nm was rising with increasing aggregation values present in the formulation. At the same time the cumulative intensity from 0 to 8.7 nm dropped with more aggregates in the sample. A disappearance of the first peak in the DLS chromatogram was observed, when aggregation exceeded 7.5%.

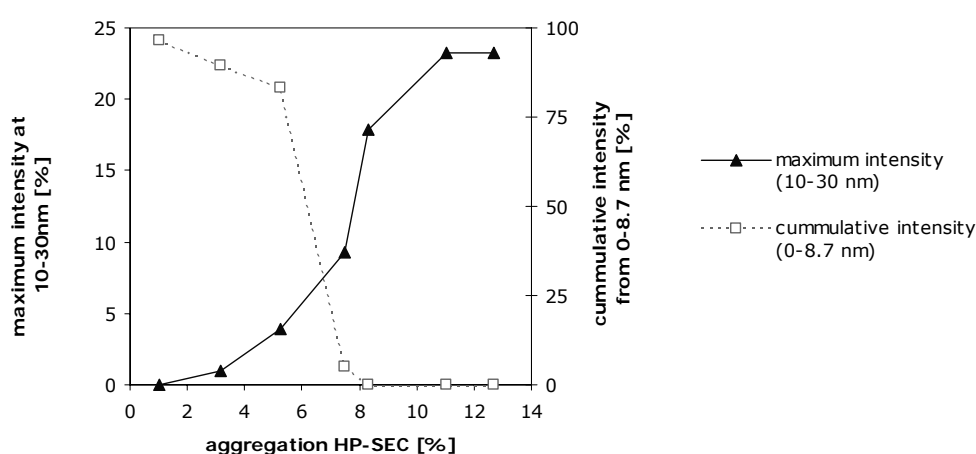


Figure 8: Maximum intensity between 10 and 30 nm and cumulative intensity from 0 to 8.7 nm in relation to aggregation (HP-SEC) for 1.7 mg/ml cytokine in SDS.

The data revealed that changes in aggregation determined with HP-SEC were reflected in the DLS size-distribution by volume. Contrary to HP-SEC, DLS measurements offered the advantage of performing the analytics of formulations in their native state. More precisely, larger turbidity-inducing aggregates, which were retained by the guard column during HP-SEC, were detected by DLS. The formulations studied by DLS were all clear with turbidity values below 3.2 FNU. Turbid samples of the HSA-containing cytokine formulations resulted in a peak at hydrodynamic radii of 50 to 70 nm and at 500 to 1500 nm (compare Chapter 2, section 3.1.4). Mahler et al. (2005) also showed that turbidity is often induced by medium-sized protein aggregates and as well that turbidity could be correlated with particle sizes of 1 and 2 μm determined by light obscuration [22]. Generally, DLS appeared to be a sensitive tool for formulation development, detecting subtle changes of protein monomers, as well as dimers and turbidity inducing aggregates. Based on these results, DLS was selected as analytical method for the stability studies.

3.2 Temperature Induced Changes of the Cytokine

Microcalorimetry is typically used to determine the melting temperature (T_m) of proteins. In the Differential Scanning Calorimetry (DSC) measurement the heat capacity of a protein solution is measured as function of temperature [26]. With increasing temperature, proteins begin to lose their native conformation and undergo unfolding, which is reflected by an endothermic transition in the DSC chromatograms [27]. The midpoint of the denaturation transition is defined as melting temperature or denaturation temperature [26]. This can be used to predict protein stability at different formulation conditions e.g. pH or excipients. A decreasing T_m is often correlated with an inferior thermal stability, which was for example shown by Remmele et al. (1998) for Interleukin-1 Receptor upon the addition of different preservatives [28]. However, an exception from this case is for example the lowering of T_m by PEG, although PEG is known to increase the stability of formulations at room temperature [29].

The DSC-scans of 1.0 mg/ml cytokine in 20 mM glycine at pH 3.0 and 5.0 are shown in Figure 9. At pH 3.0 no clear transition was detected. At pH 5.0 an exothermic shift of the baseline starting at approximately 57°C was found which could be attributed to aggregation occurring at higher temperatures [26].

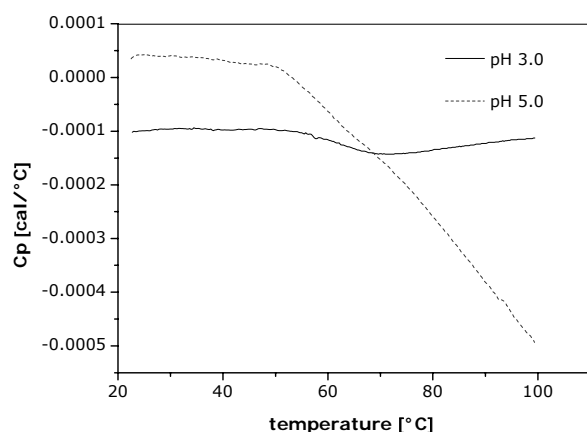


Figure 9: DSC-scan (protein scan minus buffer scan) of 1.0 mg/ml cytokine in 20 mM glycine at pH 3.0 and pH 5.0 from 20 to 100°C at 1.0°C/min.

Thus, microcalorimetry was not suitable to determine the melting temperature of the cytokine between pH 3.0 and 5.0, which would be important for formulation development. Therefore, the use of FTIR and DLS as alternative methods to determine the denaturation temperature for the cytokine was evaluated.

3.2.1 FTIR-Studies

FTIR-spectroscopy is an important tool to analyze the secondary structure of a protein. Changes in the secondary structure and the strength of the respective hydrogen bonding are reflected in the position and intensity of the C=O stretching vibrations located between wavenumbers of 1700 and 1600 cm^{-1} and the N-H and C-N bending vibrations located between 1600 and 1500 cm^{-1} . Therefore, structural changes of a protein e.g. induced by increased temperature result in changed FTIR spectra [15]. FTIR spectroscopy can be performed in transmission and in attenuated total reflection (ATR) mode. In the transmission mode the IR-beam passes the sample cell and measures the solution properties over the whole path lengths. Only clear solutions can be analyzed in the transmission cell applied for the study, as precipitating material can damage the cell. Furthermore, light scattering effects in the transmission cell can interfere with the analytics. In the ATR mode the IR-beam is reflected within the crystal and only protein in close contact to the crystal surface is analyzed. Thereby, the penetration depth of the IR-beam depends on sample properties. The advantage of the ATR mode lies in the possibility to analyze turbid solutions and suspensions as well [30]. However, care must be taken, when proteins susceptible to adsorption are analyzed.

For the FTIR-studies higher concentrated solutions containing 1.2 mg/ml cytokine were applied to achieve a better reproducibility. In order to evaluate the impact of adsorption on the measurements, solutions with 1.2 mg/ml cytokine at pH 3.0 and 5.0 were measured both in ATR and transmission mode (Figure 10).

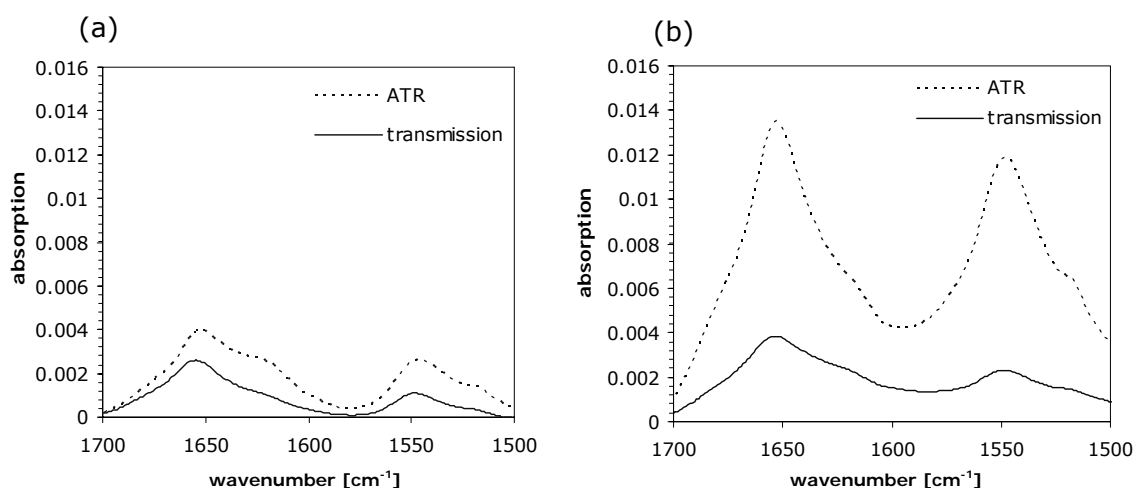


Figure 10: Comparison of spectra measured in ATR and transmission mode for 1.2 mg/ml cytokine at pH 3.0 (a) and pH 5.0 (b).

In the transmission mode the intensities of the absorption spectra at pH 3.0 and pH 5.0 were comparable, whereas a 5-fold higher intensity was measured at pH 5.0 compared to pH 3.0, when using the ATR-mode. This outcome supported the assumption that

adsorption is more pronounced at higher pH values, which is further discussed in section 3.3 of this chapter. ATR-FTIR was used to detect changes in the secondary structure of the cytokine with increasing temperature. Therefore, temperature was increased from 20 to 90°C and spectral changes were monitored for formulations with 1.2 mg/ml cytokine in 20 mM glycine between pH 3.0 and 5.5. The spectral intensities were increasing with the pH, indicating that protein adsorption was more pronounced at pH 5.5 compared to the lower pH values. At 20°C the absorption spectra at pH 3.0 and pH 3.5 exhibited a distinct peak at 1619 cm⁻¹ in the amide I region. In contrast only a shoulder was present at pH 4.2 and 5.5 (Figure 11a). In the second derivatives a better resolution of the bands was achieved (Figure 11b). The band at 1619 cm⁻¹ could be assigned to β -sheet structures, while the band at 1653 cm⁻¹ derived from α -helical structures [31,32].

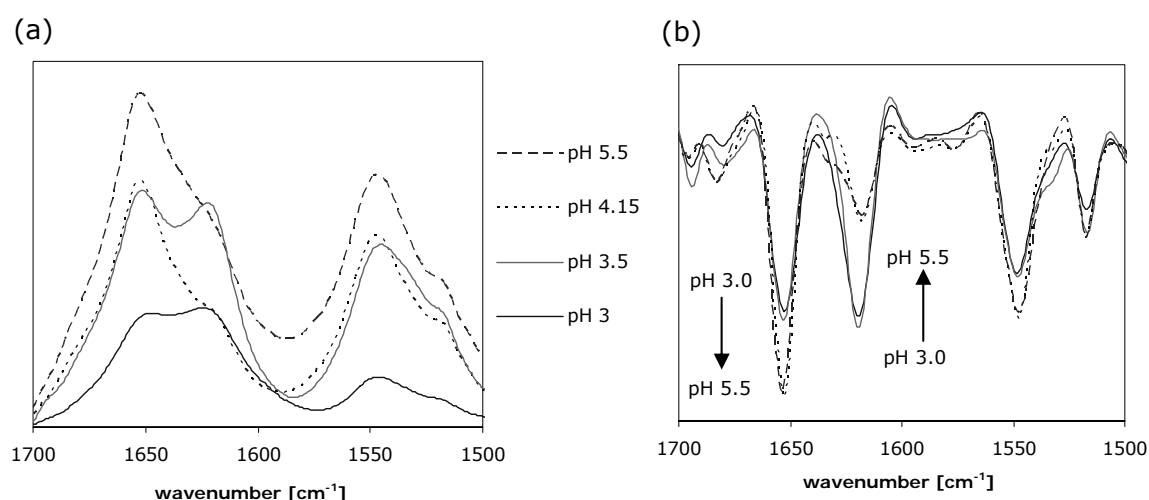


Figure 11: ATR-FTIR absorption spectra (a) and vector-normalized second derivatives (b) of 1.2 mg/ml cytokine in 20 mM glycine at pH 3.0 to 5.5.

When the pH was changed from 3.0 to 5.5 the intensity at 1619 cm⁻¹ (β -sheet) was decreasing, while an increased intensity at 1653 cm⁻¹ (α -helix) was measured. According to literature, an increased intensity at 1620 cm⁻¹ can be attributed to the formation of intermolecular β -sheets within aggregated protein molecules [33]. Meersman et al. (2002) determined a rising band at 1618 cm⁻¹, when myoglobin aggregated at elevated temperatures [34]. An increase in intensity at 1615 and 1685 cm⁻¹ for BSA [35], at 1620 cm⁻¹ for HSA [16] and at 1614 and 1685 cm⁻¹ for Interferon- γ [36] was detected when intermolecular β -sheets were formed due to the aggregation process.

However, for the cytokine HP-SEC revealed a higher degree in aggregation with 4.5% at pH 5.5, compared only 3.5% aggregates at pH 3.0. This indicated that the increase of the intensity at 1619 cm⁻¹ was not solely deriving from intermolecular aggregation. Fan et al. (2005) demonstrated structural changes as a function of pH, by a changed CD spectrum below pH 4.0 for a glycosylated form of the cytokine. Below pH 4.0 the

glycosylated cytokine exhibited a larger amount of soluble micro-aggregates and showed an improved stability resulting in a lower degree of precipitation when the temperature was increased [37]. This changed structure below pH 4.0 could be an indication for the increased intensity at 1619 cm^{-1} for the cytokine at pH 3.0. On the other hand, when comparing transmission and ATR spectra at pH 3.0 it became evident that the band intensity at 1619 cm^{-1} was less pronounced in the transmission mode, indicating that adsorbed material in the ATR-mode could be responsible for this effect.

Figure 12 shows the unprocessed absorption spectra of formulations containing 1.2 mg/ml cytokine in 20 mM glycine at a formulation pH between 3.0 and 5.5 heated from 20 to 90°C .

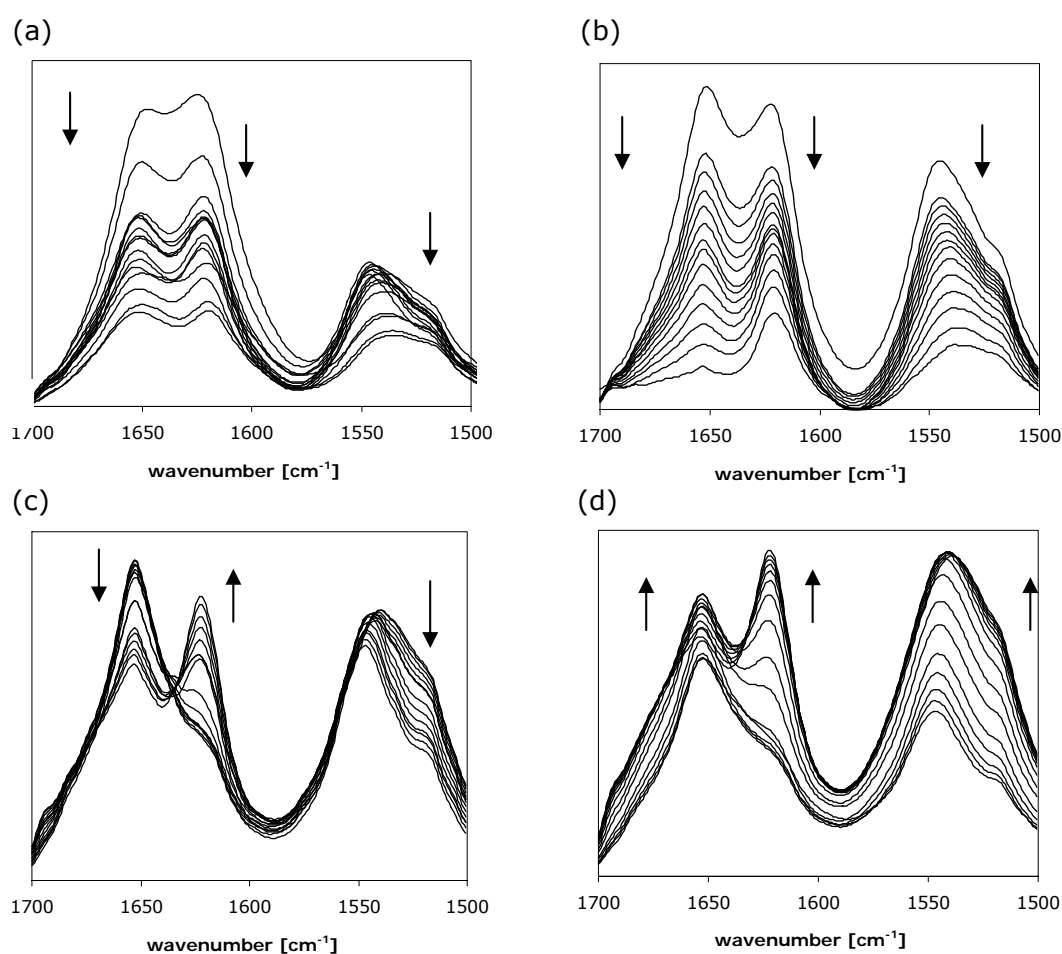


Figure 12: ATR-FTIR absorption spectra of 1.2 mg/ml cytokine in 20 mM glycine at pH 3.0 (a), pH 3.5 (b), pH 4.2 (c) and pH 5.5 (d). The arrows mark the changes when the temperature is increased from 20 to 90°C .

Generally, the intensity of the adsorption spectra increases with temperature, due to precipitation caused by the denaturation [38]. However, at pH 3.0 and 3.5 the intensity of the spectra decreased when the temperature was ramped up (Figure 12a,b). This indicated the lack of precipitation during the measurement, which was supported by the

fact that visual inspection showed clear solutions after the measurement. The cytokine, with its substantial hydrophobicity tends to adsorb on surfaces. Adsorption per se can be measured with ATR-FTIR, which was described for human calcitonin by Bauer et al. (1994), who found that the intensity of the amide I band increased by a factor of 3.4 due to adsorption [39]. The tendency of the cytokine to adsorb was pH-dependent and more distinct at pH 4.5 than at pH 3.0 (compare 3.3). A possible explanation for the decrease in spectral intensity at pH 3.0 and 3.5 is the removal of adsorbed protein from the ATR-crystal at rising temperatures. This hypothesis can be further supported by the basic principles of adsorption, considering the adsorption rate constant K_{ads} , shown in equation (2) [40].

$$\log K_{ads} = (\Delta H / 2.303 R) * 1/T + C \quad (2)$$

K_{ads} is reciprocally proportional to temperature T , with H as enthalpy, R as the universal gas constant and C as the concentration, indicating a declining strength of adsorption with increasing temperatures.

At pH 3.5 the intensity of the spectra decreased at higher temperatures. Thereby, the intensity at 1619 cm^{-1} was decreasing less than at 1653 cm^{-1} , pointing at the formation of new β -sheet structures, potentially due to aggregation. At pH 4.2 the intensity in the adsorption spectra was increasing at 1619 cm^{-1} , while only a slight reduction of overall intensity was measured in the areas of the amide I and amide II band. At pH 5.5 the intensity of the spectra raised with temperature, demonstrating that protein was precipitating, which was confirmed by the turbid nature of the solutions after the measurement.

The vector-normalized second derivatives, shown in Figure 13 offered a deconvolution of the spectra and the possibility to itemize changes in the different structural components underlying the amide I and II bands.

Overall, at pH 3.0 the spectra of the cytokine were relatively stable, with only a slight intensity increase at 1619 cm^{-1} respectively decline at 1653 and 1548 cm^{-1} suggesting a good thermal stability of the secondary structure of the cytokine. The spectral changes were more pronounced at increasing pH-values, which was already obvious in the absorption spectra. The evaluation of the second derivatives revealed that at higher pH-values the loss of α -helical structure and the formation β -sheet were more pronounced.

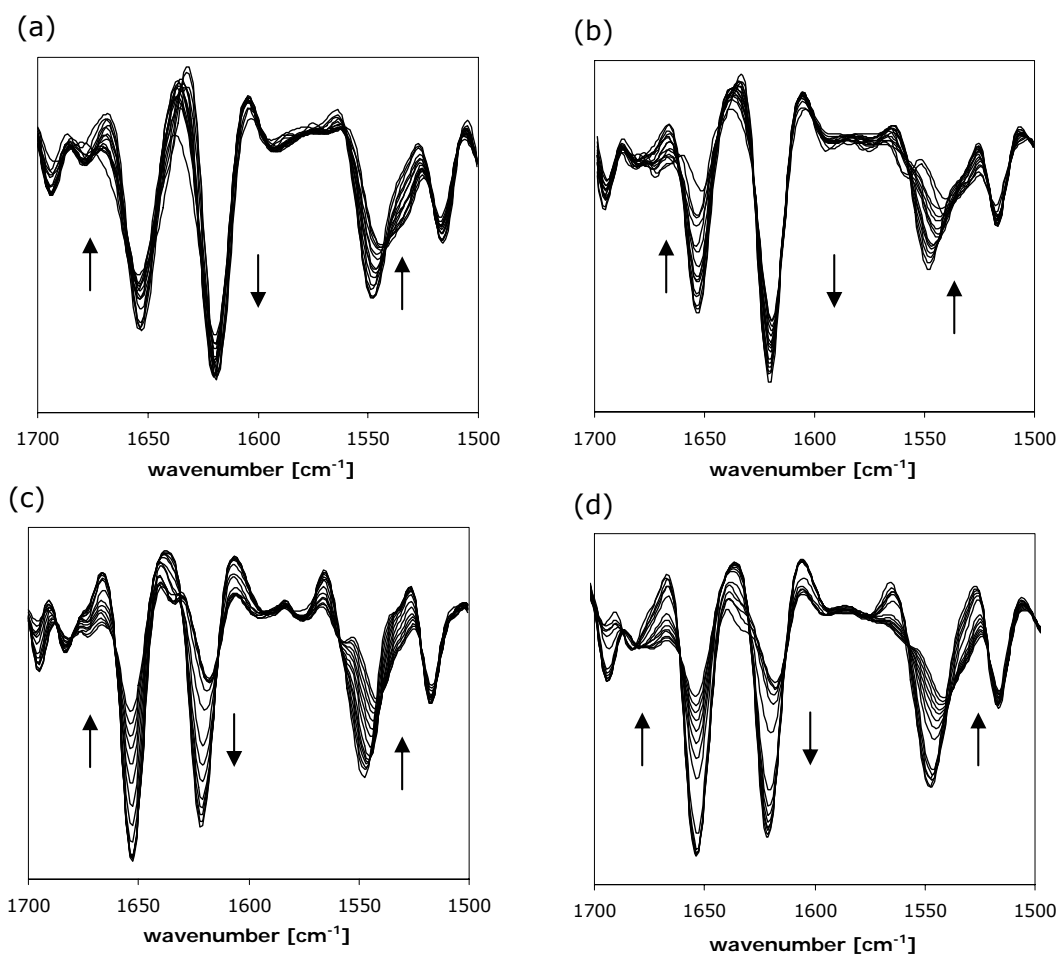


Figure 13: ATR-FTIR vector-normalized second derivatives of 1.2 mg/ml cytokine in 20 M glycine at pH 3.0 (a), 3.5 (b), 4.2 (c) and 5.5 (d). The arrows mark the changes with increasing the temperature from 20 to 90°C.

Different methods are possible to evaluate spectral changes and determine the denaturation temperature at varying conditions e.g. increasing temperatures by FTIR [41]. One possible approach is plotting the intensities of the α -helical, respectively β -sheet bands over the changing temperature. This was described by Meersman et al. (2002) for Myoglobin using the bands at 1624 and 1560 cm^{-1} and by Dong et al. (1997) for Factor XIII using the bands at 1641 and 1626 cm^{-1} [34,42]. For the cytokine the bands of 1619 and 1653 cm^{-1} were monitored over the temperature range of 20 to 90°C (Figure 14).

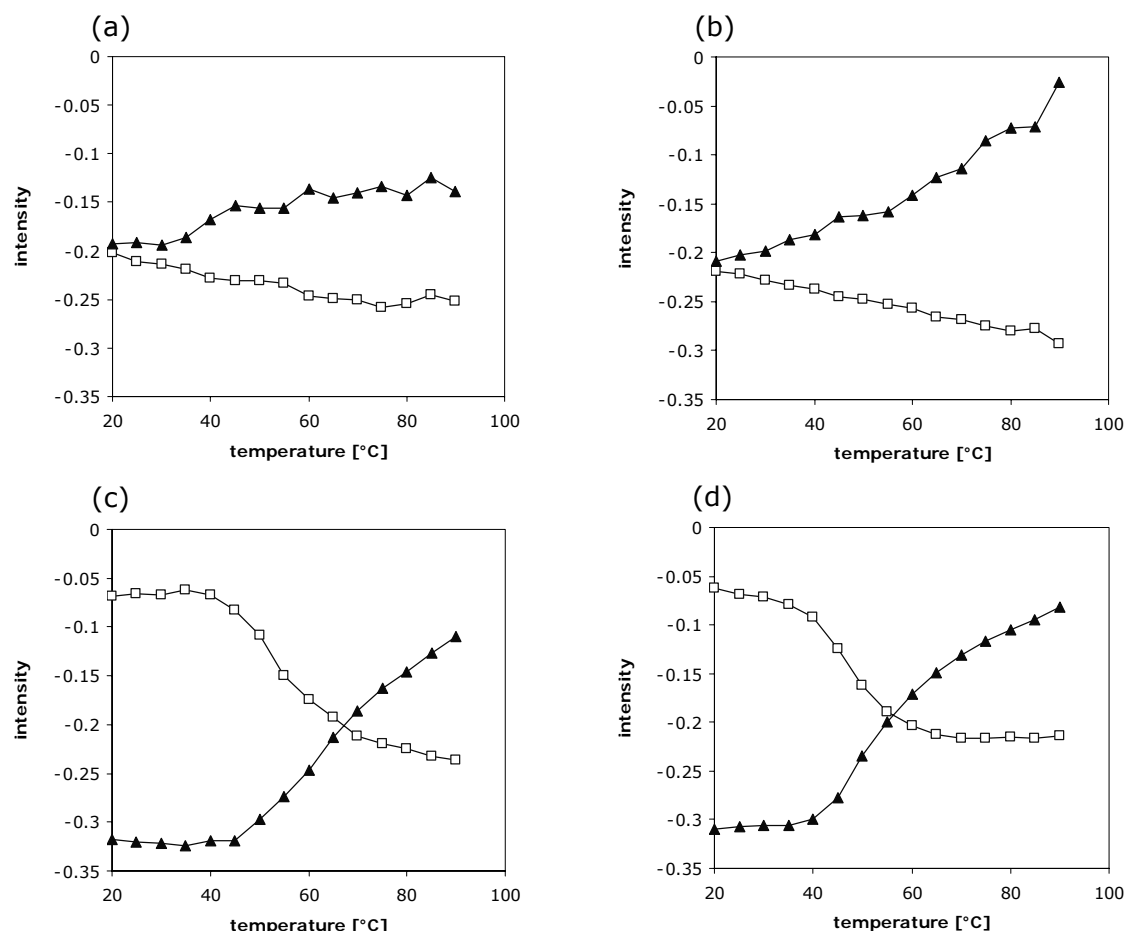


Figure 14: Intensity at 1653 cm^{-1} (\blacktriangle) and at 1619 cm^{-1} (\square) at pH 3.0 (a), pH 3.5 (b), pH 4.2 (c) and pH 5.5 (d) in the temperature range from 20 to 90°C .

At pH 3.0 and 3.5 the initial intensities of the α -helical band at 1653 cm^{-1} and the β -sheet band at 1619 cm^{-1} were similar. A continuous, almost linear intensity decrease at 1653 cm^{-1} , respectively intensity increase at 1619 cm^{-1} over the temperature range was monitored. Thereby, the absolute value of the slope was greater at pH 3.5 than at pH 3.0, pointing at a higher structural stability at pH 3.0. At pH 4.2 and pH 5.5 a higher initial intensity was measured at 1653 cm^{-1} compared to 1619 cm^{-1} . After a linear phase from 20 to 40°C the shape of the curve changed to sigmoid with a clear inflection point. This revealed a higher degree of structural alternation during the temperature increase at pH 4.2 and 5.5 compared to pH 3.0 and 3.5. At pH 3.0 and 3.5 the spectral change already started at 25°C and progressed in a linear way.

Wang et al. (2003, 2005) used a spectral correlation coefficient to show the similarity between spectra [16,17]. According to their method, the spectral correlation coefficient r was calculated for the amide I using the wavenumbers from 1700 to 1600 cm^{-1} (compare 2.8). The second derivatives of the spectra at 20°C were set as reference spectra and the spectra at higher temperatures as sample spectra. Furthermore, the ratio of the

intensities at 1619 and 1653 cm^{-1} , comparable to Goosens et al. (2003) [36] were plotted over the temperature range between 20 to 90°C and compared to the spectral correlation coefficient (Figure 15).

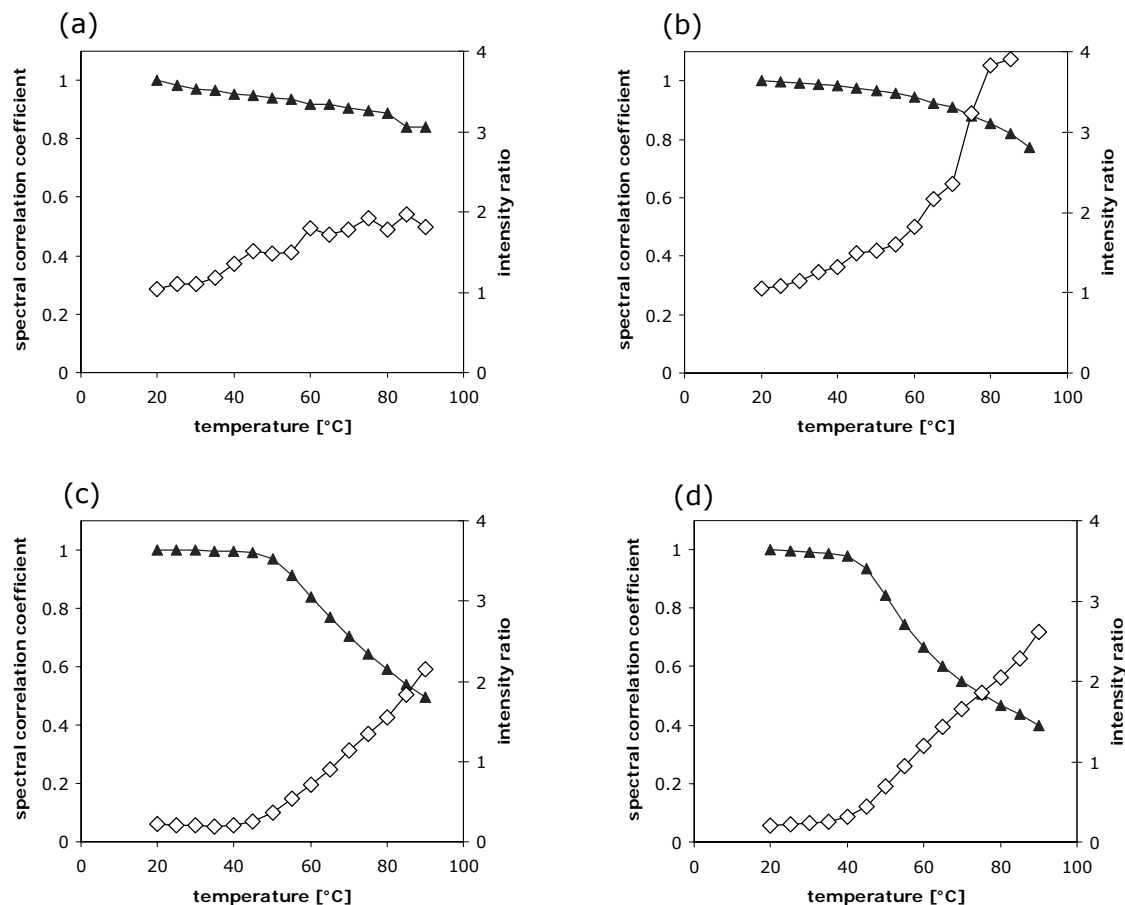


Figure 15: Spectral correlation coefficient (—▲—) and intensity ratio of 1619 cm^{-1} to 1653 cm^{-1} (—◇—) at pH 3.0 (a), 3.5 (b), 4.2 (c) and 5.5 (d) in the temperature range from 20 to 90°C.

At pH 3.0 both the intensity ratio and the spectral correlation coefficient showed a linear change in intensities. Here, the alternations were obvious already at temperatures above 25°C. First at pH 3.5 it was possible to detect an inflection point for the intensity ratio offering a value of 74°C as denaturation temperature. For pH 4.2 and pH 5.5 on the other hand constant spectral correlation coefficients, respectively intensity ratios were existent from 20 to 45°C, which is relevant for the storage of the formulations. For the higher pH-values the spectral correlation coefficient and the intensity ratio began to change at temperatures above 40 to 45°C.

For the cytokine the denaturation temperatures calculated from the intensities at 1619 and 1653 cm^{-1} , respectively the intensity ratio and the spectral correlation coefficient r are compared in Table 2.

Table 2: Denaturation temperatures (T_m) of the formulations determined from the ATR-FTIR spectra.

	intensity 1619cm ⁻¹	intensity 1653cm ⁻¹	ratio 1619cm ⁻¹ /1653cm ⁻¹	Spectral correlation coefficient r	T _m (average)
pH 3.0	-	-	-	-	
pH 3.5	-	-	74°C	-	74°C
pH 4.2	53°C	60°C	55°C	60°C	57°C
pH 5.5	50°C	47.5°C	50°C	50°C	49°C

At pH 3.0 it was not possible to determine an accurately defined transition temperature with the four different approaches. The spectra changed already above 25°C. Especially the spectral correlation coefficient and the intensity ratio revealed a linear change with increasing temperatures. At pH 3.5 only the intensity ratio of 1619 to 1653 cm⁻¹ offered a value of 74°C for T_m. The structural changes with increasing temperatures were still not pronounced enough to get results from the other methods. The transition temperature was shifted from of 57°C at pH 4.2 to 49°C at pH 5.5, indicating a decreased thermal stability.

Besides the evaluation of changes at increasing temperature, the application of FTIR-spectroscopy as tool to monitor structural changes of proteins upon storage is often found in literature. For example Kerwin et al. (1998) used FTIR spectroscopy to monitor the stability of recombinant haemoglobin upon long term storage at -20°C [43]. The application of FTIR as technique to monitor changes of the secondary structure of the cytokine was evaluated for a concentration of 1.0 mg/ml in 20 mM glycine at pH 4.0 (Figure 16). After 2 weeks storage at 2-8°C and 40°C aggregation was determined with HP-SEC and secondary structure monitored with FTIR spectroscopy. Aggregation measured by HP-SEC increased from 4.0% before storage to 4.3% after 2 weeks at 2-8°C respectively 12% at 40°C. In the FTIR spectra no significant changes were visible after 2 weeks at 2-8°C. Upon storage at 40°C on the other hand a second peak with a maximum at 1619 cm⁻¹, deriving from intermolecular β -sheet structures emerged. This experiment showed the ability of FTIR-spectroscopy to detect changes in the protein structure during storage, when using formulations with 1.0 mg/ml cytokine. As routine tool for the planned stability studies with 0.25 mg/ml cytokine on the other hand, FTIR was not suitable. The more complex formulations containing 0.25 mg/ml cytokine and further stabilizers (sugars, surfactants) showed only poor reproducibility of the spectra due to the low cytokine concentrations (data not shown).

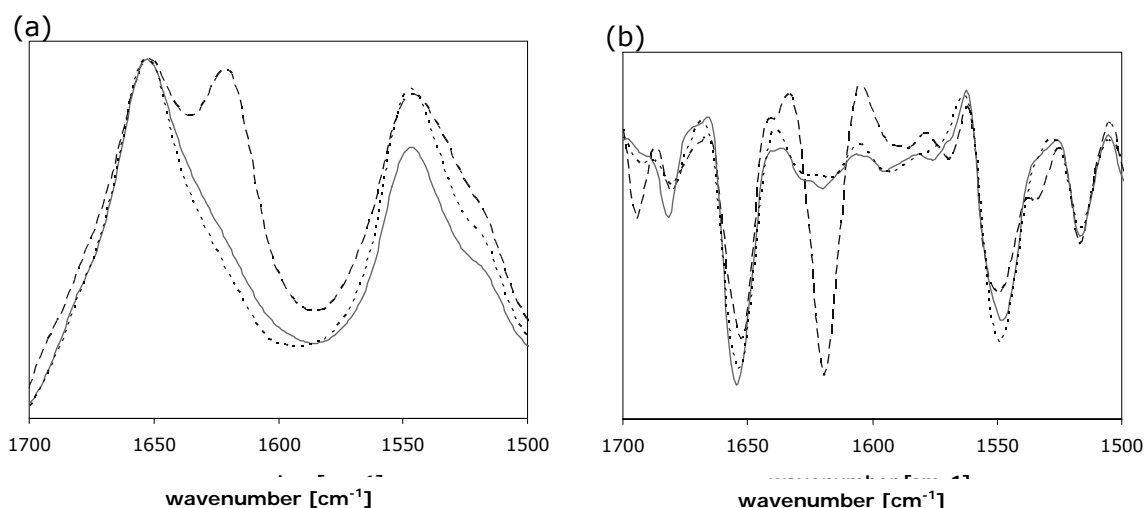


Figure 16: Adsorption spectra (a) and second derivatives (b) of 1.0 mg/ml cytokine in 20 mM glycine, pH 4.0 before storage (.....) and after 2 weeks 2-8°C (—) and 40°C (— —).

Summarizing, it can be stated that unlike microcalorimetry, FTIR-spectroscopy was capable to determine melting temperatures of the cytokine. At pH 3.0 and 3.5 a steady change in the spectrum was obvious starting already at 25°C. With increasing pH value the structural changes were more distinct and the melting temperature (average of all approaches) declined from 57°C at pH 4.2 to 49°C at pH 5.5. The melting temperature can be indicative for the stability of the protein during stability studies, especially at 25°C and 40°C storage. Therefore, higher pH values appear to be more critical regarding thermal stability of the protein during storage.

3.2.2 Dynamic Light Scattering Studies

Besides alternations in secondary structure, detectable by FTIR-spectroscopy, the size distribution of the cytokine molecules can as well change with temperature. These changes in size, induced by aggregation or precipitation might be reflected in DLS experiments. Therefore, DLS was applied to study the impact of an increasing temperature on the size distribution of 0.25 mg/ml cytokine formulated between pH 3.0 and pH 4.6. At pH 3.0 the size distribution by volume did not significantly change up to 70°C (Figure 17a). At 74°C the peak at 5 to 6 nm disappeared, whereas the second peak at 13.5 nm gained in intensity. For the formulation at pH 4.6 the enhanced formation of the second population with a maximum at 21 nm already occurred at 50°C (Figure 17b). This revealed the decreased thermal stability of the cytokine at higher pH values, which was already shown by FTIR-spectroscopy (compare 3.2.1).

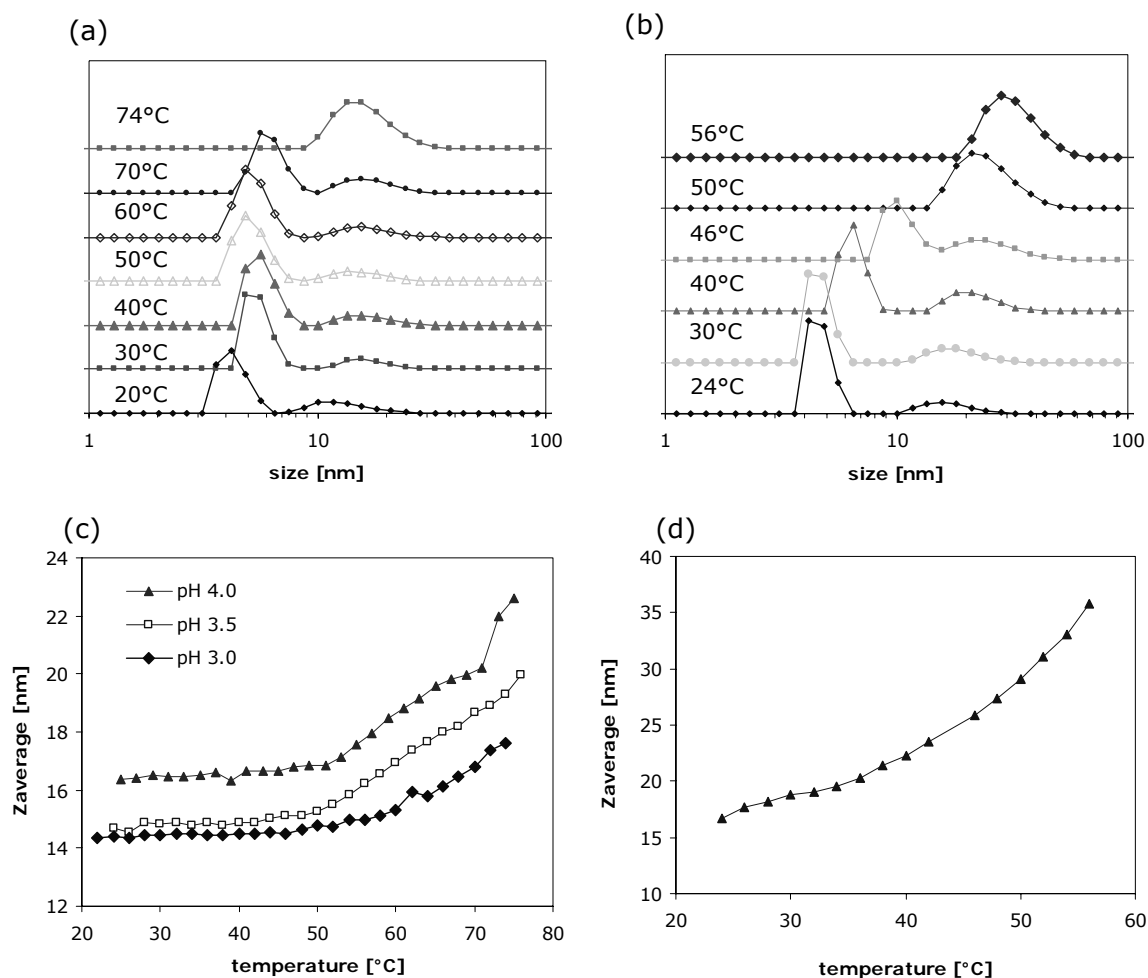


Figure 17: Size distribution by volume of 0.25 mg/ml cytokine in 20 mM glycine at pH 3.0 (a) and pH 4.6 (b) with increasing temperatures. Change in z-average of 0.25 mg/ml cytokine in 20 mM glycine at pH 3.0, 3.5 and 4.0 (c) and pH 4.6 (d) with increasing temperature.

As a method to determine the melting temperature of a protein, the z-average can be plotted as function of the temperature [44]. The use of z-average as parameter for protein solutions needs to be considered as critical, as protein solutions generally show a multimodal distribution. Z-average as the medium intensity weighted average of the correlation function offers a value for the protein size in a formulation, which is not necessarily reflecting the genuine size. However, changes of z-average with temperature can be considered to visualize changes of a protein at different conditions e.g. formulation composition or temperature [24]. To make significant statements about the size of a protein, respectively its multimeric forms, the hydrodynamic radius or diameter can be considered. Petsev et al. (2000) determined a hydrodynamic diameter using CONTIN algorithm for Apoferritin monomers at 11.4 nm, for dimers at 17.1 nm and higher aggregate at 30.0 nm after separating the fractions with size exclusion chromatography [45]. For HSA, Lin et al. (2000) measured a hydrodynamic radius of 2 to

3 nm for the monomeric form and a fraction of aggregates at 30 to 40 nm [46]. In the temperature range from 20 to 50°C, respectively 60°C, the z-average of the cytokine formulations stayed relatively constant between 14 and 15 nm for pH 3.0 and 3.5 and between 16 and 17 nm at pH 4.0 respectively (Figure 17c). When rising the temperature further, a slight increase in z-average to 17 nm at pH 3.0 and 22 nm at pH 4.0 at 75°C was measured. Increasing the temperature for formulations at pH 4.6 led to a steady increase in z-average to 36 nm already at 56°C, reflecting the decreased thermal stability of the cytokine at higher pH values. A clear determination of transition temperatures was not possible for the studied pH-values. Overall, the DLS data confirmed the decreased thermal stability at higher pH values, which was already shown by FTIR. However, DLS offered no clear values for transition temperatures and was therefore not considered further as tool to characterize the thermal stability.

3.3 Cytokine Adsorption to Vials

As the hydrophobic cytokine used in low concentrations tends to adsorb on surfaces protein adsorption was evaluated prior to performing stability studies. Protein adsorption is a complex mechanism, consisting of several steps beginning with the transport of the protein towards the surface, followed by binding, a structural rearrangement of the adsorbed molecules and finally desorption from the surface [47]. Furthermore, the adsorption process is mainly driven by hydrophobic interactions and hydrogen bonding [40]. Thereby, numerous factors can impact the kinetics and the degree of adsorption of the particular protein on surfaces, e.g. protein concentration, temperature, pH, ionic strength and the presence of further excipients [47-49]. The selection of the container material can also impact the degree of protein adsorption [12].

To circumvent the loss of cytokine due to adsorption an excess of HSA can be added to the formulation. As the use of HSA goes along with major drawbacks (compare Chapter 1) the goal was to replace HSA in the cytokine formulation and find ways to keep protein adsorption to a minimum. The goal was not to elucidate the adsorption mechanism of the cytokine, but to study the influence of various factors on the degree of adsorption and its importance for formulation development. In this initial studies, 1.0 ml of the different cytokine formulations at a concentration of 0.25 mg/ml were stored at 2-8°C in the respective container and the loss of protein content was determined by UV-spectroscopy. The focus was set on the impact of pH, container type and the addition of polysorbate 20 on the extent of adsorption.

3.3.1 Influence of pH, Glycine Concentration and Container Type on Cytokine Adsorption

The degree of protein adsorption can be influenced by the formulation pH, as the net charge of the protein, as well as the secondary structure depends on pH. Electrostatic interactions contribute to the adsorption process and adsorption is favored when surface and protein exhibit opposed charge [47]. The pH of the formulations was varied from 3.0 to 5.5 at a glycine concentration of 10 and 20 mM. As container materials 2 R vials (glass type I and I⁺) and containers made of polypropylene were evaluated.

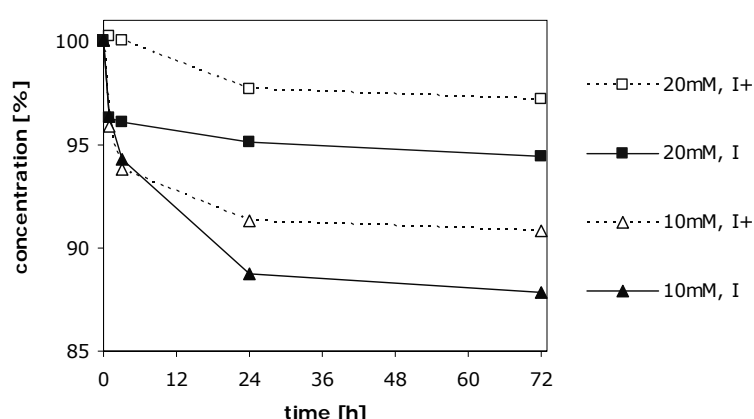


Figure 18: Protein concentration for 0.25 mg/ml cytokine with 10 and 20 mM glycine at pH 3.0 stored in glass type I and I⁺ vials for 72 h at 2-8°C.

Figure 18 shows that the decline in protein concentration at pH 3.0 was less distinct at 20 mM glycine than at 10 mM glycine. In glass type I⁺ the cytokine concentration declined to 97.2% at 20 mM and 90.8% at 10 mM glycine after 72 hours. About 3% more protein was lost on glass type I compared to glass type I⁺ for the same formulations. After 24 hours the adsorption process was almost completed. Therefore, the concentration after 24 hours was used as comparative value for the further experiments. Besides glass, polypropylene was evaluated for protein adsorption. Table 3 summarizes the protein recoveries after 24 hours at the different conditions. At 20 mM glycine the highest cytokine concentrations of 95.1% and 97.7% remained at pH 3.0 for glass type I and I⁺. Adsorption on polypropylene was unaffected by the pH of the solutions with a recovery of approximately 96% for pH 3.0 and 4.5.

Table 3: Protein concentration for 0.25 mg/ml cytokine using different formulation compositions and containers after 24 hours.

	pH 3.0	pH 4.0	pH 4.5
10 mM I	88.7	85.7	87.2
10 mM I+	91.2	92.9	95.6
20 mM I	95.1	88.6	88.1
20 mM I+	97.7	94.6	92.1
20 mM PP	96.4	-	96.1

Various factors e.g. pH, ionic strength, container type or the addition of excipients can impact the degree of cytokine adsorption. More information about the charge density on the glass surface and the protein surface, as well as the degree of electrostatic interaction and hydrophobic interactions would be necessary to offer a precise explanation. Glass surfaces are typically negatively charged due to the dissociation of silanol groups in aqueous media. A positively charged glass surface is only achieved at very acidic pH below 2 [50]. In the pH range from 3.0 to 5.5 a slight increase of the negative charge on the glass surface can be assumed. The cytokine, with a pI at 9.2 [19] should tend to a slightly higher positive charge when the pH is lowered from 5.5 to 3.0. The same tendency of an increased positive net charge density at pH 3.0 can be assumed for glycine with its pI of 6.02 at 25°C [51]. Thus, a possible explanation for the decreased adsorption at higher glycine concentrations could be a competition of glycine and the cytokine for the negatively charged glass surface.

For the development of stable cytokine formulations it is important that a higher glycine concentration was more favorable to avoid the loss of protein, best in combination with glass type I⁺. However, the loss of 15% protein after 24 hours especially in glass type I vials was unacceptably high. As HSA was to be eliminated from the formulation, the use of surfactants to reduce protein adsorption was evaluated next.

3.3.2 Influence of Polysorbate 20 on Cytokine Adsorption

The addition of surfactants is an effective approach to reduce and inhibit protein adsorption on surfaces. By adding polysorbate 20 the adsorption of albumin on silicon treated surfaces of different hydrophobicity was reduced by 15 to 90% depending on polysorbate 20 concentration and the hydrophobicity of the particular surface [52]. Surface active substances may also remove adsorbed protein from surfaces [53,54]. For the cytokine the use of polysorbate 20 to minimize protein adsorption was evaluated. Less protein was lost within 24 hours when polysorbate 20 was added to a formulation

with 0.25 mg/ml cytokine in 20mM glycine at pH 3.0 (Figure 19). The protein recovery after 24 hours could be improved from 95% without polysorbate 20 to 98% with 0.02% polysorbate 20 added to the formulation.

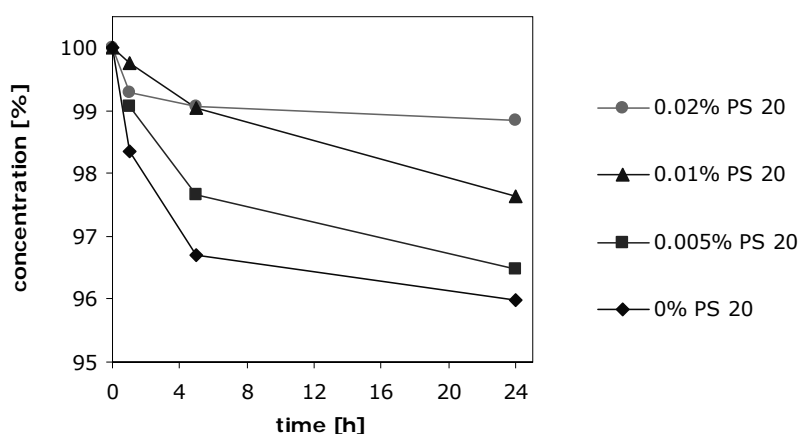


Figure 19: Protein concentration for 0.25 mg/ml cytokine in 20 mM glycine with 0.0% to 0.02% polysorbate 20 at pH 3.0 in glass type I vials over 24 hours.

Figure 20 compares the impact of polysorbate 20 on the adsorption of the cytokine on glass types I and I⁺ at pH 3.0 and 4.5. The adsorption on glass type I was inhibited to a greater extent by increasing the polysorbate 20 concentration compared to glass type I⁺, especially at pH 3.0. However, without polysorbate 20 the initial adsorption was less distinct for glass type I⁺ with 97.9% at pH 4.5 and 98.5% at pH 3.0 compared to glass type I with 93.7% at pH 4.5 and 95.2% at pH 3.0. Overall, glass type I⁺ vials were superior to glass type I vials both with and without polysorbate 20 in the formulation.

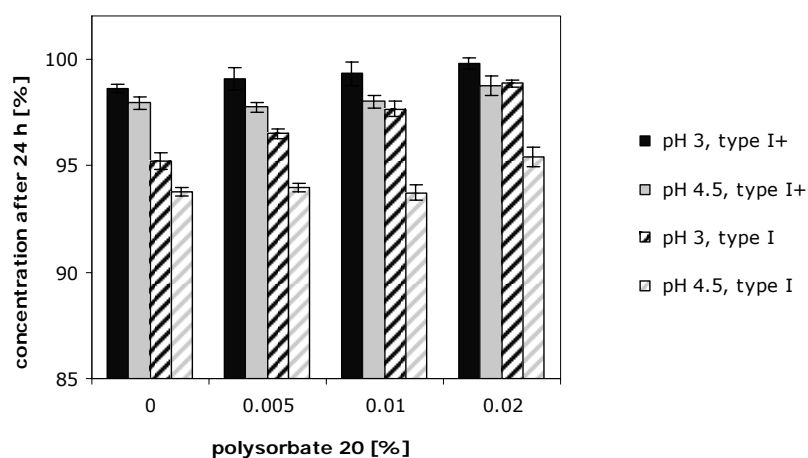


Figure 20: Protein concentration for 0.25 mg/ml cytokine in 20mM glycine (pH 3.0 and 4.5) with 0.0% to 0.02% polysorbate 20 in glass type I and I⁺ after 24 hours.

The studies showed that cytokine adsorption was dependent on glycine concentration, formulation pH and the container type used. Especially at the standard buffer concentration of 20 mM glycine a lower pH was beneficial for the cytokine in terms of adsorption. This corresponded to the ATR-FTIR spectroscopy results as less protein adsorbed on the ATR-crystal at pH 3.0 compared to pH 5.0 (compare 3.2). A buffer concentration of 20 mM glycine was favorable compared to 10mM as the decline of protein concentration was reduced at 20 mM glycine. Other possibilities to avoid protein adsorption were the addition of polysorbate 20 or the utilization of surface treated glass type I⁺. The best results with less than 1% protein loss after 24 hours were achieved by adding 0.005% to 0.02% polysorbate 20 to formulations containing 20 mM glycine at pH 3.0 and by the use of glass type I⁺. According to these investigations the use of HSA as adsorption preventing excipient could be avoided.

3.4 Short-time Cytokine Stability in Solution

Preliminary studies indicated that a pH value below 5.5 is necessary to ensure solubility and to avoid precipitation of the cytokine (compare 3.1.1). Furthermore, an increase in ionic strength by the addition of NaCl or by using higher glycine concentrations led to higher turbidity values especially at elevated pH values, reflecting protein aggregation. However, in the pH range between 3.0 and 4.5, HP-SEC revealed no significant increase in aggregation when 0.05% to 0.5% NaCl was added. As aggregation is emerging over time, it was important to evaluate the increase in aggregation during storage. Short-time stability studies over one and two weeks were conducted to elucidate the general effects of pH, ionic strength and the addition of further excipients on cytokine aggregation during storage. During these initial stability studies the focus was set on monitoring aggregation with HP-SEC, turbidity measurements and DLS.

3.4.1 Influence of pH on Cytokine Stability

To study the impact of pH on the cytokine formulations with 0.25 mg/ml cytokine in 20 mM glycine at pH 3.0, 3.5, 4.0 and 4.5 were stored for one week at 2-8°C, 25°C and 40°C. Aggregation was determined by HP-SEC and by turbidity measurement. Initial aggregation ranged between 3.3% at pH 3.0 and 4.1% at pH 4.5. When stored at 2-8°C and 25°C, the increase in aggregation was less than 0.5% for the tested pH range between 3.0 and 4.5 (Figure 21a). Storage at 40°C led to more pronounced aggregate formation at higher pH values, with 9.1% at pH 4.5 compared to 4.6% at pH 3.0. Data from turbidity measurements confirmed that formulations at pH 3.0 and 3.5 were more

stable compared to formulations at a higher pH. Turbidity ranged between 1 and 1.5 FNU for pH 3.0 and 3.5, and between 1 and 2 FNU for pH 4.0 and 4.5 (Figure 21b).

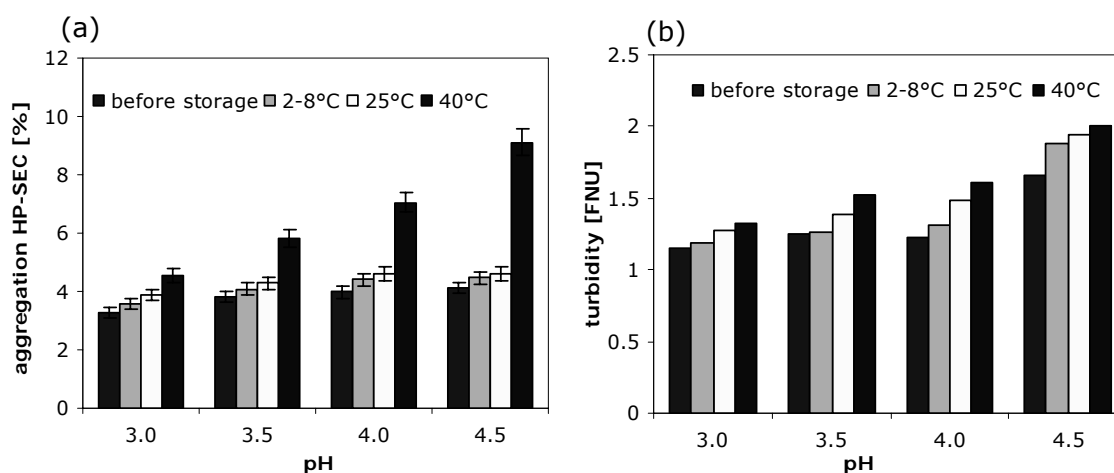


Figure 21: Aggregation determined with HP-SEC (a) and turbidity (b) of 0.25 mg/ml cytokine in 20 mM glycine after 1 week storage at 2-8°C, 25°C and 40°C.

All solutions were clear with turbidities lower than reference solution I of the European Pharmacopoeia. However, the difference between the formulations with respect to larger aggregates was less distinctive than the pH-effect on dimer and trimer formation analyzed by HP-SEC. Again it became obvious that an increase in soluble aggregates detectable by HP-SEC only has a minor impact on turbidity, which is mainly caused by medium-sized aggregates [22]. The result that a low pH was beneficial for the stability of the cytokine was confirmed with DLS (Figure 22).

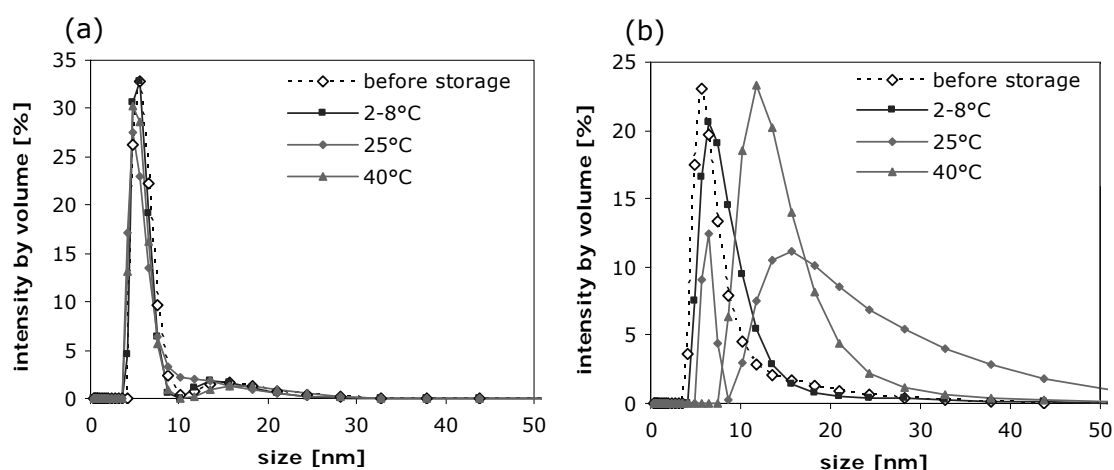


Figure 22: Size distribution by volume of 0.25 mg/ml cytokine in 20 mM glycine at pH 3.0 (a) and pH 4.5 (b) after 1 week storage.

No changes in the size distribution by volume were detected for the samples at pH 3.0 after one week at 2-8°C and 40°C. At pH 4.5 on the other hand, the size distribution by

volume was affected when the formulations were stored at 25°C and 40°C. After one week at 25°C the intensity of the peak at 5 nm decreased followed by a significant increase in the intensity at 10 to 30 nm. Storage at 40°C resulted in a disappearance of the first peak at 5 nm, while the second peak at 10 to 30 nm augmented, reflecting the increased aggregation. So far, the short-time stability study showed that aggregation detectable by HP-SEC and turbidity did not significantly increase within one week at 2-8°C and 25°C when the cytokine was formulated between pH 3.0 and 4.5. However, for the formulations at pH 4.5 DLS pointed at a changed size-distribution by volume when stored at 25°C. Storage of the samples at 40°C clearly revealed an improved stability at lower pH values. To further clarify the role of pH on cytokine stability, the impact of pH values above 4.5 was evaluated by HP-SEC in a two-week stability study (Figure 23).

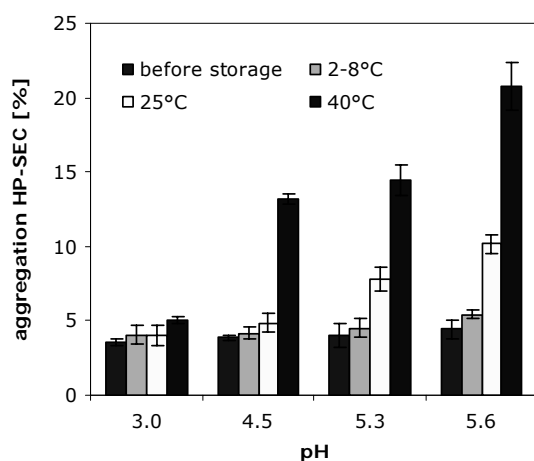


Figure 23: Aggregation determined by HP-SEC of 0.25 mg/ml cytokine in 20 mM glycine after 2 weeks storage at 2-8°C, 25°C and 40°C.

No significant increase in aggregation was determined with HP-SEC at pH 3.0 after two weeks for all storage temperatures. At pH 4.5 13.2% aggregates were measured by HP-SEC for the formulations stored at 40°C. For the formulations at pH 3.0 and pH 4.5 the total AUC in the HP-SEC chromatograms remained constant for all storage conditions, indicating the absence of substantial quantities of larger aggregates. For the cytokine formulations at pH 5.3 and 5.6 already at 25°C a substantial increase in aggregation to 7.8% and 10.2% was obvious. Even higher values of 14.5% and 20% at pH 5.3 and pH 5.6 were reached when storing the formulations at 40°C. The AUC in the HP-SEC chromatograms were significantly reduced at pH 5.2 and pH 5.6 to 92% and 93% at 2-8°C, 57% and 70% at 25°C and 33% and 59% at 40°C. The lowered AUC pointed at the formation of larger aggregates, which were retained by the guard column. Due to increased aggregation already after 2 weeks storage pH values above 4.5 will not

included for the development of a liquid formulation. For lyophilized formulations pH 5.0 could be taken in consideration, as the initial aggregation with 4.0% was not significantly higher compared to pH 4.5.

3.4.2 Influence of Ionic Strength on Cytokine Stability

So far, it could be shown that a formulation pH between 3.0 and 4.5 would be suitable for the development of liquid formulations. For this pH range the impact of increasing glycine, respectively NaCl concentrations on aggregation was further evaluated in a two week stability study at 2-8°C, 25°C and 40°C. This issue needed to be clarified in the pre-formulation study to check if NaCl can be employed for isotonicity adjustment of the final formulations. HP-SEC revealed that the formation of dimers and lower aggregates was independent of the glycine concentration when using 10 to 50 mM glycine between pH 3.0 and 4.5 (data not shown). In contrast, the addition of 0.2% to 0.9% NaCl led to a boost in aggregates after 2 weeks storage, especially at 40°C (Figure 24). Higher aggregate concentrations of about 20% were found by HP-SEC at pH 3.0 as compared to about 14% at pH 4.5 for formulations with 0.2% to 0.9% NaCl after 2 weeks at 40°C. However, the AUC was declining over storage time, particularly at pH 4.5 and with increasing NaCl concentrations, indicating the presence of larger aggregates.

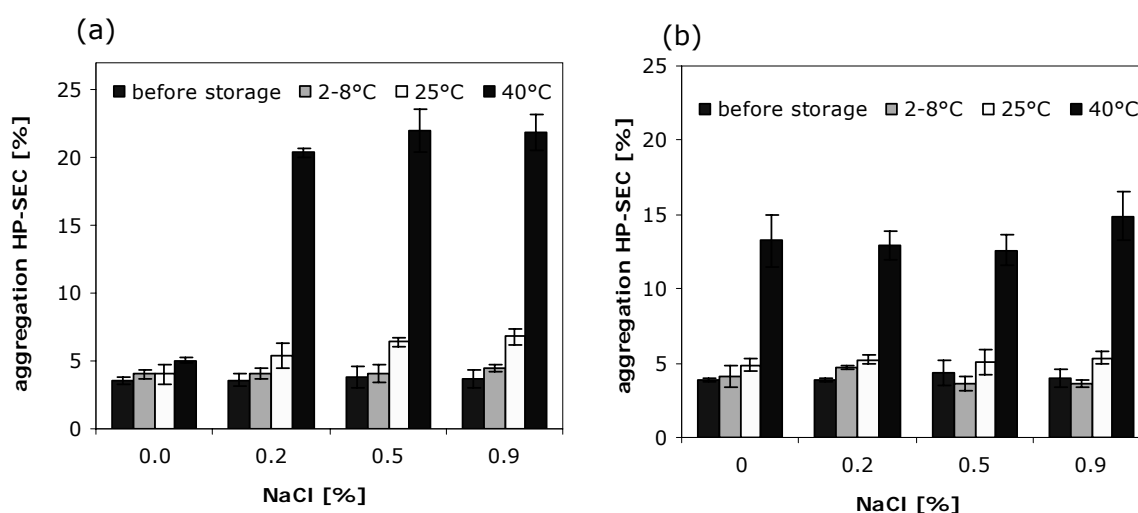


Figure 24: Aggregation determined by HP-SEC in 0.25 mg/ml cytokine in 20 mM glycine at pH 3.0 (a) and pH 4.5 (b) after 2 weeks storage at 2-8°C, 25°C and 40°C.

The formation of larger aggregates was confirmed by turbidimetry for samples with 0.2% NaCl at pH 4.5 and with 0.9% NaCl at pH 3.0 and pH 4.5 when stored for 2 weeks at 40°C (Figure 25). Without NaCl the solutions remained clear with turbidities below 3.2 after 2 weeks at 40°C, independent of the pH. When 0.2% and 0.9% NaCl were added to the formulations turbidities of about 17, respectively 24 FNU were measured for at

pH 4.5, which can be categorized as opalescent according to the European Pharmacopoeia.

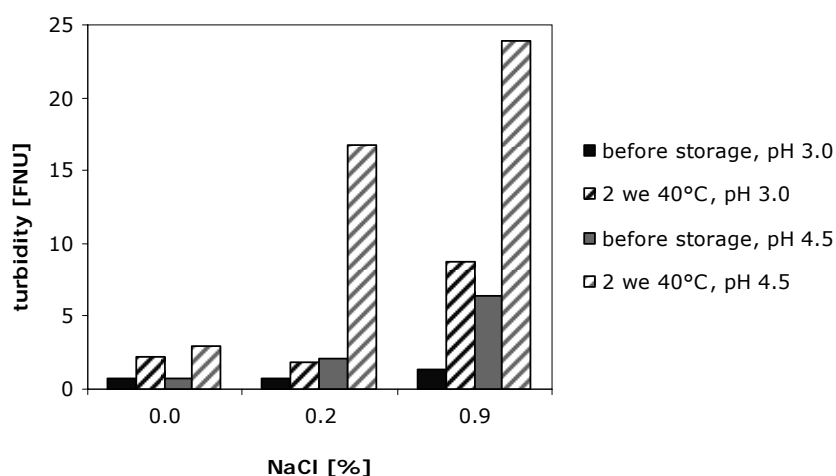


Figure 25: Turbidity of 0.25 mg/ml cytokine in 20 mM glycine at pH 3.0 and 4.5 with 0.0%, 0.2% and 0.9% NaCl before storage and after 2 weeks at 40°C.

Summarizing, the increase in ionic strength by adding 0.2 to 0.9% NaCl had a negative impact on the storage stability of the cytokine in solution, as aggregation and precipitation was fostered. Therefore, NaCl is not suitable to adjust the isotonicity of the final formulation.

3.4.3 Influence of Excipients on Cytokine Stability

Within the pre-formulation studies the impact of the excipients mannitol, trehalose and polysorbate 20 on cytokine stability with respect to aggregation was evaluated. In liquid formulations mannitol and trehalose can be used as stabilizers and simultaneously to adjust the isotonicity of the formulation, without increasing the ionic strength. Generally, sugars and sugar alcohols are preferentially excluded from the immediate vicinity of the protein surface which leads to a thermodynamically unfavorable state due to the increase in entropy. Thereby, the denaturated state of a protein exhibits a larger surface, which is more unfavorable resulting in a stabilization of the native state [55-57]. For the planned lyophilized formulations of the cytokine, mannitol as single component would not provide sufficient stabilization, as it usually crystallizes during lyophilization [58]. Only in the amorphous state mannitol is able to adequately stabilize the active protein via molecular interactions [59,60]. To provide sufficient stabilization for the protein, trehalose or sucrose as amorphous stabilizers can be added. These sugars are capable to stabilize the cytokine by acting as water substitute in the dried state and by forming an amorphous glass [61,62]. For the cytokine formulation the combination of 4.0% mannitol and 1.0%

sucrose or trehalose was used. The physico-chemical studies of the system mannitol-sucrose and the development of adequate lyophilization cycles were discussed in Chapter 5. The adsorption studies revealed that polysorbate 20 was effective in inhibiting the loss of cytokine due to adsorption on the container. Furthermore, polysorbates can inhibit aggregation which was for example shown by Kreilgaard et al. (1998) for the shaking and freezing induced aggregation of recombinant human Factor XIII [63] and by Bam et al. (1998) for the shaking induced aggregation of recombinant human Growth Hormone [64]. However, for other proteins e.g. Interleukin-1 β polysorbate 80 did not influence aggregation [65]. Therefore, the impact of 0.01% polysorbate 20 on the aggregation behavior of the cytokine was evaluated.

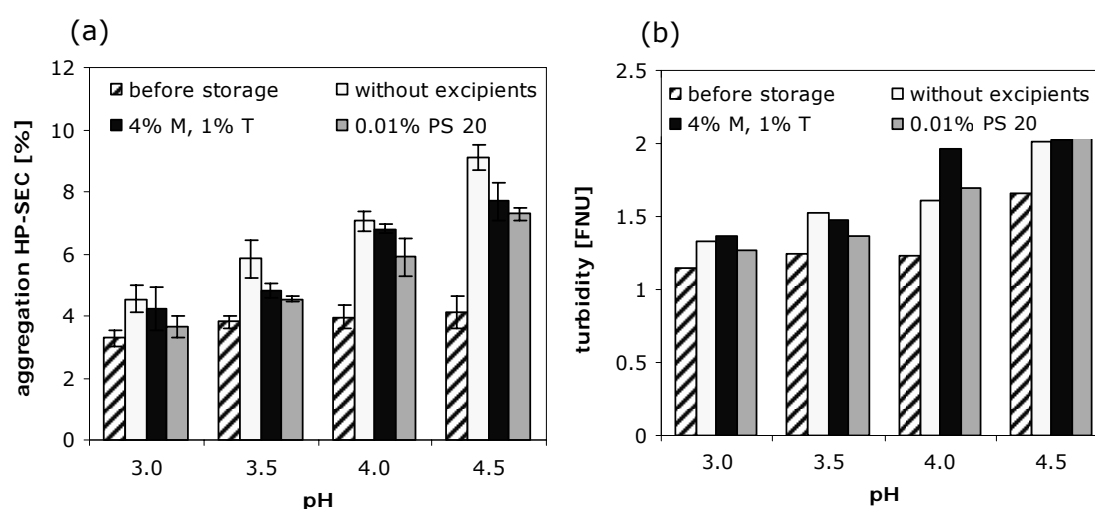


Figure 26: Aggregation determined by HP-SEC (a) and turbidity (b) of 0.25 mg/ml cytokine in 20 mM glycine with different excipients at pH 3.0, 3.5, 4.0 and 4.5 after 1 week storage at 40°C.

After one week storage at 2-8°C and 25°C HP-SEC revealed that aggregation increased less than 0.5% for formulations with 0.25 mg/ml cytokine at pH 3.0 to pH 4.5 independent of the presence of excipients. A slight stabilizing effect was achieved by the addition of mannitol-trehalose and polysorbate 20 when the samples were stored at 40°C (Figure 26a). While aggregation increased between 1.3% and 5.0% between pH 3.0 and pH 4.5 without excipients, the increase ranged between 0.4% and 3.6% when stabilizers were added. No significant differences were observed in the turbidity of the formulations with and without excipients, indicating that no larger aggregates were formed under the studied conditions (Figure 26b). Here again the formulation pH played the major role for the stability of the formulation with respect to aggregation and turbidity. For formulation development mannitol can be used to adjust the isotonicity of the formulations.

3.5 Freeze-Thaw Stability

During freezing various stress factors, e.g. the formation of ice crystals and the corresponding solid liquid interfaces, the increasing concentration of the remaining solutes, a pH shift or a phase separation can lead to damage and aggregation of proteins. These freezing induced stresses are described in detail in the reviews of Wang (2000) [2] and Arakawa et al. (2001) [57]. The freeze-thaw stability is therefore an important issue to be evaluated in the pre-formulation studies, also with respect to the planned development of lyophilized formulations. The physical stability of the cytokine during freezing and thawing was evaluated in terms of aggregation. 2 R vials containing 1.0 ml of the formulations were placed on the shelves of the freeze-drier cooled to -50°C within 2 hours. This freezing procedure was chosen as it will be used for lyophilization of the later formulations. After an isothermal phase of 2 hours at -50°C the vials were reheated to 20°C and allowed to thaw.

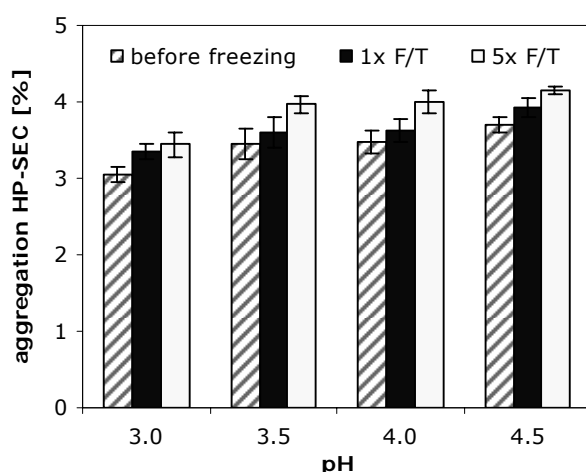


Figure 27: Aggregation determined by HP-SEC of 0.25 mg/ml cytokine in 20 mM glycine at pH 3.0 to 4.5 before and after 1 and 5 freeze-thaw cycles.

Aggregation was determined after one and five freeze-thaw (F/T) cycles for formulations with 0.25 mg/ml cytokine with 20 mM glycine at pH 3.0 to 4.5 (Figure 27). A slight increase in aggregation by approximately 0.2% after one, respectively 0.5% after five freeze-thaw cycles was found in the HP-SEC chromatograms. The AUC of the HP-SEC chromatograms was not significantly affected by the freeze-thaw cycles, which pointed at the absence of larger aggregates.

The addition of further excipients (mannitol, trehalose, sucrose and polysorbate 20) and combinations of these excipients only had a minor impact on the increase in aggregation at pH 3.0 (Figure 28a). After one cycle an average increase in aggregation of 0.2% and after five cycles of 0.5% was determined for the formulations at pH 3.0. At pH 4.5

aggregation increased by 0.25% after one freeze-thaw cycle (Figure 28b). After five cycles the formulations with 4.0% mannitol and 1.0% sucrose respectively 4.0% mannitol and 1.0% trehalose and 0.01% polysorbate 20 showed an increase in aggregation by 0.2%, compared to an increase between 0.4% to 0.8% for the other formulations.

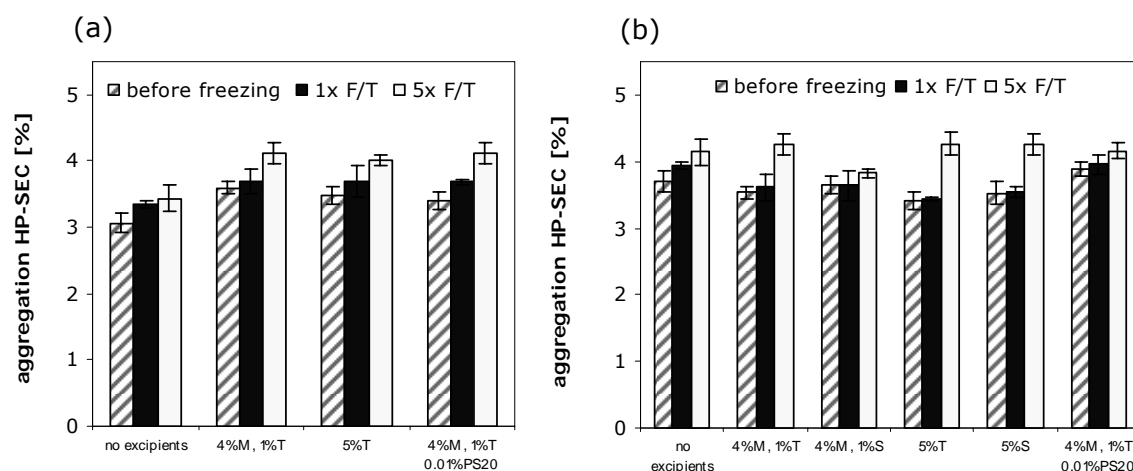


Figure 28: Aggregation determined by HP-SEC of 0.25 mg/ml cytokine in 20 mM glycine at pH 3.0 (a) and pH 4.5 (b) with combinations of mannitol (M), sucrose (S), trehalose (T) and polysorbate 20 (PS20) before and after 1 and 5 freeze-thaw cycles.

Thus, the cytokine showed an overall good stability against stresses induced by freezing and thawing, even without further excipients beside the buffering glycine. Due to this good stability the freezing step during lyophilization is not expected to cause major physico-chemical alternations of the cytokine.

3.6 Long-term Stability of Liquid and Lyophilized Formulations

The goal of the study was the development of stable, HSA-free formulations of the cytokine, as an alternative to the existing HSA-containing lyophilized formulation. Based on the results of the preformulation study, which pointed at the structural characteristics of the cytokine (compare 3.2), protein adsorption (compare 3.3) and the effect of pH, ionic strength and the addition of excipients (compare 3.4) on cytokine stability, the most promising conditions were selected. It was shown that the physical stability of the cytokine was improved at low pH between 3.0 and 3.5. A glycine concentration of 20 mM turned out to be beneficial regarding aggregation and loss of protein due to adsorption. FTIR revealed a higher fraction of β -sheet structure at pH 3.0 and 3.5, but also an increased stability against structural changes with increasing temperature. The changed secondary structure at pH 3.0 and 3.5 could be regarded as critical, as the activity of the cytokine might be changed. However, it was not an irreversible change as the amount of β -sheet was reduced in favor of α -helical structure when the pH was increased. In literature an increased thermal stability for the cytokine determined by circular dichroism and a protection of its activity at pH 2.9 was described by Boublik et al. (1990) [66]. To clarify the question how activity and secondary structure are correlated, in vitro assays for antiviral activity, e.g. antiviral yield reduction assays or cytopathic effect bioassays [67] would be necessary to quantify the biological activity of the cytokine. The first short-time stability studies indicated that storage at 2-8°C and 25°C may allow formulating the cytokine at pH 4.0 and possibly at pH 4.5. To minimize protein adsorption the addition of 0.005% to 0.02% polysorbate 20 is reasonable. For the lyophilized formulations glass type I⁺ vials could be used. For the liquid formulation the utilization of pre-filled syringes was planned, which were not available in glass type I⁺ quality. In this case the addition of polysorbate 20 could minimize protein adsorption. The addition of salt or the use of higher buffer concentrations needs to be avoided, as aggregation and precipitation were favored at higher ionic strength. In the further studies, the isotonicity of the solutions was therefore adjusted with mannitol in the liquid or with combinations of mannitol with sucrose in the lyophilized formulation. The 6 months stability study of the liquid formulations was performed in glass prefilled syringes BD Hypak SCF[®]. All liquid formulations contained 0.25 mg/ml cytokine, 20 mM glycine and 4.8% mannitol, whereas pH and polysorbate 20 concentrations were varied (Table 4).

Table 4: Overview of the liquid formulations tested for stability over 6 months.

pH	polysorbate 20 [%]
3.5	0.02
4.0	0.0
4.0	0.005
4.0	0.02
4.5	0.02

For an alternative HSA-free lyophilized formulation higher pH values were included. In the preliminary studies it could be shown that aggregation increased only marginally upon two week storage at 2-8°C for formulations at pH 5.3 and pH 5.6 (compare 3.4.1). One drawback of the higher pH values is the augmented adsorption tendency of the cytokine (compare 3.3.1). Therefore, glass type I⁺ vials were used for the lyophilized formulations in combination with polysorbate 20. The advantage of higher pH values is the possibility to use sucrose as excipient for lyophilization. At pH 3.0 the use of sucrose is not feasible due to the acid catalyzed inversion of sucrose to fructose and glucose. The inversion process can take place in lyophilized products even at very low moisture levels [68]. Therefore, mannitol employed in a concentration of 4.0% was used as bulking agent and 1.0% sucrose as lyo- and cryoprotector. The physico-chemical lyophilization behavior, as well as an adequate lyophilization cycle for the system was evaluated in Chapter 5. Again formulation pH and polysorbate 20 concentrations were varied for the lyophilized formulations (Table 5).

Table 5: Overview of the lyophilized formulations tested for stability over 6 months.

pH	polysorbate 20 [%]
4.0	0.0
4.0	0.005
4.0	0.02
4.5	0.02
5.0	0.02

The stability of the five liquid and five lyophilized formulations was evaluated over 6 months at 2-8°C, 25°C / 60% RH and 40°C / 75% RH. Stability was monitored in terms of aggregation using HP-SEC and the change of the size distribution by volume measured with DLS. Chemical modifications were detected by RP-HPLC.

3.6.1 Long-term Stability of Liquid Cytokine Formulations

The formation of dimers and lower aggregates was determined by HP-SEC after 1, 3 and 6 months storage period at 2-8°C, 25°C and 40°C (Figure 29). After 6 months storage the level of dimers and lower aggregates was increased by 0.6% at 2-8°C and by 1.4% at 25°C for formulations at pH 3.5. The most significant rise by 1.6% at 2-8°C and by 5.2% at 25°C was determined at the highest tested pH of 4.5. Aggregation stepped up drastically, when the liquid cytokine formulations were stored at 40°C. At pH 4.0 more than 40% and at pH 4.5 more than 50% dimers lower aggregates were formed, whereas only 11.5% dimers and trimers were detected at pH 3.5.

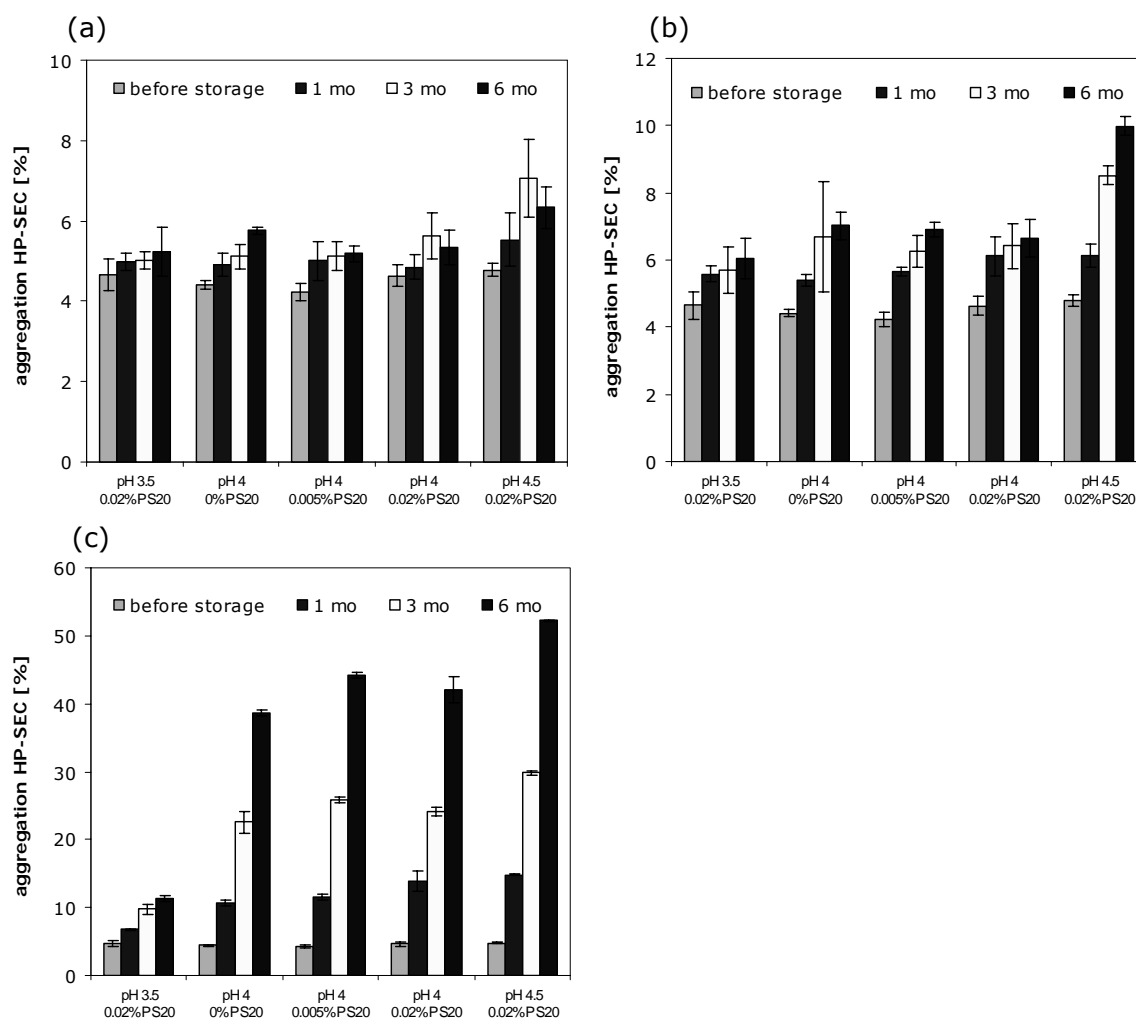


Figure 29: Aggregation determined by HP-SEC of the cytokine in the liquid formulations over 6 months during storage at 2-8°C (a), 25°C (b) and 40°C (c).

The pH-dependency of the formulation stability was in agreement with the results of the FTIR-studies (compare 3.2.1). For the cytokine formulated at pH 3.5 a denaturation temperature T_m of 74°C was determined, while pH 4.2 resulted in a T_m of 57°C. FTIR had shown that significant structural changes at pH 4.2 already started at a temperature

of 40 to 45°C. Therefore, the storage temperature of 40°C, which is only about 15°C below T_m , was already too high to assure the integrity of the cytokine. The addition of 0.005% and 0.02% polysorbate 20 to the liquid formulation at pH 4.0 had no considerable impact on the formation of aggregates. The improved stability at pH 3.5 compared to the higher pH values was further reflected in the size distribution by volume determined with DLS (Figure 30).

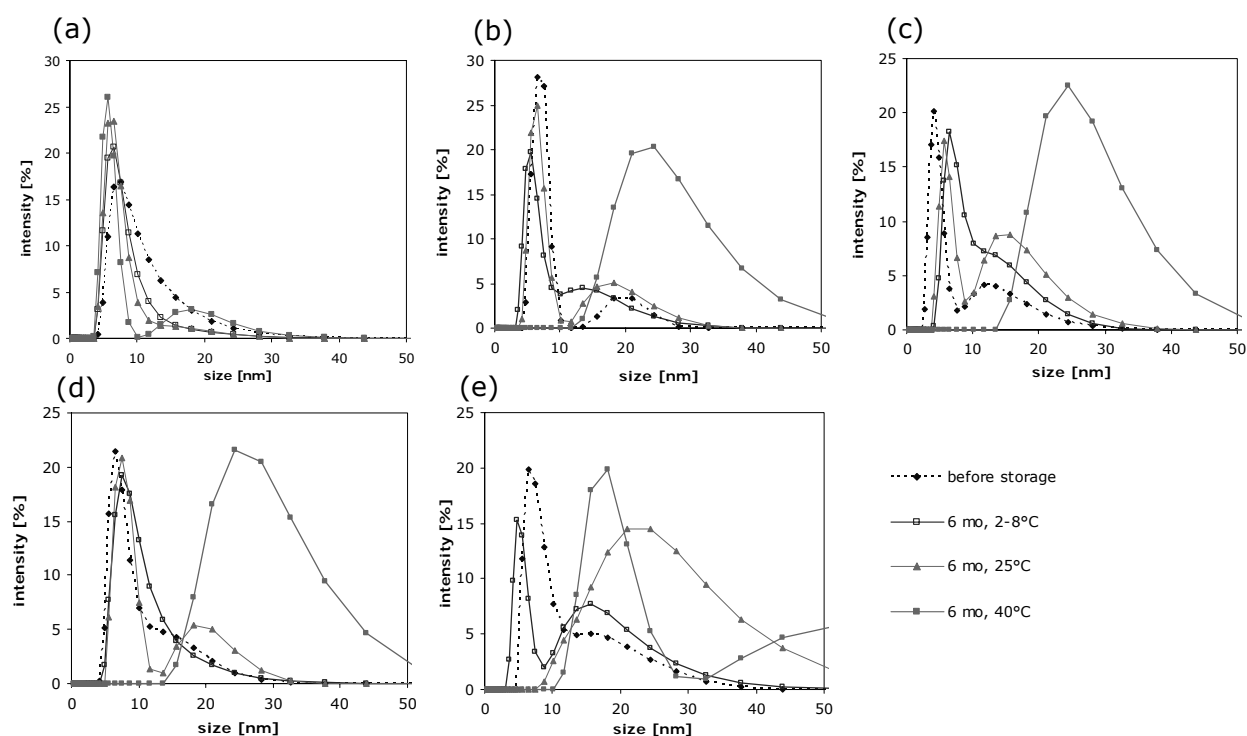


Figure 30: DLS size distribution by volume of liquid formulations at pH 3.5, 0.02% polysorbate 20 (a), pH 4.0, 0.0% (b), 0.005% (c), 0.02% polysorbate 20 (d) and pH 4.5 0.02% polysorbate 20 (e) after 6 months storage.

For the formulations at pH 3.5 a main peak at 5 nm was present after 6 months at all storage conditions. At 40°C a second peak at 10 to 30 nm appeared which reflected the significant formation of aggregates seen in HP-SEC. The samples at pH 4.0 exhibited comparable changes in the size distribution at all tested levels of polysorbate 20. Already before storage a distinct peak at 10 to 20 nm was present without and with 0.005% polysorbate 20 and a shoulder at 0.02% polysorbate 20. At 2-8°C the size distribution was slightly more stable with 0.02% polysorbate 20, as no distinct peak at 10 to 30 nm could be assigned. The decreased thermal stability of formulations at pH 4.5 becomes obvious in the drastically changed DLS size distributions. At 25°C and 40°C storage the first peak at 5 nm was no longer present and high intensities were measured above 10 nm. After storage at 40°C a second peak at about 60 nm emerged for the formulation at pH 4.5.

For the formulations stored at 2-8°C and 25°C RP-HPLC was performed to analyze the level of chemically modified cytokine. Especially at low pH values chemical modification e.g. oxidation or deamidation are more likely to occur [69,70]. Within the RP-chromatogram a met-oxidized form of the cytokine is eluting prior to the main peak followed by several peaks, which can be assigned to oligomerized protein [14]. Before storage, the formulations contained an average of 1.6% met-oxidized forms. Figure 31 shows the amount of met-oxidized cytokine after 3 and 6 months storage at 2-8°C and 25°C. Met-oxidized cytokine was formed as a function of storage time and temperature. At 2-8°C a slight rise in met-oxidized cytokine by 0.2% to 0.6% was determined after 3 months, which further increased by 1.4% to 2.4% after 6 months compared to the levels before storage. Higher values of met-oxidized cytokine were determined for the samples stored at 25°C. The data indicated a slight stabilizing effect of polysorbate 20 at pH 4.0, as here the lowest levels of met-oxidized cytokine was measured. Furthermore, the level of met-oxidized cytokine at pH 3.5 was increased after 6 months storage at 25°C compared to the higher pH values. Overall, oxidation of the cytokine should be kept low by storage at 2-8°C. As an alternative, the addition of methionine as antioxidant could be evaluated.

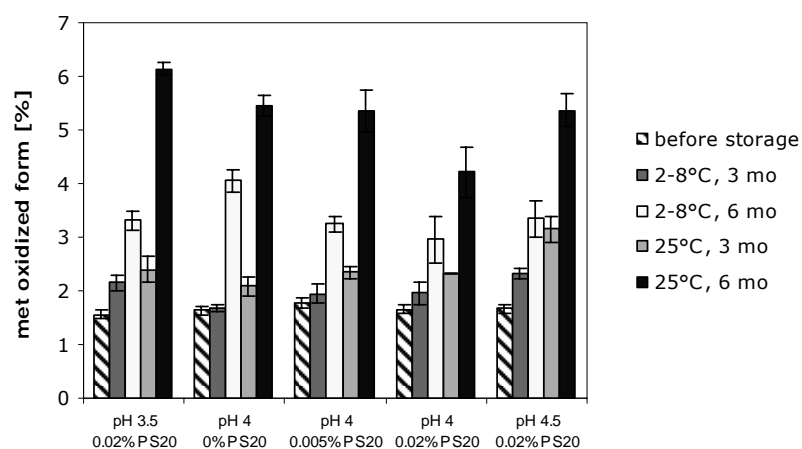


Figure 31: Met-oxidized form of the cytokine determined with RP-HPLC in liquid formulation after 3 and 6 months at 2-8°C and 25°C.

To evaluate the degree of protein adsorption in the prefilled glass syringes the protein content in the formulations was determined with UV-spectroscopy and the AUC in the HP-SEC chromatograms were considered. After storage at 2-8°C UV spectroscopy revealed a residual protein content of 96% for the formulation without polysorbate 20, while 99% were found at 0.005% polysorbate 20 and 102% at 0.02% polysorbate 20 at pH 4.0 (Figure 32a). A protein recovery of 99% at pH 3.0 and 101% at pH 4.5 was determined after one month. Especially at 40°C storage temperatures protein contents above 100%

were determined. This could be explained by light scattering effects of aggregated proteins, also evident by an increased UV-absorption at 350 nm and 550 nm. This trend was confirmed by the AUCs of the HP-SEC chromatograms (Figure 32b).

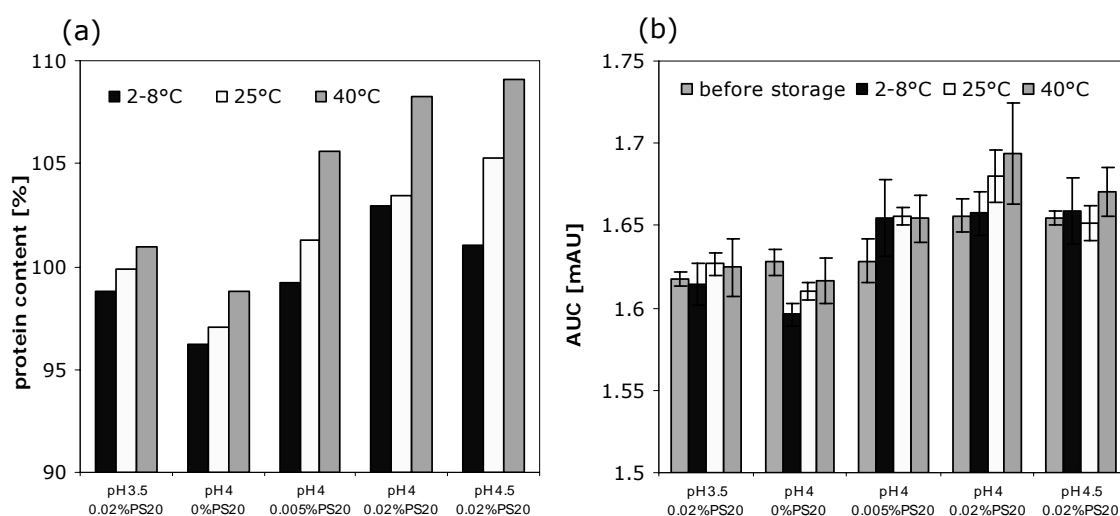


Figure 32: Protein content determined by UV-spectroscopy (a) and AUC in the HP-SEC chromatograms (b) of the liquid formulations after 1 month storage at 2-8°, 25°C and 40°C.

Summing up, the development of a liquid HSA-free formulation for the cytokine was feasible. Most suitable with respect to aggregation and formation of met-oxidized cytokine were the formulations at pH 3.5 and pH 4.0, stored at 2-8°C. Storage at 40°C facilitated the aggregation process, which was confirmed by HP-SEC and DLS. While aggregation was only slightly increased at 25°C, the formation of met-oxidized cytokine augmented significantly. To avoid adsorption of the cytokine to the glass syringes the addition of at least 0.005% polysorbate 20 was necessary. Furthermore, polysorbate 20 had a slight stabilizing effect with respect to the DLS size distribution at 2-8°C and the formation of met-oxidized cytokine.

3.6.2 Stability of Lyophilized Formulation

To stabilize the cytokine in lyophilized form pH values of 4.0 to 5.0 were selected. Mannitol was used as crystalline bulking agent and sucrose as amorphous stabilizer. Thereby, a lyophilization cycle optimized to avoid the formation of mannitol hydrate and to ensure mannitol crystallization as far as possible was used (compare Chapter 5). After lyophilization mainly δ -mannitol (peak at 9.7° 2- θ) with a smaller fraction of β -mannitol (peaks at 14.6 and 23.5° 2- θ) was present in all formulations. Figure 33 shows exemplarily the XRD patterns of the formulations at pH 4.0 without and with 0.02% polysorbate 20. In lyophilized formulation without polysorbate 20 a larger fraction of β -

mannitol is present compared to the formulations with 0.02% polysorbate 20. Polysorbate is known to influence the morphology of mannitol after lyophilization [71].

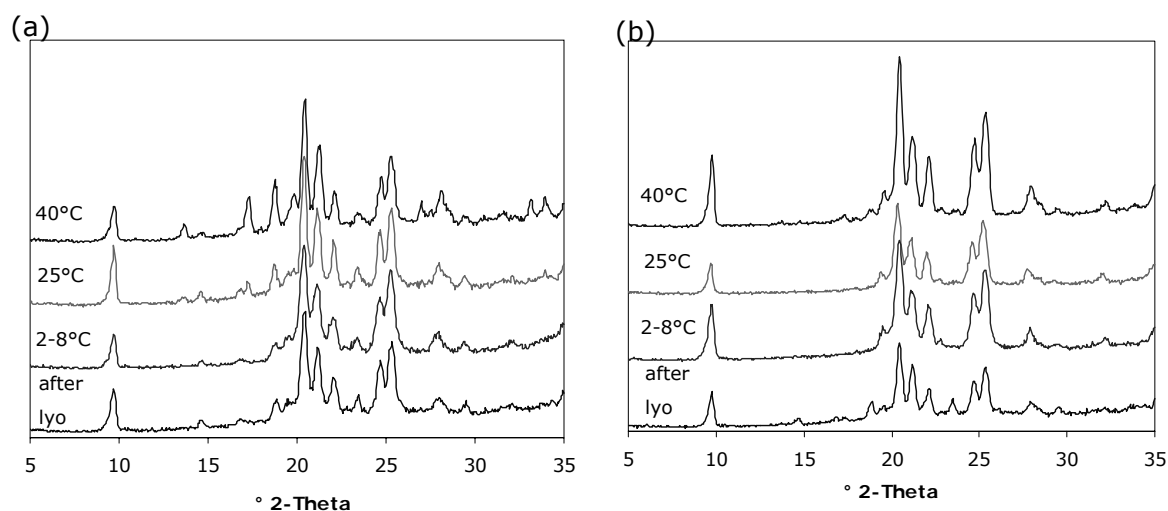


Figure 33: XRD diffraction pattern of lyophilized formulation at pH 4.0 without (a) and with 0.02% polysorbate 20 (b) after lyophilization and 6 months storage at 2-8°C, 25°C / 60% RH and 40°C / 75% RH.

Changes in the physico-chemical properties of the lyophilized products were evaluated as they may influence protein stability. However, for formulations with mannitol and HSA it could be shown in Chapter 3 that a change in the mannitol modifications and crystallinity did not affect the integrity and stability of HSA. Upon storage, slight changes could be detected in the XRD-diffraction patterns of the polysorbate 20 free samples (Figure 33a). After 6 months storage at 25°C / 60% RH and 40°C / 75% RH peaks of α -mannitol appeared at 13.6° 2- θ and 17.2° 2- θ . It was further evident that the intensity of the δ -mannitol peak at 9.7° 2- θ decreased during 6 months at 40°C / 75% RH. This could be ascribed to the fact that the δ -modification is the least stable modification of mannitol [72]. Samples with 0.02% polysorbate 20 were more stable regarding mannitol modifications with only a slight decrease in β -mannitol (Figure 33b).

After lyophilization all formulations exhibited low residual moisture levels between 0.5% and 1.0% (Table 6). This low water contents could be attributed to the high content of crystalline mannitol in the formulations. Over 6 months only a slight increase in residual moisture up to maximally 1.2% at 2-8°C and 25°C / 60% RH and maximally 1.4% at 40°C / 75% RH was measured. Water can act as reactant in chemical reactions within the lyophilized sample and as plasticizer with the consequence that the molecular mobility of the system is altered [73]. Generally, residual moisture levels of about 1% are suggested for lyophilized protein formulations [74]. However, Chang et al. (2005) showed that water in lyophilized IgG1-sucrose increased the molecular mobility in the glassy matrix, while the lowest aggregation rate was measured at intermediate water

contents of 2% to 3% [75]. The constant residual moisture level in the different lyophilized cytokine formulations over storage time could be regarded as beneficial.

Table 6: Residual moisture (RM) of lyophilized formulations stored for 6 months at 2-8°C, 25°C / 60% RH and 40°C / 75% RH (n=3).

	RM [%] after lyophilization	Storage conditions	RM [%] after 1 month	RM [%] after 3 months	RM [%] after 6 months
pH 4.0	1.03	2-8°C	0.90	0.98	1.24
0.0% PS 20		25°C / 60% RH	1.07	0.93	0.91
		40°C / 75% RH	0.86	0.98	1.17
pH 4.0	0.67	2-8°C	0.93	1.09	1.07
0.005% PS 20		25°C / 60% RH	1.03	1.00	0.92
		40°C / 75% RH	0.96	1.00	1.40
pH 4.0	0.51	2-8°C	0.86	1.03	1.03
0.02% PS 20		25°C / 60% RH	1.03	1.00	0.94
		40°C / 75% RH	1.09	1.16	1.41
pH 4.5	0.68	2-8°C	1.10	1.05	1.06
0.02% PS 20		25°C / 60% RH	1.07	1.07	1.01
		40°C / 75% RH	1.07	1.22	1.29
pH 5.0	0.57	2-8°C	0.88	1.14	1.22
0.02% PS 20		25°C / 60% RH	1.04	1.04	0.95
		40°C / 75% RH	1.06	1.12	1.24

The pre-formulation studies pointed at no significant increase in aggregation after a single freeze-thawing step (compare 3.5). After the lyophilization process no boosted aggregate formation was observed for all formulations (Figure 34). The size distributions by volume measured by DLS were equal as prior to lyophilization (data not shown). The selected excipients offered sufficient protection for the cytokine against freezing and drying induced stress. This showed that the approach of producing a lyophilized cake with highly crystalline mannitol in combination with amorphous sucrose as stabilizer in a ratio of 4:1 was feasible to stabilize the cytokine.

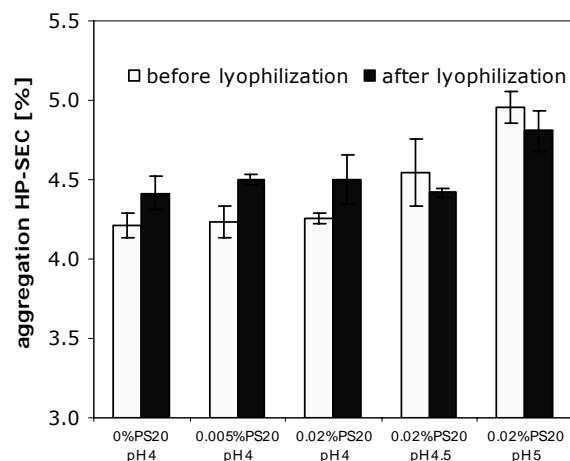


Figure 34: Aggregation determined by HP-SEC of the formulations before and after lyophilization.

The stability of the lyophilized cytokine formulations was further evaluated over 6 months at 2-8°C, 25°C / 60% RH and 40°C / 75% RH, with respect to the formation of aggregates and a met-oxidized form of the cytokine. After 6 months at 2-8°C the level of dimers and lower aggregates increased between 0.3% and 0.7% for all studied formulations, independent of formulation pH and the addition of polysorbate 20 (Figure 35a). Storage at 25°C / 60% RH and 40°C / 75% RH resulted in higher contents of dimers and lower aggregates, especially at the presence of 0.02% polysorbate 20 (Figure 35 b,c). XRD revealed that the formulations at pH 4.0 without polysorbate 20 were physico-chemically less stable and underwent morphological changes during storage (Figure 33a). Regarding aggregation on the other hand the formulations at pH 4.0 with 0.0% and 0.005% polysorbate provided an improved stability compared to the formulations with 0.02% polysorbate 20 after 6 months storage at 25°C / 60% RH and 40°C / 75% RH. The improved stabilizing conditions without or with lower polysorbate 20 concentrations outbalanced a potential detrimental effect of the change in modifications during storage (compare Chapter 4). During storage at 40°C / 75% RH the highest aggregation values were measured at pH 4.0, when comparing the formulations with 0.02% polysorbate 20 at the different pH values. For sucrose containing formulations a pH of 4.0 is critical due to the risk of the inversion of sucrose at low pH [68]. This was confirmed by the slightly brownish color of the reconstituted formulations stored at 40°C, which was distinct at pH 4.0. The discoloration induced by the Maillard reaction, occurs when sucrose undergoes inversion to fructose and glucose. The use of trehalose instead of sucrose would be an alternative approach to improve the stability of the lyophilized formulation, by avoiding the inversion of sucrose. The AUC of the HP-SEC remained at a constant level for the samples stored at 2-8°C and 25°C / 60% RH indicating that no significant loss of protein due to adsorption or precipitation occurred, which could be

attributed to the utilization of glass type I⁺ vials. Storage at 40°C / 75% RH led to a decline in the AUC due to the formation of larger aggregates.

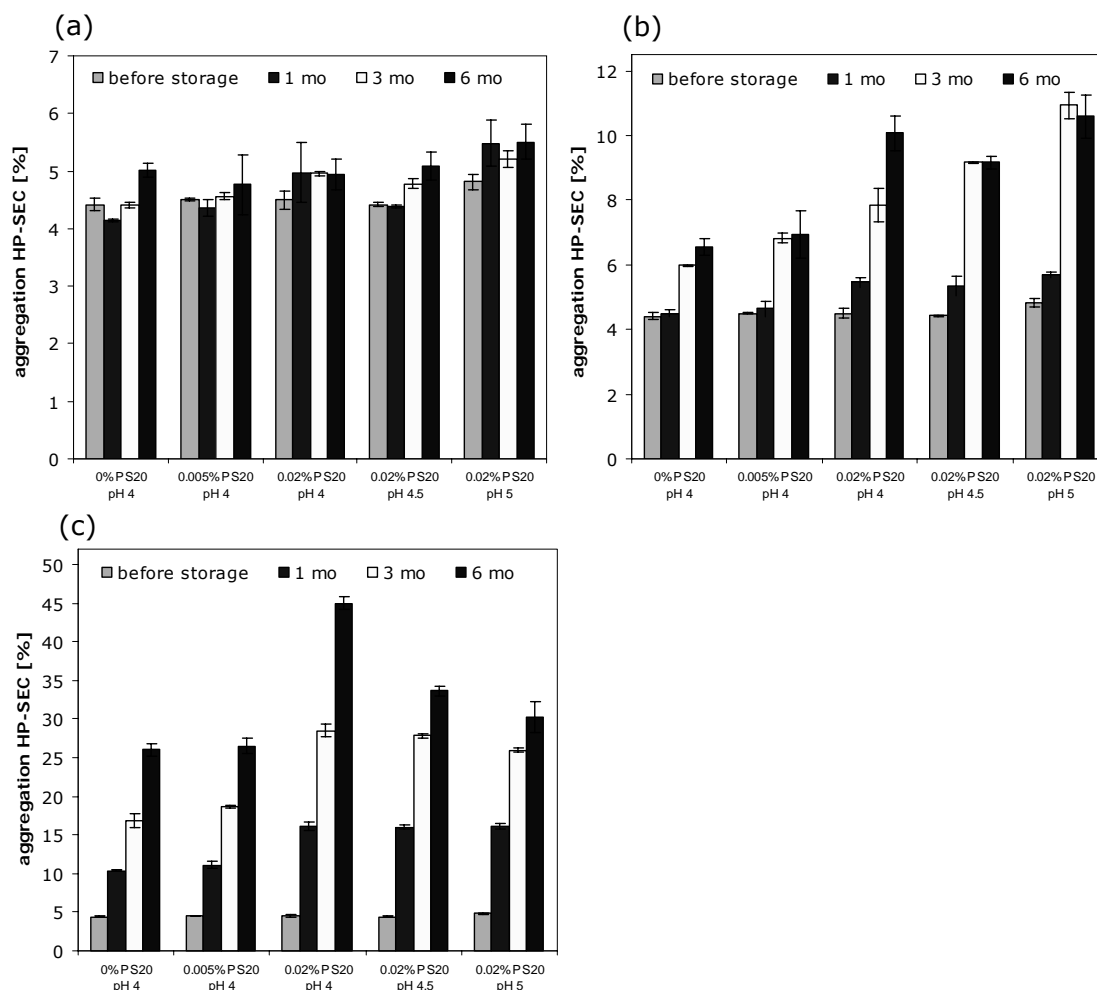


Figure 35: Aggregation determined by HP-SEC of the cytokine in the lyophilized formulations over 6 months during storage at 2-8°C (a), 25°C / 60% RH (b) and 40°C / 75% RH (c).

DLS of the formulations confirmed the results from HP-SEC (Figure 36). Here again the improved stability of samples without polysorbate 20 at pH 4.0 was evident. The size distribution by volume only changed to a moderate degree in polysorbate-free formulations when stored at 2-8°C and 25°C / 60% RH. Unlike to HP-SEC, where aggregation was comparable for samples at pH 4.0 without and with 0.005% polysorbate 20, DLS indicated a changed size-distribution by volume for the formulations stored at 25°C / 60% RH. In the presence of 0.005% polysorbate 20 the first peak was shifted to sizes of 20 to 30 nm. In addition a peak between 105 and 120 nm with intensity below 5% occurred for all samples stored at 40°C / 75% RH (not shown in Figure 36). This peak could be attributed to larger protein aggregates, which were not detected by HP-SEC but led to a decline of the AUC in the HP-SEC chromatograms. For the samples stored at 2-8°C and 25°C / 60% RH this peak was not present.

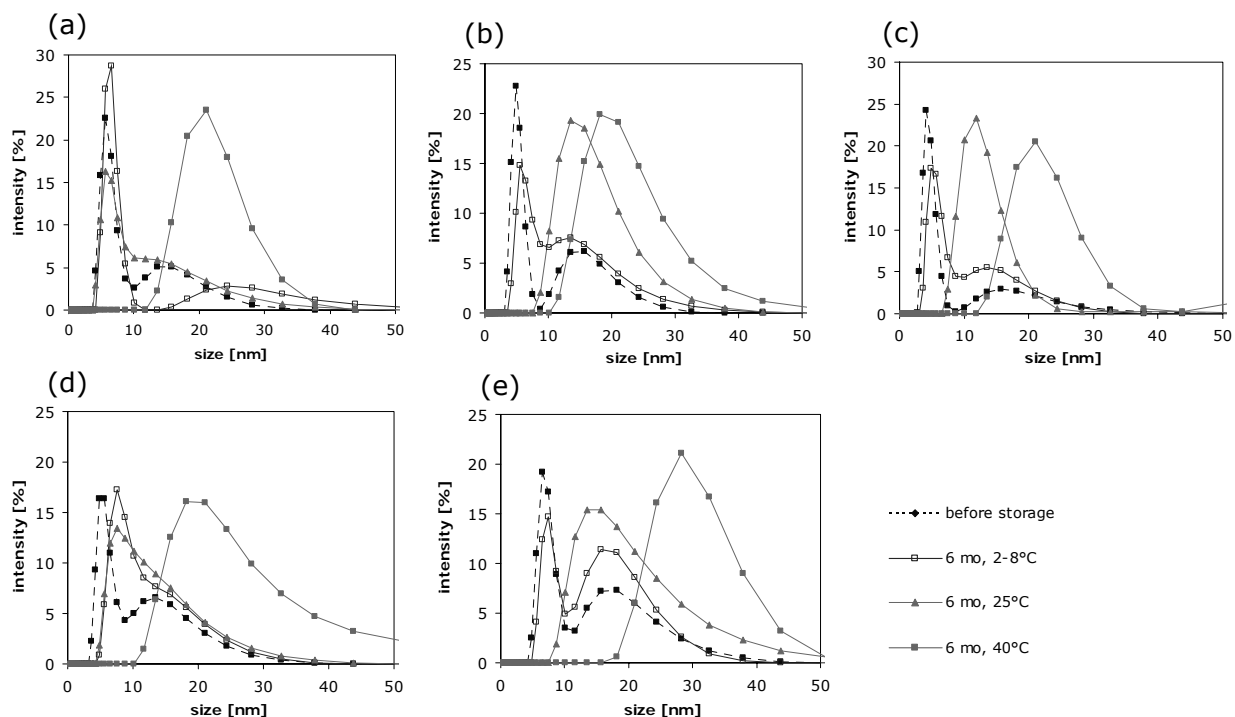


Figure 36: DLS size distribution by volume of lyophilized formulations storage at pH 4.0, 0.0% polysorbate 20 (a), 0.005% polysorbate 20 (b), 0.02% polysorbate 20 (c), pH 4.5 0.02% polysorbate 20 (d) and pH 5.0 0.02% polysorbate 20 (e) after 6 months.

The increase in met-oxidized cytokine in the lyophilized formulations was less pronounced compared to the liquid formulations (Figure 37). All samples stored at 2-8°C showed similar levels of approximately 3% met-oxidized cytokine after 6 months storage. At 25°C / 60% RH about 1% less met-oxidized cytokine was formed when 0.02% polysorbate 20 was added to the formulations.

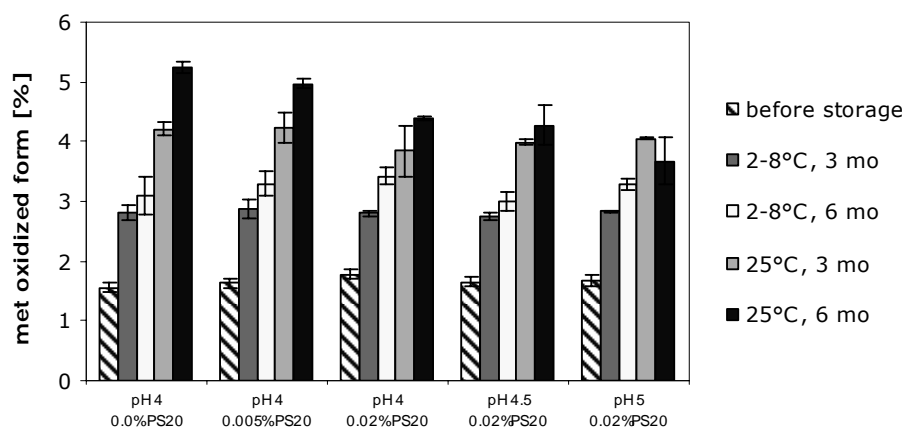


Figure 37: Results from RP-HPLC of lyophilized formulation after 3 and 6 months at 2-8°C and 25°C.

Thus, the used lyophilization cycle resulted in elegant cakes consisting of crystalline mannitol and amorphous sucrose. Low aggregation levels could be preserved upon storage at 2-8°C. The addition of 0.02% polysorbate 20 fostered aggregate formation at 25°C / 60% RH and 40°C / 75% RH, but decreased the formation of met-oxidized cytokine at 25°C / 60% RH. However, the mechanism by which polysorbate 20 increased aggregate formation in the lyophilized product during storage at 25°C / 60% RH and 40°C / 75% RH is unclear. The increased formation of aggregates induced by polysorbate 20 was not observed in the liquid formulation. The optimum stability for the lyophilized cytokine formulation could be achieved at pH 4.0 without polysorbate 20 and storage at 2-8°C.

3.6.3 Comparison of Liquid and Lyophilized Formulation

In the stability study of the liquid formulation, pH 3.5 and 4.0 turned out to be most stable regarding aggregation. The formation of the met-oxidized cytokine was independent of the pH but increased with storage time and temperature. Lyophilized formulations were stable from pH 4.0 to 5.0, when stored at 2-8°C. Again the formation of met-oxidized cytokine was independent of the formulation pH. In order to avoid protein adsorption the addition of polysorbate 20 to the liquid formulation was necessary, as the pre-filled syringes were manufactured of glass type I. Furthermore, in liquid formulation, polysorbate 20 was beneficial with respect to DLS-size distribution by volume and the formation of met-oxidized cytokine. The reduced formation of met-oxidized cytokine in presence of polysorbate 20 was as well seen for the lyophilized formulations. However, here polysorbate 20 fostered the formation of aggregates. As glass type I+ vials were employed for the lyophilized formulation, polysorbate 20 could be omitted with respect to adsorption.

4. Conclusions

The goal of the studies was to develop stable, HSA-free formulations for the cytokine as an alternative to the HSA-containing formulation. For formulation development the focus was set on the pH range between 3.0 and 5.5 in which an initial solubility of the cytokine at a constant aggregation level of about 3% to 4% was given. Above pH 5.5 precipitation of the cytokine indicated by an increased turbidity impeded a feasible formulation development. Initial characterization of the cytokine at different pH and ionic strength conditions revealed an improved stability with respect to aggregation and turbidity at a pH below 4.5 and low ionic strength. Furthermore, an improved thermal stability for lower pH values could be demonstrated by FTIR. At pH 3.0 and pH 3.5 a steady change of the FTIR-spectra with an onset above 25°C was observed. First at pH 3.5 a T_m of 74°C could be determined. With increasing pH the T_m values were lowered to 57°C at pH 4.2 and 49°C at pH 5.5. The improved thermal stability at lower pH values was also confirmed by DLS. A concentration of 20 mM glycine was selected as appropriate because the tendency of the cytokine to adsorb on glass was reduced compared to lower glycine concentration. Protein adsorption was found to be minimal at pH 3.0 using 20 mM glycine as buffer. Possible approaches to further reduce the loss of protein by adsorption were the use of glass type I⁺ and the addition of polysorbate 20 to the formulations, where more than 97% of the protein content could be recovered after 24 hours at pH 3.0 and 4.5. First short time stability studies had shown that an increase in ionic strength by adding NaCl led to a tremendous increase in aggregates and turbidity already after one week especially at 40°C. The addition of mannitol and trehalose on the other hand slightly improved the stability, with respect to aggregation.

For the storage stability study five liquid and five lyophilized formulations were selected, which contained 0.25 mg/ml cytokine, 20 mM glycine at different pH-values and polysorbate 20 concentrations. The isotonicity was adjusted with mannitol in the liquid formulation, due to the increased aggregation in presence of NaCl. For the lyophilized formulation sucrose was added as amorphous lyoprotector. Generally, aggregation levels and the formation of a met-oxidized form of the cytokine were increasing with higher storage temperature. The use of methionine as antioxidant could be an approach to reduce oxidation. For the liquid formulation aggregation increased by 0.5% for formulations with 0.02% polysorbate 20 independent of the pH. Polysorbate 20 could further reduce the loss of protein due to adsorption on the pre-filled glass syringes and the formation of met-oxidized cytokine. At pH 4.5 higher aggregation levels and a significantly changed DLS size-distribution by volume were obtained when the samples were stored at 25°C.

For the lyophilized formulations aggregation increased by 0.2% to 0.7% for all studied pH-values after 6 months at 2-8°C. Best stability with respect to aggregation was achieved for the lyophilized formulations at pH 4.0 with 0.0% and 0.005% polysorbate 20. The formation of met-oxidized cytokine on the other hand was lower in presence of polysorbate 20. For the lyophilized formulations a discoloration of the solutions after reconstitution was observed after storage at 40°C / 75% RH for pH 4.0 and pH 4.5 and at 25°C / 60% RH also for pH 4.0. The effect can be ascribed to the inversion of sucrose to the reducing sugars fructose and glucose, which is accelerated with temperature, residual moisture and lower pH. To achieve stable lyophilized formulations also at pH 4.0 and higher storage temperatures, the use of trehalose instead of sucrose could be a possible approach as trehalose shows a higher chemical stability. With lyophilization it was possible to use a higher pH of 5.0, which was not possible for the liquid formulations. When storing the liquid and lyophilized formulations for 6 months at 2-8°C good results could be achieved with all formulations. Within the studied formulations the liquid formulations at pH 3.5 and 4.0 with 0.02% polysorbate 20, as well as the lyophilized formulations at pH 4.0 with 0 and 0.005% polysorbate 20 offered the best stability at higher storage temperatures. Summarizing, it can be concluded that it is possible to stabilize the cytokine without the use of HSA as stabilizer at low pH. Aggregation and oxidation is critical at higher storage temperatures which required storage at 2-8°C. The issue of protein adsorption can be overcome by using polysorbate 20 as excipients, as well as by glass type I⁺ vials.

5. References

1. L. S. Lin, M. G. Kunitani, M. S. Hora. Interferon- β -1b (Betaseron®). A Model for Hydrophobic Therapeutic Proteins. *Pharm. Biotechnol.* **9**:275-301 (1996).
2. W. Wang. Lyophilization and Development of Solid Protein Pharmaceuticals. *Int. J. Pharm.* **203**:1-60 (2000).
3. P. McGoff, D. S. Scher. Solution formulation of Proteins/Peptides. 139-158 In E. J. McNally (eds) Protein formulation and Delivery; Drugs and the Pharmaceutical Science Volume 99, Marcel Dekker Inc, New York pp. 139-158 (2000).
4. P. J. Dawson. Effect of formulation and freeze-drying on the long-term stability of r-DNA-derived cytokines. *Dev. Biol. Stand.* **74**:273-282 (1992).
5. A. Braun, L. Kwee, M. A. Labow, J. Alsenz. Protein Aggregates Seem to Play a Key Role Among the Parameters Influencing the Antigenicity of Interferon Alpha (INF- α) in Normal and Transgenic Mice. *Pharm. Res.* **14**:1472-1478 (1997).
6. E. Hochuli. Interferon immunogenicity: technical evaluation of interferon- α 2a. *J. Interferon Cytokine Res.* **17** (Suppl. 1): 15-21 (1997).
7. A. Braun, J. Alsenz. Development and Use of Enzyme-Linked Immunosorbent Assays (ELISA) for the Detection of Protein Aggregates in Interferon Alpha (INF α) Formulations. *Pharm. Res.* **14**:1394-1400 (1997).
8. J. D. Meyer, J. E. Matsuura, J. A. Ruth, E. Shefter, S. T. Patel, J. Bausch, E. Mc Gonigle, M. C. Manning. Selective Precipitation on Interleukin-4 Using Hydrophobic Ion Pairing: A Method For Improved Analysis of Proteins Formulated with Large Excesses of Human Serum Albumin. *Pharm. Res.* **11**:1492-1495 (1994).
9. J. R. Wendorf, C. J. Radke, H. W. Blanch. Reduced Protein Adsorption at Solid Interfaces by Sugar Excipients. *Biotech. Bioeng.* **87**:565-573 (2004).
10. F. Samaritani, A. Del Rio. Human serum albumin (HSA)-free stabilized interferon liquid formulations, WO 2004096263 A2, PCT Int. Appl. (2004).
11. M. R. Duncan, J. M. Lee, M. P. Warchol. Influence of surfactants upon protein/peptide adsorption to glass and polypropylene. *Int. J. Pharm.* **120**:179-88 (1995).
12. M. S. Schwarzenbach, P. Reimann, V. Thommen, M. Hegner, M. Mumenthaler, J. Schwob, H. J. Güntherodt. Interferon α -2a interactions on Glass Vial Surfaces Measured by Atomic Force Microscopy. *PDA J. Pharm. Sci. Tech.* **59**:78-89 (2002).
13. Clarity and degree of opalescence of liquids; European Pharmacopoeia p. 27-29 (2005).
14. J. Geigert, B. A. Panschar, S. Fong, H. N. Huston, D. E. Wong, D. Y. Wong, C. Taforo, M. Pemberton. The Long-Term Stability of Recombinant (Serine-17) Human Interferon- β . *J. Interferon Res.* **8**:539-547 (1988).
15. E. A. Cooper, K. Knutson. Fourier Transform Infrared Spectroscopy Investigations of Protein Structure. in Physical Methods to Characterize Pharmaceutical Proteins. edited by J.N. Herron, Plenum Press New York 101-143 (1995).
16. S. L. Wang, S. Y. Lin, M. J. Li, Y. S. Wei, T. F. Hsieh. Temperature effect on the structural stability, similarity and reversibility of human serum albumin in different states. *Biophys. Chem.* **114**:205-212 (2005).
17. S. L. Wang, Y. S. Wei, S. Y. Lin. Subtractive similarity method used to study the infrared spectra of proteins in aqueous solution. *Vibrat. Spect.* **31**:313-319 (2003).
18. B. A. Shirley, M. Choe, M. Tellers, S. Babuka. Solubility of INF-Beta-1b in Sodium Chloride Solutions. PCT Int. Appl. WO 02/080976 A2 (2002).
19. S. Hershenson, J. Thomson. Isoelectric focusing of recombinant interferon- β . *Appl. Theor. Electrophr.* **1**:123-124 (1989).

20. K. L. Shaw, G. B. Grimsley, G. I. Yakovlev, A. A. Makarov, C. N. Pace. The effect of net charge on the solubility, activity, and stability of ribonuclease Sa. *Protein Sci.* **10**:1206-1215 (2001).
21. K. P. C. Vollhardt, N. E. Schore. *Organische Chemie*. Ed. H. Butenschön. VCH Verlagsgesellschaft mbH, Weinheim (1995).
22. H. C. Mahler, R. Müller, W. Frieß, A. Delille, S. Matheus. Induction of aggregates in a liquid IgG1-antibody formulation. *Eur. J. Pharm. Biopharm.* **59**:407-417 (2005).
23. D. Shaw, P. Dubin. Aggregation of B-Lactoglobulin. Malvern Application notes. www.malvern.co.uk. (2005).
24. P. C. Sontum, C. Christiansen. Photon Correlation Spectroscopy applied to characterisation of denaturation and thermal stability of human albumin. *J. Pharm. Biomed. Anal.* **16**:295-302 (1997).
25. J. Demeester, S. S. de Smedt, N. N. Sanders, J. Hastraete. Light Scattering. in *Methods for Structural Analysis of Protein Pharmaceuticals*, edited by W. Jiskoot and D. J. A. Crommelin, AAPS Press p. 245-277 (2005).
26. A. Schön, A. Velázquez-Compoy. Calorimetry in *Methods for Structural Analysis of Protein Pharmaceuticals*. Eds. W. Jiskoot, D. J. A. Crommelin, AAPS Press, Arlington VA, 573-591 (2005).
27. A. Cooper, M. A. Nutley, A. Wadood. Differential scanning microcalorimetry. *Protein-Ligand Interactions: Hydrodynamics and Calorimetry*, Oxford University Press. 287-318 (2001).
28. R. L. Remmele, N. S. Nightlinger, S. Srinivasan, W. R. Gombotz. Interleukin-1 Receptor (IL-1R) Liquid Formulation Development Using Differential Scanning Calorimetry. *Pharm. Res.* **15**:200-208 (1998).
29. L. L. Y. Lee, J. C. Lee. Thermal stability of proteins in the presence of poly (ethylene glycols). *Biochem.* **26**:7813-7819 (1987).
30. M. van de Weert, J. A. Hering, P. I. Haris. Fourier Transform Infrared spectroscopy. In *Methods for Structural Analysis of Protein Pharmaceuticals*. Eds. W. Jiskoot, D. J. A. Crommelin. AAPS Press Arlington 131-167 (2005).
31. D. M. Byler, H. Susi. Examination of the secondary structure of proteins by deconvolved FTIR spectra. *Biopolym.* **25**:469-487 (1986).
32. A. C. Dong, P. Huang; W. S. Caughey. Protein secondary structures in water from second-derivative amide I infrared spectra. *Biochem.* **29**:3303-3308 (1990).
33. A. C. Dong, S. J. Prestrelski, S. D. Allison, J. F. Carpenter. Infrared Spectroscopic studies of lyophilization induced protein aggregation. *J. Pharm. Sci.* **84**:415-424 (1995).
34. F. Meersman, L. Smeller, K. Heremans. Comparative Fourier Transform Infrared Spectroscopy Study of Cold-, Pressure-, and Heat-Induced Unfolding and Aggregation of Myoglobin. *Biophys. J.* **82**:2635-2644 (2002).
35. K. Murayama, M. Tomida. Head-Induced Secondary Structure and Conformation Change of Bovine Serum Albumin investigated by Fourier Transform Infrared Spectroscopy. *Biochem.* **43**:11526-11532 (2004).
36. K. Goossens, J. Helewijn, F. Meersman, M. De Ley, K. Heremans. Pressure- and temperature- Induced unfolding and aggregation of recombinant human interferon- γ : a Fourier transform infrared spectroscopy study. *Biochem. J.* **370**:529-535 (2003).
37. H. Fan, J. Ralston, M. Dibiase, E. Faulkner, C. Russel Middaugh. Solution behavior of INF- β -1a: An Empirical Phase Diagram Based Approach. *J. Pharm. Sci.* **94**:1893-1911 (2005).
38. Bruker Optics. IR-Spektroskopische Quantifizierung von Strukturänderungen in Proteinlösungen. Application Note.
39. H. H. Bauer, M. Müller, J. Goette, H. P. Merkle, U. P. Fringeli. Interfacial Adsorption and Aggregation Associated Changes in Secondary Structure of Human Calcitonin Monitored by ATR-FTIR Spectroscopy. *Biochem.* **33**:12276-12282 (1994).
40. L. Marchal-Heussler. Adsorption of Drugs. in *Cyclopeida of Surface and Colloidal Science*, Marcel Dekker, New York; pp. 294-306 (2002).

41. S. Matheus, W. Friess, H. C. Mahler. FTIR and n-DSC as analytical tools for high concentration protein formulations. *Pharm. Res.* **23**:1350-1363 (2006).
42. A. Dong, B. Kendrick, L. Kreilgaard, J. Matsuura, M. C. Manning, J. F. Carpenter. Spectroscopic Study of the Secondary Structure and Thermal Denaturation of Recombinant Human Factor XIII in Aqueous Solution. *Archives Biochem. Biophys.* **347**:213-220 (1997).
43. B. A. Kerwin, M. C. Heller, S. H. Levin, T. W. Randolph. Effects of Tween 80 and Sucrose on Acute Short-Term Stability and Long-Term Storage at -20°C of a Recombinant Hemoglobin. *J. Pharm. Sci.* **87**:1062-1068 (1998).
44. Malvern Application note: Characterization of protein melting point, www.malvern.co.uk.
45. D. M. Petsev, B. R. Thomas, S. T. Yau, P. G. Vekilov. Interaction and Aggregation of Apoferritin Molecules in Solution: Effect of Added Electrolytes. *Biophys. J.* **78**:2060-2069 (2000).
46. J. J. Lin, J. D. Meyer, J. F. Carpenter, M. C. Manning. Stability of Human Serum Albumin During Bioprocessing: Denaturation and Aggregation During Processing of Albumin Paste. *Pharm. Res.* **17**:391-396 (2000).
47. W. Norde. Adsorption of Proteins at Solid-Liquid Interfaces. *Cells Mat.* **5**:97-112 (1995).
48. F. Y. Oliva, L. B. Avelle, O. R. Cámara, C. P. De Pauli. Adsorption of human serum albumin (HSA) onto colloidal TiO₂ particles, Part I. *J. Coll. Interf. Sci.* **261**:299-311 (2003).
49. J. R. Wendorf, C. J. Radke, H. W. Blanch. Reduced Protein Adsorption at Solid Interfaces by Sugar Excipients. *Biotech. Bioeng.* **87**:565-573 (2004).
50. S. Sjöberg. Silica in aqueous Environments. *J. Non-crystall. Sol.* **196**:51-57 (1995).
51. M. Hiraki. Isoelectric point of glycine and α -alanine. *J. Biochem.* **15**:345-357 (1932).
52. M. Zhang, M. Ferrari. Reduction of Albumin Adsorption onto Silicon Surfaces by Tween 20. *Biotech. Bioeng.* **56**:618-625 (1997).
53. W. Norde, F. MackRitchie, G. Nowicka, J. Lyklema. Protein adsorption at solid-liquid interfaces: reversibility and conformation aspects. *J. Coll. Interf. Sci.* **112**:447-456 (1986).
54. M. C. Kaplan, A. Jégou, B. Chaufer, M. Rabiller-Baudry, M. C. Michalsky. Adsorption of lysozyme on membrane material and cleaning with non-ionic surfactant characterized through contact angle measurements. *Desal.* **146**:149-154 (2002).
55. T. Arakawa, S. N. Timasheff. Preferential Interactions of Proteins with Salts in Concentrated Solutions. *Biochem.* **21**:6545-6552 (1982).
56. T. Arakawa, S. N. Timasheff. Mechanism of Protein Salting In and Salting Out by Divalent Cation Salts: Balance between Hydration and Salt Binding. *Biochem.* **23**:5912-5923 (1984).
57. T. Arakawa, S. J. Prestrelski, W. C. Kenney, J. F. Carpenter. Factors affecting short-term and long-term stability of proteins. *Adv. Drug Del. Rev.* **46**:307-326 (2001).
58. A. Kim, M. Akers and S. Nail. The Physical State of Mannitol after Freeze-Drying: Effect of Mannitol Concentration, Freezing Rate and a Noncrystallizing Cosolute. *J. Pharm. Sci.* **87**:931-935 (1998).
59. K. Izutsu, S. Yoshioka, T. Terao. Effect of Mannitol Crystallinity on the Stabilization of Enzymes during Freeze-Drying. *Chem. Pharm. Bull.* **42**:5-8 (1994).
60. H. R. Costantino, J. D. Andya, P. A. Nguyen, N. Dasovich, T. D. Sweeney, S. J. Shire, C. C. Hsu, Y. F. Maa. Effect of Mannitol Crystallization on the Stability and Aerosol Performance of a Spray-Dried Pharmaceutical Protein, Recombinant Humanized Anti-IgE Monoclonal Antibody. *J. Pharm. Sci.* **87**:1406-1411 (1998).
61. J. H. Crowe, J. F. Carpenter. An infrared spectroscopic study of the interactions of carbohydrates with dried protein. *Biochem.* **28**:3916-3922 (1989).
62. F. Franks, R. H. M. Hatley, S. F. Mathias. Materials science and the production of shelf-stable biologicals. *Bio. Pharm.* **4**:38-55 (1991).

63. L. Kreilgaard, L. S. Jones, T. W. Randolph, S. Frokjoer, J. M. Flink, M. C. Manning, J. F. Carpenter. Effect of Tween 20 on Freeze-Thawing- and Agitation-Induced Aggregation of Recombinant Human Factor XIII. *J. Pharm. Sci.* **87**:1597-1603 (1998).
64. N. B. Bam, J. L. Cleland, J. Yang, M. C. Manning, J. F. Carpenter, R. F. Kelley, T. W. Randolph. Tween Protects Recombinant Human Growth Hormone against Agitation-Induced Damage via Hydrophobic Interactions. *J. Pharm. Sci.* **87**:1554-1559 (1998).
65. L. C. Gu, E. A. Erdos, H. S. Chiang, T. Calderwood, K. Tsai, G. C. Visor, J. Duffy, W. C. Hsu, L. C. Foster. Stability of Interleukin 1.β. (IL-1.β.) in aqueous solution: analytical methods, kinetics, products, and solution formulation implications. *Pharm. Res.* **8**:485-490 (1991).
66. M. Boublik, J. A. Moschera, C. Wei, H-F. Kung. Conformation and Activity of Recombinant Human Fibroblas Interferon-β. *J. Interferon Res.* **10**:213-213 (1990).
67. S. E. Grossberg, J. L. Taylor, R. E. Seibenlist, P. Jameson. Biological and immunological assays of human interferons. in *Manual of Clinical Immunology*, Editors: N. R. Rose, H. Friedman, J. L. Fahey, Am. Soc. of Microbiol. 295-299 (1985).
68. E. Y. Shalaev, Q. Lun, M. Shalaeva, G. Zografi. Acid-Catalyzed Inversion of Sucrose in the Amorphous State at Very Low Levels of Residual Water. *Pharm. Res.* **17**:366-370 (2000).
69. M. C. Manning, K. Patel, R. T. Borchardt. Stability of Protein Pharmaceuticals. *Pharm. Res.* **6**:903-918 (1989).
70. W. Wang. Instability, stabilization and formulation of liquid protein pharmaceuticals. *Int. J. Pharm.* **185**:125-188 (1999).
71. R. Haikala, R. Eerola, V. P. Tanninen, J. Yliruusi. Polymorphic changes of mannitol durino freeze-drying: effect of surface active agents. *PDA J. Pharm. Sci. Tech.* **51**:96-101 (1997).
72. L. Yu. Nucleation of One Polymorph by Another. *J. Am. Chem. Soc.* **125**:6380-6381 (2003).
73. E. Y. Shalaev, G. Zografi. How Does Residual Moisture Affect the Solid-State Degradation of Drugs in the Amorphous State. *J. Pharm. Sci.* **85**:1137-1141 (1996).
74. M. J. Pikal. Freeze-drying of Proteins. Part I: process design. *Biopharm.* **3**:18-27 (1990).
75. L. Chang, D. Shepherd, J. Sun, X. Tang, M. J. Pikal. Effect of Sorbitol and Residual Moisture on the Stabiliy of Lyophilized Antibodies: Implications for the Mechanism of Protein Stabilization in the Solid State. *J. Pharm. Sci.* **94**:1445-1455 (2005).

Chapter 7: Summary of the Thesis

1. General Introduction

The goal of the thesis was to study the impact of formulation conditions on the stability of a hydrophobic cytokine. Chapter 1 provides a general introduction into the formulation of hydrophobic proteins. Poor solubility and the tendency of hydrophobic proteins to adsorb on surfaces are the major challenges. To circumvent these problems Human Serum Albumin (HSA) is frequently used as excipient, however, its use is related to the risk of blood born pathogens and enhanced immunogenicity. Possible approaches for the development of HSA-free formulations for hydrophobic proteins are discussed. In its function as cryo- and lyoprotector HSA can be replaced by sugars, sugar alcohols or amino acids. By adjusting the formulation pH and ionic strength protein solubility can be optimized and adsorption reduced. Protein adsorption is most effectively addressed by the addition of surfactants and can be solved by the use of container materials which are less prone to adsorption e.g. glass type I⁺.

2. Characterization of Cytokine Solubility and Particle Formation in Presence of Human Serum Albumin

Based on commercially available formulations a hydrophobic recombinant human cytokine lyophilized with HSA and mannitol was used for the studies. In Chapter 2 the HSA-cytokine formulation was characterized with respect to turbidity, particle formation and protein-protein interactions. The impact of NaCl, the HSA-stabilizers Na-octanoate and Na-N-acetyltryptophanate, as well as formulation pH on the HSA-cytokine formulation was elucidated. When lowering the pH, a significant increase in turbidity with maximum values close to the isoelectric point of HSA around pH 5.0 was observed which was partially irreversible mainly due to the cytokine. The precipitated fraction was characterized by Dynamic Light Scattering, Atomic Force Microscopy, disc centrifugation and light obscuration. The main particle classes ranged between 4 to 10 nm, 20 to 50 nm and 500 to 1000 nm. A shift from smaller to larger particles was found when the pH was lowered from 7.4 to 5.0. By the addition of NaCl to the formulation the turbidity increase at pH 5.0 could be prevented. Fluorescence spectroscopy revealed weaker interactions between HSA and the cytokine at pH 4.5 in the presence of NaCl. Furthermore, studies with HSA placebo formulation demonstrated a direct stabilizing effect of NaCl on HSA, with respect to the turbidity increase at pH 5.0. At concentrations applied for the stabilization of HSA, Na-octanoate and Na-N-acetyltryptophanate only played a minor

role for the prevention of the turbidity increase at pH 5.0. Thus, it could be shown in Chapter 2 that NaCl was essential for the overall stability of the HSA-cytokine formulation.

3. Characterization of the Lyophilization Behavior of Mannitol-Human Serum Albumin-NaCl Formulations

As NaCl can impact the freezing and lyophilization behavior, the impact of NaCl on the behavior of mannitol-HSA placebo mixtures based on the cytokine-HSA formulations was studied. The freezing process of mannitol-HSA-NaCl formulations was subject of Chapter 3. Two different HSA-qualities, unstabilized-HSA and stabilized-HSA containing NaCl, Na-octanoate and Na-N-acetyltryptophanate were used. Differential Scanning Calorimetry and Low Temperature X-ray Diffraction showed that both HSA-types and NaCl could delay and inhibit the crystallization of mannitol. This effect has to be taken in consideration, as it is possible that mannitol crystallizes in an uncontrolled way upon storage. Due to the presence of the stabilizers, formulations with stabilized-HSA differed in their freezing behavior as compared to those containing unstabilized-HSA. In the particular concentration used for the stabilization of HSA, NaCl had the most distinct impact on the low temperature behavior of mannitol. Already small quantities of NaCl shifted T_g' and T_c of mannitol formulations to lower temperatures. The study demonstrated that the freezing step had a significant effect on the physico-chemical properties of the formulations which can affect the subsequent drying process and the lyophilized products.

The effect of NaCl on the overall lyophilization processes, as well as the resulting lyophilized products of mannitol-HSA-NaCl formulations was described in Chapter 4. Increasing NaCl-concentrations led to products with a lower degree of crystallinity and less compact cake structures. In the presence of NaCl the drying time was shorter due to the changed cake structure. Differential Scanning Calorimetry, X-ray Powder Diffraction and Scanning Electron Microscopy showed that NaCl-concentration and applied freezing-protocol governed the morphology of the formulations after lyophilization. Increasing NaCl concentration led to partially amorphous products. However, upon storage the amorphous state could not be preserved, with the consequence that mannitol and NaCl crystallized. The data indicated that products without NaCl were more stable in their modifications. However, the stability of HSA upon storage in the lyophilized products, monitored by a turbidity scan from pH 3.0 to 7.0 and size exclusion chromatography was improved by the addition of NaCl. This could be referred to the direct stabilizing effect of NaCl on HSA. For the studied systems the benefit of NaCl on protein stability outbalanced the observed potential drawbacks. Consequently, Chapter 3 and 4 showed the

importance of the physico-chemical characterization of the formulations used for lyophilization, when NaCl is part of the formulation. The lowering of T_g' and the inhibition of mannitol crystallization are the most distinct effects of NaCl.

4. Development of a Human Serum Albumin-free formulation for the Cytokine

One goal of the thesis was to develop a HSA-free formulation for the cytokine. In Chapter 5 the system mannitol–sucrose was evaluated as possible excipient combination for the cytokine during lyophilization. The optimum ratio of mannitol to sucrose and appropriate lyophilization cycles were evaluated with the objective to achieve a product consisting of highly crystalline mannitol in combination with amorphous sucrose. Special focus was set on the formation of the metastable mannitol hydrate, as it can cause stability problems due to the release of hydrate water. NaCl lowered the T_g' of mannitol-sucrose formulations, as it acts as plasticizer for the amorphous phase which needs to be considered to avoid collapse. Mannitol crystallization during freezing was inhibited by sucrose and NaCl. This results in partially crystalline systems which come along with the disadvantage of potential crystallization upon storage that can be detrimental for the stability of the active protein. In addition, an increased content of mannitol hydrate was found after lyophilization with annealing, which was applied to maximize mannitol crystallization. Low Temperature X-ray Diffraction experiments with 8.0% mannitol and 2.0% sucrose showed that mannitol hydrate was preferably formed at lower annealing temperatures, which was confirmed by Powder X-ray Diffraction after lyophilization. Thus, if annealing during lyophilization is necessary, a sufficiently high temperature needs to be selected. Adequate crystallization of mannitol was achieved in formulations with 4.0% mannitol and 1.0% sucrose in processes without annealing. Therefore, this system was selected for a HSA-free lyophilized formulation of the cytokine.

The development of stable, HSA-free formulations for the cytokine was outlined in Chapter 6. Pre-formulation studies revealed that sufficient cytokine solubility was given in the pH-range from 3.0 to 5.5. Above pH 5.5 a turbidity increase caused by the precipitation of the cytokine was observed. Below pH 4.5 at a low ionic strength the best stability of the cytokine with respect to aggregation and turbidity was achieved. As buffer system 20 mM glycine was selected, since lower glycine concentrations favored protein adsorption to the container and higher glycine concentrations led to an increased aggregation tendency. Protein adsorption could be minimized by the utilization of glass type I⁺ and the addition of polysorbate 20 to the formulations. The thermal stability of the cytokine, monitored by the denaturation temperature determined with Fourier Transform Infrared Spectroscopy, decreased at higher pH values.

The stability of five liquid formulations at pH 3.5 to 4.5 with 4.8% mannitol and five lyophilized formulations at pH 4.0 to 5.0 with 4% mannitol and 1% sucrose was evaluated over 6 months at 2-8°C, 25°C / 60% RH and 40°C / 75% RH. For both, liquid and lyophilized formulations the formation of met-oxidized cytokine was independent of the pH but increased with storage time and temperature. In the liquid formulations the level of met-oxidized cytokine was slightly higher compared to the lyophilized formulation. The liquid formulation at pH 3.5 and 4.0 and the lyophilized formulations between pH 4.0 and 5.0 turned out to be most stable regarding aggregation, when stored at 2-8°C. To avoid protein adsorption the addition of polysorbate 20 to the liquid formulation was necessary, as the pre-filled syringes were manufactured of glass type I. In the liquid formulation polysorbate 20 further had a slight protective effect with respect to the formation of larger protein aggregate populations detectable by Dynamic Light Scattering and the formation of met-oxidized cytokine. However, in the freeze-dried formulation polysorbate 20 fostered the formation of aggregates. As glass type I+ vials were employed for lyophilization adsorption was minimal and one could omit polysorbate 20. Overall, it was possible to stabilize the cytokine without the use of HSA at low pH.

Thus, the studies provided an extensive characterization of the hydrophobic cytokine, its stabilization with HSA and the pH dependent instability of HSA-containing systems. As an alternative a stable HSA-free formulation for the cytokine could be presented. Especially for the lyophilized formulations it could be shown that subtle changes of excipients e.g. in the NaCl content can have a detrimental impact.

Presentations and Publications associated with this Thesis

Articles

A. Hawe, W. Frieß. Physico-chemical Behavior of Mannitol, Human Serum Albumin Formulations during Lyophilization. *Eur. J. Pharm. Sci.* **28**:224-232 (2006).

A. Hawe, W. Frieß. Impact of Freezing Procedure and Annealing on the Physico-chemical Properties and the Formation of Mannitol Hydrate in Mannitol-Sucrose-NaCl Formulations. *Eur. J. Pharm. Biopharm.* **64**:316-325 (2006).

A. Hawe, W. Frieß. Freezing Behavior of Mannitol, HSA Formulations. *AAPS Pharm. Sci. Tech.* accepted (2006).

Oral Presentations

A. Hawe, W. Frieß. Development of a Formulation for a Hydrophobic Cytokine. 5th Worldmeeting on Pharmaceutics, Biopharmaceutics and Pharmaceutical Technology, Geneva, Switzerland (2006).

A. Hawe, W. Frieß. Human Serum Albumin as Stabilizing Carrier for Cytokines. Local Chapter Germany of the Controlled Release Society, Marburg, Germany (2005).

Posters

A. Hawe, W. Frieß. Human Serum Albumin as Stabilizing Excipient for Cytokines. AAPS Annual Meeting and Exposition, Nashville, USA (2005).

A. Hawe, W. Frieß. Impact of NaCl on the Physico-chemical Properties of Formulations with Mannitol and HSA during Freezing and Lyophilization. AAPS Annual Meeting and Exposition, Nashville, USA (2005).

A. Hawe, W. Frieß. Development of a Formulation for a Hydrophobic Cytokine. AAPS National Biotechnology Conference, San Francisco, USA (2005).

A. Hawe, W. Frieß. Influence of NaCl on the Crystallization Behavior of Mannitol in the System Mannitol-HSA-NaCl during Lyophilization. European Conference on Drug Delivery and Pharmaceutical Technology, Sevilla, Spain, (2004).

A. Hawe, W. Frieß. Influence of NaCl on Excipients used for Lyophilization of Proteins. Protein Stability Conference, Breckenridge, USA, (2003).

Curriculum Vitae

ANDREA HAWE

PERSONAL DETAILS

Date of birth:	August 09, 1977
Place of birth:	Munich, Germany
Nationality:	German

EDUCATION

08/2002 – 07/2006	PhD Thesis Department for Pharmacy, Pharmaceutical Technology and Biopharmaceutics Ludwig-Maximilians-University, Munich Supervisor: Prof. Dr. Wolfgang Friess
05/2002	Licence to practice as pharmacist
11/2001-05/2002	Internship at Roche GmbH, Penzberg
05/2001-10/2001	Internship in public pharmacy, Sonnenapotheke, Munich
1997-2001	Study of Pharmacy at the Ludwig-Maximilians University, Munich
08/1996 – 02/1997	Exchange student at the Georgia Southwestern State University, Americus, GA, USA
1987-1996	High School, Gymnasium Penzberg graduation with 'Abitur'